THE ROLE OF PROMYELOCYTIC LEUKAEMIA (PML) PROTEIN IN REGULATION OF ADULT SUBVENTRICULAR ZONE NEUROGENESIS

A, Deli

This dissertation is submitted to University College London for the examination of Doctor of Philosophy

University College London, 2016

DECLARATION

I, Deli A, declare that the work presented in this thesis is my own and has not been submitted for any previous degree. The collaborative contributions have been indicated clearly and acknowledged.

ACKNOWLEDGEMENTS

I would like to express my special appreciation and thanks to my supervisors, Professor Paolo Salomoni, Dr Richard Jenner and Professor Stephan Beck. Thank you Paolo for offering me the opportunity to conduct such an amazing project in your lab. I am grateful for the supervision, support, insightful discussion and invaluable advice throughout my study and your effort in reading my thesis. Some say PhD=PHD (permanent head damage), but we know there are aNSCc that can migrate… Thank you Richard for the guidance and support during my PhD, I really appreciate the weekly meetings and useful feedback from you. Thank you for providing relevant reagents and both technical and scientific advice for my project. A special thank you goes to Stephan for his kind guidance and feedback in poster sessions and giving me permission to use the equipment in his lab.

I would like to give special thanks to Professor Antonella Riccio for her advice and feedback in the joint lab meetings and my upgrade viva. I would also like to thank Professor Adrienne Flanagan for her advice in the joint lab meetings and her encouragement. I am grateful for the advice received from Professor Pierluigi Nicotera, thank you for the support. I would especially like to thank Professor Sebastian Brandner for his contributions to this project. My special thanks go to Professor William Richardson and Dr Huiliang Li for providing the access to their lab and the mouse colony.

I would like to express my gratitude to the graduate tutor, Dr Julie Olszewki, for her continual support during my Master's studies and PhD. I would like to thank all the staff in UCL animal facility and UCL Cancer Institute for their advice and help.

My deep appreciation goes out to all the members (past and current) in lab 203. I would like to thank Joanne Betts for her beautiful work and contributions to this project. I thank Sara Galavotti and David Michod for their technical support and patient training at the beginning of my PhD. Thank you Sara for your help and motivation. I would like to thank Maria Dvorkina and Sandra Cantilena for their help with the animal colonies. Special thanks go to Aikaterini Lampada for her company, support and her endless effort to remind me (and the whole Bloomsbury area) my name. I thank the two students I helped to

supervise, Sarah Oberndorfer and Salome Stierli, for their contributions and I wish them all the best. The whole lab would be at risk without the presence of Julia Hofmann. Thank you Julia for being a great neighbour. I really enjoyed our discussion (occasionally with a glass of Chardonnay) and your advice. I would like to thank Valeria Amodeo for correcting my pronunciation of “pizza” in Italian and of course, her amazing contributions to this project. I would like to thank Ana Paula Leite for her help in bioinformatics and telling me that lobster is a lot cheaper in Boston. Bonjour Ketty Kessler, thank you for the support and the effort you put into teaching me French, and I’m surprised you have very nice improvements in Chinese. I would like to thank Manav Pathania for his advice and music in the lab. I thank Qingyi Liang and Teresa Sposito for their support and help during my thesis writing and being patient for me occupying their computers. My special thanks to Natalia Izotova for her company in the lab and the funny moments she brought us. I thank Nicola Maestro and Aditya Shroff for their effort in running the lab and happy hours in the pub.

I greatly appreciate the support received from the people outside our lab. I gratefully acknowledge Manuel Beltran Nebot for his expertise in PRC2. I would like to thank Lucia Cottone and Sara Bianco for the delightful conversations. Special thanks to Dimitra Georgopoulou for the technical advice and Christopher Barrington for proofreading parts of my thesis. For the research involving neoplastic work, my gratitude goes to all the people involved in this project (see Appendix 8 for full author list). Finally, life in the lab would not have been the same without “the biggest liver”, Sussane Scheipl. Thank you for the joyful moments and company.

Last, but by no means least, I would like to thank my family. I would like to express my gratitude and respect to my parents and my sister. This PhD would not have been achievable without your support. Thank you all for your love and care during these years. Undertaking this PhD abroad has been a truly unique experience and it would not have been possible to achieve this without you being there.

To my beloved parents and sister

ABSTRACT

The control of cell fate in neural progenitor/stem cells (NPCs/NSCs) is essential for central nervous system (CNS) development. NSCs are also found within the adult brain. In particular, NSCs in the subventricular zone (SVZ) migrate through the rostral migratory stream (RMS) and terminally differentiate in the olfactory bulb (OB). However, our understanding of mechanisms regulating cell migration during SVZ neurogenesis remains limited.

Previous work from our lab showed that the promyelocytic leukaemia protein (PML), a growth suppressor inactivated in leukaemia, controls cell fate during corticogenesis, with implications for regulation of brain size. The main aim of the present work was to investigate the role of PML in the context of adult SVZ neurogenesis. Our findings show that PML loss leads to reduction of the more primitive NSC pool accompanied by expansion of transit-amplifying NPCs and neuroblasts. However, PML-deficient neuroblasts display impaired migratory capacity through the RMS, thus resulting in reduced number of terminally differentiated neurons and a smaller OB. These changes can be recapitulated *in vitro*, demonstrating an intrinsic defect of PML KO NSCs. Mechanistically, our findings suggest that PML controls NSC expansion and migration via Polycomb Repressive Complex-2 (PRC-2) - dependent suppression of a transcriptional programme involving the axon guidance genes Slit2/Robo1 and the key epithelial-to-mesenchymal transition (EMT) gene Twist1. Notably, Twist1 is part of an amplification loop for transcriptional induction of Slit2.

I was also involved in work aimed at determining whether the PML/Slit axis is functional in neoplastic settings. In this respect, alterations of adult neurogenesis are believed to lead to glioblastoma multiforme (GBM), and tumour spreading through the brain parenchyma is one of key factors underlying GBM aggressiveness. Our work revealed that a PML/Slit axis controls cell migration also in GBM cells, suggesting that mechanisms underlying cell migration are common to normal and neoplastic cells in the CNS.

Overall, these findings have important implications for our understanding of adult neurogenesis and may provide novel insights into the process of oncogenesis in the CNS.

TABLE OF CONTENTS

LIST OF FIGURES

LIST OF TABLES

LIST OF ABBREVIATIONS

4-OHT	4-Hydroxytamoxifen
APL	Acute promyelocytic leukemia
Ars-2	Arsenite-resistance protein 2
ATO	Arsenic Trioxide
ATP	Adenosine triphosphate
ATRX	Alpha thalassemia/mental retardation syndrome X-linked
bFGF	Basic Fibroblast growth factor
bHLH	Basic helix-loop-helix
Bmi1	B lymphoma Mo-MLV insertion region 1
BMP	Bone morphogenetic protein
BRGC	Brg1-dependent chromatin remodelling complex
CBP	CREB binding protein
CC	Coiled-coil
CDKi	Cyclin-dependent kinase inhibitor
ChIP	Chromatin immunoprecipitation
CML	Chronic myeloid leukaemia
CNS	Central nervous system
CSC	Cancer stem cell
CSF	Cerebrospinal fluid
DAXX	Death-associated protein 6
DCX	Doublecortin
DDR	DNA damage response
DG	Dentate gyrus
DMEM	Dulbecco's modified eagle's medium
DMSO	Dimethyl sulfoxide
DNMT	DNA methyltransferase
DSB	Double-strand break
ECL	Enhanced chemiluminescence
ECM	Extracellular matrix
EED	Embryonic ectoderm development
EGF	Epidermal growth factor

EGFR	Epidermal growth factor receptor
EGL	External granule layer
EGTA	Ethylene glycol tetraacetic acid
EMT	Epithelial-mesenchymal transition
EZH2	Enhancer of zeste homologue 2
FAO	Fatty acid oxidation
FBS	Fetal bovine serum
GBM	Glioblastoma multiforme
GC	Granule cell
GCP	Granule cell progenitor
GFAP	Glial fibrillary acidic protein
GFP	Green fluorescent protein
GLAST	Glutamate-aspartate transporter
HAT	Histone acetyltransferase
HDAC	Histone deacetylase
HGG	High grade glioma
HIRA	Histone regulator A
HRP	Horseradish peroxidase
HSC	Hematopoietic stem cell
IDH1	Isocitrate dehydrogenase 1
IF	Immunofluorescence
IGF	Insulin-like growth factor
IGL	Inner granule layer
IMDM	Iscove's modified dulbecco's medium
IPC	Intermediate progenitor cell
KMT	Lysine methyltransferase
LGE	Lateral ganglionic eminence
LIC	Leukemia-initiating cell
LOH	Loss of heterozygosity
LSD1	Lysine specific demethylase 1
MADM	Mosaic Analysis with Double Markers
MAR	Matrix attachment region
MEF	Mouse embryonic fibroblast

MET	Mesenchymal–epithelial transition
MMP	Matrix mettaloproteinase
MPNST	Malignant peripheral nerve sheath tumour
mTOR	Mammalian target of rapamycin
NCAM	Neural cell adhesion molecule
NCSC	Neural crest-derived stem cell
ND-10	Nuclear domains-10
NE	Neuroepithelium
NES	Nuclear export sequence
NF1	Neurofibromatosis type 1
NLS	Nuclear localisation signal
NSC/NPC	Neural stem cell/ Neural progenitor cell
OB	Olfactory bulb
OPC	Oligodendrocytes precursor cell
PBS	Phosphate buffer saline
PcG	Polycomb group
PDGFR	Platelet-derived growth factor receptor
PEG	Polyethylene glycol
PGC	Periglomerular cell
PI3K	Phosphatidylinositol 3-kinase
PML	Promyelocytic leukemia protein
PML-NB	PML-nuclear body
PNS	Peripheral nervous system
POD	PML oncogenic domains
PP1α	Protein phosphatase 1α
PP2A	Protein phosphatase 2
PPAR	Peroxisome proliferator-activated receptor
PRC	Polycomb repressive complex
PSA	Polysialic acid
PTEN	Phosphatase and tensin
PTM	Posttranslational modification
qPCR	Quantitative polymerase chain reaction
RARα	Retinoic acid receptor α

Rb	Retinoblastoma
RGL	Radial glia-like cell
RING	Really interesting gene
RMS	Rostral migratory stream
ROS	Reactive oxygen species
RTK	Receptor tyrosine kinase
SDF-1	Stromal cell-derived-factor-1 alpha
SDS	Sodium dodecyl sulfate
SEM	Standard error of the mean
SEZ	Subependymal zone
SGZ	Subgranular zone
SHH	Sonic hedgehog
shRNA	Short hairpin RNA
Sox2	SRY-box transcription factor 2
srGAP1	Slit-Robo Rho GTPase activating protein 1
SUZ12	Suppressor of zeste 12 protein homolog
SVZ	Subventricular zone
T-ALL	T cell acute lymphoblastic leukaemia
TEMED	Tetramethylethylenediamine
TGF-β	Transforming growth factor β
TRIM	Tripartite motif
TSP2	Thrombospondin 2
TSS	Transcription start site
VEGF	Vascular endothelial growth factor
WHO	World Health Organisation
γH2AX	Phosphorylated histone H2AX

Chapter 1

Introduction

1 Introduction

1.1 An overview

It is well established that adult stem cells contribute to tissue homeostasis and tissue regeneration in different organs due to their landmark capabilities: self-renewal and generation of mature progeny cells within a given tissue. Likewise, the existence of adult neural stem cells (aNSCs) is central to the persistence of adult neurogenesis and brain plasticity throughout life. In mammals, the fully developed central nervous system (CNS) comprises three differentiated neural cell types: neurons, astrocytes and oligodendrocytes. In adulthood, the production/replacement of these mature cells from aNSCs are essential for normal brain function as well as under hazardous conditions (e.g. injury). The maintenance of aNSCs pool, the production of desired cells and subsequent migration of cells to the destination in need are under tight control from both extrinsic and intrinsic programmes. Importantly, alterations of these normal processes give rise to disease, including brain cancer. The key hallmarks of brain cancer are the ability to proliferate indefinitely and to invade through the brain parenchyma. Interestingly, normal neural cells and brain cancer cells migrate through the same routes (myelin, vessels, soma), suggesting similar underlying mechanisms.

Key nuclear functions such as transcription and chromatin regulation are believed to play a crucial role in the orchestration of adult neurogenesis, and their deregulation can lead to brain tumourigenesis. In particular, our laboratory has a long-standing interest in an interchromatin subdomain called the Promyelocytic Leukaemia nuclear body (PML-NB), which has been implicated in various cellular functions as well as in tumour suppression. Notably, its essential component PML plays an important role in maintaining the stem cell pool in both normal and cancerous settings, indicating an oncogenic side of PML. Importantly, previous work from our group has implicated PML in regulation of cortex development via controlling cell cycle progression of NSCs, unravelling a novel role of PML in CNS neurogenesis and stem cell fate. Therefore, it was tempting to delineate its role in adult neurogenesis with potential implications for our understanding of brain tumour pathogenesis.

1.2 PML and PML-NB

The promyelocytic leukaemia (PML) protein was originally identified in acute promyelocytic leukaemia (APL) of the reciprocal chromosomal translocation at the breakpoint t (15; 17). This results in the juxtaposition of most of PML and the retinoic acid receptor α (RARα) gene coding sequences**,** generating the oncogenic PML-RARα fusion gene (de The et al. 1991; Kakizuka et al. 1991; Grimwade and Solomon 1997). The PML-RARα fusion protein is the main oncogene of APL (Grimwade and Solomon 1997; Melnick et al. 1999) (further discussed below). Structurally, PML belongs to the tripartite motif (TRIM) family of proteins (TRIM19), characterized by a really interesting gene (RING) domain, two zinc-finger motifs B-boxes and a coiled-coil (CC) domain (RBCC) (**Fig. 1.1A**) (Jensen et al. 2001; Reymond et al. 2001). TRIM protein members have been implicated in a number of biological and physiological processes, many of which are achieved through their ability to form high molecular weight complexes by homo-multimerisation or hetero-multimersation (Reymond et al. 2001; Borden 2002; Napolitano and Meroni 2012). Notably, the CC domain is responsible for the homo-multimerisation of TRIM proteins and is indispensable for the formation of high order protein complexes and subcellular compartments, both in the nucleus and in the cytoplasm (Reymond et al. 2001).

The human PML gene is located on chromosome 15q22, which consists of nine exons (Jensen et al. 2001). The N-terminal tripartite motif within exon 1 to exon 3 is highly conserved, while the C-terminal exons are subject to alternative splicing, resulting in seven PML isoforms (PML-I to PML-VII) (Jensen et al. 2001; Reymond et al. 2001). Most PML isoforms harbour nuclear localisation signal (NLS) in exon 6 (Condemine et al. 2006), which explains their predominant nuclear localisation. However, it has been reported that PML-I contains a nuclear export sequence (NES) in exon 9 (Condemine et al. 2006) and its cytoplasmic form exerts crucial functions. In particular, a

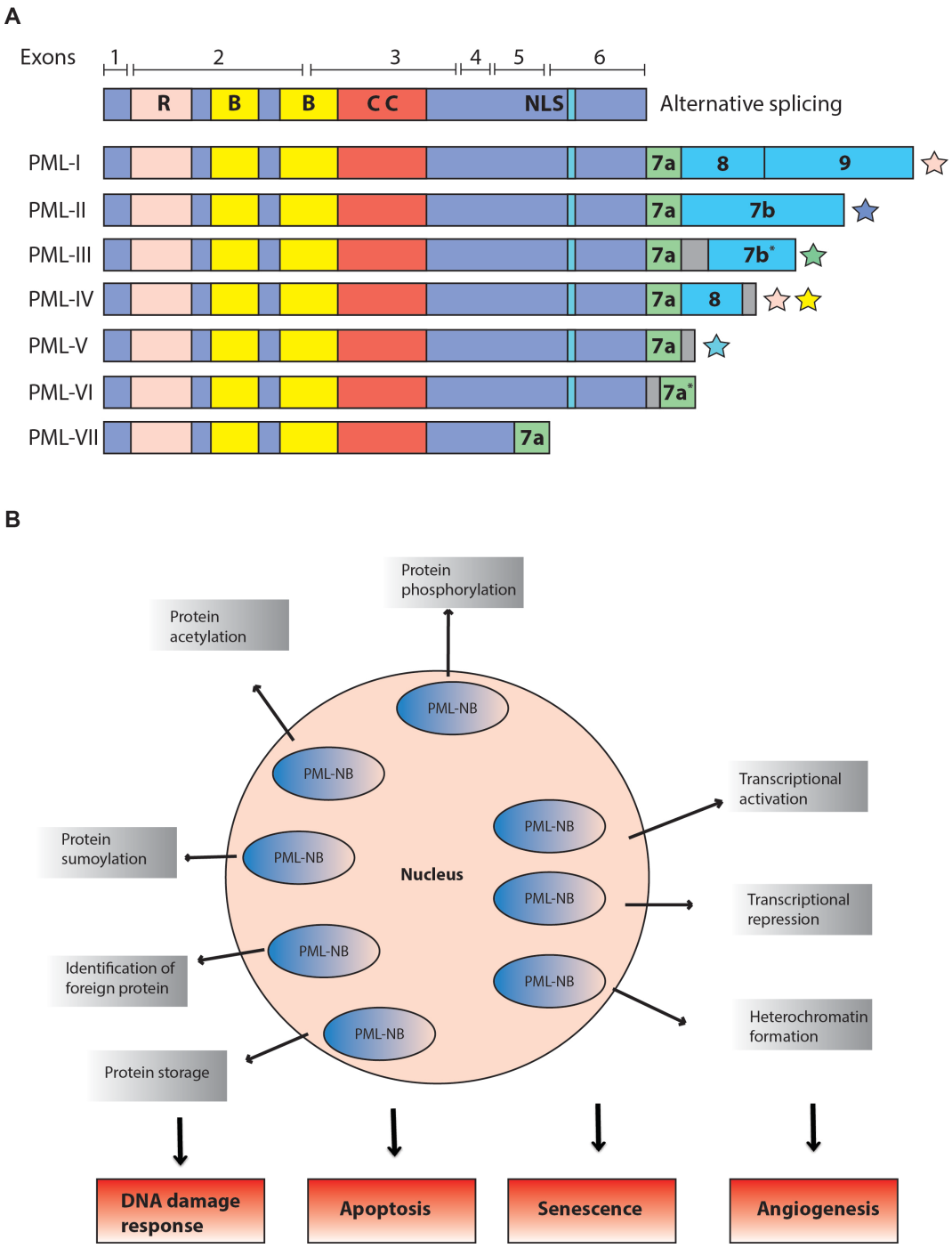

Figure 1.1: The PML protein isoforms and functional diversity of PML-NBs.

(A) Alternative splicing of PML C-terminus generates seven isoforms. All PML isoforms harbor the RBCC motif within the first three exons. A nuclear localisation signal (NLS) is located in exon 6 whereas PML-I harbors a nuclear export sequence (NES) in exon 9. (B) The many functions regulated by PML-NBs are categorized into: protein identification and storage, post-translational modification of proteins and regulation of nuclear activities. Many of these functions require recruitment of other proteins onto this nuclear hub. R, RING domain; B, B-box; CC, coiled-coil domain; NLS, nuclear localisation signal. Adapted from (Bernardi and Pandolfi 2007).

study has shown that PML cytoplasmic isoform is an essential modulator of transforming growth factor β (TGF-β) signalling (Lin et al. 2004; Salomoni and Bellodi 2007). Notably, among all the isoforms, PML-I is the most evolutionarily conserved as it shares high homology with murine isoforms. In addition, it is also the most abundant isoform *in vivo* (Condemine et al. 2006; Salomoni et al. 2008).

PML is the essential constituent of a nuclear domain of the interchromatin space (see **Table 1**) termed the PML-nuclear body (PML-NB). These macromolecular structures were also known previously as Kremer bodies, nuclear domains-10 (ND-10) and PML oncogenic domains (PODs) (Bernardi and Pandolfi 2007; Lallemand-Breitenbach and de The 2010). PML-NBs are nuclear spherical bodies, ranging from 0.3 to 1.0 μm in width and normally number 5-30 per cell in most mammalian cell types. However, the size and the number of PML-NBs depend on the cell type and cell cycle phase (Koken et al. 1995; Dellaire and Bazett-Jones 2004; Dellaire et al. 2006; Bernardi and Pandolfi 2007). PML contributes to formation of PML-NBs in part due to its RBCC domain. For instance, the RING motif has been reported to carry E3 ubiquitin ligase activity in the context of other proteins (Joazeiro and Weissman 2000; Meroni and Diez-Roux 2005; Deshaies and Joazeiro 2009; Ikeda and Inoue 2012; Metzger et al. 2012), but whether PML can act as an E3 ligase remains to be formally demonstrated. Irrespective of its putative enzymatic function, mutations in the PML RING domain disrupt PML-NBs formation *in vivo* potentially due to its role in mediating protein-protein interactions (Borden et al. 1995). Moreover, mutants in the zinc fingers called B-boxes disrupt PML-NBs *in vivo* but without affecting the multimerisation with wild-type PML *in vitro* (Borden et al. 1996). One mechanism by which B-boxes affect protein-protein interactions is via SUMOylation-dependent recruitment of PML-NB components (Zhu et al. 2005a) (further elaborated below). Additionally, the coiled-coil domain has been shown to be indispensible for PML-NBs formation and growth suppressor activity *in vivo* (Fagioli et al. 1998) (see also below).

Table 1: Summary of nuclear microdomains

Nuclear domain	Size (μm)	Number/cell	Major constituent
Nuclear speckle	0.8-1.8	25-50	SRSF1/2, Malat1
PML-nuclear body	0.3-1.0	5-30	PML
Paraspeckle	0.5	10-20	PSP1, p54nrb, Neat1
Polycomb body	0.3-1.0	12-16	Bmi1, Pc2
Nuclear stress body	0.3-3.0	2-10	HSF1, HAP
Cajal body	0.1-2.0	0-10	Coilin, SMN
Histone locus body	0.2-1.2	2-4	NPAT, FLASH
Nucleolus	0.5-8.0	1-4	RNA Pol I
Perinucleolar compartment	0.2-1.0	1-4	PTB, CUGBP
Clastosome	0.2-1.2	0-3	19S, 20S proteasome

***Adapted from (Mao et al. 2011)**

Phosphorylation and sumoylation are the two well-characterised post-translational modifications (PTMs) of PML (Chang et al. 1995; Duprez et al. 1999; Zhu et al. 2005a). For example, phosphorylation on Serine (Ser) and Tyrosine (Tyr) residues of PML (Chang et al. 1995) following stress conditions such as DNA damage contributes to PML-mediated tumour suppressive effects, for instance induction of apoptosis or sequestration of MDM2 (Yang et al. 2002). Importantly, sumoylation of PML is required for recruitment of essential components such as Sp100 and Death-associated protein 6 (DAXX) to PML-NBs (Ishov et al. 1999; Lallemand-Breitenbach and de The 2010). Indeed, the biogenesis of PML-NBs has been proposed as a multi-step event involving sumoylation: non-sumoylated PML proteins first dimerise via RBCC motif (coiled-coil domain) and subsequently multimerise to form primary PML-NBs. Following PML sumoylation, a higher order of protein structures is formed, resulting in recruitment of SUMO binding motif-containing/sumoylated partners to the SUMO binding motif/sumoylated PML to generate mature PML-NBs (Shen et al. 2006; Lallemand-Breitenbach and de The 2010) (see also below). It is important to note that the PML RING domain is required for PML

sumoylation, thereby generating PML-NBs (Shen et al. 2006), suggesting that PML may mediate its own sumoylation by acting as E3 ligase for SUMO.

1.2.1 Different roles of PML-NBs

As mentioned above, PML is believed to contribute to the recruitment of many proteins into PML-NBs either transiently or constitutively (Zhong et al. 2000; Shen et al. 2006), with functions including DNA damage response, apoptosis and tumour suppression (Shen et al. 2006; Lallemand-Breitenbach and de The 2010) (Alcalay et al. 1998; Ishov et al. 1999; Li et al. 2000; Bernardi and Pandolfi 2007) (**Fig. 1.1B** and further elaborated below). Notably, PML has been implicated in nuclear aggregate degradation (Janer et al. 2006), in particular those implicated in neurodegenerative polyglutamine (polyQ) disorders. One of the PML isoforms, PML IV, contributes to the formation of nuclear bodies associated with proteasomal subunits (reminiscent of clastosomes, see **Table 1**), which in turn recruit soluble mutant ataxin-7 and trigger its proteasome-dependent proteolysis (Janer et al. 2006).

Importantly, PML-RARα has been implicated in interacting directly or indirectly with chromatin remodellers (Hofmann & Salomoni 2016). For example, PML-RARα (through PML moiety) interacts with histone H3K9-specific methyltransferase SUV39H1 (Carbone et al. 2006), in which PML-RARα binding facilitates H3K9me3 establishment at the promoter of RARβ2, a well-established target of PML-RARα. Moreover, PML-RARα interacts with Polycomb repressive complex 2 (PRC2) components SUZ12, EED and EZH2 (see below **1.5.2** for more detailed discussion on PRC complexes) and recruits PRC2 to the RARβ2 promoter leading to increased H3K27me3 repressive mark levels (Villa et al. 2007). In addition, the chromatin modifier DAXX (Hollenbach et al. 2002; Kuo et al. 2005) interacts with PML-RARα and is believed to contribute to neoplastic transformation (Zhu et al. 2005a; Zhou et al. 2006). Interestingly, PML-RARα affects the chromatin state indirectly through modulating expression levels of histone demethylases, including JMJD3 and SETDB1, all of which are PML-RARα targets (Martens et al. 2010).

Notably, chromatin regulators have been found localised to PML-NBs. For instance, the histone acetyltransferase CREB binding protein (CBP) /p300 has

been proposed to be responsible for p53 acetylation through its localisation to PML-NBs (Pearson et al. 2000). Furthermore, the histone deacetylase I (HDAC I) and co-repressors c-Ski, N-CoR and mSin3A, have been reported to interact with PML, mediating transcriptional repression (Khan et al. 2001). Interestingly, PML positively regulates the expression of the stem cells factor Oct4 and is essential for an open chromatin state (more accessible) of the Oct4 promoter in stem cells in part by interacting with Brg1-dependent chromatin remodelling complex (BRGC) (Chuang et al. 2011). In addition, it has been reported that PML-NBs non-randomly associate with genomic regions where transcription is active and a histone-encoding gene cluster is strongly associated with PML-NBs in S phase (Wang et al. 2004b; Ching et al. 2005; Dellaire et al. 2006). Another study has shown that PML interacts directly with SATB1, and the two proteins colocalise within PML-NBs. Moreover, SATB1/PML complex binds to matrix attachment region (MAR) and regulates formation of chromatin-loop structures (P et al. 2007). Interestingly, as mentioned above, DAXX is a component of PML-NBs and it has been recently identified as a novel histone chaperone for the histone H3.3 variant (Drané et al. 2010; Lewis et al. 2010a; Michod et al. 2012; Salomoni 2013) (also discussed also below). Despite these studies, the precise role of PML and PML-NBs in chromatin remodelling still needs to be fully elucidated.

1.2.2 PML in cancer pathogenesis and stem cell / cancer stem cell regulation

PML exerts a *Yin and Yang* fashion in the context of cancer. PML was first identified as a tumour suppressor in APL, where its normal function is disrupted via the dominant negative effects of the PML-RARα fusion protein (de The et al. 1991; Kakizuka et al. 1991; Grimwade and Solomon 1997; Mazza and Pelicci 2013) (Note: I will not cover here retinoic acid signalling but I will be happy to discuss this during the viva). A number of studies have revealed that PML exerts a tumour suppressive effect through regulation of the p53 and pRb tumour suppressors downstream of oncogenic RAS (Alcalay et al. 1998; Fogal et al. 2000; Guo et al. 2000; Pearson et al. 2000; Salomoni and Pandolfi 2002; Vernier et al. 2011; Acevedo et al. 2016) and by suppressing PTEN-PI3K-Akt-mTOR pathway (Trotman et al. 2006; Song et al. 2008) (**Fig. 1.2**). Moreover,

mounting evidence suggests that PML expression is decreased or lost in several human cancers of multiple histologic origins, including lung cancer, prostate cancer, breast carcinoma, colon adenocarcinoma and nervous system tumours (Gurrieri et al. 2004; Dvorkina et al. 2016). Intriguingly, a recent study from our lab shows that low PML expression is strongly associated with tumour recurrence in neuroblastoma (Dvorkina et al. 2016). Mechanistically, the PML-I isoform (not PML-IV) contributes to tumour suppression via upregulation of thrombospondin-2 (TSP-2) to inhibit angiogenesis (Dvorkina et al. 2016). Furthermore, PML has also been implicated in antiviral response (Chelbi-Alix et al. 1995; Lavau et al. 1995; Chelbi-Alix et al. 1998; McNally et al. 2008; Geoffroy and Chelbi-Alix 2011). For instance, PML expression was induced by interferon along with the number and size of PML-NBs (Chelbi-Alix et al. 1995; Lavau et al. 1995; Chelbi-Alix et al. 1998). Of note, it has been proposed that viruses evade cellular resistance for viral infections by co-localising with PML and disrupt PML-NBs (Geoffroy and Chelbi-Alix 2011). Additionally, PML confers antiviral function by inducing p53-dependent apoptosis of infected cells (McNally et al. 2008). In this way, it has been proposed that PML eliminates infected cells as they are susceptible to oncogenic transformation.

Although many studies have suggested that PML works via regulating the localisation of nuclear factors to PML-NBs (e.g. p53 (Ferbeyre et al. 2000; Pearson et al. 2000; Bernardi and Pandolfi 2003; Louria-Hayon et al. 2003); **Fig. 1.2**), there is also evidence of PML-NB-independent mechanisms. For instance, PML regulates p53 stability via sequestration of Mdm2 in the nucleolus after cellular stress (i.e. DNA damage), challenging the canonical model by which PML regulates p53 and adding additional layer of complexity on PML in tumour suppression.

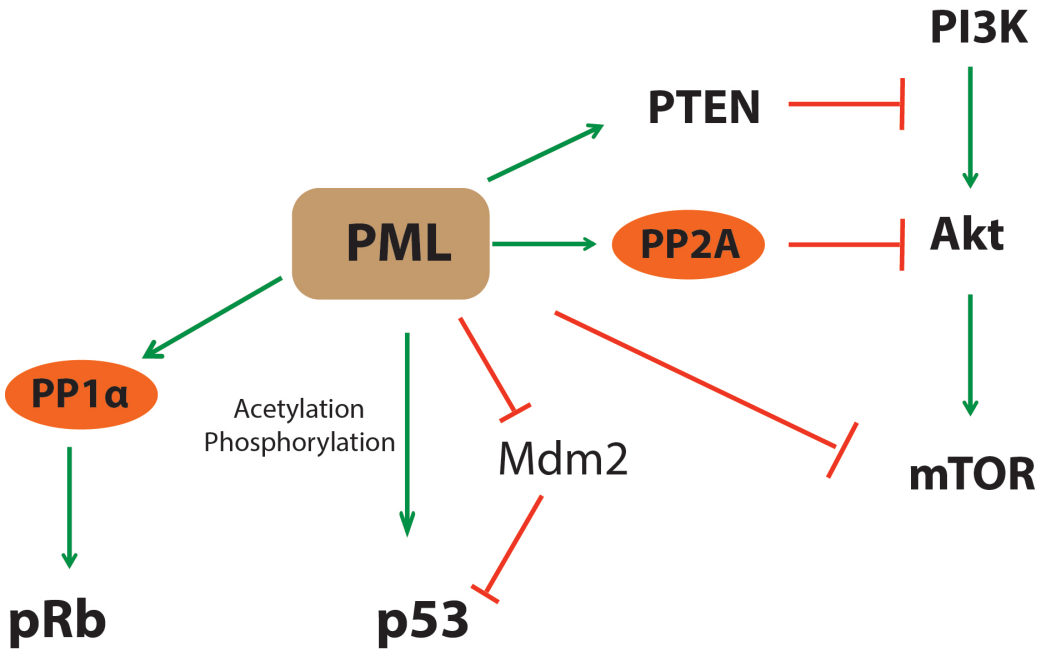

Figure 1.2: Role of PML in regulating cell growth and apoptosis pathways.

PML colocalises with pRb to the PML-NBs and activates pRb via PP1 α -dependent dephosphorylation, thereby preventing cell cycle progression. Conversely, PML loss leads to pRb hyperphosphorylation, thus inhibiting E2F binding capacity and subsequent growth suppressive effect. PML also recruits p53 to the PML-NBs and regulates p53 through post-translational modifications, including acetylation (Ser 15) and phosphorylation (Lys 382). In addition, PML indirectly regulates p53 stability via Mdm2 sequestration, thus preventing Mdm2-dependent p53 degradation. Finally, PML inhibits Akt via protein phosphatase 2 (PP2A)-mediated dephosphorylation of Akt as well as by inhibiting mTOR. Additionally, PML inhibits PI3K/Akt pathway through sustaining PTEN, which acts as an inhibitor of PI3K/Akt pathway. Adapted from (Salomoni et al. 2012).

Interestingly, there is also evidence supporting PML oncogenic functions within established tumours (Ito et al. 2008; Carracedo et al. 2012; Ito et al. 2012) in part by maintaining the stem cell/cancer stem cell (CSC) pool of chronic myeloid leukaemia (CML). Specifically, PML is highly expressed in hematopoietic stem cells (HSCs) and leukaemia-initiating cells (LICs) and contributes to their maintenance. Interestingly, rapamycin treatment restores the phenotypes observed in PML-deficient HSCs and LICs, indicating PML maintains HSCs and LICs pool by suppressing mTOR activity (Ito et al. 2008). In addition, a recent study suggests that PML maintains HSCs via promoting fatty acid oxidation (FAO) by regulating PPAR-δ. As a result, PML loss (or inhibition of PPAR-δ expression or FAO) results in symmetric stem cell division, leading to loss of HSCs self-renewal capacities and exhaustion of HSCs (Ito et al. 2012). More specifically, PML negatively regulates PPAR-δ coactivator 1A (PGC1A) acetylation and actively regulates PPAR signalling and FAO, which promotes ATP production. Interestingly, a similar pathway was shown to control breast cancer cells survival (Carracedo et al. 2012). Accordingly, PML expression in breast cancer is correlated with poor prognosis (Carracedo et al. 2012). In this respect, a previous study reported that PML controls mammary gland development, and its loss disturbs the balance of two distinct mammary luminal cell progenitor populations (Li et al. 2009b). It would be interesting to determine whether a similar FAO pathway (see above) is also involved in normal homeostasis and potential transformation in the mammary gland.

These studies suggest that PML may represent a potential therapeutic target in a number of human neoplasms. In this respect, APL patients treated with arsenic trioxide (As_2O_3) alone have up to 70% cure rate and this is due to As_2O_3-induced degradation of the oncogenic fusion protein PML-RARα (Lallemand-Breitenbach et al.). Intriguingly, it has been shown that this degradation is in part mediated by direct binding of As_2O_3 cysteine residues within the RBCC motif of PML and further triggering PML oligomerisation and enhanced sumoylation-induced degradation (Zhang et al. 2010). Of note, As_2O_3-induced production of reactive oxygen species (ROS) promotes PML oligomerisation, which leads to cysteine oxidation to promote formation of covalent disulphide bonds and further results in PML ubiquitylation and PML-NBs degradation (Jeanne et al. 2010; Zhang et al. 2010).

Collectively, these studies highlight the complex and multifaceted role of PML/PML-NBs in contributing to distinct cellular functions as well as in oncogenesis. Importantly, the emerging involvement of PML in stem cell biology has added another layer of complexity to its function (**Fig. 1.3**). On one hand, its targetting in cancer stem cells could limit tumour recurrence and/or resistance to therapy. On the other hand, increasing PML expression could be beneficial to support haematopoiesis as well as stem cell function in other tissues.

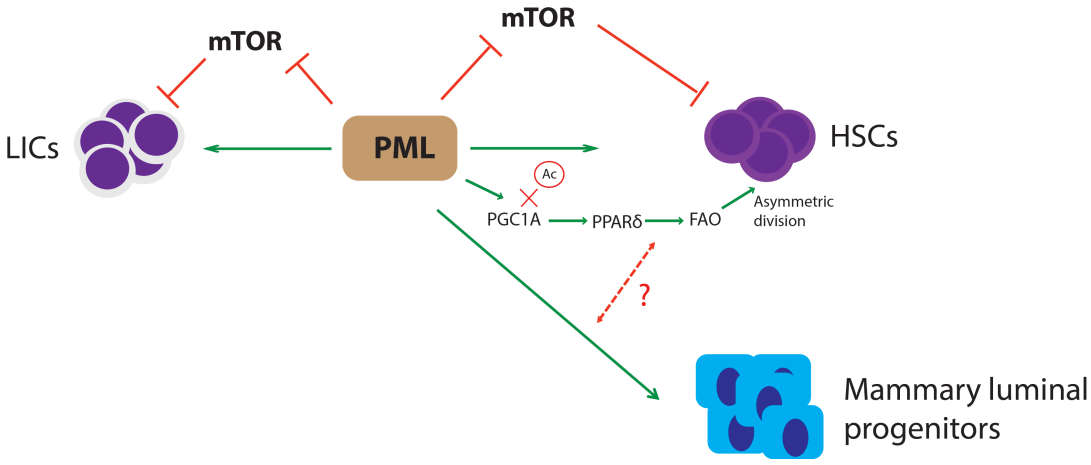

Figure 1.3: Emerging role of PML in stem cell/cancer stem cell maintenance.

PML facilitates the maintenance of both cancer and non-cancerous stem cells. More specifically, PML maintains hematopoietic stem cells (HSCs) and leukaemia-initiating cells (LICs) via inhibition of mTOR. Notably, PML also maintains HSCs through regulating metabolism, by which PML facilitates deacetylation of PGC1A and resulting in PPAR δ activation and fatty acid oxidation (FAO) to enhance ATP production. PPAR δ /FAO thus promotes asymmetric division of HSCs to repopulate the stem cell pool. PML also controls mammary gland development. It is unclear whether PML regulates mammary luminal progenitors through a similar metabolic pathway observed in HSCs.

1.3 Stem cells in adult tissues

Small populations of somatic stem cells are required for tissue homeostasis and tissue regeneration in different organs throughout life (Weissman 2000; Barker et al. 2010; Biteau et al. 2011). It has also been proposed a model whereby these subpopulation of cells represent units of evolution (Weissman 2000): based on this model, germline stem cells outcompete the “losers” for gonad niches in protochordate colonial tunicates and mice, and somatic hematopoietic stem cells (HSCs) in mice and humans also compete for bone marrow niches for clonal expansion (Weissman 2000; Weissman 2015). At the single cell level, stem cell are defined by their ability for self-renewal, which is to maintain/regenerate themselves over a long period of time, and the capability to differentiate into specialised cell types within respective tissues (Barker et al. 2010). Based on their potential to give rise to differentiated cell types, stem cells are classified hierarchically with descending order as: totipotent, pluripotent, multipotent, oligopotent and unipotent over developmental stages (Wagers and Weissman 2004), with unipotent cells only being able to generate one mature cell type. As such, adult stem cells are characterised by their abilities for self-renewal and multipotency. Contrary to the relatively quiescent stem cells, transit-amplifying cells, their direct progeny, are fast-cycling and will terminate as functional cells within the tissue after a limited rounds of cell division (Barker et al. 2010), with different kinetics/dynamics in physiological conditions versus in response to stimuli or injury (Charruyer et al. 2009). Importantly, the differentiation process needs to be tightly regulated as emerging evidence has shown that alterations of cell plasticity and cell fate/lineage specification due to oncogenic insult can lead to neoplastic transformation and cancer development (Hanahan and Weinberg 2011). In particular, the fact that stem cells persist longer than other cells together with their proliferative potential make them susceptible to accumulate mutations throughout life, which can trigger oncogenic transformation and eventually result in cancer development (Reya et al. 2001; Li and Neaves 2006). Several lines of evidence suggest the existence within established tumours (see also above) of a subpopulation of stem cell-like (cancer stem cells, CSCs) with the ability to self-renew, at least to partially differentiate to other cell types (tumour bulk) and disseminate and metastatise to distant

organs (Reya et al. 2001; Hanahan and Weinberg 2011; Nguyen et al. 2012). However, it is important to note that CSCs are not necessarily solely derived from transformation of normal stem cells, as restricted progenitor cells or mature cells may also become transformed to acquire the properties of CSCs (Reya et al. 2001).

1.4 NSCs and adult neurogenic niches

The existence of adult neural stem/precursor cells (aNSCs) in the mammalian brain has revolutionised our understanding of brain plasticity and has added an additional layer of complexity to brain functions (Reynolds and Weiss 1992; Bond et al. 2015). Like other somatic stem cells, NSCs are rare and exert the fundamental functions of stem cells: self-renewal and the ability to generate a heterogeneous cell progeny upon differentiation (multipotency) (Doetsch et al. 1999b; Gage 2000; Bond et al. 2015). Upon activation, aNSCs undergo two modes of division: symmetric division that generates either two aNSCs or two progenitor cells, or asymmetric division give rise to one aNSC to maintain the stem cells pool and one progenitor cell (Morrison and Kimble 2006). In particular, aNSCs are able to give rise to neurons, the functional building blocks of information transmission, and glia cells (astrocytes and oligodendrocytes), which support the normal functions of neurons (Nait-Oumesmar et al. 1999; Gage 2000; Picard-Riera et al. 2002; Menn et al. 2006; Gonzalez-Perez et al. 2009; Gage and Temple 2013; Ortega et al. 2013b; Lim and Alvarez-Buylla 2014; Xing et al. 2014; Bond et al. 2015).

In the adult mammalian brain, there are two main neurogenic niches where aNSCs are found (**Fig. 1.4A**): the subgranular zone (SGZ) of the dentate gyrus (DG) within the hippocampus and the subventricular zone (SVZ; also termed as subependymal zone, SEZ) lining the lateral ventricles in the forebrain (Zhao et al. 2008; Urban and Guillemot 2014). In brief, SGZ NSCs within the DG named radial glial-like cells (RGL, type B cells) generate intermediate progenitor cells (IPCs, type D cells), which in turn produce neuroblasts after a limited expansion. Newborn neuroblasts undergo tangential migration along the SGZ and eventually integrate as dentate granule neurons (type G cells) in dentate granule cell layer (van Praag et al. 2002; Ehninger and Kempermann 2008;

Urban and Guillemot 2014). With regard to SVZ NSCs, it has been proposed recently that slow-dividing embryonic radial glial cells (RGCs) are the source of SVZ aNSCs (Fuentealba et al. 2015; Furutachi et al. 2015). SVZ aNSCs (type B cells) are able to produce transit-amplifying progenitor cells (TAPs, type C cells) upon activation. After a few divisions, type C cells in turn generate migrating neuroblast cells (type A cells), which form a chain ensheathed by glial cells and migrate anteriorly through the rostral migratory stream (RMS) using a chain migration mechanism. Once they reach the olfactory bulb (OB), they then migrate radially, further develop and integrate into the existing neural circuits as local interneurons (Temple and Alvarez-Buylla 1999; Alvarez-Buylla and Garcia-Verdugo 2002). More specifically, newborn inhibitory interneurons develop into granule cells (GCs) and periglomerular cells (PGCs) located in the granule layer and glomerular layer, respectively (Kosaka et al. 1995; Carleton et al. 2003; Nagayama et al. 2014). Moreover, GCs and PGCs can be further divided into several subtypes. Based on their localisation in granule cell layers and the expression status of calcium-binding protein calretinin ($CalR^+$), GCs are subdivided into superficial GCs (superficial granule layer), deep GCs (deep granule layer) and $CalR^+$ GCs (Price and Powell 1970; Orona et al. 1983; Jacobowitz and Winsky 1991; Alvarez-Buylla et al. 2008). In terms of PGCs, there are $CalR^+$ PGCs, tyrosine hydroxylase-expressing (TH^+) dopaminergic PGCs and calbindin ($CalB^+$) PGCs (Kosaka et al. 1997; Parrish-Aungst et al. 2007; Alvarez-Buylla et al. 2008). The existence of these subtypes highlights the extensive heterogeneity and complexity of OB neurons. Of note, this continual SVZ-RMS-OB chain migration serves as the fundamental basis of production/replacement of OB neurons throughout life in rodents.

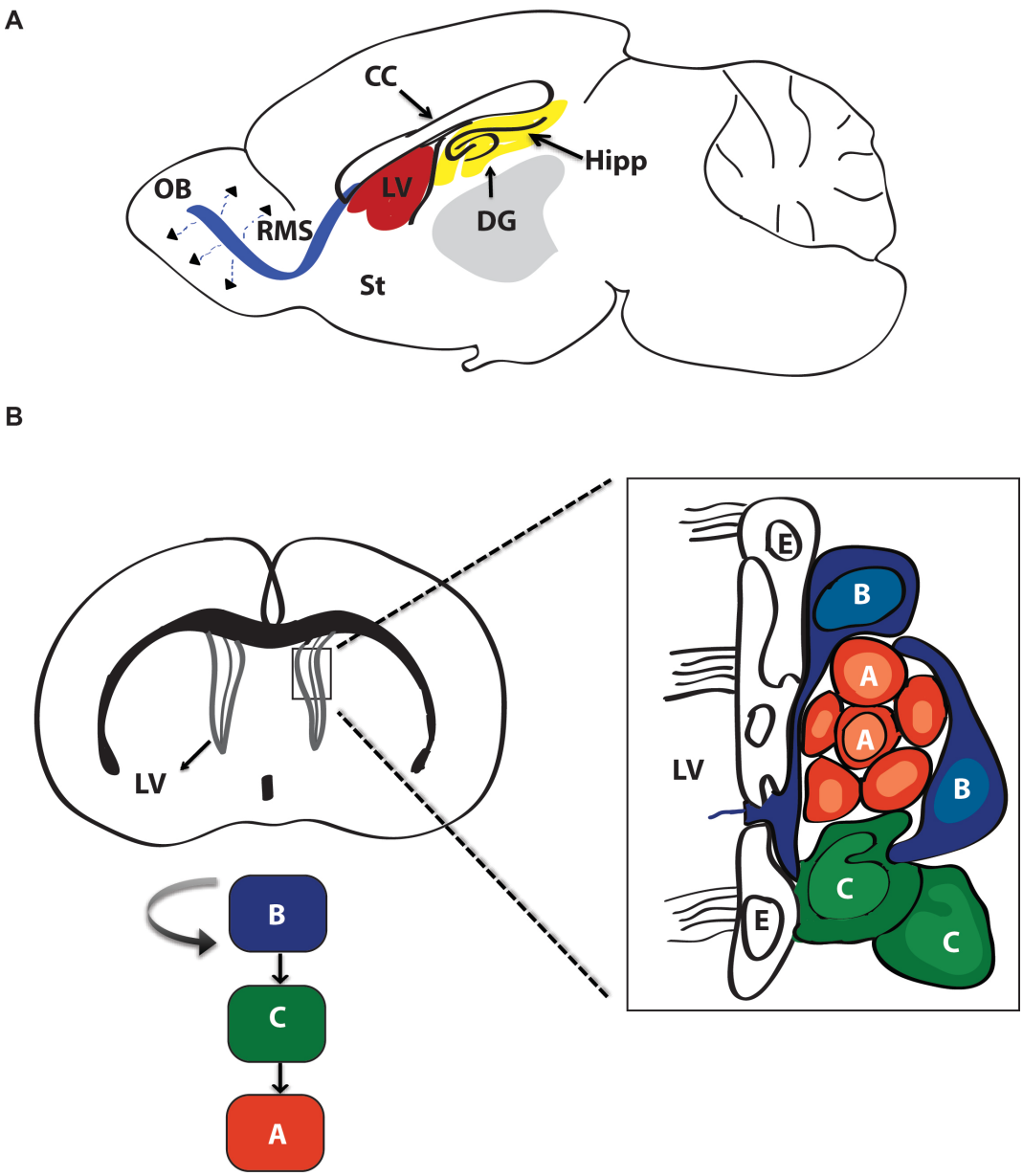

Figure 1.4: Neurogenic niches in adult mammalian brain and cytoarchitecture of the subventricular zone.

(A) A sagittal view of the two neurogenic niches in an adult mammalian brain, showing the subgranular zone (SGZ) along the dentate granule cell layer of the hippocampus and the subventricular zone (SVZ) in the forebrain lining the lateral ventricle. St, striatum; CC, corpus callosum; LV, lateral ventricle; OB, olfactory bulb; DG, dentate gyrus; RMS, rostral migratory stream; Hipp, hippocampus. Red: SVZ. Yellow: SGZ. (B) A coronal view of the organisation of the SVZ. Of note, ependymal cells have multiple cilia to contact the CSF where as type B1 cells make contact with CSF using single cilium. B, SVZ astrocytes; C, transit-amplifying progenitor cells; A, migrating neuroblasts. Adapted from (Alvarez-Buylla and Garcia-Verdugo 2002; Bond et al. 2015).

1.4.1 Rodent SVZ organisation/cellular composition

The organisation of SVZ and its cytoarchitecture provide the environmental support for NSCs within this niche (**Fig. 1.4B**). The SVZ is positioned next to the ependymal cell layer, which splits the SVZ from the ventricle cavity (Alvarez-Buylla and Garcia-Verdugo 2002; Zhao et al. 2008). The composition of cells within the SVZ display heterogeneity that can be defined based on their morphology and molecular markers (see **Table 2**): ependymal cells (E cells) separate SVZ from the ventricular space, which is filled with cerebrospinal fluid (CSF) and the astrocytic stem cells (type B1 cells) undergo asymmetric divisions to produce transit-amplifying progenitor cells (type C cells). Notably, E cells have multiple cilia to contact the CSF whereas B1 cells make connection with the ventricular space via a single cilium (Doetsch et al. 1999b; Alvarez-Buylla and Garcia-Verdugo 2002), resembling the neuroepithelial stem cells in the embryo (Cohen and Meininger 1987). Type C cells in turn give rise to migrating neuroblasts (type A cells), which are ensheathed by astrocytic type B2 cells thereby forming a cylindrical morphology. Of note, B2 cells do not connect to the CSF (Doetsch et al. 1999b; Imayoshi et al. 2008b; Bond et al. 2015). Thus, the adult SVZ in rodents can be subdivided into three compartments: layer I contains the ependymal cells and the apical astrocytic B cells; layer II contains the type C and type A cells in conjunction with the cell body of B cells; layer III is composed of basal B cells adjacent to blood vessels (Alvarez-Buylla and Garcia-Verdugo 2002; Bond et al. 2015).

Table 2: Cellular composition of SVZ and their molecular markers

Composition of SVZ	Molecular markers
Ependymal cells (E cells)	CD24; S100β; Nestin; Vimentin
Astrocytes (B1 cells)	CD133; GFAP; Nestin; Vimentin
Astrocytes (B2 cells)	GFAP; Nestin; Vimentin
Transit-amplifying progenitor cells (C cells)	Ascl1; Nestin; Dlx1
Neuroblasts (A cells)	DCX; PSA-NCAM; βIII-tubulin; Nestin

***Adapted from (Capilla-Gonzalez et al. 2015)**

It has been suggested that SVZ type B cells and type A cells are dividing in addition to type C cells (Lois and Alvarez-Buylla 1994; Menezes et al. 1995; Alvarez-Buylla and Garcia-Verdugo 2002). Moreover, there is evidence that type E ependymal cells function as neural stem cells *in vivo* and generate OB neurons (Johansson et al. 1999), although the stem cell nature of type E cells is being debated. These studies raise the question: what are the genuine aNSCs within SVZ? Interestingly, a study has shown that a mixture of B and C cells are capable to differentiate into A cells whereas no self-renewal of A cells was found when cultured *in vitro* (Lim and Alvarez-Buylla 1999; Alvarez-Buylla and Garcia-Verdugo 2002), suggesting A cells are not stem cells. Furthermore, another important study has shown that following the treatment of Ara-C, an antimitotic drug, C and A cells were eliminated. However, only the remaining B cells divide to repopulate C and A cells, indicating that SVZ B cells are indeed NSCs *in vivo*, further supported by the finding that they are able to grow as multipotent neurospheres *in vitro* (Doetsch et al. 1999a; Alvarez-Buylla and Garcia-Verdugo 2002).

As mentioned above, there are several OB neuron subtypes developed via the SVZ-RMS-OB route. Interestingly, it has been proposed that the heterogeneity of OB interneurons stems from the heterogeneity of the SVZ NSCs (Merkle et al. 2007; Alvarez-Buylla et al. 2008; Merkle et al. 2014). Particularly, the spatial organisation of NSCs within SVZ contributes to their multifaceted developmental potential. As mentioned earlier, aNSCs derive from embryonic RGCs (Fuentealba et al. 2015; Furutachi et al. 2015). Likewise, this conservation is also true with respect to the adult SVZ region and the developing lateral ganglionic eminence (LGE), as a common pattern of transcription factors is found expressed in both regions, including Ascl1 and Pax6 (Stenman et al. 2003; Parras et al. 2004; Guillemot 2005; Kohwi et al. 2005; Alvarez-Buylla et al. 2008).

Notably, a landmark study utilising adenovirus-expressing Cre recombinase system targeting neonatal brain has shown that RGCs from different regions within the SVZ give rise to distinct types of OB neurons *in vivo* (Merkle et al. 2007). For instance, the CalB^{+} PGCs are derived from ventrolateral SVZ, whereas dorsal subpallial SVZ predominantly give rise to superficial GCs. Intriguingly, this regional specification is shared by the aNSCs as aNSCs

generate similar OB neurons as RGCs targetted in the matching region (Merkle et al. 2007). Furthermore, grafting experiments relocating postnatal SVZ NSCs from one region to another demonstrate that SVZ NSCs possess regional specification and which is sustained in propagating cells *in vitro* (Merkle et al. 2007), indicating location-based plasticity is established at an early stage during development and is maintained after birth (Alvarez-Buylla et al. 2008). Another study has reported that this regional specification seems to be retained *in vitro* under a defined monolayer based cell culture system mimicking entire events during SVZ neurogenesis (Scheffler et al. 2005). Furthermore, a recent study has reported four previously unknown OB interneuron subtypes (type 1-4) that are derived from domains within the anterior ventral ventricular (V)-SVZ region, which accounts for less than 5% of the V-SVZ surface area. In addition, Nkx6.2^{+} and Zic^{+} aNSCs contribute to the generation of these interneuron subtypes, with their expression correlating with the spatial origin of these novel OB interneurons, indicating the complexity of aNSC heterogeneity even within restricted microdomains (Merkle et al. 2014). Collectively, these studies suggest that SVZ NSCs are not homogenous and they are the source of heterogeneous OB interneurons.

1.4.2 Regulation of SVZ aNSC self-renewal and entry into differentiation

As mentioned above, multipotent aNSCs should in theory be able to give rise to all the mature cell types, including neurons, astrocytes and oligodendrocytes. However, several recent studies challenged the multipotent nature of aNSCs (Bonaguidi et al. 2011; Ortega et al. 2013a; Bond et al. 2015; Calzolari et al. 2015). There is one study utilising *in vitro* live imaging and single-cell tracking of cultured mouse adult SVZ NSCs and revealed that these NSCs generate either oligodendrocytes or neurons, but never both (Ortega et al. 2013a). Another study using *in vivo* clonal labelling of individual adult SVZ NSCs and found that the self-renewal rate of aNSCs and the diversity of OB interneuron subtypes generated from aNSCs decline with age (Calzolari et al. 2015). In addition, one *in vivo* study combining clonal-tracing and fate-mapping techniques has shown that SGZ NSCs give rise to neurons and astrocytes only (Bonaguidi et al. 2011). Collectively, these studies suggest that endogenous aNSCs have limited differentiation potential. Intriguingly, it has been speculated

that aNSCs are indeed multipotent, however, the neurogenic niches may suppress their lineage specification potential (Bond et al. 2015). Evidence supporting this came from *in vitro* studies showing that aNSCs from both SGZ and SVZ are able to give rise to all the neural lineages (Reynolds and Weiss 1992; Palmer et al. 1997; Bond et al. 2015). However, SGZ aNSCs give rise to dentate granule neurons and astrocytes whereas SVZ aNSCs generate OB interneurons as well as corpus callosum oligodendrocytes *in vivo* (Bond et al. 2015), suggesting that neurogenic niches may shape the lineage specification potential of adult NSCs.

Indeed, the regulation of adult NSCs is orchestrated both extrinsically and intrinsically. Extrinsic cues from the niche have been reported to regulate aNSCs in a number of circumstances. For instance, E cells within the SVZ express Noggin, an antagonist of bone morphogenetic protein (BMP), to promote neurogenesis and neuronal differentiation by blocking endogenous BMP signalling (Lim et al. 2000). In addition, a recent study has shown that endothelial cells in the SVZ maintain aNSC quiescence by expression of ephrinB2 and Jagged1, which suppress cell-cycle progression and inhibit differentiation by inducing stemness genes. *In vivo* deletion of either gene results in aNSC depletion (Ottone et al. 2014). Another study has found that endothelial cells in mouse SVZ secrete neurotrophin-3, which is required for aNSC quiescence and maintenance (Delgado et al. 2014). Moreover, one study has shown that EGFR-expressing progenitor cells in mouse SVZ affect the number and self-renewal ability of aNSC via Notch signalling (Aguirre et al. 2010), reinforcing the importance of cell-cell interaction within the niche in regulation of aNSCs. Intriguingly, one study has reported that GDF11 found in the blood of young mice contribute to vascular remodelling and promotes an increase in SVZ aNSC number and neurogenesis, which is linked to an improvement in olfactory discrimination in aged mice (Katsimpardi et al. 2014). This study highlights the significance of extrinsic systemic circulating factors that are able to affect aNSCs.

Intrinsic programmes, such as transcription factor networks, underpin one of the most potent mechanisms involved in regulation of aNSC self-renewal and differentiation. For example, one study has shown that the SRY-box transcription factor 2 (Sox2) can be directly activated by arsenite-resistance

protein 2 (Ars-2) in order to promote aNSC self-renewal in adult SVZ (Andreu-Agullo et al. 2012), suggesting an overlapping transcriptional role of Sox2 in regulation of aNSC homeostasis in both SGZ and SVZ. Interestingly, another paper has found that the basic helix-loop-helix (bHLH) transcription factor Olig2 is expressed in SVZ aNSCs and is necessary to direct them toward astrocytic and oligodendrocytic differentiation patterns (Marshall et al. 2005). Another bHLH transcription factor, Ascl1, was found expressed in a subset of type B1 cells in SVZ and Ascl1 is known to be essential for neuronal and oligodendroglial specification (Schuurmans and Guillemot 2002; Parras et al. 2004; Kohwi et al. 2005). Moreover, Id1, also a bHLH family member, is highly expressed in B1 cells in adult SVZ. Of note, the level of Id1 seems to be crucial for aNSC self-renewal (Nam and Benezra 2009). Another transcription factor, FoxO3 has been reported to express in adult SVZ NSCs and have roles in preventing premature depletion of aNSCs thus contributing to aNSC maintenance (Renault et al. 2009). Finally, the orphan nuclear receptor Tlx has been reported to be expressed in adult SVZ B cells. Interestingly, Tlx ablation leads to complete abolishment of SVZ neurogenesis, indicating the crucial role of Tlx in adult SVZ NSCs homeostasis (Liu et al. 2008).

Importantly, cell cycle regulators have been implicated in regulation of SVZ NSC self-renewal and differentiation (Salomoni and Calegari 2010). For instance, it has been shown that depletion of cyclin-dependent kinase inhibitor (CDKi) $p21^{Cip1}$ results in SVZ NSCs exhaustion both *in vivo* and *in vitro*, suggesting $p21^{Cip1}$ is necessary for NSCs life-long maintenance (Kippin et al. 2005). Moreover, another recent paper has shown that $p21^{Cip1}$ negatively regulates Sox2 expression through directly binding to its enhancer, therefore regulating adult SVZ NSCs expansion (Marques-Torrejon et al. 2013). This study also highlights the crosstalk between transcription factors and cell cycle regulators, implicating a dynamic regulation network of intrinsic modulators.

1.4.3 Regulation of RMS migration

As mentioned above, the continual migration of newly generated neuroblasts from SVZ via RMS underpins OB neurogenesis. It has been reported that at E15 in rodents, cells expressing neuronal markers are beginning to line up in chains, exhibiting the hallmark of postnatal RMS (Pencea and Luskin 2003).

Once established, this route from SVZ to OB is a 5mm long journey and is maintained throughout adulthood (Lois and Alvarez-Buylla 1994; Doetsch and Alvarez-Buylla 1996). Notably, similar to SVZ aNSCs, this chain migration is subject to dynamic regulations by intrinsic and extrinsic factors. Intrinsic factors have been implicated in regulating cell morphology and motility during SVZ-RMS migration (Francis et al. 1999; Kappeler et al. 2006; Koizumi et al. 2006; Ocbina et al. 2006; Hirota et al. 2007; Mejia-Gervacio et al. 2011; Capilla-Gonzalez et al. 2015). For instance, cyclin-dependent kinase 5 (CDK5), a serine/threonine kinase, has been implicated in regulation of neuronal migration (Dhavan and Tsai 2001). CDK5 conditional deletion in mice results in irregular chain formation and impairments in orientation and speed of neuroblast migration, which leads to an accumulation of neuroblasts in SVZ and RMS (Hirota et al. 2007). Ion transporter NKCC1 has been implicated in cell size control through its regulation of cellular volume (Lytle and Forbush 1996; Strange 2004). Intriguingly, one study has shown that NKCC1 controls neuroblast migration in RMS in mice and its activity is required for normal migratory speed (Mejia-Gervacio et al. 2011). Another example is doublecortin (DCX), a microtubule-associated protein that is highly expressed in migrating neurons (Gleeson et al. 1999). An *in vitro* study has shown that DCX knockdown by RNA-interference reduced SVZ cell migration, while re-expression of DCX after knockdown rescued migration (Ocbina et al. 2006). Moreover, DCX deletion *in vivo* results in decreased RMS migration as cells migrate in a disorganised manner in association with bipolar morphology (Kappeler et al. 2006; Koizumi et al. 2006).

With regard to extrinsic programmes, mounting evidence has shown that multiple factors control RMS migration via cell-cell interaction and cell-extracellular matrix (ECM) interaction (Bonfanti et al. 1992; Yang et al. 1992; Tomasiewicz et al. 1993; Cremer et al. 1994; Hu et al. 1996; Peretto et al. 1997; Jacques et al. 1998; Mason et al. 2001; Hack et al. 2002; Emsley and Hagg 2003; Bonfanti 2006; Courtes et al. 2011; Mobley and McCarty 2011). As mentioned earlier, migrating neuroblasts are ensheathed by astrocytes termed gliotubes (Jankovski and Sotelo 1996; Peretto et al. 1997; Alvarez-Buylla and Garcia-Verdugo 2002). Although it has been reported that the chain migration is independent of astrocytes (Wichterle et al. 1997), these astrocytes may

secrete factors that facilitate neuroblast migration as well as provide pro-survival and directional guidance to migrating neuroblasts (Mason et al. 2001; Alvarez-Buylla and Garcia-Verdugo 2002), highlighting the importance of cell-cell interaction in the RMS. In addition, the polysialylated form of neural cell adhesion molecule (PSA-NCAM) has been reported to be expressed in migrating neuroblasts throughout RMS (Bonfanti and Theodosis 1994; Bonfanti 2006). Notably, PSA-NCAM has been implicated in providing intercellular space between migrating neuroblasts and the ensheathed astrocytic gliotubes to stimulate their movement (Yang et al. 1992; Hu et al. 1996). Importantly, NCAM mutant (loss of NCAM-180, the long cytoplasmic domain) shows a decrease in RMS migration (Ono et al. 1994), and PSA-NCAM-deficient mice exhibit a reduction in overall brain weight and a profound decrease in OB size (Cremer et al. 1994).

The cell-ECM interaction also contributes to the establishment of a pro-migratory environment in RMS. For example, the transmembrane receptors integrins mediate interactions between the cytoskeleton and the extracellular matrix (Hynes 2002). Ablation of integrin β8 in mice results in aberrant chain migration and a reduced OB (Mobley and McCarty 2011). In addition, α6β1 integrin has been shown to be essential for chain migration (Jacques et al. 1998; Emsley and Hagg 2003). Furthermore, the ECM glycoprotein Reelin, functions as a detachment signal in the postnatal mouse brain. Specifically, cells detach from Matrigel in response to addition of exogenous Reelin, whilst in a Reelin mutant line, where secretion of the protein is impaired, the switch from tangential chain migration to radial migration in OB is abolished (Hack et al. 2002).

Another part of this dynamic regulatory network is the presence of soluble factors and secreted proteins that act as chemoattractant or chemorepellent signals during RMS migration. The secreted protein Sonic hedgehog (Shh) displays various types of functions during development (Ingham and McMahon 2001; Varjosalo and Taipale 2008), such as regulation of cell proliferation and differentiation. Interestingly, several studies have shown that in the adult mouse brain, Shh functions as chemoattractant in the context of chain migration (Angot et al. 2008; Hor and Tang 2010; Ihrie et al. 2011). In this respect, migrating neuroblasts in SVZ-RMS express Shh receptor Patched,

and blockage of Shh signalling impairs neuroblast migration (Angot et al. 2008). Another example is the family of Netrin proteins, which regulate axon guidance in the developing nervous system (Kennedy et al. 2006). A recent study has shown that deletion of the Netrin receptor Neogenin, leads to accumulation of neuroblasts in the RMS accompanied by decreased migration to the OB, an effect that has been recapitulated *in vitro* (O'Leary et al. 2015). Importantly, the axon guidance regulators and chemorepellent Slits (Slit1-Slit3) and their receptors Robo proteins (Robo1-Robo4) (Brose et al. 1999; Long et al. 2004) have been implicated in CNS cell proliferation and RMS migration (Hu 1999; Wu et al. 1999; Nguyen-Ba-Charvet et al. 2004; Kaneko et al. 2010; Borrell et al. 2012; Blockus and Chedotal 2014) (further discussed in the Results chapters). In particular, Slit1 and Slit2 are found expressed in the adult septum and have roles in orientating and inhibiting SVZ cell migration (Nguyen-Ba-Charvet et al. 2004). Collectively, these studies highlight the crucial roles of intrinsic and extrinsic factors in controlling cell migration in the adult SVZ-RMS-OB route.

1.4.4 Migration upon injury

It has long been believed that OB is the only destination for SVZ-RMS migration in adult rodents (Alvarez-Buylla and Garcia-Verdugo 2002). Intriguingly, there is evidence suggesting that migrating neuroblasts persist in RMS even after elimination of OB (Kirschenbaum et al. 1999), indicating that OB is not essential for RMS migration. Another study has revealed additional migratory pathways in which young neurons migrate from the SVZ to different forebrain areas, including cortex, striatum and nucleus accumbens (Inta et al. 2008), suggesting the capability of these cells to migrate across the brain parenchyma in addition to the RMS/OB route. In this respect, there is a large body of literature proposing that SVZ-derived neuroblasts are able to migrate to injury sites and subsequently conduct repair processes in the adult brain (Arvidsson et al. 2002; Goings et al. 2004; Imitola et al. 2004; Sundholm-Peters et al. 2005; Liu et al. 2006a; Yamashita et al. 2006; Nait-Oumesmar et al. 2007; Del Carmen Gomez-Roldan et al. 2008; Kojima et al. 2010; Otero et al. 2012; Kang et al. 2013; Capilla-Gonzalez et al. 2014). Importantly, this aberrant migration upon injury is regulated by variety of different factors. For instance, a

number of growth factors have been implicated in this migration, including fibroblast growth factor-2 (FGF-2) (Lachapelle et al. 2002), epidermal growth factor (EGF) (Sundholm-Peters et al. 2005), insulin-like growth factor-1 (IGF-1) (Yan et al. 2006) and vascular endothelial growth factor (VEGF) (Wang et al. 2007). Additionally, cytokines/chemokines also contribute to the recruitment of migrating cells to the damage sites upon injury (Imitola et al. 2004; Jaerve and Muller 2012; Capilla-Gonzalez et al. 2015). For example, following injury, SVZ neurogenesis is increased, and stromal cell-derived-factor-1 alpha (SDF-1) directs newly generated neurons migrate into the injury site (Imitola et al. 2004; Capilla-Gonzalez et al. 2015). Moreover, ECM-associated proteins have been found to function in injury-induced migration (Barkho et al. 2008; Courtes et al. 2011). For example, matrix metalloproteinases (MMPs), which are known to regulate ECM remodelling during development (Vu and Werb 2000) have been implicated in injury-induced migration. In particular, a study has reported that in response to injury-induced factors (SDF-1 and VEGF), MMP-3 and MMP-9 are upregulated in neuroblasts mediating their migration, whereas blockage of either MMP-3 or MMP-9 impairs the differentiation capacity of aNSCs as well as the injury-induced migration (Barkho et al. 2008). Furthermore, one study has found that the ECM glycoprotein Reelin is upregulated in damaged sites, triggering the redirection of neuroblasts from RMS to the injury site (Courtes et al. 2011).

Importantly, there is also evidence that aNSCs themselves can migrate to the site of injury (Faiz et al. 2015). In particular, in response to endothelin-1 and pial vessel disruption-induced stroke in the cortex, neurospheres with extended self-renewal capacity could be derived from the SVZ as well as from the site of injury in the cortex, but not from the uninjured cortex. Of note, NSCs isolated from the site of injury originated from SVZ aNSCs. In this respect, the same study provided some evidence that SVZ aNSCs themselves migrate to the site of injury and give rise to reactive astrocytes that facilitate scar formation and they could be converted into neurons by forced Ascl1 expression (Faiz et al. 2015). This study sheds light on the intrinsic migratory ability of SVZ aNSCs upon injury.

Collectively, these studies highlight the complexity of adult SVZ neurogenesis and in particular how two highly interconnected processes, differentiation and

migration contribute to continuous generation of neural cells during the lifespan of rodents in both physiological settings and upon injury.

1.4.5 Human vs Rodent SVZ

Given the plasticity of SVZ NSCs in rodents, it was tempting to investigate if this niche and the migration route are comparable in human, which may shed light on potential therapeutic strategies aimed at promoting tissue repair upon injury or in pathological conditions caused by neuronal loss (Trounson and McDonald 2015). However, the characterisation of adult human SVZ has revealed a considerable degree of difference compared to rodents (**Fig. 1.5**) (Quinones-Hinojosa et al. 2006; Gonzalez-Perez 2012). As described earlier, based on the spatial organisation and cellular compartment, the adult SVZ in rodents can be segregated into three layers. Intriguingly, using intraoperative and postmortem samples, it has been shown that the cytoarchitecture of the human SVZ is different from the mouse SVZ (Quinones-Hinojosa et al. 2006; Gonzalez-Perez 2012) and there are four layers: layer I contains ependymal cells; layer II is predominantly devoid of cells, generating a hypocellular gap; layer III is composed of a ribbon of astrocytes and layer IV is characterised as a transitional area adjacent to the brain parenchyma.

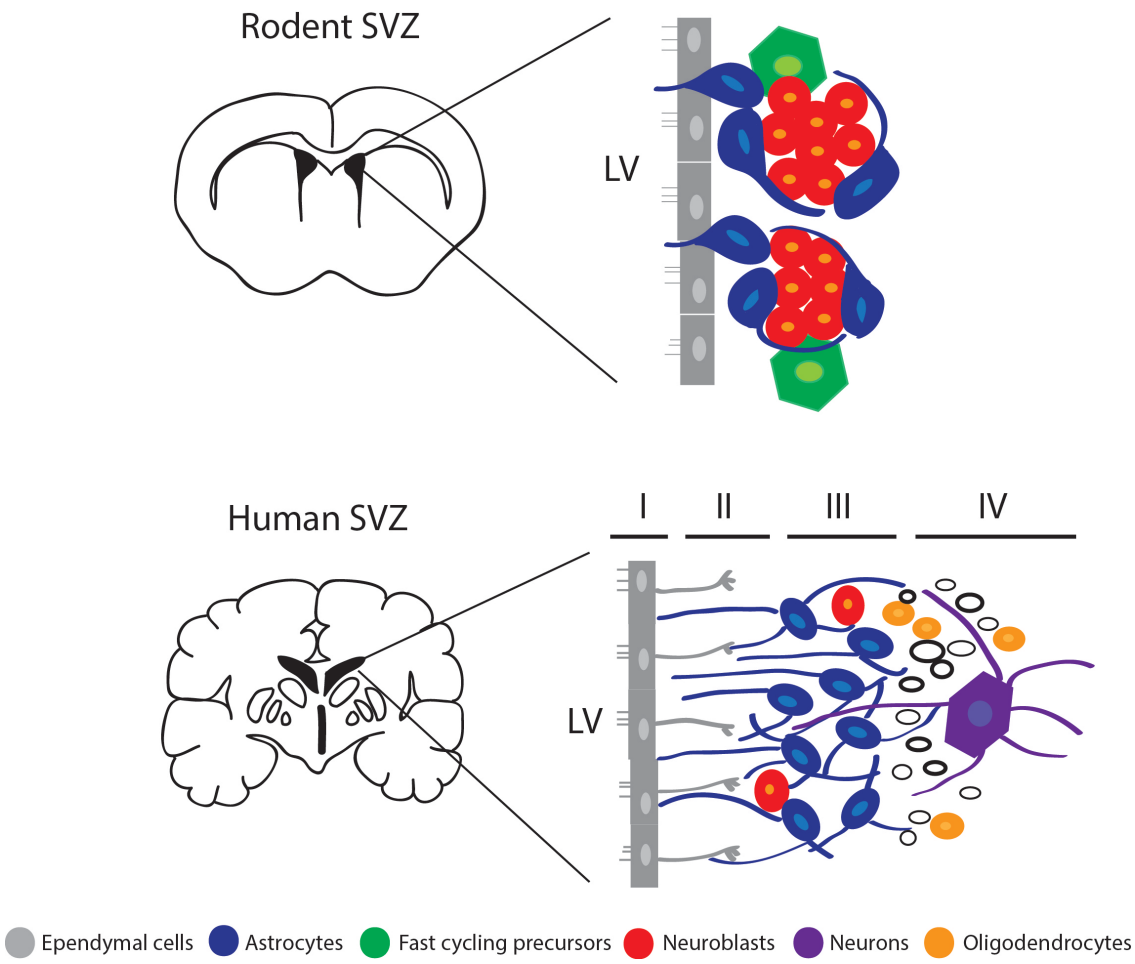

Figure 1.5: Cytoarchitecture of rodent and human SVZ.

Schematic representation of coronal views of rodent and human SVZ. LV, lateral ventricle; SVZ, subventricular zone. Note that unlike rodent SVZ, in human SVZ there is a hypocellular layer, layer II, which separates the astrocytes ribbon layer III from the ependymal layer I. Adapted from (Capilla-Gonzalez et al. 2014).

Although extensive studies have well documented the existence of adult human DG neurogenesis (von Campe et al. 1997; Eriksson et al. 1998; Sahay and Hen 2007; Spalding et al. 2013), with regard to adult SVZ neurogenesis and RMS migration, a number of studies have drawn controversial conclusions. While some groups have reported adult neurogenesis/chain migration in the human brain (Curtis et al. 2007; Wang et al. 2011), there is a lack of strong evidence to support the existence of human SVZ-RMS-OB neurogenesis (Sanai et al. 2004; Quinones-Hinojosa et al. 2006; Sanai et al. 2011). Moreover, a recent study utilised carbon dating technique to investigate cell turnover rate in human OB and failed to provide evidence supporting the existence of neurogenesis in human OB (Bergmann et al. 2012). However, a subsequent study has reported the generation of striatal neurons from human SVZ and that this integration route into the striatum is devoid in rodents (Ernst et al. 2014), suggesting the existence of adult stem cells in the human SVZ. It is important to highlight that there is evidence suggesting that neuroblast-like cells (PSA-NCAM^{+}) exist in human infant SVZ (less than one year old) (Weickert et al. 2000). Furthermore, another paper has shown that a marked rostral extension of neuroblasts of the lateral ventricle in human foetal brain was observed (Guerrero-Cazares et al. 2011). Of note, these migrating neurons appear to be developmental-dependent, where they persist in RMS in infants but gradually decrease with maturation (Sanai et al. 2011). Thus it has been proposed that chain migration is a transient process that only takes place during infant development in humans (Quinones-Hinojosa et al. 2006).

Taken together, these studies suggest that aNSCs are present in both humans and rodents, but there are substantial differences in their capacity to differentiate depending on whether they are located in the SVZ or DG. Further research into this area is needed.

1.5 Epigenetic mechanisms controlling neurogenesis

During development, multicellular organisms require tight control on gene expression to achieve their biological and physiological tasks. At the cellular level, gene expression is controlled via coordination of various intrinsic and extrinsic stimuli that are pivotal for the establishment of the appropriate cellular

identity (Levine and Davidson 2005; Alberts 2008). Aberrant gene expression contributes to a number of pathological conditions, including cancer (Hanahan and Weinberg 2011). Control of gene expression is exerted by transcription factors in association/coordination with a number of epigenetic mechanisms regulating chromatin function and structure. By definition, epigenetics is the study of heritable changes in gene expression that do not involve alteration in DNA sequence (Jaenisch and Bird 2003; Felsenfeld 2014). To date, several epigenetic mechanisms have been identified, including DNA and histone modifications, chromatin remodelling and non-coding RNAs-mediated regulation (Jaenisch and Bird 2003; Piunti and Shilatifard 2016) (further elaborated below). Among such mechanisms, histone modifiers, in particular, the Polycomb group (PcG) proteins have been extensively studied in the context of stem cell biology (Sparmann and van Lohuizen 2006; Aloia et al. 2013) and play key roles during neurogenesis (Hirabayashi and Gotoh 2010; Ma et al. 2010; Aloia et al. 2013; Yao et al. 2016) (see below). I will now summarise research in this area and then focus on mechanisms that are relevant to my thesis work.

1.5.1 Histone modifications

Genetic information in eukaryotes is compacted into chromatin (**Fig. 1.6A**). The basic building block of chromatin is termed the nucleosome, where four core histones, H2A, H2B, H3 and H4, assembly into an octamer which is wrapped around by a superhelix that consists of 147bp DNA (Kornberg 1974; Kornberg and Thomas 1974; Kouzarides 2007). This DNA-histone structural unit is essential for modulating and storaging genetic information. Histones are highly conserved from yeast to mammals and they are involved in a number of cellular and molecular programmes, including DNA replication, recombination, repair and importantly, transcription regulation (Bottomley 2004; Kouzarides 2007; Felsenfeld 2014). Histones modulate DNA accessibility either by relaxing chromatin into euchromatin (less condensed, more accessible) or by promoting chromatin aggregation into heterochromatin (highly condensed, inaccessible) (Felsenfeld and Groudine 2003; Bottomley 2004; Kouzarides 2007). Notably, a number of covalent modifications/PTMs regulate chromatin organisation by modifying specific amino acids within the N-terminal tail of core histones,

including phosphorylation, acetylation, methylation, sumoylation, ubiquitylation, deamination, ADP ribosylation and proline isomerisation (Kouzarides 2007). It has been postulated that histone modifications affect transcription by modulating physical histone/DNA interaction as well as by recruiting non-histone 'reader' proteins with various functions ranging from chromatin remodelling to further histone modifications (Li et al. 2007). Moreover, increasing evidence suggest that alterations of chromatin structure contribute to transformation and malignancy through deregulated gene expression and genome instability (Esteller 2007).

Regulation of histone acetylation by histone acetyltransferases enzymes (HATs) and histone deacetylase enzymes (HDACs) (Marks et al. 2001; Roth et al. 2001) represents a well-documented example of how histone modifications associate with different transcriptional states. Specifically, histone lysine acetylation is associated with transcription activation since this modification neutralises the basic charge of lysine and further destabilises the structure of chromatin in order to promote transcription (Allfrey 1966; Tse et al. 1998; Zheng and Hayes 2003). Conversely, transcriptional repression is correlated with histone lysine deacetylation since hypoacetylation leads to reduced accessibility to transcription factors (Nan et al. 1998; de Ruijter et al. 2003; Kouzarides 2007). In addition, evidence also supports that both HATs and HDACs have target substrates that are non-histone proteins, including the transcription factors p53, E2F, TFIIE, TFIIF and GATA1 (Khochbin et al. 2001; Marks et al. 2001; Roth et al. 2001; de Ruijter et al. 2003).

Another well-studied covalent modification is methylation. Histone methylation on specific lysine site is mediated by a number of "writers": lysine methyltransferases (KMTs) and is reversibly removed by the "erasers": lysine-specific demethylases (KDMs) (Zhang and Reinberg 2001). Interestingly, in contrast to other modifications such as histone acetylation/deacetylation, histone methylation was long believed to be an irreversible mark until the discovery of lysine specific demethylase 1 (LSD1) (Shi et al. 2004), which facilitates the removal of mono- and di-methyl marks. Importantly, unlike other modifications, histone lysine methylation results in more complicated consequences, as lysine is susceptible to be added from one methyl group up to three methyl groups (Margueron and Reinberg 2011). Hence, gene

activation or repression can be marked by the level as well as the site of lysine methylation. For instance, actively transcribed genes are associated with trimethylation on H3K4 and H3K36 whereas repressed genes are enriched for trimethylation on H3K9 and H3K27 (Martin and Zhang 2005; Kouzarides 2007). However, the presence of active or repressive histone methylation marks is not simply a binary state, as evidence has shown that many genes display occupancy of both marks (Bernstein et al. 2006; Voigt et al. 2013). In this respect, the “bivalent status” of certain genomic regions is believed to be essential during development as it maintains the genes in a poised state, rendering them ready for activation if necessary. It is important to note that more evidence is required to establish the concept of bivalency as it has been challenging to prove that the two antagonist modifications are present in the same cell and same gene.

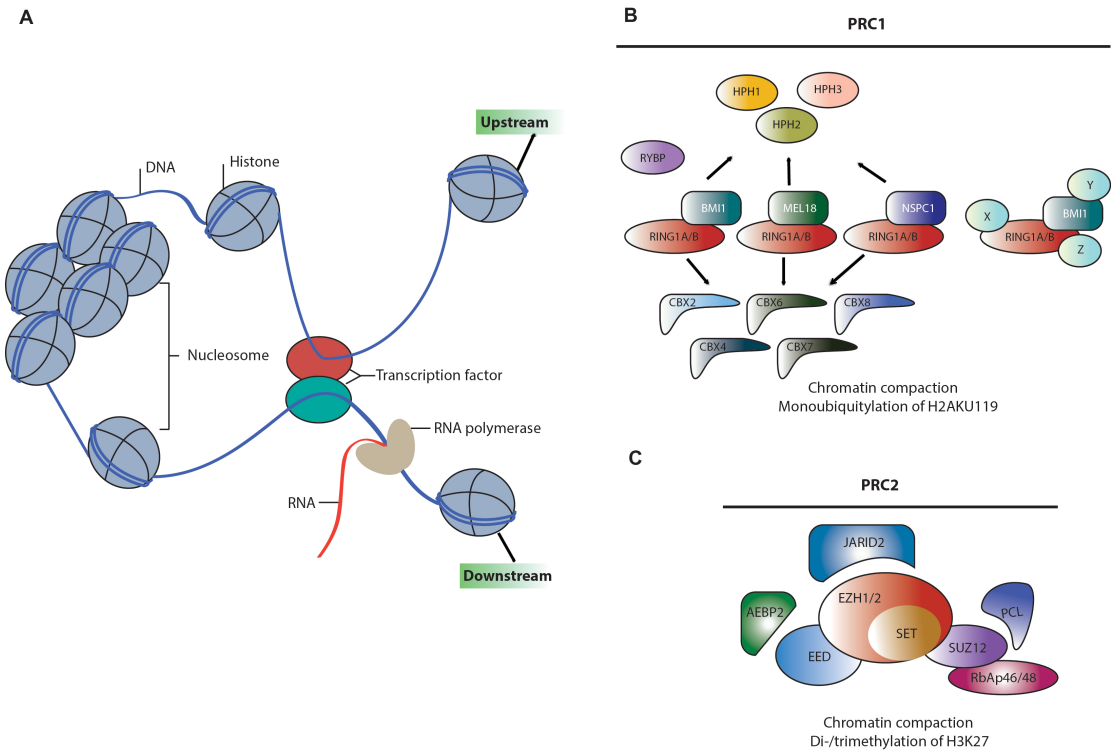

Figure 1.6: Schematic views of chromatin organisation and composition of Polycomb Repressive Complexes PRC1 and PRC2.

(A) Illustration of chromatin organisation in the eukaryotic nucleus. Nucleosomes are the major protein components of chromatin; comprising two copies of the core histones: H2A, H2B, H3 and H4 to form the octamer with ~147bp DNA wrapped around. This highly compact organisation is key to genetic information storage and gene regulation. (B) Composition of PRC1. Ring1a and Ring1b are two core components of PRC1 and they function as E3 ubiquitin ligase to establish H2AK119Ub. Bmi1 has been implicated in regulation of stem cell development. (C) Composition of PRC2. EZH1/2 are responsible for di-/trimethylation of H3K27. Notably, Jarid2, Aebp2 and Pcl are newly identified PRC2 components. Adapted from (Margueron and Reinberg 2011; Yao et al. 2016).

1.5.2 Polycomb Repressive Complexes

The Polycomb group (PcG) proteins are multiprotein complexes that exhibit histone methyltransferase activity (Muller et al. 2002; Blackledge et al. 2014; Piunti and Shilatifard 2016). The *Polycomb* (*Pc*) was originally identified in *Drosophila* and encodes a repressor required for proper body segmentation (Lewis 1978). It is now well established that PcG proteins are highly conserved from *Drosophila* to mammals (Levine et al. 2002; Margueron and Reinberg 2011; Aloia et al. 2013) and they function as "gene silencers" during development to maintain the repression state of key genes (Boyer et al. 2006; Sparmann and van Lohuizen 2006; Aloia et al. 2013). Together with their functional antagonist Trithorax group (TrxG) proteins, which maintain/activate gene expression, these two groups of proteins are essential for the maintenance of proper gene expression pattern during development and throughout adulthood (Schuettengruber et al. 2007). In mammals, there are two well-characterized families of PcG proteins, the Polycomb Repressive Complex 1 (PRC1) and PRC2 (Sparmann and van Lohuizen 2006; Aloia et al. 2013). Moreover, another two families have been identified in *Drosophila*, including Polycomb Repressive Deubiquitinase (PR-DUB) and PHO Repressive Complex (PhoRC) (Klymenko et al. 2006; Scheuermann et al. 2010).

The distinct components of PRC1 and PRC2 facilitate their role in histone modifications as well as in gene repression (Sparmann and van Lohuizen 2006). The composition of PRC1 is diverse (**Fig. 1.6B**), with two core components Ring1a/b together with Bmi1, Nspc1 or Mel18 (Whitcomb et al. 2007; Aloia et al. 2013). Ring1a and Ring1b function as E3 ubiquitin ligases that facilitate histone H2A monoubiquitylation at lysine 119 (H2AK119Ub) (Wang et al. 2004a). Other constituents, for example, Bmi1 and Mel18 are known to modulate enzyme activity of PRC1 (Brunk et al. 1991; Kanno et al. 1995; Aloia et al. 2013). Notably, PRC1 can be grouped into canonical PRC1 or non-canonical PRC1 based on the presence or absence of Cbx proteins (Gao et al. 2012; Aloia et al. 2013; Blackledge et al. 2014). Functionally, canonical PRC1 is able to bind H3K27me3 marks deposited by PRC2 via Cbx proteins whereas non-canonical Rybp-containing PRC1 can be recruited to specific unmethylated CpG island through its subunit Kdm2b (Garcia et al.

1999; Farcas et al. 2012; Gao et al. 2012; Hisada et al. 2012; Tavares et al. 2012; Aloia et al. 2013; He et al. 2013; Wu et al. 2013; Blackledge et al. 2014).

The PRC2 complex is more conserved through evolution, from *Drosophila* to mammals (**Fig. 1.6C**), consisting of EED, EZH1/2, SUZ12 and RbAp46/48 subunits (Whitcomb et al. 2007; Margueron and Reinberg 2011). Notably, SUZ12 is required for the stability of the EZH2 catalytic subunit (Cao and Zhang 2004; Pasini et al. 2004). Additionally, Jarid2, Aebp2 and Pcl1/2/3 have been recently identified as PRC2 components, by their interaction with other PRC2 components as well as their capabilities to modulate PRC2 enzyme activity (Cao and Zhang 2004; Nekrasov et al. 2007; Peng et al. 2009; Li et al. 2010; Margueron and Reinberg 2011).

Gene silencing by PRC1 and PRC2 is achieved in part through their modifications of histones. PRC1 facilitates histone H2A monoubiquitylation at lysine 119 (H2AK119Ub) through ubiquitin ligases Ring1a and Ring1b, whereas PRC2 di- and tri-methylate lysine27 of histone 3 via EZH1 and EZH2 (Lund and van Lohuizen 2004; Kouzarides 2007). Interestingly, a study suggests a progressive H3K27 methylation pattern, where H3K27me3 is derived from monomethylation of H3K27me2 (Zee et al. 2010). In addition, a recent study has shown that PRC1 (Ring1b) is able to repress gene expression by chromatin compaction, but independently of its enzymatic activity (Eskeland et al. 2010). Of note, PRC1 and PRC2 activities have been reported to be interdependent. Specifically, H3K27me3 deposited by PRC2 serves as a docking site for PRC1, suggesting a cascade model whereby PRC2-mediated gene repression is amplified by PRC1 recruitment/activation (Wang et al. 2004c). However, a recent paper suggests that PRC1-mediated H2AK119Ub is independent of PRC2-deposited H3K27me3 (Tavares et al. 2012). Intriguingly, another recent paper has reported that variant PRC1-dependent (non-canonical PRC1) H2AK119Ub is able to recruit PRC2 and H3K27me3 (Blackledge et al. 2014), indicating a non-canonical recruitment process as well as the involvement of PRC1 in H3K27me3 establishment and maintenance.

1.5.3 PRC1 and PRC2 in regulation of neurogenesis

As mentioned above, PcG proteins play important roles during development and disease. For instance, Bmi1, a PRC1 component, was identified as an oncogene that promotes B- and T-cell lymphomas development together with c-MYC (Haupt et al. 1991; van Lohuizen et al. 1991). In addition to cancer, accumulating evidence suggests its role in maintenance of NSCs (Molofsky et al. 2003; Fasano et al. 2007; Fasano et al. 2009; He et al. 2009). It has been reported that Bmi1 is required for SVZ aNSC self-renewal (Molofsky et al. 2003). Specifically, Bmi1 knockout mice lead to postnatal depletion of SVZ NSCs rather than more committed progenitors, and this effect is mediated by increased expression of the Polycomb target and cell cycle inhibitor $p16^{Ink4a}$ (Molofsky et al. 2003). Interestingly, acute reduction of Bmi1 using shRNA impairs proliferation of NSCs both in embryonic and adult, and this defect is mediated by another cell cycle inhibitor, $p21^{Cip1}$ (Fasano et al. 2007). Moreover, Bmi1-overexpression *in vitro* promotes NSCs self-renewal via repression of $p21^{Cip1}$, and cooperation with forebrain-specific transcription factor Foxg1 underpins regulation of stemness (Fasano et al. 2009). However, constitutive overexpression of Bmi1 using Nestin-Bmi1-GFP mice revealed that Bmi1-overexpression has no profound effects in NSCs proliferation and SVZ-OB neurogenesis *in vivo*, suggesting discrepancies between *in vivo* and *in vitro* studies (He et al. 2009). In addition, Bmi1-overexpression also induces oxidative stress-induced DDR and elevated γH2AX foci formation in neurospheres, resulting in increased apoptotic cell death (Acquati et al. 2013). Finally, another PRC1 component, Ring1b, has also been implicated in neurogenesis. Tissue specific Ring1b knockout ($Ring1b^{f/f}$;Nestin-Cre-ERT2) leads to prolonged neurogenic phase of NPCs, thereby delaying the astrogenic phase during neocortical development (Hirabayashi et al. 2009).

PRC2 subunits have also been well documented to have roles in neural development. For example, EZH2 knockout or EED knockdown prolonged the neurogenic phase thereby delaying the onset of neurogenic to astrogenic transition (Hirabayashi et al. 2009). Intriguingly, EZH2 has been reported to be responsible for inhibition of astroglial differentiation but not neuronal differentiation *in vivo* via directly repression of glial fibrillary acidic protein (GFAP) promoter (Sparmann et al. 2013). In addition, this phenotype requires

interaction with Chd4, a NuRD complex member, suggesting the coordination of PcG protein and HDACs in regulation of neurogenesis (Sparmann et al. 2013). Moreover, Emx1-Cre driven deletion of EZH2 in cortical progenitors at E9.5, prior to the onset of neurogenesis, leads to accelerated neurogenesis and a substantially thicker cortex by E14 (Pereira et al. 2010). More specifically, EZH2 loss results in removal of H3K27me3 repressive mark in cortical progenitors, leading to gene derepression and ultimately shifting the balance toward differentiation rather than self-renewal (Pereira et al. 2010). A very recent paper has shown that EZH2 conditional inactivation in the cerebellar primordium results in cerebellar hypoplasia, and this is due to the dysregulated transcriptional programmes that mediate increased GABAergic neurons production at the expense of Purkinje cells (Feng et al. 2016). Interestingly, another recently published paper has reported that EZH2 knockdown in chick embryo neural tubes leads to disorganised neuroepithelium (NE) structure and EZH2 preserves NE structure through targeting the $p21^{Cip1}$ promoter (Akizu et al. 2016). Finally, another PRC2 component, SUZ12, which is required for stability and activity of PRC2 (Cao and Zhang 2004; Pasini et al. 2004), has been implicated in brain malformations (Miro et al. 2009). In particular, loss of one allele of SUZ12 leads to cerebellar herniation, an enlarged brainstem as well as a smaller occipital cortex, indicating a haploinsufficient role of SUZ12 in CNS development (Miro et al. 2009). Collectively, these studies shed light on the key contributions of PcG proteins to neurogenesis. However, the involvement of PcG proteins in the context of adult SVZ neurogenesis remains only partially understood.

1.6 Brain cancer as a disease of aberrant neurogenesis

Alterations of the neuro/gliogenesis process are believed to underlie neoplastic transformation during development as well as in the adult brain (further discussed below). Glioblastoma multiforme (GBM) remains the most prevalent and aggressive primary brain tumour in adults despite intensive research efforts in the last 20 years (Maher et al. 2001; Sanai et al. 2005). According to the World Health Organisation (WHO), GBMs are classified as grade IV gliomas and characterised by their highly proliferative, invasive nature compared to lower grade astrocytomas as well as by the presence of necrosis

and glomeruloid microvascular proliferation at the histological levels (Kleihues et al. 2002). Adult GBMs can be classified into two groups: primary GBM and secondary GBM (Ohgaki and Kleihues 2013). Primary GBMs develop predominantly in older patients without histological presence of a less malignant precursor lesion, whereas secondary GBMs mainly develop from lower grade astrocytomas in younger patients with a better prognosis (Ohgaki et al. 2004; Ohgaki and Kleihues 2013). The hallmarks of primary GBMs are loss of heterozygosity (LOH) of chromosome 10q (carrying PTEN), mutation/amplification of epidermal growth factor receptor (EGFR), deletion of $p16^{Ink4a}$ and overexpression of Mdm2. With regard to secondary GBMs, they are characterised by amplification of platelet-derived growth factor A (PDGFA)/platelet-derived growth factor receptor α (PDGFα), mutations in p53/pRb and LOH of chromosome 19q (Furnari et al. 2007; Wen and Kesari 2008; Ohgaki and Kleihues 2013). Intriguingly, with the help of genome-wide analysis, two predominant molecular pathways have been identified being dysregulated in human GBMs: inactivation of the tumour suppressive p53 and pRb pathways and gain of receptor tyrosine kinase (RTK) signalling (Cancer Genome Atlas Research 2008; Parsons et al. 2008; Brennan et al. 2013), which have been associated with disruption of cell cycle regulation and apoptosis as well as aberrant RTK cascades (Furnari et al. 2007). Notably, a gain-of-function point mutation (R132H) in isocitrate dehydrogenase 1 (IDH1) has been identified as a specific marker for secondary GBMs, with implications for epigenetic modifications affecting both DNA and histones (Yan et al. 2009; Killock 2016).

Importantly, integrated genomic analysis has identified several molecular subtypes of GBMs using gene expression-based molecular classification: proneural, neural, classical and mesenchymal (Verhaak et al. 2010). For instance, the classical subtype is characterised by loss of PTEN and amplification of EGFR, whereas the mesenchymal subtype is depicted by loss of tumour suppressor neurofibromatosis type 1 (NF1). This classification approach provides insight into the heterogeneity within GBMs and permits the better clinical assessment of GBMs.

In addition to the characterisation of different subtypes based on molecular profiling, the identification of cell of origin is of crucial importance as this not

only fosters our understanding for the biology of tumour initiation, maintenance and progression but also promotes better clinical treatment strategies (**Fig. 1.7**). In this respect, the term “cell of origin” refers to normal cells within the brain that are susceptible to oncogenic insults and subject to subsequent transformation into GBMs (Visvader 2011). It is now believed that cells harbouring NSC/neural progenitor cell (NPC) properties may serve as the cell of origin of adult GBMs (Holland et al. 2000; Sanai et al. 2005; Vescovi et al. 2006; Alcantara Llaguno et al. 2009; Jacques et al. 2010; Zong et al. 2015). In addition to the SVZ lining the lateral ventricles and DG within the hippocampus (Eriksson et al. 1998; Sanai et al. 2004), NSCs have been also isolated from subcortical white matter of the adult human brain that are competent to give rise to neurons and glia both *in vitro* and *in vivo* (Nunes et al. 2003), suggesting that different NSC types could act as cell of origin of GBM. Of note, the proliferative ability and developmental plasticity render NSCs/NPCs susceptible to accumulating more mutations and transformation in response to oncogenic stimuli compared to other mature cells (Sanai et al. 2005). Most evidence comes from studies based on mouse models, which have provided convincing and insightful findings with regard to cell(s) of origin of GBM (**Fig. 1.7**). For instance, concomitant mutations of p53 and NF1 tumour suppressor genes in NSCs give rise to glioma and early p53 inactivation preceding or concomitant NF1 loss is essential for tumour formation (Zhu et al. 2005b). This is further corroborated using mouse models with combined mutation/deletion of the key tumour suppressors found dysfunctional in human GBM, including p53, pRb, NF1 and PTEN (Holland et al. 2000; Alcantara Llaguno et al. 2009; Jacques et al. 2010). These studies not only highlighted the importance of NSCs in GBM formation but also established the crucial genetic events underlying its pathogenesis.

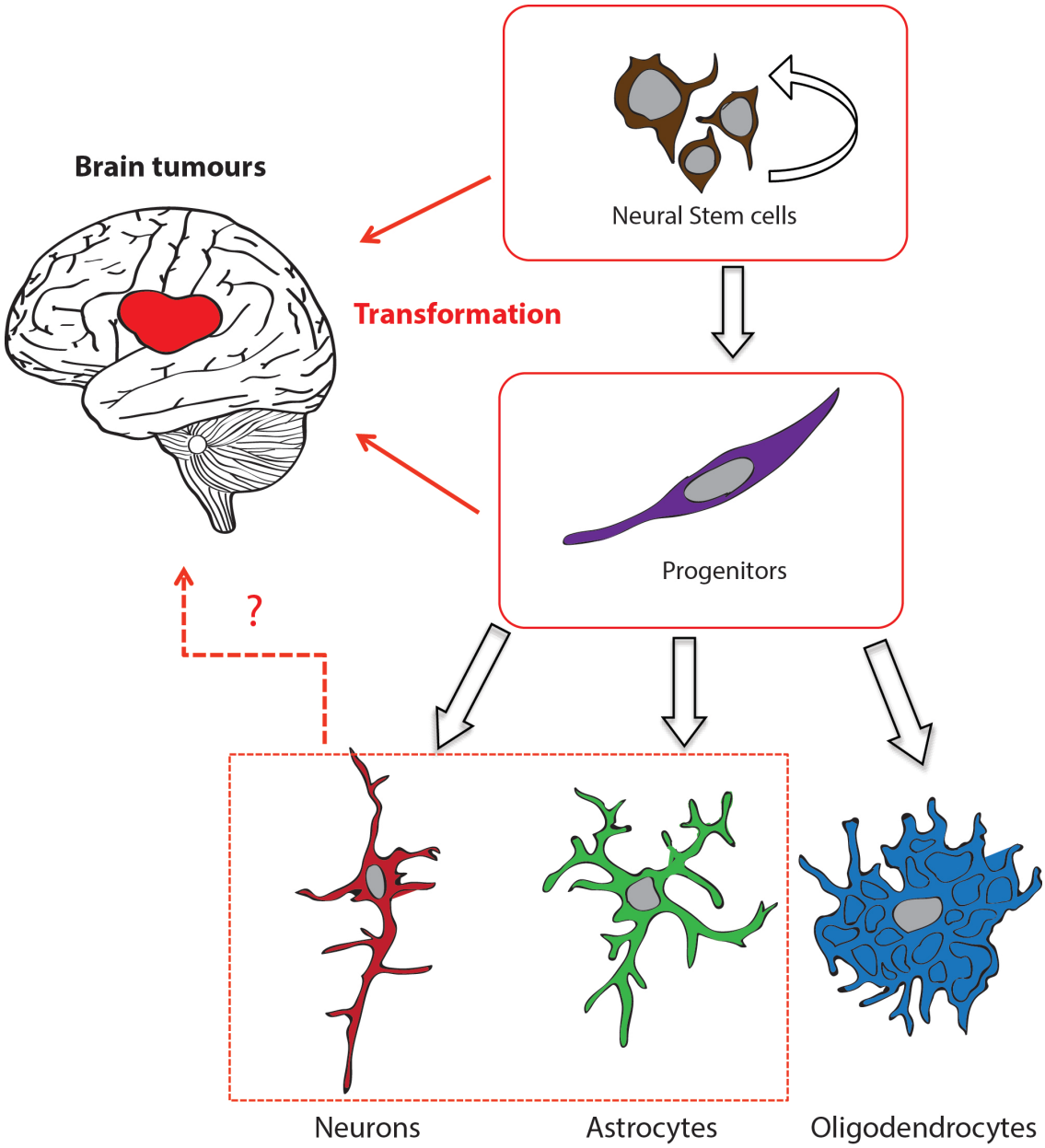

Figure 1.7: Cell of origin of GBM.

NSCs and progenitors (both neural progenitors and oligodendrocytes progenitors) are well established as cell of origin of GBM. This is predominantly due to their persistence through adulthood, which leads them to be susceptible to oncogenic transformation. Notably, transformation of differentiated progenies may also give rise to brain tumours (dashed box and arrow), this is consistent with the hypothesis that CSCs may not necessarily be derived from transformation of stem cells. Adapted from (Liu et al. 2011; Friedmann-Morvinski et al. 2012; Casarosa et al. 2013).

However, evidence suggests that other cell types act as cell of origin of gliomas in addition to NSCs. One study has shown that more than 20% of high-grade gliomas developed far away from the NSCs niches upon concomitant disruption of p53, PTEN and with or without pRb inactivation in adult GFAP-CreER mice (Chow et al. 2011), suggesting astrocytes are able to serve as the cell of origin of gliomas as well.

Moreover, there is also evidence suggesting that differentiated cells can also serve as the cell of origin of gliomas. However, this requires them to acquire “stemness” properties through dedifferentiation. More specifically, in response to lentiviral-induced silencing of p53/NF1 or activation of Ras (H-Rasv12)/p53 silencing, neurons and astrocytes are able to undergo dedifferentiation and subsequently initiate and maintain malignant gliomas (Friedmann-Morvinski et al. 2012). Notably, these gliomas belong to the mesenchymal subtype as described before (Friedmann-Morvinski et al. 2012).

Interestingly, oligodendrocytes precursor cells (OPCs) have been reported as being the cell of origin of gliomas. The most striking evidence coming from a study using Mosaic Analysis with Double Markers (MADM) showed that following concurrent p53/NF1 mutations a significant aberrant growth prior to transformation was restricted to OPCs (but not NSCs or other lineages derived from NSCs), raising the possibility that OPCs act as the cell of origin of gliomas. Moreover, this study also suggests that OPCs outcompete NSCs with regard to cell of origin of gliomas in this scenario (Liu et al. 2011).

Collectively, these studies provide important evidence delineating cell of origins of GBMs as well as reinforcing the complexity of GBMs.

Another key feature of GBMs is their altered/augmented migration/invasion capabilities (Furnari 2007; Cuddapah 2014). In contrast to other solid tumours, which predominantly metastasise to distant organs, GBMs mainly infiltrate within the brain, with very few reports of extracranial metastases (Beauchesne 2011; Cuddapah et al. 2014; Hamilton et al. 2014). Our understanding with respect to GBM invasion/migration remains limited, as genomic studies have failed to report genetic alterations affecting direct regulators of cell invasion in GBM. As a result, there are few insights into which key cell migration regulators underlie cell invasion in GBMs. However, it is important to note that GBM cells

exploit similar routes as neuroblasts and neurons, indicating potential shared mechanisms facilitating GBM cells to infiltrate the brain parenchyma (Arvidsson et al. 2002; Goings et al. 2004; Zhang et al. 2007; Faiz et al. 2015). Therefore, it is imperative to delineate if similar molecular mechanisms are being exploited by both normal cells and transformed GBM cells, further facilitating our understanding of GBM pathogenesis.

1.6.1 Epigenetic alterations in brain cancer

As mentioned above, histones are targets for various PTMs that have implications in altering the properties of the nucleosome as well as the associated factors. Importantly, the existence of histone variants, which exert distinct properties compared to their canonical counterparts, add more complexity to this scenario (Kamakaka and Biggins 2005). In mammals, histone variants are categorised into three groups corresponding to their canonical partners: H2A variants (e.g. H2A.Z, H2A.X), H2B variants and H3 variants (e.g. CENP-A, H3.3) (Skene and Henikoff 2013; Maze et al. 2014; Zink and Hake 2016). In addition, there are numerous H1 variants, however, their biological roles remain incompletely understood (Parseghian et al. 2001; Kamakaka and Biggins 2005; Happel and Doenecke 2009; Terme et al. 2011; Maze et al. 2014; Zink and Hake 2016). Notably, the key feature of histone variants is their distinct incorporation pattern throughout cell cycle compared to canonical histones; histone variants are deposited into chromatin and their expression is not restricted to S phase whereas canonical histones are incorporated in a replication-dependent way, with significantly higher level during S phase (Kamakaka and Biggins 2005; Skene and Henikoff 2013). Intriguingly, mounting evidence has implicated mutations in the histone variant, H3.3, in brain cancer (Khuong-Quang et al. 2012; Schwartzentruber et al. 2012; Sturm et al. 2012; Wu et al. 2012; Bender et al. 2013; Chan et al. 2013; Jones et al. 2013; Lewis et al. 2013; Venneti et al. 2013; Zhang et al. 2013). The H3.3 protein is encoded by the *H3f3a* and *H3f3b* genes in both mice and humans (Wells et al. 1987; Albig et al. 1995; Witt et al. 1997; Yuen and Knoepfler 2013). Importantly, H3.3 is predominantly deposited in transcriptionally active regions, marked by H3K4me3 (Delbarre et al. 2013; Yuen and Knoepfler 2013). However, evidence also suggests that H3.3 is able

to incorporate into telomeres and pericentric repeats, sites of heterochromatin that are associated with the transcription-inactive state (Drane et al. 2010; Lewis et al. 2010b; Szenker et al. 2011; Yuen and Knoepfler 2013; Elsasser et al. 2015). Incorporation of histone variants into dedicated regions relies on their dedicated histone chaperones (De Koning et al. 2007). Specifically, H3.3 is guided into euchromatin regions by histone regulator A (HIRA) (Tagami et al. 2004) and positioning into telomeric and pericentromeric heterochromatin regions is directed by DAXX and α-thalassemia X-linked mental retardation protein (ATRX) (Drane et al. 2010; Elsaesser and Allis 2010; Goldberg et al. 2010; Delbarre et al. 2013). Importantly, recent work from our lab has demonstrated that the PML-NB constituent DAXX is responsible for H3.3 loading at regulatory elements of immediate early genes upon neuronal activation (Michod et al. 2012). In addition, work from David Allis' group showed that H3.3 accumulates in neuronal and glial chromatin during ageing and the activity-dependent deposition of H3.3 is mediated by HIRA (Maze et al. 2015). Finally, our unpublished data and existing literature have shown that the DAXX/ATRX complex is found in PML-NBs (Xue et al. 2003; Berube et al. 2008; Delbarre et al. 2013), suggesting the potential involvement of PML in regulation of H3.3 deposition (Salomoni 2013). Of note, both ATRX and DAXX are found mutated in various tumours, including glioma and neuroblastoma, indicating the potentially crucial role of alterations of the DAXX/ATRX-H3.3 pathway in tumour development (Heaphy et al. 2011; Jiao et al. 2011; Cheung et al. 2012; Jiao et al. 2012; Liu et al. 2012).

As mentioned above, mutations in histone gene itself, particularly in H3.3, have been implicated in paediatric GBM (Khuong-Quang et al. 2012; Schwartzentruber et al. 2012; Sturm et al. 2012; Bjerke et al. 2013; Chan et al. 2013; Jones et al. 2013; Lewis et al. 2013; Venneti et al. 2013; Zhang et al. 2013) and other diseases (Attieh et al. 2013; Behjati et al. 2013). In this respect, heterozygous histone mutations in the human *H3F3A* gene result in K27M (lysine 27 to methionine) and G34R/V (glycine 34 to arginine/valine) mutants in N-terminal tail of H3.3 (Yuen and Knoepfler 2013). In addition, these two mutations are mutually exclusive in paediatric GBM (Schwartzentruber et al. 2012; Sturm et al. 2012) and are found in tumours arising in different CNS anatomical regions (**Fig. 1.8**) (Sturm et al. 2012; Bjerke et al. 2013; Yuen and

Knoepfler 2013), indicating potentially different cells of origin. Furthermore, patients harbouring K27M are younger than G34R/V patients (Schwartzentruber et al. 2012; Sturm et al. 2012), suggesting that H3.3K27M may contribute to tumour formation in NSCs at an earlier developmental stage (Chan et al. 2013). Importantly, K27M and G34R/V are found concurrently with other classical tumour-related mutations in gliomas. Specifically, K27M is associated with mutations in TP53, DAXX/ATRX, NF1, PDGFRA, KRAS, BRAF and FGFR1 (Khuong-Quang et al. 2012; Schwartzentruber et al. 2012; Jones et al. 2013; Yuen and Knoepfler 2013; Zhang et al. 2013), whilst G34R/V mutations are found associated with TP53, DAXX/ATRX and PDGFRA (Schwartzentruber et al. 2012; Yuen and Knoepfler 2013). It is thus proposed that H3.3K27M and H3.3G34R/V are "driver mutations" by which they function as "second hit" (Knudson 1971) following somatic mutations that collectively contribute to the onset of tumour formation (Khuong-Quang et al. 2012; Schwartzentruber et al. 2012; Yuen and Knoepfler 2013).

H3.3K27M has been functionally linked to PRC2. In particular, it leads to global decrease of H3K27me3 level in brain tumour cells as well as in human embryonic kidney (HEK) cells, mouse embryonic fibroblasts (MEF) and human astrocytes (Chan et al. 2013; Lewis et al. 2013). More specifically, this driver mutation affects the enzyme activity of EZH2, the PRC2 catalytic subunit (Chan et al. 2013; Lewis et al. 2013). Intriguingly, though K27M impairs global level of H3K27me3, this effect exerts distinct enrichment levels at a set of genes with various biological functions (Chan et al. 2013). More specifically, one subset of genes (group A) with loss of H3K27me3 at promoters is associated with neurobiological processes (e.g. ligand-receptor interactions, synaptic transmission). Another subset of genes (group C) with gain of H3K27me3 at promoters is involved in cancer pathways (e.g. $p16^{Ink4a}$). Interestingly, group A genes also possess higher enrichment of H3K4me3 at promoters, an active mark, indicating the antagonist features of H3K27me3 and H3K4me3 in gene expression. Moreover, group C genes are defined as bivalent genes marked by the high density of both H3K27me3 and H3K4me3 at promoter regions (Chan et al. 2013).

The involvement of PRC2 and H3K27me3 has been well documented in a number of cancers. PRC2 has been implicated as an oncogene in a number of

different cancers. For instance, high level of EZH2 is associated with prostate cancer, breast cancer, lung cancer and liver cancer (Varambally et al. 2002; Sudo et al. 2005; Bachmann et al. 2006; Hussain et al. 2009; Kim and Roberts 2016). This oncogenic role has been further supported by studies revealing that gain-of-function point mutations of EZH2 resulting increased H3K27me3 levels lead to lymphomagenesis (Morin et al. 2010; Sneeringer et al. 2010; McCabe et al. 2012; Kim and Roberts 2016). In particular, high-EZH2 expression was observed in CSCs purified from human breast cancer and EZH2 was required for their maintenance (Chang et al. 2011). Taken together, these studies shed light on the potential oncogenic role of PRC2/EZH2 in adult GBM.

Interestingly, EZH2 may also bear tumour suppressive effect as loss-of-function EZH2 mutations have been implicated in a number of cancers, including T cell acute lymphoblastic leukaemia (T-ALL) (Ernst et al. 2010; Nikoloski et al. 2010; Ntziachristos et al. 2012; Simon et al. 2012; Sashida et al. 2014; Kim and Roberts 2016). Other PRC2 subunits have also been implicated as tumour suppressors. For example, mutations in SUZ12 and EED are associated with T-ALL and malignant peripheral nerve sheath tumours (MPNSTs) (Ntziachristos et al. 2012; Simon et al. 2012; Lee et al. 2014; Kim and Roberts 2016). This context-dependent manner provides hints with respect to PRC2/H3K27me3 in brain cancers. More specifically, it is known that H3K27me3 has a tumour suppressive role in paediatric GBM (Bender et al. 2013; Chan et al. 2013; Lewis et al. 2013) (see above), however, in the context of adult GBM, like many other tumours, it can exert oncogenic effects. Intriguingly, this context-dependent, double-faceted property of PRC2 resembles the role of PML in tumourigenesis.

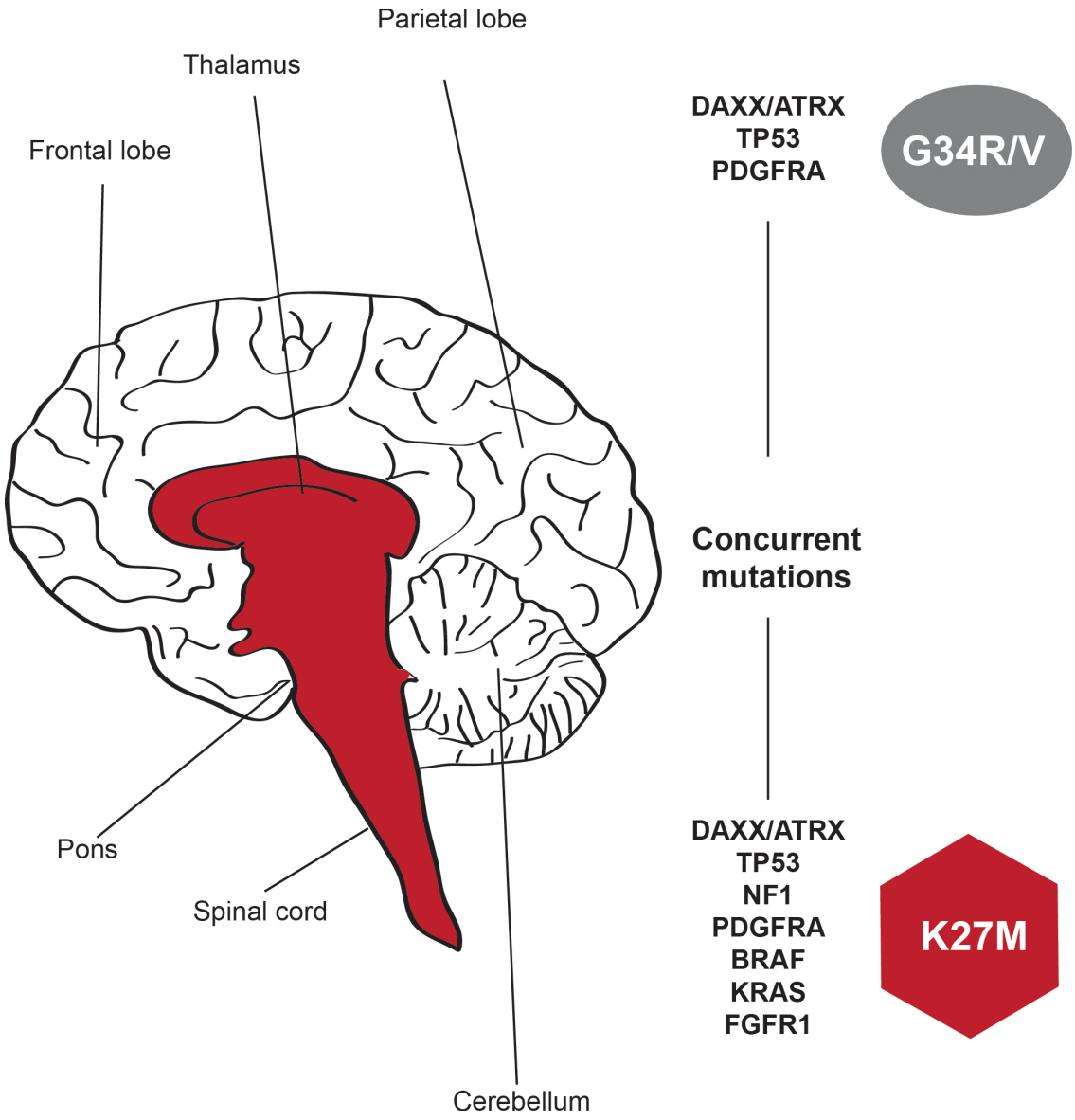

Figure 1.8: Distribution of H3.3 driver mutations in the CNS.

It is important to note that H3.3K27M mutations localise mainly to midline locations (red): spinal cord, thalamus, pons and brainstem. In addition, K27M patients are typically younger than G34R/V patients, indicating an earlier developmental onset of tumour growth. Moreover, K27M is associated with mutations in DAXX/ATRX, TP53, NF-1 PDGFRA, BRAF, KRAF and FGFR1. K27M mutation results in decreased EZH2 enzyme activity and thus leading to a decreased global H3K27me3 level. Adapted from (Yuen and Knoepfler 2013).

1.7 PML in the central nervous system

As mentioned earlier, our previous work has revealed an unexpected role of PML in regulation of corticogenesis through its ability to regulate NSCs proliferation (Regad et al. 2009). Specifically, this study found that PML expression is restricted to the NPCs/NSCs in the developing neocortex (**Fig. 1.9**). Interestingly, PML loss affects radial glia cells expansion and impairs generation of basal progenitor, resulting in reduced neuronal output and a thinner cortex (Regad et al. 2009). Notably, layering of the cortex was not affected, suggesting that PML loss negatively influenced differentiation throughout corticogenesis. Mechanistically, PML, pRb and protein phosphatase 1α (PP1α) form a nuclear complex in NPCs, whereby PML regulates pRb by facilitating PP1α-dependent dephosphorylation. Thus, PML loss leads to hyperphosphorylation of pRb and therefore abolishes its cell cycle inhibitory effect.

Previous studies had suggested an involvement of PML in the nervous system (Gray et al. 2004; Woulfe et al. 2004; Villagra et al. 2006; Woulfe et al. 2007; Regad et al. 2009). Following our report, it has been shown that PML is expressed in different parts of adult brain, including hippocampus, cerebellum, cortex and brain stem, and that germline PML knockout (KO) results in abnormalities in learning and spatial memory (Butler et al. 2013). More recently, another study has reported that PML is expressed in the suprachiasmatic nucleus, which is responsible in regulating circadian rhythm, and PML expression level shows a highly regulated pattern during circadian period (Miki et al. 2012). Furthermore, an *in vitro* study using a neuronal culture system (which lacks glia) has shown that PML expression level is low in neurons, however, neuronal stimulation leads to significant upregulation of PML protein levels (Korb et al. 2013). In addition, PML has been implicated in synaptic plasticity, given the fact that PML interacts with Arc, which is involved in synaptic plasticity and memory formation (Bloomer et al. 2007; Korb et al. 2013). Another study has reported that PML activates NeuroD expression following formation of a complex with forkhead protein FoxO1 (Kitamura et al. 2005), implicating a role of PML in neuronal differentiation. Importantly, a

previous study from our group has shown that PML regulates neurogenesis in the developing cortex (Regad et al. 2009). This study reveals an unexpected role of PML in central nervous system (CNS) stem cells and neurogenesis. Taken together, these studies provide evidence for the multiple and dynamic roles of PML in CNS stem cells, neurogenesis and normal adult brain functions.

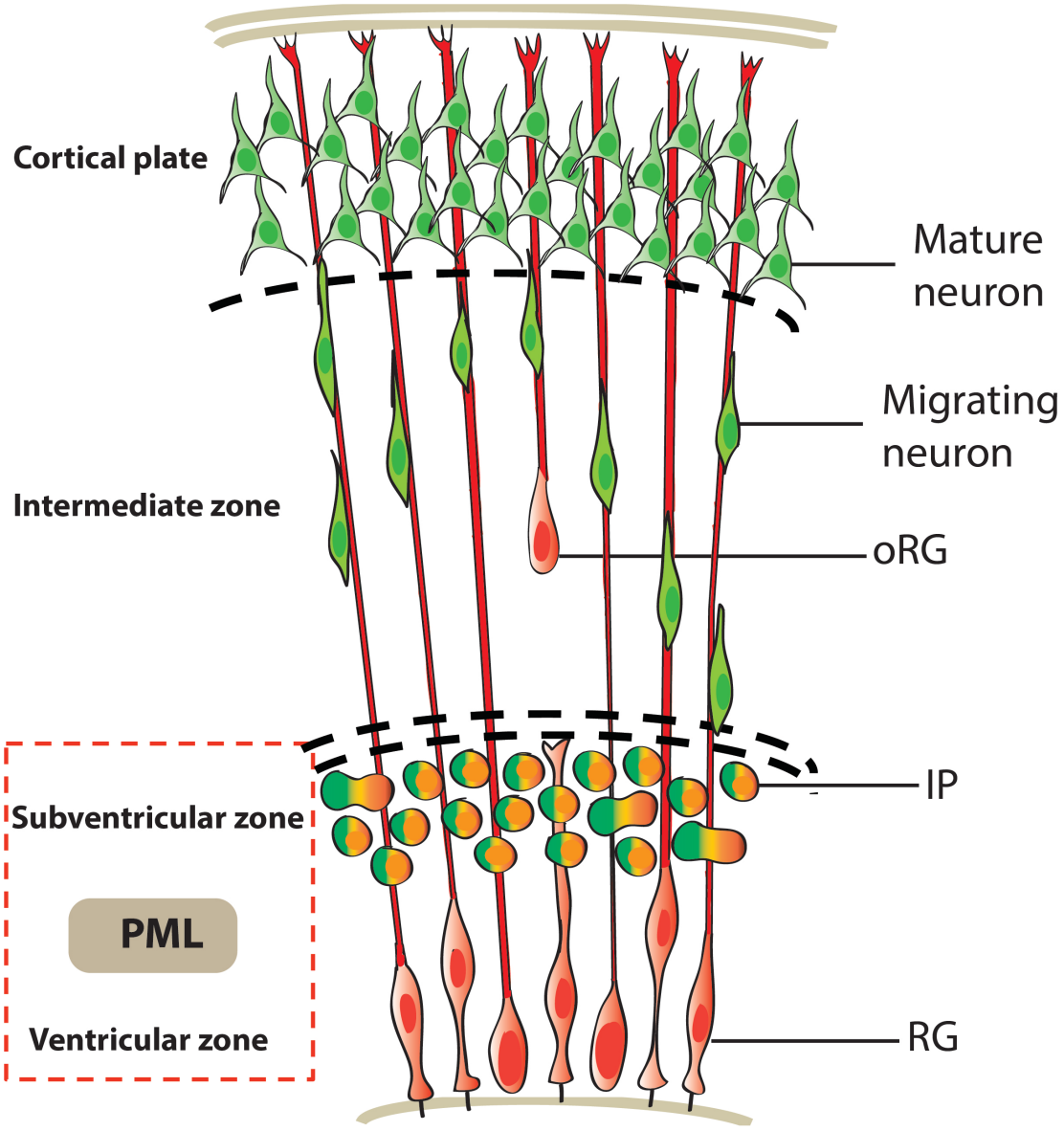

Figure 1.9: Schematic illustration depicting rodent corticogenesis and PML expression is restricted in neural progenitor cells (NPCs) in the developing neocortex.

Intermediate progenitor (IP) cells in the subventricular zone (SVZ) are derived from radial gilal (RG) cells located in the ventricular zone (VZ). IP cells in turn generate neurons that migrate radially via RG fibers (red) to the cortical plate. Notably, previous work from our lab has shown that PML expression is restricted in NPCs located in VZ during neocortex development and its expression retains confined in VZ/SVZ postnatally (dashed red box). A subset of outer SVZ radial glia-like (oRG) cells are also indicated, which are generated from RG via asymmetric divisions. Adapted from (Lui et al. 2011).

1.8 Supporting data on the effect of PML loss on adult neurogenesis

(generated before the start of my thesis work)

Based on our findings on the role of PML in CNS development, we hypothesised that PML could also play a role in regulation of adult neurogenesis. To address this, a number of experiments were carried out by a former postdoctoral researcher, Joanne Betts, to study the impact of PML loss on adult SVZ neurogenesis.

1.8.1 PML is expressed in the SVZ/OB niche

To investigate the expression of PML in adult mice (6-month old) SVZ NSCs, fate-mapping experiments were performed using a nucleoside analogue of thymidine, 5-bromo-2'-deoxyuridine (BrdU), indexing S-phase synthesis of the cell cycle. In brief, Edu injections were carried out intraperitoneally in $PML^{+/-}$ mice once daily for 12 consecutive days to guarantee the incorporation by slow-cycling type B NSCs as well as the fast-proliferating type C progenitor cells. Mice were subsequently sacrificed at two time points: 1-month (**Fig. 1.10A**) or 1-day (**Fig. 1.10B**) after the last injection. The differentiated cells in OB and the label-retaining NSCs residing in the SVZ can be detected at the 1-month time point, whereas the 1-day time point identifies the fast cycling type C cells in SVZ as well as the newly generated neuroblasts that migrate away from SVZ. PML was successfully detected in a subset of Edu^+ and $GFAP^+$ NSCs within SVZ (**Fig. 1.10A**), type C cells (**Fig. 1.10B**) and in doublecortin positive (DCX^+) migrating neuroblasts (**Fig. 1.10C**). The expression of PML in SVZ NSCs could be recapitulated *in vitro* using cells extracted from SVZ propagating adherently (**Fig. 1.10D**) or as neurospheres (data not shown). Thus, PML expression in NSCs was confirmed both *in vivo* and *in vitro*. In addition, PML expression was found absent in βIII-tubulin$^+$ (Tuj1, neuronal marker) and $GFAP^+$ (glia marker) differentiated cells (**Fig. 1.10E**) and this reduced expression pattern was confirmed both at mRNA and protein levels by triggering NSCs into differentiation *in vitro* (**Fig. 1.10F**).

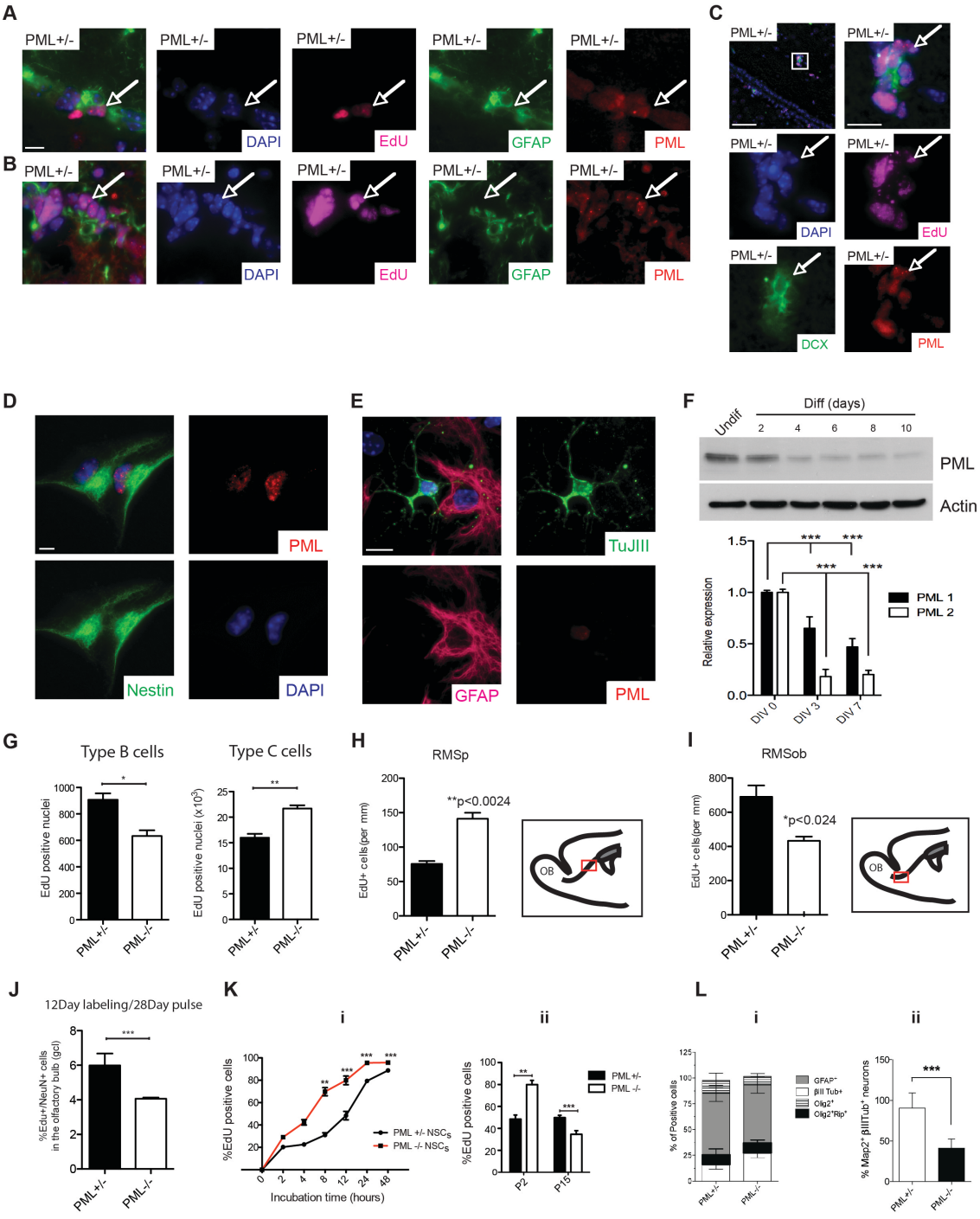

Figure 1.10: Supporting data of phenotypes caused by PML loss.

These results were conducted by a previous postdoctoral researcher Joanne Betts. (A) PML is expressed in SVZ NSCs. Staining was carried out in coronal sections for mice sacrificed at 1-month time point, indexing the label-retaining NSCs in SVZ. Scale bar=50μm. (B) Staining of coronal sections at 1-day time point, identifying PML expression in type C cells as well as in (C) migrating neuroblasts. Scale bar=50μm. (D) PML expression in adherent NSCs *in vitro*. Scale bar=25μm. (E) PML expression is virtually absent in differentiated cell types, identified by co-staining of βIII-tubulin (Tuj1) and GFAP. Scale bar=20μm. (F) PML mRNA and protein is gradually

decreased in cells undergoing differentiation at different time points. (G) Quantification shows decreased number of type B cells within SVZ in $PML^{-/-}$ mice compared to $PML^{+/-}$ mice. Conversely, quantification reveals an increased production of type C cells in $PML^{-/-}$ mice compared to $PML^{+/-}$ mice. (H) Staining and quantification reveals an increased number of migratory neuroblasts (DCX^{+}) entering the region of posterior RMS in PML-deficient mice, whereas (I) shows a decreased number of neuroblasts migrating to RMS region proximal to OB. (J) Staining and quantification shows a significant reduction of OB neurons within the granule cell layer in $PML^{-/-}$ mice compared to control mice.(K) *In vitro* Edu incorporation reveals a higher percentage of Edu+ cells upon PML loss at all time points, indicating accelerated proliferation (i) whereas fewer label-retaining NSCs were propagated at later passages upon PML loss (ii), suggesting an exhaustion of NSCs. (L) Differentiation assay shows PML loss results in increased induction of neuronal generation (i) but a less terminally differentiated phenotype *in vitro.* Values represent mean ± SEM (n=3; *$p<0.05$; **$p<0.01$; ***$p<0.001$, unpaired t-test).

1.8.2 PML loss affects adult neurogenesis

To determine the impact of PML loss on adult neurogenesis, the abovementioned fate-mapping experiments were performed in $PML^{+/-}$ and $PML^{-/-}$ mice. At the 1-month time point, there was a significant reduction of type B label-retaining cells in $PML^{-/-}$ mice SVZ compared to $PML^{+/-}$ control mice (**Fig. 1.10G**). Conversely, at the 1-day time point, Edu injections identified more type C cells in $PML^{-/-}$ mice SVZ than $PML^{+/-}$ mice (**Fig. 1.10G**). To determine whether increased production of type C cell correlated with augmented migrating neuroblasts, the posterior region of RMS (RMSp) and proximal region to the OB (RMSob) in $PML^{+/-}$ and $PML^{-/-}$ mice at 1-day time point after last Edu injection (labeling migratory neuroblasts) were examined. Quantification of DCX^{+} and Edu^{+} cells in the posterior RMS (RMSp) revealed a significantly increased number of migratory neuroblasts entering the RMS in $PML^{-/-}$ mice compared to PML control mice (**Fig. 1.10H**). In contrast, a reduced number of neuroblasts were found in RMS region proximal to the OB (RMSob) in $PML^{-/-}$ mice (**Fig. 1.10I**), indicating a defect in SVZ-RMS-OB migration in PML-deficient mice, though the entry into differentiation was augmented. This is in line with the reduced number of newly generated OB neurons in $PML^{-/-}$ mice following quantification of Edu^{+} and $NeuN^{+}$ cells (**Fig.1.10J**) at the 1-month time point.

In vitro, the Edu incorporation assay revealed that $PML^{-/-}$ SVZ NSCs contained higher amount of Edu^{+} cells than $PML^{+/-}$ cells when normalised to total amount of $DAPI^{+}$ cells (**Fig. 1.10K,i**), mimicking PML loss increased proliferation *in vivo.* Moreover, at later cell passages, a reduced number of Edu^{+} cells were revealed in $PML^{-/-}$ cells (**Fig. 1.10K,ii**), suggesting exhaustion of NSCs similar to *in vivo*. Finally, induction of NSCs differentiation and subsequent staining and quantification revealed that $PML^{-/-}$ cells more frequently entered neuronal differentiation (**Fig. 1.10L, i**), however, less terminally differentiated neurons were produced from $PML^{-/-}$ NSCs (**Fig. 1.10L,ii**), recapitulating the pattern *in vivo.* Taken together these results suggest that PML loss results in increased proliferation of progenitor cells, at the expense of NSC pool, and reduced neuroblast migration in RMS as well as impaired differentiation in the OB both *in vivo* and *in vitro.*

1.9 Outstanding questions and hypotheses

Given the existing literature and previous published and unpublished work from our group, three main outstanding questions remain:

1. What is the role of PML in regulation of cell migration and SVZ/OB neurogenesis? Unpublished work from Joanne Betts suggests that PML may play a role in cell migration in addition to aNSC self-renewal and progenitor expansion. However, evidence is needed to prove that PML loss indeed affects the cumulative neuronal output in the OB and as a result its size. Furthermore, evidence is needed to prove that migration defects could be recapitulated *in vitro*, in a NSC-intrinsic fashion.

2. What are the molecular mechanisms underlying PML function in adult SVZ neurogenesis? Published work from our group shows that during corticogenesis PML regulates NSC expansion via regulation of the growth suppressor pRb. Therefore, it is possible that PML regulates aNSC migration through regulation of cell cycle. However, it cannot be excluded that PML controls migration by directly modulating pathways that are involved in cell migration.

3. What is the role of PML upon neoplastic transformation?
Unpublished work from Joanne Betts suggests PML is enriched in GBM belonging to the mesenchymal subtype and its expression is correlated with poor prognosis. Accumulating evidence supports a role of PML in maintaining both cancer and non-cancerous stem cells. Furthermore, NSCs serve as the cell of origin of GBM. One of the key features of GBM is the aggressive invasion through the brain parenchyma and brain cancer cells and normal neuroblast/NSC use the similar migratory routes. Thus it is important to determine the involvement of PML under neoplastic transformation to gain insight with respect to its role in brain tumourigenesis.

1.10 Aims

1. To investigate the phenotypic changes caused by PML loss during adult SVZ neurogenesis
2. To determine the molecular mechanisms underlying PML role in regulation of adult SVZ neurogenesis

1.11 Potential impact

This study has the potential to provide key insights into fundamental mechanisms underlying neurogenesis, in particular cell migration. Moreover, as alterations of neurogenesis underlie cancer development in the CNS, this work could have implications for our understanding of the process of neoplastic transformation.

Chapter 2

Materials and Methods

2 Materials and Methods

2.1 Materials

2.1.1 Animals

The *PML*$^{-/-}$ mice were a generous gift from P.P. Pandolfi (Beth Israel Deaconess Medical Center), as described previously (Regad et al. 2009), and the PML conditional KO (*PML*$^{F/F}$) mice were derived from Taconic Artemis. The PML RingMut mice constitutively express PML with a double mutation (Cys31Ala, Cys34Ala), disrupting the first zinc ion-binding site of the RING domain (Moravcsik et al. 2013). Mice were maintained, bred, and subjected to procedures under the Project Licenses 80/2325, and 70/8240, which were issued by the Home Office.

2.1.2 Antibodies

Table 3: Antibodies for immunofluorescence and western blotting

Antibody	Condition	Supplier	Cat.
Bmi1	WB: 1/500	Santa Cruz	sc10745
EZH2	WB: 1/1,000	Cell Signaling	4509
GFAP	IF: 1/2,000	DAKO	P0488
H3	WB: 1/50,000	Abcam	ab1791
H3K27Ac	WB: 1/2,000	Abcam	ab4729
H3K27me3	WB: 1/2,000 IF: 1/2,000	Millipore	07-449
H3K4me3	WB: 1/2,000	Millipore	7473
Map2	IF: 1/100	Abcam	ab11267
Nestin	IF: 1/100	Millipore	MAB353
PML	IF: 1/100 WB: 1/500	Millipore	5718
SUZ12	WB: 1/500	Santa Cruz	sc46264
Tubulin	WB: 1/50,000	Sigma Aldrich	T5168
Twist1	WB: 1/50	Abcam	ab50887
β-actin	WB: 1/5,000	Sigma Aldrich	A5441
βIII-tubulin	IF: 1/1,000	Covance	MMS435P
γH2AX	IF: 1/500	Millipore	MB5636

Table 4: Secondary antibodies for western blotting

Antibody	Condition	Supplier	Cat.
ECL Anti-Mouse IgG	WB: 1/50,000	GE Healthcare	NA931V
ECL Anti-Rabbit IgG	WB: 1/50,000	GE Healthcare	NA934V

Table 5: Secondary antibodies for immunofluorescence

Antibody	Condition	Supplier	Cat.
Anti-Mouse IgG Alexa Fluor 568	1/1,000	Life Technologies	A11019
Anti-Rabbit IgG Alexa Fluor 568	1/1,000	Life Technologies	A11008

Table 6: Antibodies for ChIP

Antibody	Supplier	Cat.
H3	Abcam	ab1791
H3K4me3	Millipore	7473
H3K27me3	Millipore	07-449
Polyclonal Rabbit anti-Mouse IgG	Dako	Z0259

2.1.3 Buffers and solutions

Phosphate buffered saline (PBS): 137mM NaCl, 2.7mM KCl, 10mM Na_2HPO_4, 2mM KH_2PO_4, pH 7.4.

PBS-Tween (PBS-T): PBS containing 0.1% (v/v) Tween-20.

TBS: 20mM Tris-HCl pH 7.6, 150mM NaCl

TBS-Tween (TBS-T): TBS containing 0.1% (v/v) Tween-20.

5X Laemmli buffer: 2mM β-mercaptoethanol, 250mM Tris pH 6.8, 0.125% bromphenol blue, 10% SDS, 50% glycerol.

1X Tris-acetate-EDTA (TAE): 1mM EDTA, 20mM acetic acid, 40mM Tris, pH 8.0.

5X DNA loading dye: 10mM EDTA pH 8.0, 100mM Tris pH 8.0, 0.5% bromophenol blue, 50% glycerol.

5X Polyethylene glycol (PEG): 50mM PEG (Sigma Aldrich, 89510), 410mM NaCl, 0.2% 1M Tris pH 7.5.

LB Broth: 5g/L yeast extract, 10g/L NaCl, 10g/L tryptone.

1X SDS-Page running buffer: 25mM Tris-HCl, 192mM glycine, 0.1% SDS

1X Transfer buffer: 25mM Tris-HCl, 192mM glycine, 20% Methanol

2X HEPES: 1.5mM Na_2HPO_4, 50mM HEPES, 280mM NaCl, adjust pH to 7.05.

RIPA buffer: 0.5mM EDTA, 0.5mM $MgCl_2$, 50mM Tris pH 8.0, 150mM NaCl, 1% Triton-X, 0.5% SDS, supplemented with 1:100 protease inhibitor cocktail, and phosphatase inhibitor (1mM NaVO4, 50mM NaF) before cell lysis.

Isotonic buffer (nuclear protein extraction): 5mM MgCl2, 20mM Tris pH7.5, 100mM NaCl, 10% glycerol, 0.2% NP-40, 0.5mM DTT, 1:500 Pimix

High salt buffer (nuclear protein extraction): 0.5mM DTT, 50mM Tris pH7.5, 600mM NaCl, 10% glycerol, 0.2% NP-40, 1:500 Pimix.

8% Acrylamide gel (20ml): 9.4ml H_2O, 5.3ml 30% Acrylamide mix, 5.0ml 1.5M Tris pH 8.8, 0.1ml 20% SDS, 0.2% APS, 12ul TEMED.

10% Acrylamide gel (20ml): 7.9ml H_2O, 6.7ml 30% Acrylamide mix, 5.0ml 1.5M Tris pH 8.8, 0.1ml 20% SDS, 0.2% APS, 8ul TEMED.

15% Acrylamide gel (20ml): 4.6ml H_2O, 10.0ml 30% Acrylamide mix, 5.0ml 1.5M Tris pH 8.8, 0.1ml 20% SDS, 0.2% APS, 8ul TEMED.

Cell lysis buffer (ChIP): 10mM EDTA, 50mM Tris pH 7.5, 150mM NaCl, 1%Triton, 0.5% deoxycholate, 1% SDS.

Wash buffer 1 (ChIP): 0.5mM EGTA, 10mM EDTA, 10mM Hepes pH7.5, 0.75% Triton X-100.

Wash buffer 2 (ChIP): 0.5mM EGTA, 1mM EDTA, 10mM Hepes pH7.5, 200mM NaCl.

Lysis/Sonication buffer 3: 10mM EDTA, 50mM Tris pH 7.5, 150mM NaCl, 0.5% Deoxycholate, 1% Triton-X.

PBS/BSA blocking solution: 0.25g of BSA (Sigma Aldrich, A7906) in PBS to a final volume of 50ml. Vortexed intensively to fully dissolve BSA. 0.22μM syringe filtering was required.

Wash buffer A (ChIP): 1mM EDTA, 50mM Tris pH 8.0, 150mM NaCl, 0.1% SDS, 0.5% Deoxycholate, 1% NP40.

Wash buffer B (ChIP): 1mM EDTA, 50mM Tris pH 8.0, 500mM NaCl, 0.1% SDS, 0.5% Deoxycholate, 1% NP40.

Wash buffer C (ChIP): 50mM Tris pH 8.0, 250mM LiCl, 0.5% Deoxycholate, 1% NP40, 1mM EDTA.

2.1.4 Plasmids

For knockdown studies, pGIPZ vectors were derived from the UCL Cancer Institute Cancer Genomic Engineering (CAGE) facility. Bmi1-overexpression, and FUGW vectors were derived from Addgene. The p-MIG-Cre-ERT2-GFP vector was a generous gift from the Hugues de Thé lab at Université Paris Diderot. Additionally, the pTT28-His-tagged Robo1N plasmid was a kind gift from Lisa Robinson, The Hospital for Sick Children.

2.1.5 Primers

Primers were purchased from Invitrogen. Lyophilized primers were reconstituted by nuclease-free H_2O into 100μM for storage in -20°C. Primers for qPCR were designed as intron spanning, and primers for ChIP-qPCR were designed using Ensemble, and validated by presence of CpG island using UCSC Genome Browser.

Table 7: Primers for PML germline KO genotyping

	Sequence
Forward 1 (5'-3')	TTTCAGTTTCTGCGCTGCC
Forward 2 (5'-3')	CGACCACCAAGCGAAACA
Reverse (5'-3')	TTGGACTTGCGCGTACTGTC

Table 8: Primers for PML conditional KO genotyping

	Sequence	
Forward (5'-3')	CAAAGCCACACCATACTCATCC	PML F/F
Reverse (5'-3')	AAGGAGGCTCTAGGACCTAGAGG	

Forward (5'-3')	CAAAGCCACACCATACTCATCC	Recombination
Reverse (5'-3')	AAGGAGGCTCTAGGACCTAGAGG	

Forward (5'-3')	GACAAGCGTTAGTAGGCACAT	Flippase
Reverse (5'-3')	GGCAGAAGCACGCTTATCG	

Table 9: Primers for PML RingMut genotyping

	Sequence
Forward (5'-3')	CAACTCCCAGCAACCACATGG
Reverse (5'-3')	GCCGCATGTCAGCTCAATGAC

Table 10: List of primers for qPCR and ChIP-qPCR

Gene	Forward (5'-3')	Reverse (5'-3')
GAPDH	ACCACAGTCCATGCCATCAC	TCCACCACCCTGTTGCTGTA
Twist1	GGACAAGCTGAGCAAGATTCA	CGGAGAAGGCGTAGCTGAG
Slit1	CAAGAACATCCCACGGAACAC	TCCACAGCTCCGATCTGGTT
Slit2	CCATGTAAAAATGATGGCACCTG	ATCACAGTCCTGACCCTTGAA
Robo1	CCTTCAGACCTGATCGTCTCC	TGAGCGCGGGTCATCTTTG
Scratch1	CTCTTCGGCAGACCTCGAC	CCATCGTAGACCGACGCAG
E-Cadherin	CAGCCTTCTTTTCGGAAGACT	GGTAGACAGCTCCCTATGACTG
N-Cadherin	CCAGCAGATTTCAAGGTGGAC	TTACAGCTACCTGCCACTTTTC
Snail1	CACACGCTGCCTTGTGTCT	GGTCAGCAAAAGCACGGTT
Fra1	ATGTACCGAGACTACGGGGAA	CTGCTGCTGTCGATGCTTG
Zeb2	ATTGCACATCAGACTTTGAGGAA	ATAATGGCCGTGTCGCTTCG
MMP3	CGATGGACAGAGGATGTCAC	GACTGGGTACATCAGAGCTTCA
MME	GGGAGGCTTTATGTGGAAGC	CCGGATTTGTGCAATCAAGT
Bmi1	AAACCAGACCACTCCTGAACA	TCTTCTTCTCTTCATCTCATTTTTGA
$p16^{Ink4a}$	CGTACCCCGATTCAGGTG	ACCAGCGTGTCCAGGAAG
$p21^{Cip1}$	TCCACAGCGATATCCAGACA	GGACATCACCAGGATTGGAC
$p57^{Kip2}$	CAGGACGAGAATCAAGAGCA	GCTTGGCGAAGAAGTCGT
Ascl1	CCCCAACTACTCCAACGACT	AAGTCCATTCCCAGGAGAGC
Ccnd2	CCCGACTCCTAAGACCCATC	TGCGAAGGATGTGCTCAATG
Promoter	**Forward (5'-3')**	**Reverse (5'-3')**
Twist1	CTTGCCACTACTGCTGTCAC	TGCGAACCATTCAAAACCGA
Slit2	TGTCGGGAAGTGGAGAAGAC	AACAGTAATGGTGGCCCTGA
Robo1	GGGAGCCTGAGATGGAAAGG	GTTTCCTCCCTCTCCAGCC

2.2 Methods

2.2.1 DNA extraction for genotyping

Ear snips, or cell pellet were used as starting materials. DNA extraction was performed using REDExtract-N-Amp™ Tissue PCR Kit (Sigma Aldrich). For each tube/sample, 40µl Extraction Solution + 10µl Tissue Preparation Solution was mixed, and the sample was fully immersed into this reaction mix. Incubation was carried out using a dry water bath (LabScientific) at 50°C for 20 mins, and a subsequent 3 mins at 95°C. The 40µl Neutralisation Solution was mixed by vortexing it with the 50µl reaction mix. For genotyping PCR, 4µl DNA was used.

2.2.2 DNA sequencing

Desired plasmid DNA was prepared in an appropriate concentration together with defined sequencing primers following the instructions from the company (Source Bioscience). Data were retrieved using 4Peaks software, and sequence alignment was carried out by EMBOSS Needle.

2.2.3 Genotyping

To determine the $PML^{F/F}$/WT alleles and flippase transgene, PCR programme was carried out by: initial denaturation at 95°C for 5 mins; denaturation at 95°C for 30 secs; annealing at 60°C for 30 secs; and extension at 72°C for 1 min. Amplification was repeated for another 34 cycles from the denaturation step: final extension at 72°C for 10 mins. Expected amplicons were WT: ~170bp; $PML^{F/F}$: ~289bp; and flippase transgene: ~340bp. See **Table 8** for primers.

To determine the recombination upon 4-OHT treatment, PCR programme was carried out by: initial denaturation at 95°C for 5 mins; denaturation at 95°C for 30 secs; annealing at 60°C for 30 secs; and extension at 72°C for 1 min 30 secs. Amplification was repeated for another 34 cycles from the denaturation step: final extension at 72°C for 10 min. Expected amplicons: Recombined: ~300bp; and $PML^{F/W}$: ~1.5Kb. See **Table 8** for primers.

To determine the PML RingMut, PCR programme was carried out by: initial denaturation at 95°C for 5 mins; denaturation at 95°C for 1 min; annealing at 57°C for 1 min; and extension at 72°C for 1 min. Amplification was repeated for another 34 cycles from denaturation step: final extension at 72°C for 6 mins. Expected amplicons: WT: ~200bp; and RingMut: ~254bp. See **Table 9** for primers.

To determine the PML WT/KO alleles, PCR programme was carried out by: initial denaturation at 95°C for 10 mins; denaturation at 94°C for 1 min; and annealing at 59°C for 1 min. Amplification was repeated for another 34 cycles from denaturation step: final extension at 72°C for 1 min. Expected amplicons: WT: ~400bp; and KO: ~600bp. See **Table 7** for primers.

2.2.4 Agarose gel electrophoresis

PCR products were visualised, and separated by agarose gel electrophoresis. Concentration of agarose gel (Sigma Aldrich, A9539) was determined by the size of the amplicons, which ranged from 1% to 2%. For genotyping, samples were loaded directly. For other reactions, DNA was mixed with DNA loading dye (into 1X concentration), and electrophroresis was performed for approximately 25 mins at 100V. After electrophoresis using a PowerPac^{TM} Power Supply (Bio-Rad), bands were visualised using a G:BOX Gel imaging system (Syngene).

2.2.5 Measurement of OB size

Briefly, the whole brain was dissected from two adult mice, and the whole brain was isolated carefully using dedicated surgical tools. The brains were placed horizontally in a 10cm petri dish, and photos were taken using a Nikon D3S Digital SLR camera with a Nikon AF Micro Nikkor 60mm f/2.8D macro lens. Quantification was achieved using ImageJ area measurement. Finally, OB size was determined by plotting the area of the OB over the area of the rest of the brain.

2.2.6 Isolation of SVZ aNSCs

The isolation of adult mouse NSCs/progenitors was performed as previously described (Pollard et al. 2006). Essentially, the olfactory bulbs, cerebellum, and brainstem were removed from the dissected brain, and an area encompassing the SVZ surrounding the lateral wall of the forebrain ventricle was dissected under microscope. Tissue was subsequently incubated in Accutase (STEMCELL Technologies) for 25 mins at 37°C, and mechanically dissociated. Cells were plated onto a laminin-coated petri dish/flask in NeuroCult Proliferation Kit (STEMCELL Technologies, 05702) medium supplemented with 10 ng/mL of both bFGF-2, and EGF (Peptrotech).

2.2.7 Tissue culture

Human embryonic kidney cells (HEK 293T) were maintained in a DMEM (1X) + GlutaMAX^{TM}-I medium with 10%FBS (LifeTechnologies, 31966-021). Phoenix

cells were maintained in an IMDM+GlutaMAX^{TM}-I medium with 10% FBS, and aNSCs were cultured in a NeuroCult^{TM} Proliferation Kit (STEMCELL Technologies) supplemented with 10 ng/mL of both bFGF-2, and EGF (Peptrotech). HEK 293T and Phoenix cells were dissociated from the petri dish using 1X Trypsin (Gibco), and the aNSCs were dissociated from the tissue culture flask using Accutase (STEMCELL Technologies, 05702). Cell number and size were determined by Vi-CELL XR (Beckman Coulter). All cells were maintained at 37°C with 5% CO_2. HEK 293T and Phoenix cells were cryopreserved using a defined medium containing 10% DMSO, 45% DMEM/IMDM, and 45% FBS, and stored in -80°C for short-term storage, and in liquid nitrogen for long-term storage. The aNSCs were cryopreserved using a defined medium containing 10% DMSO with 90% NeuroCult^{TM} Proliferation medium, snap frozen on dry ice, and transferred at -80°C overnight, and in liquid nitrogen the following day. Cells were thawed in a water bath at 37°C before transferring the cell suspension in a 15ml Falcon tube with a pre-warmed medium. Cell suspension was subjected to centrifugation at 1,200 rpm for 4 mins, and supernatant containing DMSO was completely removed. Cell pellet was resuspended in a normal expansion medium, and plated onto a petri dish/tissue culture flask.

2.2.8 Immunofluorescence

A total of 60,000 cells/well were plated onto laminin-coated glass coverslips in a 24-well plate prior to fixation. The following day, fixation was performed in 4% PFA for 10 mins. The cells were washed three times in PBS, and permeabilised in a 0.5% Triton solution (in PBS). Blocking was subsequently performed in 5% goat serum (in 0.1% PBS-Tween (v/v)) for 1 hour at room temperature. Primary incubation was carried out by a diluting antibody (**Table 3**) in blocking solution, and incubated overnight at 4°C. The following morning, cells were washed 3 times with 0.1% PBS-Tween, and incubated with secondary antibodies (in blocking solution, described in **Table 5**) for 1 hour (covered with foil). Cells were washed 3 times with PBS, and counterstained with Hoescht (1:10,000 in PBS) for 15 mins at room temperature (covered with foil), and mounted. Staining was examined under a fluorescence microscope

(Zeiss AxioImager A1), and at least 5 different scopes were taken for quantification purpose.

2.2.9 Differentiation assay

A total of 200,000 cells/coverslip were plated at day 0 in a normal expansion medium onto laminin-coated glass coverslips. The following day, the expansion medium was replaced with medium supplemented only with bFGF-2 (10ng/mL), and cells were incubated for additional 3 days. A NeuroCult™ Differentiation Kit (STEMCELL Technologies, 05704) was subsequently introduced for 5 days. Cells were then fixed, and subjected to immunofluorescence.

2.2.10 EdU incorporation assay *in vitro*

A total of 50,000 cells were plated on top of laminin-coated coverslips in 24-well plates, and after 24 hours, EdU (10μM) was added to the medium. After 2 hours, cells were fixed in 4% PFA for 10 minutes. Edu was detected using a Click-iT® EdU Alexa Fluor® 555 Imaging Kit (Applied Biosystem) as per the manufacturer's instructions. Nuclei were stained with DAPI for 15 minutes, and coverslips were mounted for microscopy using FluorSave™ Reagent (Millipore). Quantification was performed by counting Edu-positive cells over the number of total DAPI-positive live cells in at least 5 different areas/coverslips.

2.2.11 RNA extraction

A total of 300,000 cells per well were plated onto a 6-well plate the day before the experiment. Cells were harvested using Accutase, and subjected to RNA extraction using the RNeasy® Plus Mini Kit (QIAGEN, 74134). β-mercaptoethanol (β-ME) was added to Buffer RLT Plus in a 1:100 (v/v) ratio before use. Cells were disrupted and homogenised using Buffer RLT Plus (+β-ME), and vortexing for 30 secs. Lysates were transferred to a gDNA Eliminator column, and centrifugation was performed at 11,000 rpm for 30 secs to remove genomic DNA from lysates. A 1:1 (v/v) ratio of 70% ethanol was added to the flow-through, and the total mixture was transferred to an RNeasy spin column,

and subjected to centrifugation at 11,000 rpm for 15 secs. Column-bound total RNA was washed twice with Buffer RPE, first at 11,000 rpm for 15 secs, and once again at 11,000 rpm for 2 mins. Final elution was performed using 30µl RNase-free H_2O, and by centrifugation at 11,000 rpm for 1 min. RNA concentration was determined by ND-1000 NanoDrop^{TM} Spectrophotometers (ThermoScientific).

2.2.12 Reverse transcription (cDNA synthesis)

Reverse transcription was performed using High Capacity cDNA Reverse Transcription Kits (Applied Biosystems). 500ng-1µg RNA was added into the 2X reaction mix containing RT Buffer, RT Random Primers, dNTP Mix, MultiScribe^{TM} Reverse Transcriptase, and RNase-free H_2O in a final volume of 20µl. The PCR programme was perform as follows: 25°C for 10 mins; 37°C for 120 mins; and 85°C for 5 mins. cDNA was further diluted for subsequent real-time PCR analysis.

2.2.13 Real-Time PCR (qPCR)

Real-time PCR was performed using 2X Fast SYBR Green Master Mix (Applied Biosystems), dedicated primers (**Table 10**), RNase-free H_2O, and cDNA in a final volume of 20µl (cDNA were loaded as replicates). PCR programme was performed as follows: 50°C for 2 mins; 95°C for 10 mins; 95°C for 15 secs (40 cycles); and 60°C for 1 min in a 7500 Fast Real-Time PCR System (Applied Biosystems). Relative abundance of gene expression was normalised to GAPDH mRNA, and calculation was generated using the $2^{-\Delta\Delta Ct}$ method as previously described (Livak and Schmittgen 2001).

2.2.14 Chromatin immunoprecipitation (ChIP)

Chromatin pulled down by immunoprecipitation was employed to study the DNA-protein interaction. Protocol was adapted from original protocol by Dr Suzana Hadjur (UCL Cancer Institute).

2.2.14.1 Cell fixation and crosslinking

A total of $5x10^6$ cells were plated onto a T75 flask, and expanded to obtain sufficient starting materials. Ideally, cells were grown into 80% confluent per flask. Cells were collected by Accutase, and washed once with PBS. Cell number was determined by Vi-CELL XR (Beckman Coulter), and $12x10^6$ cells were pelleted down per condition ($PML^{+/-}$ or $PML^{-/-}$). Cell pellet was resuspended in a normal proliferation medium containing 1% formaldehyde (FA) (in total 10ml) for a fixation of 10 mins at room temperature. Fixation was quenched by adding 0.125M glycine (solution turned yellow) for 5 mins at room temperature, and rotating on a tube roller (STAR LAB). Cell pellet was subjected to centrifugation at 2,500 rpm for 5 mins at 4°C, and supernatant was removed. Cell pellet was washed twice in ice-cold PBS, and spun down at 2,500 rpm for 5 mins at 4°C. The fixed, washed pellet could be snap frozen, and stored at -80°C.

2.2.14.2 Preparation of nuclear extracts

Following fixation and crosslinking, cell pellet was resuspended in a 10ml Wash buffer 1, and incubated by rotating on a tube roller for 10 mins at 4°C. Centrifugation was performed at 2,500 rpm for 5 mins at 4°C, and supernatant was removed. Cell nuclei were resuspended in 10ml Wash buffer 2, and incubated by rotating on a tube roller for 10 mins at 4°C. Centrifugation was performed at 2,500 rpm for 5 mins at 4°C, and supernatant was removed. Cell lysis was carried out using lysis/sonication buffer 3 containing 1% SDS with protease, and phosphatase inhibitors in a total volume of 300µl. Cell lysis was performed for 30 mins on ice. Meanwhile, Diagenode Bioruptor was pre-cooled to 4°C.

2.2.14.3 Sonication

Sonication was performed at 4°C, and programme was setup consisted of 15 cycles (30 secs on, 30 secs off) on high power. Sonication was repeated 3 times to reach 45 cycles in total. After every 15^{th} cycle, the sonicator was allowed to cool down for 3 mins prior to the next round commencing. After

sonication, 5µl of sample was taken in a pre-chilled eppendorf tube (left on ice), and the remaining sample was centrifuged at 13,000 rpm for 30 mins at 4°C. An additional 5µl sample was taken in a pre-chilled eppendorf tube, and the remaining chromatin could be stored at -80°C. To check the sonication efficiency, de-crosslinking was performed by adding 5µl Proteinase K (BioLine Reagen), and 90µl 100mM Tris pH7.5. De-crosslinking mixture was incubated overnight at 65°C, and the following morning, the mixture was incubated with 2µl RNase for 1 hour. DNA was purified using QIA Quick PCR Purification Kit (QIAGEN, 228106), as per the manufacturer's instructions. Fragmentation could be visualised by running on a 2% agarose gel, and ideally, the band smear should be restricted to 200bp~500bp.

2.2.14.4 Chromatin immunoprecipitation

Dynabeads Protein G (Life Technologies, 1004D) blocking was performed for 1 hour in cold room using freshly prepared PBS/BSA. Chromatin and BSA-blocked beads were incubated for 2 hours in cold room, and then overnight in 3µg of anti-H3, anti-H3K27me3, anti-H3K4me3, and anti-IgG (see **Table 6**). The following day, sequential washing steps were performed using wash buffer A, wash buffer B, and wash buffer C as follows: once with wash buffer A, quickly inverted while on the magnet rack; twice with wash buffer A, rotating for 10 mins on a windmill; once with wash buffer B, quickly inverted while on the magnet rack; an additional time with wash buffer B, rotating 10 mins on a windmill; once with wash buffer C, quickly inverted while on the magnet rack; and an additional time with wash buffer C, rotating 10 mins on a windmill. During the washing steps, a magnet rack was used to segregate magnetic beads from the wash buffers. After the washing steps were completed, protein-DNA de-crosslinking was performed using buffer (1% SDS, 0.1M $NaHCO_3$, Proteinase K) at 65°C overnight, while shaking on a Thermomixer (Eppendorf), which was also used during RNAse-A treatment for an additional 2 hours at 37°C the following morning. The samples were purified using the phenol-chloroform method.

2.2.14.5 ChIP-qPCR

To determine the enrichment of relevant histone marks at the level of gene promoter regions, ChIP-qPCR promoter primers were designed (**Table 10**). PCR programme was performed as follows: 50°C for 2 mins; 95°C for 10 mins; 95°C for 15 secs (40 cycles); and 60°C for 1 min on a 7500 Fast Real-Time PCR System (Applied Biosystems). Amplification was performed using 2X Fast SYBR Green Master Mix (Applied Biosystems), and calculation was carried out by the percentage input formula:

$100 \times 2 \wedge (Ct_{adjusted\ input} - Ct_{IP})$

In the percentage input formula, input was adjusted by subtracting 6.644 (Log_2100), and the data were normalised to the enrichment of H3, and to the PML control cells (as 1).

2.2.15 Total protein extraction

Between 600,000 and 800,000 cells were plated onto a T25 flask the day before extraction. The following day, cells were washed once in PBS, which was previously collected by Accutase. The RIPA buffer was freshly prepared before the experiment. Cell pellet was resuspended in RIPA buffer, and incubated on ice for 20 mins. Sonication was performed (SONICS) twice using 30% power for 4 secs (on ice). Lysates were subjected to centrifugation at 13,200 rpm for 5 mins. Supernatant was collected, and transferred to a pre-chilled eppendorf tube, and protein concentration was determined by BCA assay. As soon as the concentration was measured, a 5X Laemmli buffer was added to extracts.

2.2.16 Nuclear protein extraction

A total of $5X10^6$ cells were plated onto a T75 flask with normal expansion medium the day before extraction. The following day, the medium was removed, and cells were washed once with PBS, and collected using Accutase. An isotonic buffer, and high salt buffer were freshly prepared prior to the experiment. Cell pellet was firstly lysed with isotonic buffer, and homogenisation was performed rigourously in an up and down motion using a P1000 Gilson for at least 3 cycles (10 mins on ice, 10 mins for

homogenisation). To assess the efficiency for homogenisation, cell lysates were stained with trypan blue (1:1 ratio), which enables faint blue nuclei with stark nuclear membrane to be observed under microscope. Nuclei were pelleted by centrifugation at 13,200 rpm for 20 mins at 4°C. Cytosolic supernatant was transferred to another fresh pre-chilled eppendorf tube, and the cell nuclei pellet was further lysed by high salt buffer for 30 mins on ice. Sonication was subsequently performed (SONICS) twice using 20% power for 15 seconds (on ice). Lysates were subjected to centrifugation at 13,200 rpm for 5 mins, and nuclear extract was collected, and transferred to a fresh pre-chilled eppedorf tube. Protein concentration was determined by BCA assay. As soon as the concentration was measured, a 5X Laemmli buffer was added to the extracts.

2.2.17 Measurement of protein concentration

Protein concentration was determined using a colorimetric BCA Protein Assay Kit (Pierce, 23225). The working solution was made by mixing 1ml BCA Reagent A+20µl BCA Reagent B per sample, and the 2µl protein sample was mixed with working solution by vortex, and subjected for incubation in a water bath at 37°C for 45 min. A standard curve was generated from the gradient BSA protein concentration (blank, 0.5, 1, 1.5, 2, 3,4, 6, 8, 10, unit: µg/µl), and was used to determine the desired protein concentration. The colorimetric readout was measured by a Spectrophotometer (Jenway, LAB070) at 562 nm.

2.2.18 Western blotting

Protein extracts were adjusted to equal volume using a 1X Laemmli buffer, which generated an equal amount and volume of protein extracts per sample. Based on the size of the proteins, acrylamide gel (8%, 10%, and 15%), and Criterion™ TGX Stain-Free™ Precast Gels (Bio-Rad) were used to separate the proteins. Electrophoresis was performed in freshly prepared in an 1X SDS-Page running buffer, and electrophoretic protein transfer was carried out using a wet Criterion Blotter (Bio-Rad) onto an Amersham Protran Nitrocellulose Blotting Membrane (GE Healthcare, 10600002) in a freshly prepare 1X Transfer buffer. For acrylamide gels, a 150 mins protein transfer was performed at 60V, and for precast gels, a 60 mins protein transfer was

performed at 100V with ice cubes. Protein transfer was visualised by a short incubation of Ponceau S (Sigma Aldrich) staining of nitrocellulose membrane, and blocking was performed in dried skimmed milk (5%, Marvel) with PBS-T for 1 hour at room temperature. Primary antibody incubation (**Table 3**) was performed on a tube roller (STAR LAB) at 4°C overnight, and the following day, washing was performed in PBS-T 3 times for 10 mins each. Secondary antibody (**Table 4**) was performed at room temperature for 1 hour, and a protein of interest was subsequently detected using Pierce ECL Western Blotting Substrate (Thermo Scientific, 32106) with Super RX-N film (Fujifilm). Notably, for Twist1, SuperSignal® West Dura Extended Duration Substrate (Thermo Scientific, 34076) was employed.

2.2.19 Extracellular Matrix (ECM) assay

ECM assay was performed using BD BioCoat Matrigel Invasion Chambers (BD Bioscience, 354480), and Falcon Translucent Insert (BD Bioscience, 353097) as control inserts as per the manufacture's instructions. Essentially, 50,000/well were plated in invasion and migration chambers, and 40ng/mL of both bFGF-2, and EGF were used as chemoattractant in the bottom wells. Cells were immersed in the normal culture conditions for incubation, and after 48 hours, cells were fixed using 100% methanol (pre-chilled in -20°C) for 2 mins, and stained with DAPI for 30 mins at room temperature. Images were obtained using a fluorescence microscope (Zeiss AxioImager A1), and quantification of DAPI-positive cells was undertaken using Cell Profiler with optimised pipeline. An invasion index was plotted as the number of DAPI-positive cells passing invasion chambers, divided by the number of cells passing control chambers. For the supernatant ECM assay, $5x10^6$ cells were plated onto a T75 flask with 12ml medium the day prior to the experiment to obtain sufficient materials. The following day, the medium from $PML^{+/-}$ and $PML^{-/-}$ cells was taken, and filtered through a 0.45µm cell strainer. Medium from $PML^{-/-}$ cells was used on top of PML control cells. Remaining steps were carried out as above.

2.2.20 Plasmid DNA purification

A JetStar^{TM} 2.0 Plasmid Purification Kit (Genomed) was used for purification of plasmid DNA. Desired plasmid DNA was inoculated overnight with 200ml LB

medium supplemented with 100μg/ml ampicillin (Sigma Aldrich). The following day, bacteria were concentrated by centrifugation at 12,000g for 3 mins, and supernatant was removed. Pellet was lysed in Buffer E1 (supplemented with RNase) fully until homogeneous. Cell suspension was mixed with Buffer E2 gently, with no vortex, until homogeneous, and incubated at room temperature for 5 mins. The mixture was neutralised by Buffer E3 immediately by inverting the tube up and down several times until homogeneous. Mixture separation was performed by centrifugation at 12,000g for 10 mins, and the supernatant was loaded onto an equilibrated column (using Buffer E4) to allow the DNA to be bounded by the column. Washing was performed once using Buffer E5, elution was subsequently performed using Buffer E6, and precipitation of DNA was carried out using isopropanol. Precipitate was concentrated by centrifugation at 12,000g for 30 mins, and supernatant was removed and pellet DNA was washed once with 70% ethanol at 4°C. Purified DNA pellet was air-dried at room temperature for approximately 10 mins, and dissolved in nuclease-free H_2O. DNA concentration was determined the following day by NanoDrop™ Spectrophotometers (Thermo Scientific).

2.2.21 Virus particle production

Lentivirus production was achieved using HEK 293T cells, and retrovirus production was performed using Phoenix cells. For lentivirus, $6X10^6$ HEK 293T cells were plated onto a 15cm dish with 20ml DMEM (10% FBS) at day 0. The following day, transfection (per plate) was carried out using solution containing 24ug plasmid of interest, 15.6ug pCMV-HIV-1, 7.2ug pCMV-VSV-G, 100uL $CaCl_2$ (2.5M), and 900uL H_2O. The mixture was mixed by vortexing, and equilibrated for 30 mins at room temperature. Precisely 1,000uL pre-warmed (37°C) 2X HEPES was subsequently introduced into the DNA-calcium chloride mixture, mixed by pipetting up and down, and incubated for exactly 1 min. The transfection mixture was introduced to each HEK 293T cells plate drop by drop, and the plate was stirred gently. The medium was changed after 8 hours, and after 48 hours (from the time the medium was changed), viral supernatant was collected, and subjected to polyethylene glycol (PEG) precipitation.

For retrovirus, 2.5X10^6 Phoenix cells were plated onto a 10cm dish with 10ml IMDM (10% FBS) at day 0. The following day, transfection (per plate) was performed using 20ug plasmid of interest, 1.2ug packaging plasmid (SARA III vector, Salomoni lab), 250uL $CaCl_2$ (1M), and H_2O to a final volume of 1,000ul. The mixture was mixed by vortexing, and equilibrated for 30 mins at room temperature. 1,000uL pre-warmed (37°C) 2X HEPES was subsequently introduced into the DNA-calcium chloride mixture, and mixed by pipetting up and down, and incubated for exactly 1 min. The transfection mixture was introduced to each Phoenix cell plate drop by drop, and the plate was gently stirred. The medium was changed after 8 hours, after 36 hours (from the time the medium was changed), viral supernatant was collected, and subjected to PEG precipitation.

2.2.21.1 PEG precipitation for virus particle concentration

5X PEG was prepared as described previously. PEG solution was mixed well, and heated in a microwave. The pH level was adjusted to 7.2, and the solution was autoclaved, and stored in a fridge (4°C) for long-term usage. For virus particle precipitation, supernatant was collected and centrifuged at 3,000g for 15 mins. Upper phase supernatant was filtered via a 0.45um PVDF filter to eliminate cell debris, and the supernatant was transferred to a sterile vessel, with 1 volume of cold 5X PEG added. The solution mix was refrigerated at 4°C overnight. The following day, the viral-supernatant/PEG mixture was centrifuged at 1,500g for 30 mins at 4°C. Upper phase supernatant was discarded, and residual solution was further centrifuged at 1,500g for 5 minutes at 4°C. The supernatant was carefully removed, and viral pellet was resuspended in cold PBS. Virus particles were aliquoted in PCR tubes, and stored at -80°C. Titration was determined by serial infection, and analysed by FACS (see the following paragraph).

2.2.21.2 Virus tittering by FACS analysis

Virus tittering was performed using HEK 293T cells, and the day prior to the experiment, 70,000 cells/well were plated onto a 24-well plate in a final volume of a 500µl medium. In total, 8 wells were needed for each virus: 6 wells were plated for serial dilution; and an additional 2 well were also plated, one for cell

counting prior to transduction, and one for untransduced control. The following day, 1 well was used to determine the cell number prior to transduction. Serial dilutions of the virus particles were performed using DMEM medium (+10% FBS) in eppendorf tubes, and to obtain 10^{-2} to 10^{-7} dilutions, a 2.5µl stock virus was added to 247.5µl medium for a final volume of 250µl (10^{-2} well). In next tube, 25µl of virus from 10^{-2} well was added into 225µl medium for a final volume of 250µl (10^{-3}). Serial dilutions were further performed until the 10^{-7} dilution was obtained. Following this process, the medium from 24-well was removed. Subsequently, 200µl of diluted virus particles were added to corresponding wells, leaving 1 well for untransduced control. Cells were incubated overnight at 37°C, and after 24 hours, the medium containing virus particles was removed, and replaced with fresh DMEM medium (+10% FBS). Cells were incubated at 37°C for an additional 48 hours. At 72 hours post transduction, GFP expression should range from around 100% to 0% when viewed under a fluorescent microscope. Flow cytoemetry was performed for the wells obtaining approximately 5% to 2% GFP^+ cells. The following equation was used to determine the tittering of virus:

$$T=(P \times N) / (D \times V)$$

In this equation, T is the final titer of virus (TU/ml), P is the percentage of GFP^+ cells (e.g. N = 0.2 for 20% GFP^+ cells), N is the number of cells prior to transduction, D is the dilution factor (e.g. 10^{-4} = 0.0001), and V is the volume of virus-containing medium (200µl).

2.2.22 Virus transduction of aNSCs

80,000 cells/well in a 12-well plate were plated in a final volume of 500µl medium the day prior to transduction. Cells should be approximately 60% confluent, and look healthy. The medium was changed the following morning 1 hour prior to transduction. For retrovirus transduction, 5µg/ml polybrene was added to the medium, and cells were transduced with virus using appropriate MOI (MOI1, or MOI 2) for at least 1 hour, and up to 6 hours. Virus-containing medium was removed and replaced with normal proliferation media. Ideally, viral vector carrying fluorescent reporter should be visualised under a fluorescent microscope 48 hours post-transduction, and based on the

percentage of reporter^{+} cells, cell sorting may be carried out. For viral vector containing resistance (e.g. puromycin), 72 hours post-transduction selections were performed.

2.2.23 Robo1N purification

A total of 2x10^{6} HEK 293T cells were plated onto a 10cm petri dish with 10ml DMEM medium. 20µg of pTT28-His-tagged Robo1N plasmid was transfected to obtain sufficient starting materials. After 120 hours incubation, the medium was collected, and subjected to centrifugation at 4,000g for 15 mins. Supernatant was filtered through a 0.45µm cell strainer, and purification was performed using the Ni-NTA Superflow Cartridges (QIAGEN, 30760). Essentially, a syringe (50ml) was filled with Buffer NPI-10, and the buffer was expelled by air depressing. The syringe was attached to the cartridge inlet, and the cartridge outlet stopper was removed. The cartridge was equilibrated using 10 column volumes of buffer. The syringe was then removed, and lysate was applied to the cartridge. Washing was performed by applying a fresh syringe with 10 column volumes of Buffer NPI-20, and the protein was eluted using Buffer-NPI 250, and concentrated by Amicon® Ultra Centrifugal Filters (Millipore). Protein concentration was determined by BSA assay, as described previously.

2.2.24 Statistical analysis

All values and graphs were expressed as mean ± SEM (standard error of the mean), and statistical analyses were performed using unpaired two-tailed *t* tests, unless specified (GraphPad Prism). A statistically significant difference was indicated by a P value of less than 0.05.

Chapter 3

Results

3 Results

3.1 PML loss results in reduced olfactory bulb size

Based on the data that PML loss leads to impaired cell migration in SVZ-RMS-OB route and impaired differentiation in OB (Joanne Betts), it was speculated that this process may affect the overall neuronal output displayed in OB. Therefore, the present research investigates the effect of PML loss on OB size. To test this effect, dissection and measurement of the whole brains were performed from four pairs of adult mice (6-months-old, same gender within each pair). OB size was measured and plotted as the ratio between the areas of OB and the rest of the brain using specific software solutions (see **Materials and Methods**). Interestingly, quantification revealed a significant reduction of OB size in $PML^{-/-}$ mice compared to $PML^{+/-}$ mice (**Fig. 3.1A**). Our previous work has demonstrated that PML loss leads to a smaller brain at birth, whilst adult mice display only a 10% thinning of the cortex wall, and no differences in overall brain size (Regad et al. 2009). Nonetheless, the present research aims to formally exclude the possibility that the reduced OB size was due to reduced overall brain size. Therefore, data were plotted as the rest of the brain, and OB-only (**Fig. 3.1B**). Indeed, no difference was found in size of the rest of the brain between $PML^{+/-}$ and $PML^{-/-}$ mice. However, the OB size itself was significantly smaller in $PML^{-/-}$ mice than in control mice (**Fig. 3.1B**), indicating the difference from the ratio was primarily due to the difference in OB size. In addition, and as reported previously, the phenotypes of $PML^{+/+}$ and $PML^{+/-}$ mice were undistinguishable (Regad et al. 2009). To further confirm this finding with regard to adult OB size, an additional four pairs of mice were used to conduct the measurement. As expected, no differences were found in neither in the ratio of OB size (**Fig. 3.1C**) nor the rest of brain or OB-only (**Fig. 3.1D**) between $PML^{+/+}$ and $PML^{+/-}$ mice.

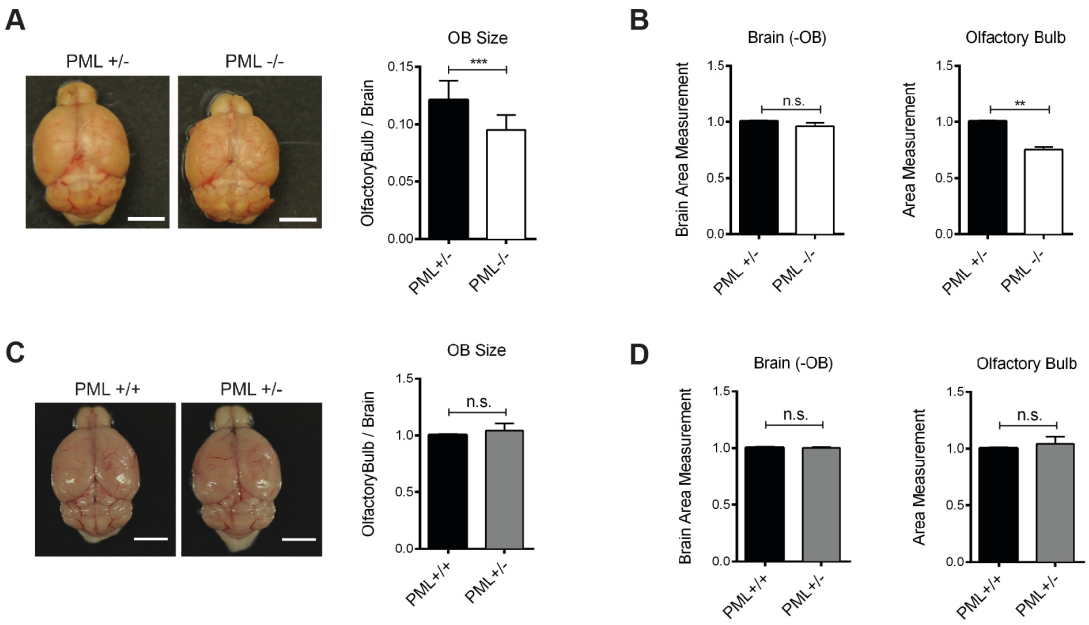

Figure 3.1: PML loss results in reduced olfactory bulb size.

(A) Representative images revealed reduced OB size in $PML^{-/-}$ mice. Histograms plot the ratio of the OB size over the rest of the brain, and the values represent mean ± SEM (n = 4; ***p < 0.001, paired ratio t-test), and scale bar = 5mm. (B) Although, a reduction in OB size had no affect on the rest of the brain (-OB) in $PML^{-/-}$ mice compared to control mice. Values represent mean ± SEM (n = 4; **p < 0.01; n.s. = non-significant, paired ratio t-test). (C), (D) Representative images and quantification revealed no difference in OB size, or in the separate measurement for the rest of the brain, and OB-only between $PML^{+/+}$, and $PML^{+/-}$ mice. Values represent mean ± SEM (n = 4; n.s. = non- significant, paired ratio t-test).

3.2 PML loss affects cell migration *in vitro*

Subsequently, the present research investigated whether the changes in cell migration observed *in vivo* could be recapitulated *in vitro*. aNSCs were used as an *in vitro* model system, as this allowed investigation of the intrinsic nature of phenotypic changes observed *in vivo,* as well as studying the underlying molecular mechanisms. Moreover, aNSCs have been suggested to acquire migratory properties in response to injury (Faiz et al. 2015). Adult NSCs (6-month) were extracted from the SVZ region, and grown *in vitro* as adherent cells (Pollard et al. 2006). These adherent NSCs could then be propagated *in vitro* with the presence of EGF and b-FGF in a defined serum-free medium (Conti et al. 2005; Pollard et al. 2006; Pollard et al. 2008). This *in vitro* system makes it possible to study a number of aNSC biological features and behaviours such as migration, proliferation, and differentiation (Reynolds and Weiss 1992; Palmer et al. 1995; Doetsch et al. 1999a; Laywell et al. 2000; Gregg and Weiss 2003). To assess the cell migration capability, extracellular matrix (ECM) transwell assays were employed (**Fig. 3.2A**). The manufacturer's conditions were amended to use 4x grow factors as chemoattractant in the bottom chamber (see **Materials and Methods**). $DAPI^{+}$ cells passing the ECM at 48 hours were captured (**Fig. 3.2B,i**), and subsequent quantification (**Fig. 3.2B,ii**) revealed that $PML^{-/-}$ cells had significantly impaired migration compared to $PML^{+/-}$ control cells (**Fig. 3.2C**). Interestingly, a similar pattern of impaired migration was observed (**Fig. 3.2D**) in cells derived from a PML knock-in mutant mouse (PML RingMut), which expresses wild-type PML, but lacks PML-NBs (Moravcsik et al. 2013), indicating that PML promotes cell migration via a PML-NB-dependent mechanism. Notably, the observed differences in cell migration through the ECM were not due to changes in cell size (~13μm for both control and PML-deficient cells).

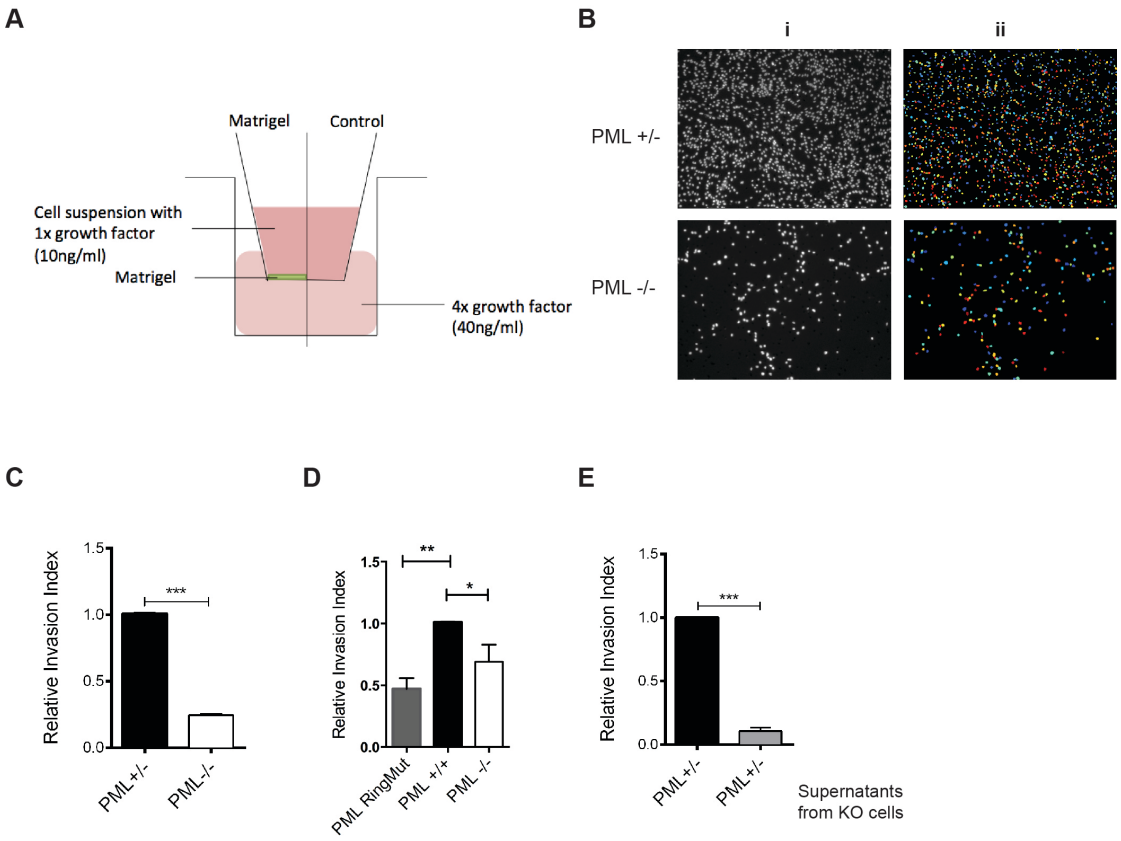

Figure 3.2: PML loss affects cell migration *in vitro*.

(A) Schematic illustration details the conditions optimised for *in vitro* ECM assay. Importantly, the Matrigel, and control inserts were placed into separate wells based on experimental design. (B) (i) Representative images illustrate DAPI^{+} cells passing the ECM at the 48h time point; (ii) Representative images illustrate the quantification of DAPI^{+} cells using Cell Profiler with optimised pipeline outlining the cells. (C) ECM assay revealed impaired migration upon PML loss compared to PML$^{+/-}$ cells. Values represent mean ± SEM (n = 3; ***p < 0.001, unpaired t-test). (D) ECM assay revealed impaired migration in PML RingMut, and PML$^{-/-}$ cells compared to PML$^{+/+}$ cells. Values represent mean ± SEM (n = 3; *p < 0.05; **p < 0.01, one-way ANOVA). (E) ECM assay using supernatants from PML$^{-/-}$ cells on top of PML$^{+/-}$ cells revealed a similar migration-compromised pattern as observed in PML$^{-/-}$ cells. Values represent mean ± SEM (n = 3; ***p < 0.001, unpaired t-test).

However, the observed differences could not only be due to changes in intracellular signalling pathways controlling cell movement, but also to altered secretion of factors affecting cell migration in an autocrine or paracrine fashion. To test this hypothesis, we set up ECM assays based on incubation with supernatants from control or PML-deficient cells (see **Materials and Methods**). Supernatants from PML$^{-/-}$ cells (cultured for 24 hours before experiment)

severely impaired migration of $PML^{+/-}$ cells (**Fig. 3.2E**), indicating that soluble factors could influence the defect migration upon PML loss in an autocrine or paracrine fashion.

3.3 Discussion

Previous work from our lab has demonstrated the role of PML in embryonic CNS neurogenesis, with implications for regulation of neural stem/precursor cell fate, and cortex development and size (Regad et al. 2009) (see **Fig. 1.9**). However, the role of PML in adult neurogenesis has remained unexplored. Supporting data produced by Joanne Betts demonstrates that PML is expressed in aNSCs derived from SVZ, as well as in type C cells and migrating neuroblasts in RMS, although its expression gradually decreases alongside differentiation. This finding indicated the potential roles of PML in aCNS stem cells and SVZ-RMS-OB neurogenesis, in addition to its role during embryonic CNS development. Indeed, PML loss leads to increased proliferation of aNSCs both *in vivo,* and *in vitro* (**Fig. 1.10G & K, i**). It has also been demonstrated that PML interacts with pRb and p53 to control cell growth (Alcalay et al. 1998; Fogal et al. 2000; Guo et al. 2000; Pearson et al. 2000; Salomoni and Pandolfi 2002; Vernier et al. 2011; Acevedo et al. 2016). In this respect, previous work from our lab has demonstrated that PML regulates embryonic neurogenesis through its ability to control phosphorylation level of pRb in NPCs (Regad et al. 2009). Also in adult settings, phosphorylation levels of pRb were increased in $PML^{-/-}$ cells compared to $PML^{+/-}$ cells (Joanne Betts, **Appendix 1. A**). Interestingly, re-expression of PML-I isoform in PML-deficient cells inhibited pRb phosphorylation, and led to reduced proliferation (**Appendix 1. B**). In contrast, a PML mutant lacking the RING domain, and unable to form PML-NBs had no effect. Furthermore, PP1α and pRb colocalise in PML-NBs in WT cells, but not in PML-deficient cells (**Appendix 1. C**). Finally, p53 and p21 protein levels were decreased in $PML^{-/-}$ cells (**Appendix 1. D**), indicating that the observed increase in proliferation upon PML loss may also partially depend on p53.

It has been demonstrated that the turnover rate of OB neurons is from at least 10,000 cells per day to 80,000 per day (Kaplan et al. 1985; Lois and Alvarez-

Buylla 1994). Our findings have demonstrated that PML loss reduced the number of migratory neuroblasts in the RMS region proximal to OB, and reduced the number of *de novo* generated, mature neurons production in OB. Notably, there was no difference in cell death observed by active caspase-3 staining between $PML^{+/-}$ and $PML^{-/-}$ in RMS migration (Joanne Betts, data not shown), excluding the possibility that reduced migration was due to enhanced level of cell death. Future experiments could be performed by measuring the thickness of RMS, as a previous study has demonstrated that after removal of OB, chain migration continued along the RMS but the RMS increased in volume (Kirschenbaum et al. 1999). Therefore, an observation of a thicker and bigger RMS in $PML^{-/-}$ mice would be expected.

Due to the reduction in OB size, it would be also be worthwhile investigating the functional consequences of this impairment. It has been demonstrated that the ability to discriminate between two distinct odorants is not affected by impairment in adult OB neurogenesis (Imayoshi et al. 2008a; Lazarini et al. 2009). However, a number of other phenotypes have been reported, including the detection threshold of an odorant, short-term and long-term olfactory memory, and perceptual learning ability (Breton-Provencher et al. 2009; Moreno et al. 2009; Valley et al. 2009; Sultan et al. 2010). Therefore, it could be investigated if these functions are affected between PML control and PML-deficient mice, as this research may provide more information about the potency of the effect of OB neurons replacement in adulthood. In addition, mating behaviour may also be affected in $PML^{-/-}$ mice, as a previous study has demonstrated that intact olfactory input is essential in masculine sexual behaviour in male mice (Rowe and Edwards 1972). Furthermore, it has also been reported that approximately 50% of the newborn OB neurons are eliminated one month after reaching the OB due to programmed cell death (Winner et al. 2002). Therefore, it would be interesting to also study the survival of newborn OB neurons and how effectively integrate into the existing circuit.

As discussed in Introduction, a plethora of factors that regulate RMS cell migration *in vivo* have been well established, making it difficult to propose if this defect is due to NSC-intrinsic behaviour using a germline model in which all cells are PML-deficient. Therefore, the present study uses an *in vitro* system for isolation, and propagation of NSCs, which allowed the intrinsic nature of the

cell migration phenotype to be studied, and mechanistic studies to be performed (see below sections from **3.7**). Notably, the impaired cell migration upon PML loss could be recapitulated *in vitro* using ECM assay. Moreover, it seems PML depends on intact PML-NBs to promote migration, because PML RingMut cells displayed a similar pattern of migration defects observed in PML-deficient cells. Future experiments could be conducted by staining migratory neuroblasts (DCX^+) in PML RingMut RMS in comparison to PML control, and PML-deficient mice to confirm this phenotype *in vivo*, as well as measuring the OB size in PML RingMut mice to confirm the phenotypic changes.

Interestingly, the ECM assays based on the addition of supernatants from control, and PML-deficient cells revealed the potential involvement of soluble factors in regulating NSC migration *in vitro*, providing guidance to identify the underlying mechanisms. As described in the Introduction, the SVZ-RMS-OB migration is regulated by a summation of different factors, including cell-cell, and cell-ECM interactions, as well as the chemoattractant or chemorepulsive factors. Supernatants ECM assay from the present study suggests that soluble factors secreted from $PML^{-/-}$ aNSCs may contribute to the migration defect. Indeed, soluble factors have been implicated in regulating migration from SVZ to OB. For example, within the SVZ niche, the contact with CSF via ependymal cilia, and single cilium from type B1 cells is central for sensing the systemic factors circulating around and through CSF (Doetsch et al. 1999b; Alvarez-Buylla and Garcia-Verdugo 2002; Bond et al. 2015). Interestingly, aberrant cilia formation from mutant mice leads to defective migration from SVZ to RMS (Sawamoto et al. 2006), suggesting that contact with the CSF, and the soluble factors therein, are important in mediating cell migration. Moreover, it has been suggested that along the journey of RMS migration, the directional migration is guided partially through secreted factors from the septum (opposing the direction of RMS migration), or OB (Hu and Rutishauser 1996; Coskun and Luskin 2002; Sun et al. 2010), reinforcing the contribution of secreted factors to cell migration in the SVZ/RMS/OB route.

Finally, supporting data (Joanne Betts) has suggested that PML loss leads to increased entry into differentiation, but an impaired production of mature neurons in vitro (Fig. 1.10L), suggesting the phenotypic changes in response to PML in vivo could be caused by a combination of different mechanisms, such

as aberrant migration and/or altered differentiation (further discussed below page 106 and page 116).

3.4 PML loss affects expression of axon guidance regulators

Next, the present study investigated the molecular mechanisms underlying the defect in cell migration. As discussed previously, ECM supernatants assay suggests soluble factors may be involved in migration phenotype. The long migratory route that cells within the SVZ-RMS-OB niche need to follow during differentiation requires a tight control by both intrinsic, and extrinsic factors (Lois and Alvarez-Buylla 1994; Mason et al. 2001; Lim and Alvarez-Buylla 2016). OB, and other structures, such as septum, are known to secrete signals guiding chain migration (Hu and Rutishauser 1996; Coskun and Luskin 2002; Sun et al. 2010). However, an interesting study demonstrated that RMS migration was not affected upon removal of OB in the short-term (Kirschenbaum et al. 1999), indicating that gradients of factor secreted by the OB alone are not sufficient to support SVZ to OB migration. Notably, it has been reported that migrating neuroblasts secrete chemorepulsive signal Slit (Nguyen-Ba-Charvet et al. 2004; Kaneko and Sawamoto 2007; Eom et al. 2010; Kaneko et al. 2010), and Slit1 is essential in regulating neuronal migration in adult SVZ-RMS-OB, whereas Slit1 and Slit2 are vital in the developing forebrain (Hu 1999; Wu et al. 1999; Nguyen-Ba-Charvet et al. 2004; Yeh et al. 2014).

Therefore, a panel of genes encoding soluble factors/receptors that are known to regulate migration in the CNS (e.g. Slit/Robo family members) (**Fig. 3.3A**), as well as more generally genes involved in regulation of cell migration, including metalloproteinases (MMP3, MME), and epithelial-mesenchymal transition factors (Scratch 1, E-cadherin, Twist1, Snail1, N-Cadherin, Fra1, Zeb2) (**Fig. 3.3B**) were checked by qPCR. Interestingly, among these genes, the Slit2 gene was found to be significantly upregulated in PML-deficient cells compared to $PML^{+/-}$ cells (**Fig. 3.3A**), and this observation was consistent in independent NSC preparations. Moreover, Slit2 was found upregulated (albeit not statistically significant due to variations between repeats, see **Appendix 6. A** for details) in PML RingMut cells, displaying a similar pattern as observed in $PML^{-/-}$ cells (**Fig. 3.3A**), indicating the requirement of PML-NBs in repression of Slit2. In addition, Robo1, the cognate receptor of Slit2, was also found upregulated in $PML^{-/-}$ cells (**Fig. 3.3C**). As discussed in the Introduction, the high affinity binding of Slit1 to Robo inhibits RMS cell migration in the adult

brain (Nguyen-Ba-Charvet et al. 2004), and further discussion on the literature can be found below. However, though highly expressed in NSCs (not shown), no alterations in expression of the ligand Slit1 and its cognate receptor Robo2 were found in either germline PML KO, or PML KI cells (**Fig. 3.3C**). Notably, the upregulation of Slit2 in PML$^{-/-}$ cells was also confirmed at the protein level (**Fig. 3.3D**).

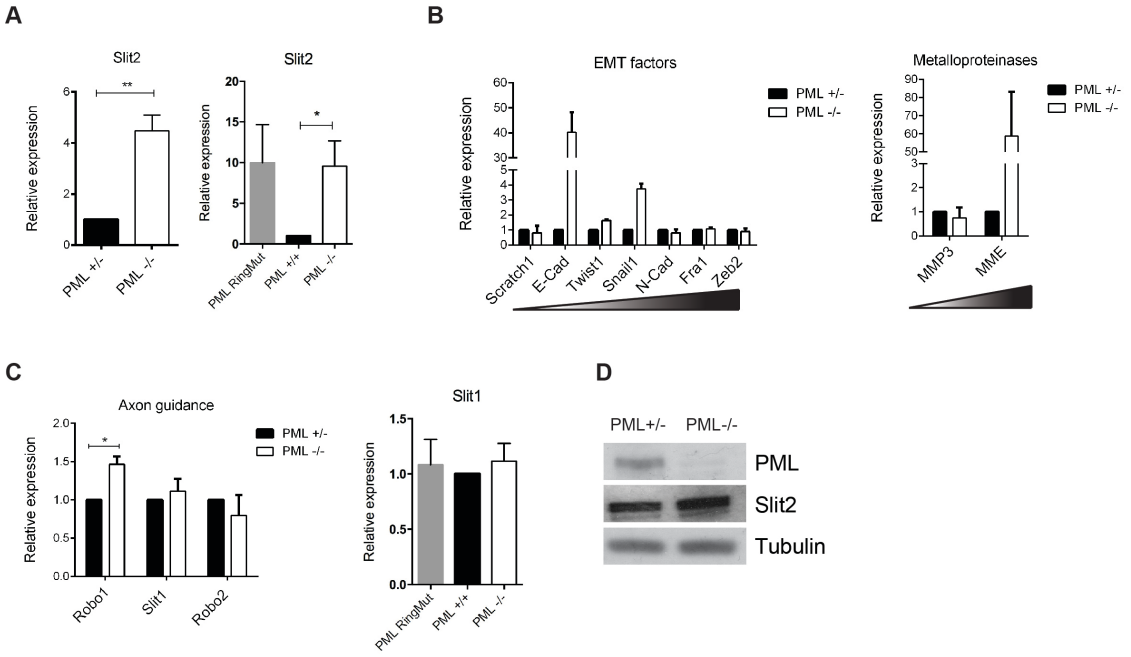

Figure 3.3: PML loss affects expression of axon guidance regulators.

(A) qPCR analysis demonstrated upregulation of Slit2 in PML-deficient cells, as well as in PML RingMut cells. Values represent mean ± SEM (n = 3; *p < 0.05; **p < 0.01, unpaired t-test). (B) qPCR analysis of expression pattern of EMT-related genes, and metalloproteinases genes. Genes were arranged from left to right based on their expression level (from low to high). (C) qPCR analysis revealed the expression pattern of Slit2 receptor, Robo1, and Slit1/Robo2 (the other ligand-receptor). A similar expression pattern was found in PML RingMut cells. Values represent mean ± SEM (n = 3; *p < 0.05, unpaired t-test). (D) Representative Western blotting (WB) analysis confirmed upregulation of Slit2 protein in PML$^{-/-}$ cells compared to PML$^{+/-}$ cells. Tubulin was used as loading control.

To determine whether these changes could be repeated upon acute PML loss, a PML conditional knockout (KO) system ($PML^{F/F}$) generated by our lab was used. Essentially, the PML exon3 is flanked by two loxP sites, enabling recombination via introduction of Cre recombinase (**Fig. 3.4A**). SVZ NSCs were isolated and propagated from $PML^{F/F}$, and control ($PML^{F/W}$) mice and cells were transduced with p-MIG-Cre-ERT2-GFP virus. Acute PML loss could be achieved by treatment with 4-hydroxytamoxifen (4-OHT), as detected by DNA recombination (**Fig. 3.4B**), and protein degradation (**Fig. 3.4C**). Utilising this system, Slit2 upregulation was confirmed in 4-OHT-treated $PML^{F/F}$;CreERT2 cells upon acute PML loss both at mRNA (**Fig. 3.4D**), and protein level (**Fig. 3.4E**).

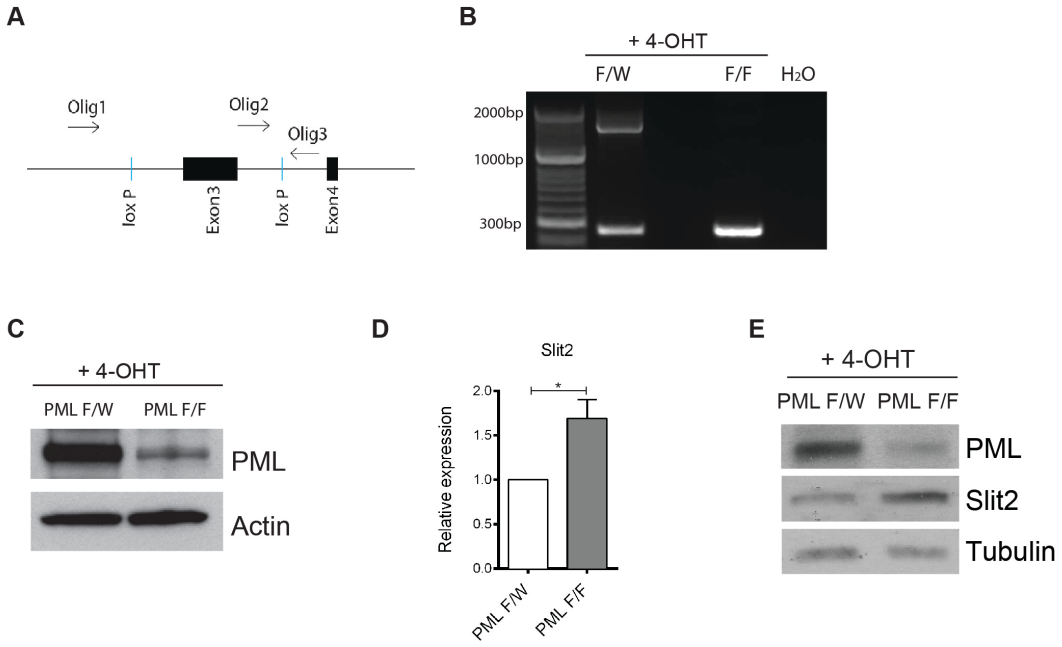

Figure 3.4: PML acute loss affects Slit2 expression.

(A) Schematic illustration demonstrates that exon3 of PML is flanked by two loxP sites, with dedicated oligos to amplify specific bands for genotyping. (B) Gel electrophoresis illustrates recombined band (~300bp) upon 4-hydroxytamoxifen (4-OHT) treatment amplified by defined oligos. (C) WB analysis confirmed conditional deletion/disruption of PML upon 4-OHT treatment. β-Actin was used as loading control. (D) qPCR analysis revealed upregulation of Slit2 in response to 4-OHT treatment-induced acute PML loss. Values represent mean ± SEM (n = 3; *p < 0.05, unpaired t-test). (E) WB analysis confirmed upregulation of Slit2 upon acute PML loss. Tubulin was used as loading control.

3.5 Slit/Robo signalling is required for PML-mediated regulation of cell migration

It was subsequently investigated whether PML promotes cell migration through repression of Slit2/Robo1 signalling. Therefore, attempts were made to knock down Slit2 using small interfering RNA hairpins (shRNA). All available (7) pGIPZ lentiviral shSlit2 clones from Cancer Institute shRNA core facility were produced as high-titer lentiviral supernatants, and transduced into $PML^{+/-}$ and $PML^{-/-}$ cell (see **Materials and Methods**), using a Scramble (Scrbl) sequence as control. Unfortunately, none effectively silenced Slit2 in $PML^{-/-}$ cells (**Fig. 3.5**). Based on a previous study (Wu et al. 1999), I employed Robo1N, a truncated mutant form of Robo receptor lacking the intracellular domain that functions as a decoy receptor via competitive binding to Slit2 (Patel et al. 2012), and blocking its association with Robo1 on the cell surface. I assisted Valeria Amodeo, a postdoctoral researcher in the lab, with experiments using this system.

An ECM assay utilising recombinant Slit1 (rSlit1), and Slit2 (rSlit2) proteins was performed to determine whether Slit proteins affected cell migration in aNSCs, and if so, which ones. rSlit1 had no effect on cell migration in either $PML^{+/-}$, or $PML^{-/-}$ cells (**Appendix 2. A**). However, rSlit2 impaired migration in $PML^{+/-}$ cells, but this effect was not further exacerbated in $PML^{-/-}$ cells, suggesting that PML works through repression of Slit2 (**Appendix 2. A**). To formally demonstrate that Slit2 was required for the effect of PML loss on cell migration, a His-tagged Robo1N form from transfected HEK 293T was isolated using affinity purification based on nickel columns (see **Materials and Methods** for further details). Robo1N successfully rescued the migration defect of $PML^{-/-}$ cells, and this effect was abolished by the addition of rSlit2 (**Appendix 2. B**), suggesting that not only is Slit2 (not Slit1) the main factor in regulating cell migration in aNSCs, but this repulsive effect is also mediated through its cognate receptor Robo1. This finding provides important insight into the novel role of Slit2 in adult CNS cell migration. Collectively, these data suggest that PML regulates cell migration via repression of Slit2/Robo1 signalling.

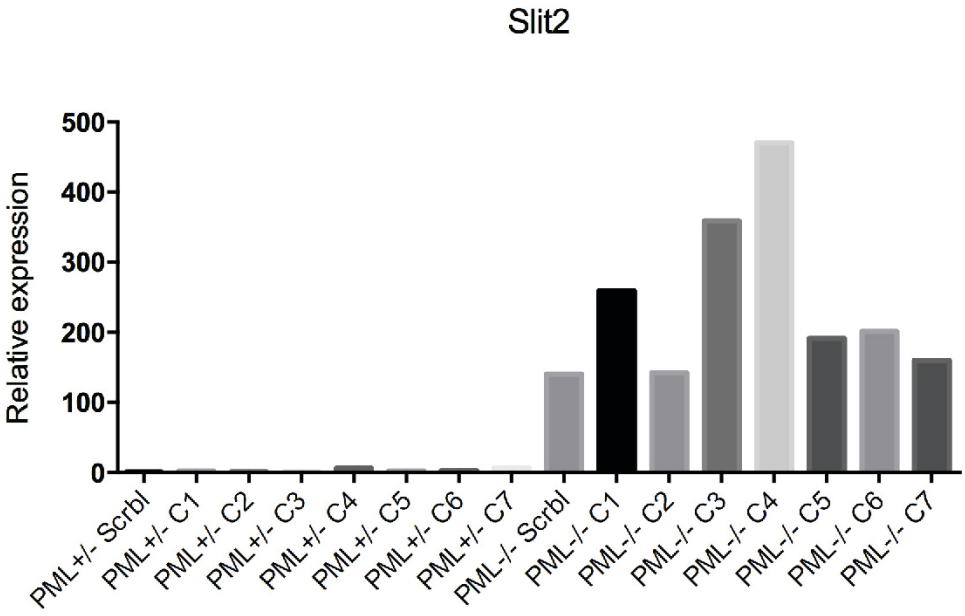

Figure 3.5: Unsuccessful Slit2 knockdown using small interfering RNA hairpins.

qPCR analysis revealed unsuccessful Slit2 knockdown in $PML^{-/-}$ cells using pGIPZ lentiviral shRNA. C1-C7: clone 1 to clone 7 for shSlit2 (see Materials and Methods for more information).

3.6 Discussion

As discussed previously in the Introduction (page 35; page 37), a number of chemotropic factors regulate adult neurogenesis, and RMS migration. The defect in cell migration upon PML loss could be repeated *in vitro* using ECM assay, and importantly, ECM assays based on supernatants derived from control or KO cells revealed the potential involvement of soluble factors in this respect. In the present study, the chemorepulsive glycoprotein Slit2, and its cognate receptor Robo1, were shown to be significantly upregulated in SVZ aNSCs upon PML loss. Importantly, Slit2 upregulation was confirmed in two different genetic models (PML germline KO and PML conditional KO), and mouse strains (129sv and C57BL/6), reinforcing the argument that Slit2 is indeed a target of PML. Slit proteins, and Robo receptors were originally implicated in axon guidance during development (Brose et al. 1999; Long et al. 2004; Blockus and Chedotal 2014). In addition, when considering CNS neurogenesis in rodent, both Slit1 and Slit2 (Bagri et al. 2002), and both Robo1 and Robo2 (Lopez-Bendito et al. 2007), have been involved in axonal pathfinding in the forebrain. Furthermore, Slit and Robo have been found to regulate cell migration, as well as cell proliferation in CNS both in embryonic, and adult neurogenesis (Hu 1999; Li et al. 1999; Wu et al. 1999; Nguyen-Ba-Charvet et al. 2004; Andrews et al. 2006; Andrews et al. 2008; Kaneko et al. 2010; Borrell et al. 2012; Blockus and Chedotal 2014). Interestingly, Slit1 has been reported to impede RMS cell migration toward the OB in the adult brain (Nguyen-Ba-Charvet et al. 2004), but the role of Slit2 in this context was not explored. The present research demonstrates that Slit2 represses cell migration in aNSCs, suggesting that Slit2 can be a key mediator of the cell migration phenotype observed in PML-deficient cells. Moreover, there may be a context-dependent expression manner to consider, as Slit1 has been observed to be expressed, and to play a role in neuroblast cells, whereas, based on our results, Slit2 could be NSC-specific in the adult brain. To test this hypothesis, ongoing experiments using established *in vitro* neuroblasts migration assay (O'Leary et al. 2015) would provide more evidence of this claim.

As detailed in the Introduction (page 23 and **Fig. 1.2** page 25), PML interacts with pRb and p53, with implications for growth and tumour suppression

(Salomoni and Pandolfi 2002). Moreover, it has been demonstrated that in embryonic neurogenesis, PML partially regulates cell fate via control of pRb phosphorylation in eNPCs (Regad et al. 2009). Our unpublished data reveal that PML loss also results in hyperphosphorylation of pRb in aNSCs, (Joanne Betts, **Appendix 1. A**). Therefore, it can be hypothesised that PML could regulate migration in a cell cycle-dependent manner. In addition, as shown before that PML indirectly stabilises p53 protein levels (**Appendix 1.D**) by preventing Mdm2-dependent p53 degradation (**Fig. 1.2**), it is therefore possible that the migration phenotype is also dependent on p53.

However, expression of SV40 LargeT, which inhibits both pRb, and p53 in $PML^{+/-}$, and $PML^{-/-}$ cells, affects proliferation (**Appendix 4. A**), whilst it enhanced rather than decreased cell migration (**Appendix 3. A**, **B; work performed by Valeria Amodeo**). This finding is in line with the expression pattern of Slit2 upon SV40 LargeT expression, in which Slit2 expression was unaffected in $PML^{+/-}$ cells, and was augmented in $PML^{-/-}$ cells (**Appendix 3. C**). These data suggest that PML controls aNSCs migration through Slit2/Robo1 independently of its role in controlling cell proliferation, and the migration defects upon PML loss is independent of pRb, and p53.

To determine whether PML controls cell migration through repression of Slit2, gene knockdown experiments were initially performed. However, as discussed above, it seemed all the available pGIPZ clones failed to knock down Slit2. Due to limited time, additional gene silencing strategies were not employed (e.g. CRISPR/Cas9). A previous study utilised Robo1N, a mutant form of Robo receptor lacking transmembrane and intracellular domains, to competitively inhibit Slit/Robo signalling (Wu et al. 1999). Based on the work by Wu et al. (1999), and a recent study using Robo1N to disrupt Slit2/Robo1 pathway (Patel et al. 2012), experiments in the present study were designed employing Robo1N to determine if Slit2 acts downstream PML to inhibit migration. In support of the hypothesis stated in the present study, Robo1N rescued the migration in PML-deficient cells, and this effect was abolished by addition of rSlit2. Interestingly, no effect was observed upon addition of rSlit1, reinforcing the proposal that Slit2, not Slit1, underlies the migration defects upon PML loss in aNSCs. Notably, it was rSlit2, not rSlit1, impaired migration phenotype in PML control cells (**Appendix. 2A**), suggesting Slit2 is the target responsible for

migration phenotype downstream PML. However, addition of both rSlit1 and rSlit2 in $PML^{-/-}$ cells seemed to rescue migration phenotype (statistically significant, **Appendix. 2A**). If the quantification inconsistency could be ruled out (as no statistical significant was shown in **Appendix. 2B** with respect to rSlit2 in $PML^{-/-}$ cells), this could be due to a potential negative feedback loop between Slit family members in the context of PML loss, as excessive amount of Slit1 could repress Slit2 pathway, thus ameliorating migration, and forced addition of Slit2 in $PML^{-/-}$ cells could also trigger the "Slit burden" in the cell (see also page 140 in GBM settings).

Ultimately, these results identify a novel axis, whereby the growth suppressor PML controls cell migration via repression of Slit2. Therefore, future *in vivo* work could be designed to investigate RMS migration/OB size via modulation of Slit2 expression/activity. A method currently being established in our lab, *in utero* or early postnatal electroporation of NSCs (Pathania et al, manuscript in preparation), would allow others in the lab to express Robo1N in $PML^{-/-}$ and control mice (or tamoxifen-treated $PML^{f/f}$;NestinCreERT2 mice, currently available in our colony), and analyse whether the phenotype could be reverted upon inhibition of Slit2 signalling. Because a previous study has demonstrated that Slit1 is the principal factor in impeding neuroblast migration (Nguyen-Ba-Charvet et al. 2004), it would also be rational to include Robo2N to test whether Slit1 and Slit2 function cooperatively in these settings. Similar experiments could be conducted by using shRNAs against Slit1 or Slit2, or gRNA sequences along with Cas9.

It cannot be excluded that the role of Slit2/Robo1 depends on the developmental stage, given that one study has demonstrated Robo1 mutant mice displayed smaller OB size at E18.5 (Borrell et al. 2012), indicating a pro-migratory (instead of anti-migratory) or pro-differentiation function of Slit2/Robo1 signalling during development. Therefore, crossing a Slit2 conditional KO mouse line with NestinCreERT2 mice would enable researchers to monitor the effect of Slit2 loss at postnatal stages.

3.7 The EMT factor Twist1 regulates Slit2 expression downstream PML

Mechanisms underlying PML-mediated regulation of Slit/Robo signalling were investigated next. Among the genes that were differentially expressed upon PML loss (see **Fig. 3.3 A&B**), the transcription factor Twist1 was upregulated in $PML^{-/-}$ cells (**Fig. 3.6A**), as well as in PML RingMut cells (**Fig. 3.6B**), whilst its RNA levels were almost undetectable in control cells. Further validation was subsequently performed using immunoblotting, which demonstrated marked induction of Twist1 in $PML^{-/-}$ cells (**Fig. 3.6C**), and PML RingMut cells (**Fig. 3.6D**). However, in $PML^{+/-}$ and $PML^{+/+}$ cells, Twist1 was not detected [in accordance to qPCR data (Ct > 35)]. It is important to note that at Twist1 was marginally regulated by PML at early passage (passage<3), while its RNA and protein levels became undetectable in control cells in later passage. Moreover, when compared with $PML^{-/-}$ cells, Twist1 expression was over-amplified in PML RingMut cells, leading to an induction for more than 60-fold. One can speculate that PML RingMut has a selection preference towards cells overexpressing Twist1.

Twist1 belongs to the bHLH family of transcription factors (Imayoshi and Kageyama 2014), and is a master regulator of epithelial-to-mesenchymal transition (EMT) (Yang et al. 2004), which is a crucial process contributing to neural crest development as well as to the onset and progression of tumour spreading (metastasis) (Thiery 2002; Kalluri and Weinberg 2009; Thiery et al. 2009) (further discussed below page 113). However, there is no existing literature investigating the expression, or functions of Twist1 in aNSCs. I investigated other genes involved in EMT, and associated either directly or indirectly with Twist1, including the “cadherin switch” genes E-cadherin, N-cadherin (Wheelock et al. 2008), Scratch1 (Itoh et al. 2013), Snail, and Zeb (Peinado et al. 2007; Xu et al. 2009; Lamouille et al. 2014) and Fra1 (Caramel et al.) (**Fig. 3.3B**). EMT regulators interact with each other, and it is known that Snail1 is able to induce Twist1 (Peinado et al. 2007; Xu et al. 2009; Lamouille et al. 2014), and Twist1 is required to maintain EMT upon Snail1-induced EMT initiation (Tran et al. 2011), indicating a functional feedback loop between the EMT transcription factors. This is in line with the data that Snail1 was upregulated earlier than Twist1 upon PML loss at early passage (**Fig. 3.3B**).

Notably, although E-cadherin was found upregulated in PML$^{-/-}$ cells compared to PML$^{+/-}$ cells, its expression levels in general were remarkably low according to the Ct values (> 33). In contrast, the mesenchymal marker N-cadherin, Snail, and Zeb were found highly expressed, but levels were not affected by PML loss.

Although Twist1 is predominantly a transcriptional repressor, and an inducer of cell migration, its role in the context of aNSCs had not been studied previously. To investigate this, gene knockdown experiments using pGIPZ vectors expressing shTwist1 or Scrbl shRNAs in both PML-deficient and control cells were performed. Upon GFP-cell sorting, it could be demonstrated that Twist1 was successfully silenced in PML$^{-/-}$ cells to a considerable degree (**Fig. 3.7A;** its expression is almost undetectable in control cells). Surprisingly, Slit2 and Robo1 expression levels were downregulated upon Twist1 KD in PML-deficient cells (**Fig. 3.7B**), suggesting Twist1 may act as a transcriptional activator of Slit2 and Robo1 downstream PML loss. To further evaluate the functional consequences of Twist1 KD, ECM assays were performed. Interestingly, Twist1 KD rescued cell migration in PML-deficient cells (**Fig. 3.7C**), in accordance with the observed Slit2 and Robo1 downregulation (**Fig. 3.7B**).

To investigate if Twist1 upregulation may underlie other phenotypic changes observed upon PML loss in addition to cell migration, cell proliferation upon Twist1 KD in PML-deficient cells was analysed. Quantification of Edu^{+} cells revealed that proliferation decreased to control levels in PML$^{-/-}$ cells upon Twist1 KD (**Fig. 3.7D**), suggesting that Twist1 acts downstream PML loss to positively regulate adult NSCs proliferation, as well as cell migration. Work by Joanne Betts and Valeria Amodeo (see **Appendix 4**) has demonstrated a correlation between increased proliferation, and induction of γH2AX^{+} DNA damage foci upon PML loss *in vitro,* and *in vivo*, as an index of replicative stress (further discussed below). Quantification of percentage of dense foci (>10 foci) revealed a decreased level of γH2AX foci formation upon Twist1 KD (**Fig. 3.7E**), which was in line with the reduction in proliferation rate. Furthermore, because work from Joanne Betts demonstrated that PML-deficient cells display an intrinsic defect in differentiation (**Fig. 1.10L**), *in vitro* differentiation assay was subsequently employed to assess the differentiation pattern in the context of Twist1 KD. To this end, aNSCs were plated on laminin-

coated coverslips supplemented with normal proliferation media at day 0. EGF and b-FGF were sequentially removed to trigger differentiation, and cells were kept in a defined differentiation media until day 8 (see **Materials & Methods** page 81). Interestingly, quantification of βIII-tubulin^{+} and GFAP^{+} cells (**Fig. 3.7F**) revealed that Twist1 KD did not revert the differentiation changes observed in PML-deficient cells.

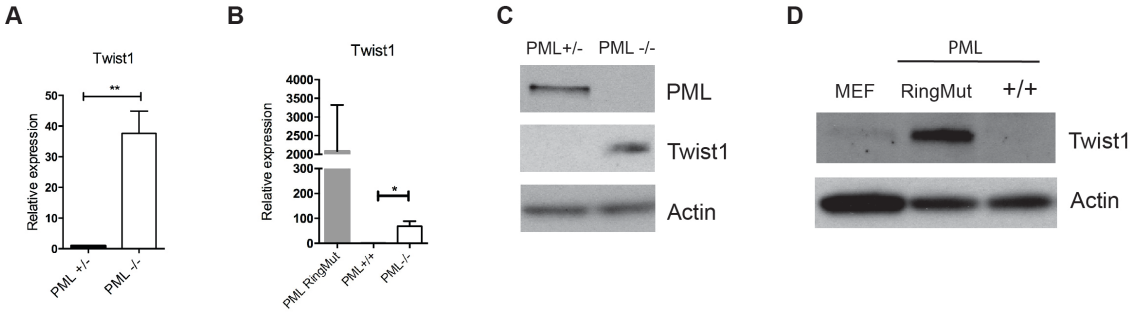

Figure 3.6: EMT factor Twist1 is expressed in aNSCs and repressed by PML.

(A) Twist1 was found consistently upregulated in PML$^{-/-}$ cells, and (B) massively in PML RingMut cells. Values represent mean ± SEM (n = 3; *p < 0.05; **p < 0.01, unpaired t-test). (C) WB analysis confirmed Twist1 expression at protein level in adult NSCs in response to PML loss, and (D) in PML RingMut. Mouse embryonic fibroblast (MEF) extract was used as positive control for Twist1, and β-Actin was used as loading control.

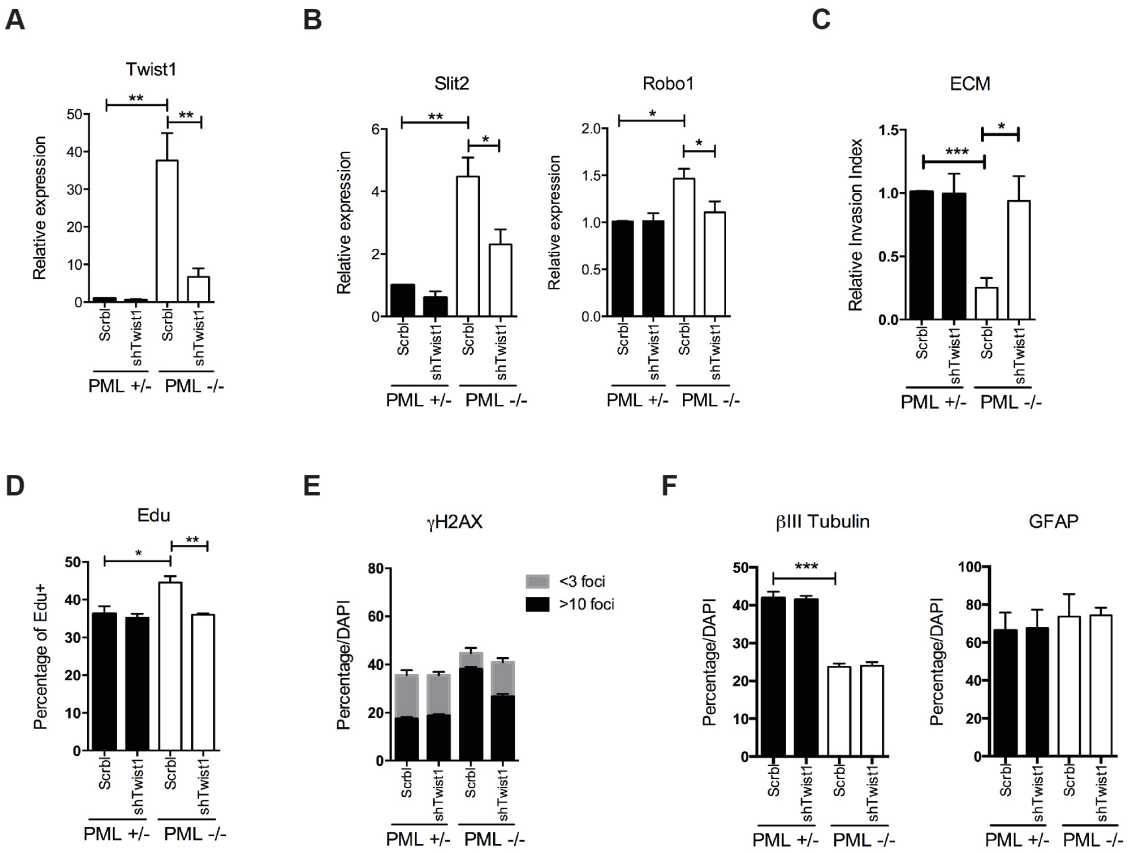

Figure 3.7: Twist1 regulates Slit2 expression downstream PML and play a role in migration and proliferation phenotypes.

(A) qPCR confirmed Twist1 knockdown (KD) in PML$^{-/-}$ cells. Values represent mean ± SEM (n = 3; **p < 0.01, unpaired t-test). (B) qPCR analysis revealed that Slit2/Robo1 expression was affected downstream upon Twist1 KD. Values represent mean ± SEM (n = 3; *p < 0.05; **p < 0.01, unpaired t-test). (C) ECM assay revealed rescued migration capability upon Twist1 KD. Values represent mean ± SEM (n = 3; *p < 0.05; ***p < 0.001, unpaired t-test). (D) Edu assay demonstrated impaired proliferation upon Twist1 KD, and phenocopying PML control cells. Values represent mean ± SEM (n = 3; *p < 0.05; **p < 0.01, unpaired t-test). (E) Quantification of γH2AX foci revealed a decreased level of foci formation (> 10 foci) upon Twist1 KD. Foci formation was subdived into two groups: less than 3 foci or nuclei (< 3 foci), and greater than 10 foci or nuclei (> 10 foci). Values represent mean ± SEM (n =3). (F) Quantification of differentiation assay revealed cell fate specification was not affected by Twist KD. Values represent mean ± SEM (n = 3; ***p < 0.001, unpaired t-test).

3.8 Discussion

Our findings demonstrate that Twist1 is involved in regulation of cell migration, and proliferation downstream PML. As previously detailed, Twist1 is the master regulator of EMT, a biological process that contributes to normal development, wound healing, tissue fibrosis, and cancer progression (Kalluri and Weinberg 2009; Thiery et al. 2009), and its reverse process is termed mesenchymal-epithelial transition (MET) (Kalluri and Weinberg 2009; Thiery et al. 2009). Essentially, the EMT programme during tumour invasion and metastasis involves several sequential steps, including dissociation from primary tumour site, spreading into the circulation system (blood vessels/lymphatic system), dissemination into distant organs, and establishment as a secondary tumour (Yang et al. 2004; Thiery et al. 2009; Hanahan and Weinberg 2011).

EMT transition is accompanied by the downregulation or loss of epithelial marker genes (e.g. E-cadherin), and upregulation of mesenchymal maker genes (e.g. N-cadherin) (Lamouille et al. 2014), indicating the essential role of molecular signature in this event. Notably, one of the hallmarks of EMT is “cadherin switch”, by which downregulation of E-cadherin, and upregulation of N-cadherin foster the dissociation with epithelia, and subsequent transition into pro-migratory/pro-invasive mesenchymal cells (Wheelock et al. 2008; Lamouille et al. 2014).

As discussed, Twist1 belongs to the family of bHLH transcription factors, some of which have been previously implicated in cell fate determination, and lineage specification in CNS stem cells (Imayoshi and Kageyama 2014). For instance, Ascl1 promotes neuronal differentiation during embryonic neurogenesis (Parras et al. 2002; Schuurmans and Guillemot 2002; Parras et al. 2004; Urban and Guillemot 2014). In proliferating aNSCs (from DG within SGZ), Ascl1 protein is destabilised by E3-uniquitin ligase Huwe1, with the latter being required for inducing a quiescent state in proliferating aNSCs, and thus protecting them from exhaustion (Urban et al. 2016). Moreover, accumulated Ascl1 promotes aNSCs proliferation in Huwe1 WT mice via activation of Cyclin D1/D2 (Urban et al. 2016).

Twist1 was found expressed in neurons in embryonic/foetal human brain (Elias et al. 2005), suggesting potential involvement of Twist1 in neurogenesis.

However, to our knowledge, its role in CNS stem cells is unknown. Findings from the present study suggest that Twist1 may be involved in CNS neurogenesis, and that it is repressed by PML to undetectable levels. Notably, neural crest-derived stem cells (NCSCs) are multipotent, self-renewing cells in peripheral nervous system (PNS) (Binder et al. 2011). At the molecular level, NCSCs differ from NSCs by the expression of distinct marker genes, including Sox10 and p75, and can be reprogrammed through direct transdifferentiation from PNS to CNS stem cells (Binder et al. 2011; Weber et al. 2015). Interestingly, NCSCs derived from mouse palate do not induce CNS stem cell marker genes under reprogramming conditions, characterised by sustained expression of neural crest marker genes, including Twist1 (Weber et al. 2015). Given that PML loss activates Twist1 expression, it is plausible to speculate that PML may play a role in repressing NCSC fate in NSCs by inactivating Twist1.

In addition to its role in promoting mesoderm development (Chen and Behringer 1995; Fuchtbauer 1995; Gitelman 1997; O'Rourke and Tam 2002; Zhao and Hoffman 2004; Figeac et al. 2007; Pan et al. 2009; Qin et al. 2012), increased Twist1 expression has been associated with a number of solid tumours (Maestro et al. 1999; Rosivatz et al. 2002; Hoek et al. 2004; Watanabe et al. 2004; Entz-Werle et al. 2005). In particular, Twist1 has been consistently implicated in triggering EMT programme in the context of tumour progression and metastasis (Yang et al. 2004; Elias et al. 2005; Kwok et al. 2005; Lee et al. 2006; Puisieux et al. 2006; Ansieau et al. 2008; Luo et al. 2008; Vesuna et al. 2008; Li et al. 2009a; Hong et al. 2011). One of the best-characterised roles of Twist1 in this scenario is its ability to promote cell invasion/migration, including in human glioma (Elias et al. 2005; Mikheeva et al. 2010). However, given the low-migratory state of $PML^{-/-}$ cells, the overexpression pattern of Twist1 upon PML loss doesn't fit with its canonical role. In this respect, Twist1 KD rescued the migration capability in $PML^{-/-}$ cells. Furthermore, this finding correlated with reduced expression of Slit2, and Robo1, suggesting that Twist1 represses migration in aNSCs via induction of Slit2/Robo1.

Generally, findings from the present study indicate that Twist1 repression in aNSCs is permissive for cell migration, which is contradictory to findings observed in other tissues. To further address if Twist1 regulates migration in

aNSCs via Slit2, experiments could be designed to overexpress Slit2 in $PML^{-/-}$;Twist1-KD cells, to check if Slit2 overexpression is able to impair migration phenotype that rescued by Twist1-KD in $PML^{-/-}$ cells, or to introduce Robo1N in $PML^{+/-}$;Twist1-overexpressing cells, and study whether the effects on cell migration/invasion are reversed by disruption of Slit2-Robo1 pathway.

Interestingly, Twist1 KD impaired proliferation to the level observed in PML controls cells, suggesting a causal link between Twist1 expression level and proliferation state. Indeed, one study has previously demonstrated that Twist1 positively regulates keratinocyte proliferation, specifically, that Twist1 KD in primary keratinocytes impairs G1/S transition by affecting the level of c-Myc, Cyclin E1, and E2F1 (Srivastava et al. 2016). This function is shared by another bHLH member, Ascl1, which promotes NPCs expansion through direct regulation of cell cycle progression genes, including E2F1 (Castro et al. 2011), suggesting that Ascl1, like Twist1, is a positive regulator of proliferation of CNS stem cells via direct interaction with cell cycle genes. Interestingly, Ascl1 expression was found upregulated (albeit marginally) in $PML^{-/-}$ cells (**Appendix 6. B**). This finding is in line with the activation of its target, Cyclin D2 (Ccnd2) upon PML loss (**Appendix 6. B**). However, this pattern was not found upon PML acute loss (**Appendix 6. B**). Further work needs to be conducted to study the potential involvement of Ascl1 in the context of Twist1-KD, and their potential interaction in adult CNS stem cells upon PML loss.

Finally, our data reveal a link between the increase in proliferation in aNSCs and γH2AX foci formation (my work and findings by Joanne Betts, unpublished). In addition, previous work has demonstrated that NPCs display replication-associated DNA damage during early development as a result of the enhanced replicative rate (McKinnon 2009; McKinnon 2013; Wei et al. 2016). A recent study demonstrated that aphidicolin-induced replication stress in aNSCs induce genomic instability at a set of fragile sites (Wei et al. 2016). Therefore, it is reasonable to propose that impaired proliferation upon Twist1 KD leads to a decreased level of replication stress, and thus less γH2AX foci formation. Work by Joanne Betts (not shown) reported that a pharmacological inhibitor of the ATM kinase decreased DNA damage foci in PML-deficient cells. Furthermore, work from Valeria Amodeo in the lab revealed that inhibition of pRb/p53 via expression of SV40 LargeT was sufficient to induce proliferation and DNA

damage foci in control cells, further suggesting that enhanced proliferation leads to replication stress in aNSCs (**Appendix 4**).

Furthermore, there was no effect observed on *in vitro* differentiation upon Twist1 KD, indicating PML regulates differentiation through other mechanisms. Because cell cycle has been demonstrated to control NSC differentiation (Salomoni and Calegari 2010), future experiments could be conducted to investigate the differentiation pattern in cells expressing SV40 LargeT. Moreover, Slit-Robo signalling has been implicated in differentiation of cortical interneurons (Andrews et al. 2008), and therefore it would be interesting to study the effects of Slit2/Robo1 using recombinant Slit2 or Robo1N on differentiation, because Twist1 affects expression of Slit2 upstream.

Ultimately, the results found in the present study suggest that PML inhibits Slit2/Robo1 via transcriptional repression of Twist1. However, evidence for Twist1 upregulation *in vivo* was lacking. Therefore, immunohistochemistry/immunofluorescence was performed in brain sections from PML-deficient, and control brains using different anti-Twist1 antibodies (commercially available, and obtained from Gongda Xue, Friedrich Miescher Institute, Switzerland). Unfortunately, results were not consistent due to the extremely low quality of all available antibodies tested. Only one experiment demonstrated co-staining of label-retaining NSC (Edu^+) with Twist1 in the PML-deficient SVZ, but the finding could not be reproduced (data not shown).

3.9 PRC1 component Bmi1 is not part of the mechanism

The PRC1 component Bmi1 (Joanne Betts, data not shown) was one of the genes upregulated in PML-deficient cells, and acts cooperatively with Twist1 in a feedback loop fashion to induce EMT (Yang et al. 2010a). Therefore the present study investigated whether Bmi1 could also be involved in the phenotypic changes caused by PML loss in aNSCs. The initial experiments were carried out by knockdown of Bmi1 in $PML^{-/-}$ cells using shRNA to check if Bmi1-KD mimics phenotypes observed in PML control cells. However, none of the constructs were able to achieve this (data not shown). Thus, to determine if Bmi1 overexpression mimics PML loss, $PML^{+/-}$ cells were transduced with the lentivirus overexpressing Bmi1, with FUGW as a control (Fasano et al. 2007). Bmi1-overexpression (OE) was confirmed by immunoblotting (**Fig. 3.8A**), and qPCR (**Fig.3.8B**). Due to findings examined the existing literature, relevant CDKi were then examined upon Bmi1-OE. Importantly, $p16^{Ink4a}$ is a well-known target of Bmi1, and has been identified as a regulator of G1/S transition, which is found deregulated in a number of cancers including brain cancer (Molofsky et al. 2003; Leung et al. 2004). In addition, $p21^{Cip1}$ has been identified as a target of Bmi1 (Fasano et al. 2007), with implications in NSC self-renewal, as well as for the NPCs maintenance in the forebrain (Kippin et al. 2005). Moreover, $p57^{Kip2}$, which belongs to the same Cip/Kip family as $p21^{Cip1}$, acts as a tumour suppressor for its implications in inhibition of angiogenesis, tissue invasion, and metastasis, as well as in promoting cell differentiation and apoptosis (Kavanagh and Joseph 2011). Interestingly, increasing evidence suggests that $p57^{Kip2}$ participates in CNS development (Itoh et al. 2007; Joseph et al. 2009; Jadasz et al. 2012; Furutachi et al. 2013). In particular, a recent study revealed that deletion of $p57^{Kip2}$ triggers increased neurogenesis in the short-term, but leads to NSC exhaustion and impaired neurogenesis in the long-term (Furutachi et al. 2013), which shares a similar phenotype of PML loss. Surprisingly, gene expression analysis revealed that all Bmi1 target genes tested were upregulated instead of downregulated upon Bmi1-OE (**Fig.3.8C**), and therefore challenging the canonical role of Bmi1, at least in an aNSC context. Furthermore, Edu assays indicated that Bmi1 overexpression did not result in accelerated proliferation (**Fig.3.8D**), but did lead to an elevated level of γH2AX foci formation (**Fig. 3.8E**). Interestingly, induction of differentiation

revealed that Bmi1-OE results in an increased percentage (~15%) of βIII-tubulin^{+} neurons generated, although no difference was found in astrocytic lineage (**Fig. 3.8F**), suggesting a pro-neurogenic differentiation pattern in response to Bmi1-OE. Therefore, these results indicate that Bmi1-OE in PML controls cells partially phenocopies PML loss in NSCs. Despite these preliminary data, we were unable to confirm Bmi1 upregulation in subsequent experiments performed using new aNSC preparations (**Appendix 6. C**; further discussed below).

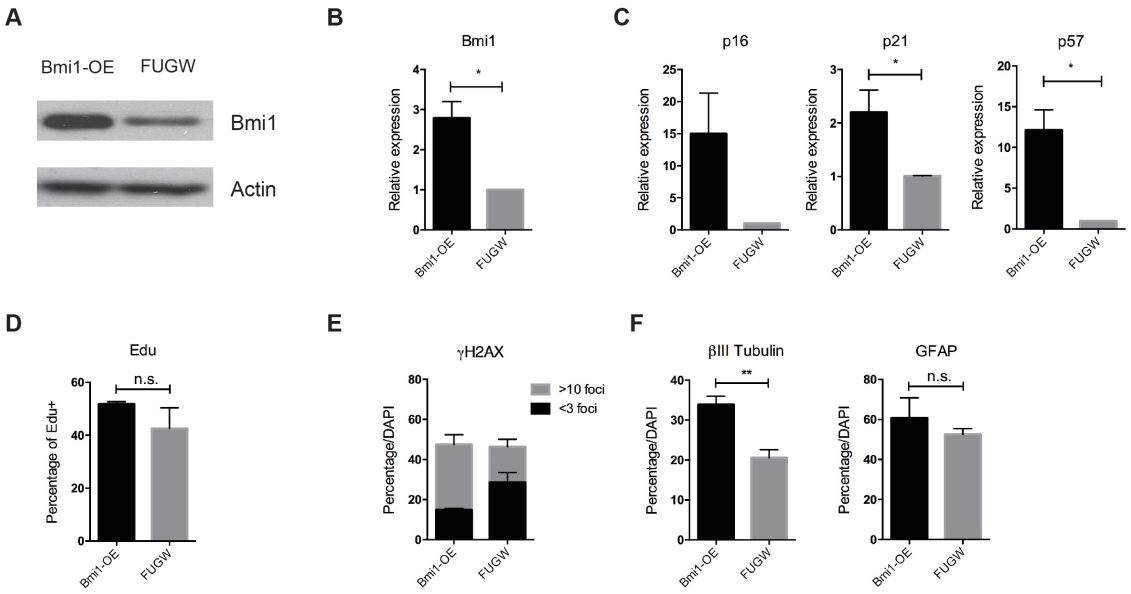

Figure 3.8: Role of Bmi1 downstream PML loss is unclear.

(A) Representative WB validation of Bmi1-overexpression (OE) in PML control cells at protein level. FUGW empty vector was used as control, and β-actin was used as loading control. (B) qPCR analysis revealed Bmi1-OE in PML control cells. Values represent mean ± SEM (n = 3; *p < 0.05, unpaired t-test). (C) qPCR analysis revealed an unexpected pattern of Bmi1 target genes. Values represent mean ± SEM (n = 3; *p < 0.05, unpaired t-test). (D) Edu assay demonstrated that no difference in proliferation was found upon Bmi1-OE. Values represent mean ± SEM (n = 3; n.s. non significant unpaired t-test) (E) Bmi1-OE led to elevated level of γH2AX foci formation (>10 foci). (F) Differentiation assay revealed Bmi1-OE results in more neuronal specification, while no difference was observed in astrocytic-lineage production. Values represent mean ± SEM (n = 3; **p < 0.01, n.s.= non significant, unpaired t-test).

3.10 Discussion

As an oncogene, overexpression of Bmi1 has been reported in a number of different tumours, including human medulloblastomas, breast cancer, prostate cancer, lung cancer, and myeloid leukaemia (Vonlanthen et al. 2001; Kim et al. 2004; Leung et al. 2004; Sawa et al. 2005). Importantly, increasing evidence suggests that Bmi1 contributes to the maintenance, and self-renewal of stem cells, in particular, neural stem cells (Lessard and Sauvageau 2003; Molofsky et al. 2003; Fasano et al. 2009). Moreover, a recent study proposed the possibility to target cancer-initiating cells self-renewal machinery by inhibiting Bmi-1 to achieve abrogation of their tumourigenic potential (Kreso et al. 2014). Because it has been proposed that brain cancers arise from multipotent neural stem cells (Singh et al. 2004; Sanai et al. 2005; Vescovi et al. 2006), targeting the subpopulation cells with "stemness" would be an effective therapeutic strategy. The present study assessed whether Bmi1 contributes to the phenotypes caused by PML loss, by overexpressing Bmi1 in control aNSCs to firstly determine whether it could phenocopy PML loss. Contrary to expectations, Edu assay revealed no effect in cell proliferation. Moreover, the known Bmi1 targets CDKi that have roles in neurogenesis were found upregulated upon Bmi1-OE. This finding is in contrast to a study, which has revealed increased Bmi1 (~2 fold) expression in NSCs promotes proliferation (Yadirgi et al. 2011). However, a recent study has demonstrated that Bmi1 overexpression in granule cell progenitors leads to decreased proliferation (Behesti et al. 2013), and this decrease may due to the induction of compensatory mechanisms to counteract oncogenic Bmi1 overexpression. Given the gene expression pattern upon Bmi1-OE observed in the present study, where CDKi $p16^{Ink4a}$, $p21^{Cip1}$, and $p57^{Kip2}$ were found derepressed in response to Bmi1-OE, it is plausible to suggest that sustained oncogenic Bmi1 expression activates compensatory effects, partially by upregulation of CDKi to attenuate tumourigenic potential. In addition, elevated γH2AX foci formation (>10 foci) was found in cells overexpressing Bmi1 compared to control, mimicking the effect of PML loss (Joanne Betts, data not shown). As discussed previously, an increased γH2AX level may be linked to replication-induced stress. However, if no difference in proliferation upon Bmi1-OE is considered, induction of γH2AX foci may not due to the replication stress. Indeed, a study

has reported that Bmi1 overexpression *per se* leads to more γH2AX foci formation (Acquati et al. 2013). Additionally, although γH2AX foci can be established in as short as 30 minutes after DSB formation (Rogakou et al. 1999), a study conducted by Kinner et al (2008) suggests that γH2AX foci remain elevated even after DSBs have been rejoined. This finding is consistent with a study demonstrating that after irradiation, Bmi1 was found enriched at chromatin, and colocalised with ATM, and γH2AX (Facchino et al. 2010). Similarly, additional studies are needed for instance, using ATM inhibitor, to demonstrate that Bmi1-OE leads to DSBs. Importantly, the differentiation assay conducted in the present study revealed an interesting pattern. Given that Bmi1-OE triggers increased neuronal production, even though preliminary, this finding suggests that this differentiation pattern might function as another counteractive mechanism to attenuate the Bmi1-induced oncogenic transformation. Contrary to expectations, it ultimately appears that Bmi1 overexpression in PML control cells only partially mimics PML loss. Ideally, additional studies should be carried out in the context of Bmi1-knockdown in PML KO cells to investigate whether it phenocopies PML control cells. Unfortunately, gene expression analysis has revealed that in other preparations of aNSCs, no difference was found with regard to Bmi1 expression level between $PML^{+/-}$ and $PML^{-/-}$ cells (**Appendix 6. C**), suggesting that this pathway may not be a relevant downstream target of PML. Therefore, the present research focusses on the investigation of mechanisms underlying Twist1, and Slit/Robo regulation downstream PML.

3.11 PML regulates Twist1/Slit2/Robo1 via Polycomb Repressive Complex 2-mediated repression

Findings previously discussed have demonstrated that Twist1 and Slit2/Robo1 are part of a PML-controlled pathway for regulation of cell migration in aNSCs. Therefore, the question as to how PML regulates these genes is an interesting one to pose. Notably, experiments employing acute PML gene loss (see above) demonstrate that while Slit2 is upregulated 5 days after 4-OHT treatment (**Fig. 3.9A**), Twist1 was clearly induced at 14 days (**Fig. 3.9B**). These data suggest that Twist1 is not the primary regulator of Slit2, and it could be rather part of an amplification loop, as overexpression of Twist1 in $PML^{+/-}$ cells is sufficient to induce Slit2/Robo1 albeit at a lower extent than in PML-deficient cells (**Fig. 3.9C**). It has been reported that prolonged EZH2 depletion in GBM leads to upregulation of Twist1 (de Vries et al. 2015). Moreover, Slit2 has been reported to be repressed by EZH2 in prostate cancer (Yu et al. 2010). Intriguingly, Twist and Slit family members are derepressed upon cerebellar EZH2 deletion (Feng et al. 2016). Finally, EZH2 has been demonstrated to interact with PML-RARα (as well as PML itself) fusion protein (Villa et al. ; Villa et al. 2007). Thus, it is conceivable to hypothesise that PML could regulate expression of Twist1 and Slit2/Robo1 via an epigenetic mechanism involving PRC2.

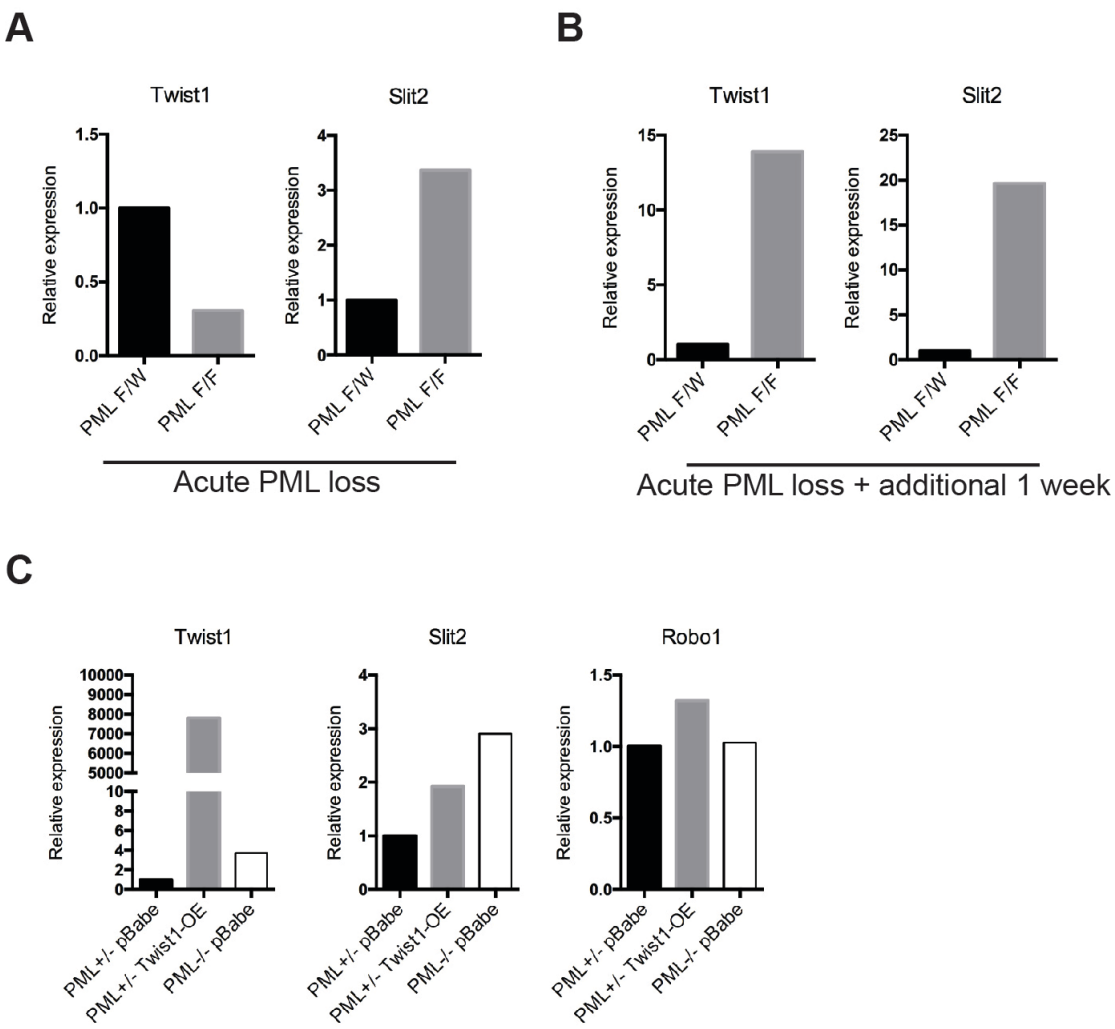

Figure 3.9: A Twist1-mediated amplification loop for induction of Slit2 upon PML loss in aNSCs.

(A) Slit2, not Twist1, was found upregulated upon acute loss (5-day post-4-OHT treatment) (n = 1). (B) Following prolonged incubation (one additional week+5-day post 4-OHT treatment), Twist1 was found upregulated after Slit2 upon PML loss (n = 1). (C) Overexpression of Twist1 in PML control cells led to no induction of Slit2, and Robo1 (n = 1). Experiments were carried out in cultured aNSCs. Same PML conditional KO system was employed as described in **Fig. 3.4**.

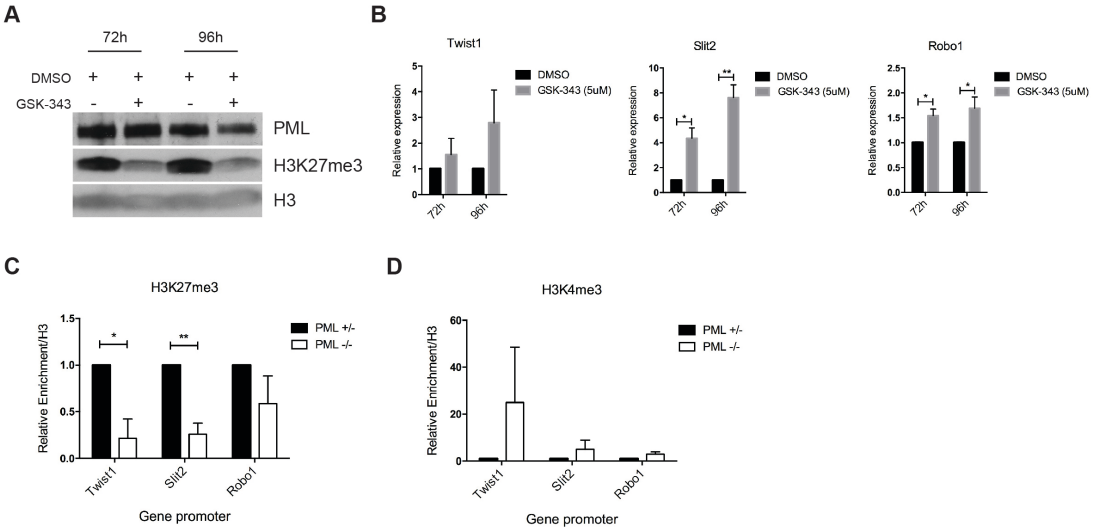

Figure 3.10: Twist1, Slit2 and Robo1 are PRC2 targets and PML loss affects H3K27me3 levels at their promoters.

(A) GSK-343 treatment revealed decreased total H3K27me3 level in $PML^{+/-}$ cells. DMSO was used as treatment control. (B) qPCR analysis revealed derepression of Ezh2 targets, Twist, Slit2, and Robo1 in response to GSK-343 treatment. Values represent mean ± SEM (n = 3; *p < 0.05; **p < 0.01, unpaired t-test). (C) ChIP-qPCR analysis revealed significantly less H3K27me3 enrichment at the promoter regions of target genes. Values represent mean ± SEM (n = 3; *p < 0.05; **p < 0.01, unpaired t-test). (D) ChIP-qPCR analysis revealed increased H3K4me3 enrichment at the promoter regions of target genes. Values represent mean ± SEM, (n = 3).

To first establish the link between PRC2 and the genes of interest, the pharmacological agent GSK-343 was used, which is a highly-selective, and potent inhibitor of EZH2 (Verma et al. 2012). As expected, treatment of $PML^{+/-}$ cells with GSK-343 led to reduced total H3K27me3 levels compared to DMSO-treated controls (**Fig. 3.10A**). Notably, Twist1, Slit2, and Robo1 were found upregulated after 48 hours of treatment (**Fig. 3.10B**). Furthermore, PML acute loss didn't result in Twist1 upregulation (**Fig. 3.9A**), suggesting Twist1 is not the direct target of PML. It could be that PML loss leads to reduced PRC2 and H3K27me3 mark, which results in immediate de-repression of Slit2 (**Fig. 3.9A&B**). Slit2 will then in turn promotes Twist1 expression, favouring cells that overexpress Twist1 and this is further stabilised by the reduced H3K27me3 mark. The is in line with the data that GSK-343-induced de-repression of Twist1 was slower than Slit2 (**Fig. 3.10A&B**), indicating a positive feedback loop between Twsit1 and Slit2.

Secondly, it was evaluated whether PML loss affected H3K27me3 levels at the promoter regions of Twist1, Slit2, and Robo1 by chromatin immunoprecipitation (ChIP)-qPCR using primers specific for the respective promoter regions (see **Table 10;** primers were validated using UCSC Genome Browser showing overlapping CpG islands, **Appendix 6. D**). Indeed, PML loss led to reduced H3K27me3 enrichment at gene promoter regions of these genes (**Fig. 3.10C**). This reduction correlated with increased levels of the Trithorax-dependent H3K4me3 mark (albeit not statistically significant) (**Fig. 3.10D**), correlating with the transcriptional activation of these genes.

To provide insights into the underlying mechanisms of this effect, the expression levels of the two core PRC2 components, EZH2, and SUZ12 were analysed. As mentioned in Introduction (page 50), EZH2 is the catalytic component of PRC2 for establishing H3K27me3 mark and it regulates expression of developmental genes, whereas SUZ12 is required for the activity and stability of PRC2 complex (Cao and Zhang 2004; Lund and van Lohuizen 2004; Pasini et al. 2004; Kouzarides 2007). Findings revealed that EZH2, the catalytic subunit of PRC2 was downregulated at the protein level in $PML^{-/-}$ cells compared to $PML^{+/-}$ cells (not mRNA, **Appendix 6. E**) (**Fig. 3.11A**). Although no difference was found at protein level (data not shown), SUZ12 mRNA was found downregulated upon PML loss in two genetic models (**Appendix 6. E**).

Reduced EZH2 levels are expected to lead to a global decrease in H3K27me3, and H3K27me3 levels were indeed reduced in $PML^{-/-}$ cells compared to $PML^{+/-}$ cells (**Fig. 3.11A**). No differences were detected with regard to global H3K27Ac, and H3K4me3 levels (Valeria Amodeo, **Fig. 3.11B**). This global reduction pattern of H3K27me3 was further corroborated using immunofluorescence (**Fig. 3.11C**), and by utilising PML conditional KO system upon acute PML loss (**Fig. 3.11D**). Based on previous studies reporting an interaction between PML and EZH2 (Villa et al. 2007), we speculate that PML may directly interact with EZH2 in aNSCs, and in turn affecting its stability. This hypothesis is currently under investigation, but initial experiments have failed to detect an interaction between PML, and either EZH2, or SUZ12 in human glioblastoma cells (Valeria Amodeo, unpublished).

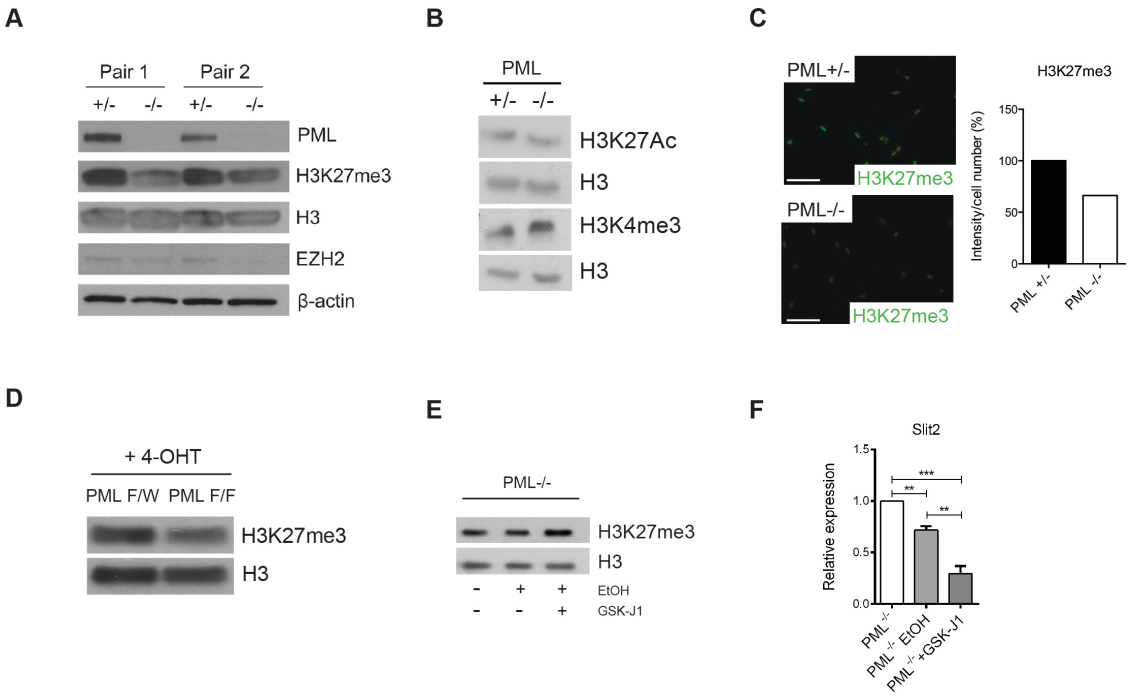

Figure 3.11: PML loss affects PRC2 component and H3K27me3 levels globally.

(A) Representative WB revealed reduced total H3K27me3 level as a result of reduced Ezh2 protein level in $PML^{-/-}$ cells compared to $PML^{+/-}$ cells. H3 was used as histone loading control. (B) WB analysis revealed that no differences were found in H3K27Ac, and H3K4me3 levels in $PML^{-/-}$ cells compared to $PML^{+/-}$ cells. H3 was used as histone loading control. (C) Representative images of reduced H3K27me3 in $PML^{-/-}$ cells by immunofluorescence staining. (D) WB analysis demonstrated reduced H3K27me3 upon acute PML loss in response to 4-OHT treatment. H3 was used as histone loading control. (E) WB revealed inhibition of JMJD3, and UTX in $PML^{-/-}$ cells using GSK-J1 rescued H3K27me3 levels compared to EtOH-treated control cells. Cells were treated with GSK-J1 (50nM) and EtOH for 48 hours, and H3 was used as histone loading control. (F) qPCR analysis revealed that Slit2 expression was found reduced upon GSK-J1 treatment in $PML^{-/-}$ cells. Values represent mean ± SEM (n = 3; **p < 0.01; ***p < 0.001; one-way ANOVA, and unpaired t-test). Note, experiments in (B), (E) and (F) were performed by Valeria Amodeo.

Based on these findings, it was investigated whether changes in H3K27me3 are responsible for the observed transcriptional activation of the Slit2 gene. Therefore, together with Valeria Amodeo in the lab, the GSK-J1 compound was used, which inhibits both JMJD3, and UTX, the demethylases of H3K27me3 (Kruidenier et al. 2012; Heinemann et al. 2014). GSK-J1 treatment in $PML^{-/-}$ cells increased H3K27me3 levels (**Fig. 3.11E**), and accordingly, significantly reduced Slit2 expression (**Fig. 3.11F**). Ultimately, these results suggest that PML regulates Slit2 expression through modulation of H3K27me3 levels.

To further corroborate these findings, a paediatric GBM-associated H3.3K27M mutant histone variant was used, and as discussed in the Introduction, leads to global reduction of H3K27me3 levels by inhibiting EZH2 enzymatic activity (Schwartzentruber et al. 2012; Bender et al. 2013; Chan et al. 2013; Lewis et al. 2013). To establish this system, NSCs derived from 15-day and 6-month old mice were transduced, with H3.3K27M, wild type (WT) H3.3, and control GFP. This model was used to further study the correlation between H3K27me3 and Slit2. A global reduction of H3K27me3 levels was observed in H3.3K27M-transduced NSCs in comparison to WT H3.3 and empty vector (**Appendix 5. A**). In response to reduced global H3K27me3 levels (Valeria Amodeo, **Appendix 5. A**), Slit2 was found upregulated in H3.3K27M-expressing cells (Valeria Amodeo, **Appendix 5. B**). Interestingly, this effect was also observed in WT H3.3 cells, suggesting that both WT and mutant H3.3 can promote Slit2 upregulation potentially by different mechanisms (further discussed below). According to the effect on Slit2 expression, both WT H3.3 and H3.3K27M significantly impaired migration, and this effect was not further amplified in $PML^{-/-}$ cells (Valeria Amodeo, **Appendix 5. C**).

3.12 Discussion

The present study demonstrates that the EMT master regulator Twist1, and axon guidance genes Slit2/Robo1 may underpin the effect of PML loss on aNSC migration. Although in germline PML KO cells, all these genes were upregulated, Twist1 appeared to be induced later than Slit2 upon acute PML loss (**Fig. 3.9A&B**), suggesting that Twist1 regulates Slit2 as part of an amplification loop rather than a main mechanism. Therefore, it is important to determine the mechanism by which PML regulates their expression levels. Interestingly, Twist1, and Slit2 are targets of PRC2 (Yu et al. 2010; de Vries et al. 2015), and PML has been demonstrated to interact with PRC2 (Villa et al. 2007). Interestingly, a recent study reported that Twist1, and Slit family members are targets of EZH2 in embryonic cerebellum (Feng et al. 2016), reinforcing the link between PRC2 and Twist1/Slit2, and their involvement in CNS neurogenesis. Finally, PRC2 has been implicated in regulating CNS neurogenesis in the embryonic and adult brain (Hirabayashi et al. 2009; Pereira et al. 2010; Hwang et al. 2014; Yao and Jin 2014; Zhang et al. 2014), and radial neuronal migration in cerebral cortex (Zhao et al. 2015). Therefore, it is plausible to consider PRC2 in this respect. Indeed, all the genes investigated in the present study were found to be targets of PRC2, and PML loss resulted in decreased levels of H3K27me3 at the promoter regions of these genes, suggesting that PML regulates Slit2 via PRC2. In this respect, findings in the present study demonstrate that in $PML^{-/-}$ cells, EZH2 protein levels were reduced, which correlated with a global decrease in H3K27me3 (**Fig. 3.11A**). This finding provides an epigenetically controlled mechanism by which alteration of PRC2 component, and H3K27me3 downstream PML could affect the expression levels of transcriptional programmes that are key to regulating cell migration in the adult CNS. We are currently investigating the composition of the PRC2 complex to determine whether PML loss only affects EZH2 levels, or more generally the stability of the complex (Cao and Zhang 2004; Pasini et al. 2004). Furthermore, it would be important to study EZH2, and H3K27me3 genome-wide in PML-deficient cells using ChIP-Seq, as this investigation could provide important insights into the actual impact of PML loss on their chromatin enrichment. Furthermore, PML has been reported to be associated with chromatin, although this claim is debated (P et al. 2007). In this respect, PML

binds matrix-associated regions in the genome. Therefore, it might also be informative to attempt PML qPCR or ChIP-Seq. However, availability of antibodies could be an issue given the potentially low affinity of PML for chromatin or the transient nature of these interactions. Based on preliminary data in the lab, PML does not seem to associate with the promoter region of Slit2 by using a commercially available antibody.

Further experimental investigations are also needed with respect to the relationship between Twist1 and EZH2, as one study has reported a contradictory finding that in bone marrow-derived mesenchymal stem cells, Twist1 induces EZH2, in turn leading to increased H3K27me3 (Cakouros et al. 2012). Based on our data, and existing literature, it is tempting to investigate if Twist1-KD/Twist1-OE affects the stability of PRC2, and in turn the levels of H3K27me3, which would allow determination of whether a complex feedback loop exists.

More work could also be conducted using *in vivo* models. For instance, a previously described EZH2 conditional KO line could be used to assess whether EZH2 loss affects Slit/Robo, and phenocopies the changes caused by PML loss in adult neurogenesis. In addition, a study has revealed that selective EZH2 inhibition via ZLD1039 potently blocks H3K27me3, and this drug can be delivered through oral gavage in mice (Song et al. 2016). Based on this finding, treatment could be carried out to determine if EZH2 inhibition mimics PML loss. Finally, to further corroborate these findings, GSK-J1 inhibitor treatment in PML-deficient mice may allow us to determine if a rescue of H3K27me3 levels could revert phenotypic changes caused by PML loss.

Finally, experiments based on the expression of H3.3K27M in aNSCs suggest that H3.3K27M-mediated inhibition of EZH2 leads to Slit2 upregulation, and reduced invasion. EZH2 is found highly expressed in a number of human cancers (Varambally et al. 2002; Bracken et al. 2003), and therefore, inhibition of EZH2 has been reported to exert tumour suppressive effects (Fiskus et al. 2006; Tan et al. 2007; Wilson et al. 2010). This finding is contrary to its effect in paediatric tumours, in which K27M is associated with marked invasion through brain parenchyma. However, it was observed in the present study that Slit2 was also induced in WT H3.3-expressing cells, which may due to the reported H3.3 enrichment in H3K4me3, as well as in other active marks (Loyola et al.

2006). Interestingly, a recent study has demonstrated that the width of H3K4me3 is associated with tumour suppressor activity (Chen et al. 2015). More specifically, broad H3K4me3 correlates with increased transcription elongation, and enhancer activity, including at the Slit2 locus in lung tissue (Chen et al. 2015). The trend of greater H3K4me3 levels at the Slit2 promoter in PML-deficient aNSCs suggest that this could be a mechanism contributing to Slit2 upregulation following a drop in H3K27me3 levels. Of note, loss of PML and H3.3K27M have cumulative effect on Slit2 expression, suggesting that Slit2 derepression in $PML^{-/-}$ cells is not solely due to a H3.3K27M-induced loss of H3K27me3. Likewise, H3.3K27M could act via a different mechanism as H3.3WT on Slit2 induction. Therefore, I believe it would be worth testing this hypothesis in future research.

Chapter 4

Discussion and Conclusions

4 Discussion and Conclusions

This project set out to determine the role of PML in regulation of adult SVZ/OB neurogenesis and cell migration. Control of cell cycle and cell migration underpins neurogenesis during development as well as in adulthood. This study has shown that PML loss results in reduced OB size and it affects aNSC migration *in vitro*. Our work has identified that PML controls cell migration in aNSCs through transcriptional control of the axon guidance gene Slit2 independently of its ability to regulate cell cycle. My data suggest that PML represses Slit2 via control of the repressive mark H3K27me3. Furthermore, I found that the EMT factor Twist1 contributes to regulation of Slit2 downstream PML and PRC2, revealing a previously unknown feedback loop for control of cell migration in aNSCs.

PML controls OB size

The present study shows that PML loss results in reduced number of slow-proliferating aNSC and increased entry into differentiation. However, PML loss impairs neuroblast migration in RMS and leads to a smaller OB size. Further work could be carried out in the future on the OB phenotype (see also **3.1 Discussion**). There exists a considerable degree of heterogeneity of OB interneuron subtypes. However, it is known that the production of diversity OB interneuron subtypes is not simply occurring at the time migrating neuroblasts entering the OB. This heterogeneity is derived from the aNSC niche itself, and different regions within the SVZ give rise to defined OB interneuron subtypes (Merkle et al. 2007; Alvarez-Buylla et al. 2008; Merkle et al. 2014). In this respect, our study leaves a number of specific questions unanswered: i) What subtype of aNSCs does PML affect? ii) If so, does it correlate to the generation of a specific OB neuron subtype and ultimately the OB size phenotype? To this end, we can utilize the mouse model of glutamate-aspartate transporter (GLAST) promoter (GLAST-CreERT2) (Mori et al. 2006; Ninkovic et al. 2007; DeCarolis et al. 2013; Benedykcinska et al. 2016) crossing to the Confetti multicolour Cre reporter as established recently (Calzolari et al. 2015), enabling us to target and follow the progeny of single aNSC in long-term. This will

provide us with more insight into the role of PML in regulating stem cell fate and lineage specification in adult CNS.

A novel PML/Slit2 axis for regulation of adult neurogenesis

Our work showed the first time that Slit2 has a role in inhibition of cell migration in SVZ-derived aNSCs downstream PML. In contrast, Slit1 is not regulated by PML and fails to affect cell migration in aNSCs. A previous study reported that Slit1, not Slit2, exerts chemorepulsive function in adult RMS migration (Nguyen-Ba-Charvet et al. 2004). However, we cannot rule out the possibility that Slit functions are context-dependent and cell type-specific, as the abovementioned study reported that Slit1 is itself expressed in type A cells along the RMS (Nguyen-Ba-Charvet et al. 2004). In this respect, we have not studied the respective levels of Slit1 and Slit2 during differentiation in our model system. Future experiments can be carried out to study the expression of Slit proteins in more committed cells along RMS in control and PML-deficient brains, as this will provide hints on whether a transition/switch of Slit proteins occurs throughout the SVZ-OB route and what is PML role in their regulation depending on the differentiation stage. Such experiments are being designed in the lab to study the expression of Slit1 and Slit2 in neuroblast cells first *in vitro* (O'Leary et al. 2015) and then *in vivo*.

We showed in the present study that Slit2 binds to its cognate receptor Robo1 to inhibit aNSC migration in a collective fashion. It is known that the Slit2-Robo1 signalling pathway negatively regulates Cdc42 activity and cell cytoskeleton remodelling (Wong et al. 2001). Mechanistically, Slit2 binds to Robo1 receptor, which in turn activates the Slit-Robo Rho GTPase-activating protein 1 (srGAP1), resulting in inactivation of GTPase Cdc42, activation of another GTPase RhoA and ultimately decreased actin polymerization and cell migration (Wong et al. 2001; Yiin et al. 2009; Sit and Manser 2011). In my study, no difference was observed with respect to cytoskeleton following F-actin staining between PML control cells and $PML^{-/-}$ cells (data not shown). However, further work is needed to more thoroughly examine the changes in cytoskeleton upon PML loss, as well as the mode of migration. Similar to the glial-dependent neuronal migration in the cerebral cortex, chain migration of neuroblasts in anterior SVZ requires nuclear-centrosome coupling (Wong et al.

2001; Schaar and McConnell 2005). In this respect, neuronal migration occurs via repetition of two key events: 1) leading process extension, and 2) movement of the cell body and translocation of the nucleus (Tsai and Gleeson 2005). Interestingly, the positioning of centrosome in the leading process and the subsequent nuclear translocation toward the centrosome constitutes the key feature of migration, since alteration in these two sub-events has been linked to a cell migration defect (Solecki et al. 2004; Tanaka et al. 2004; Koizumi et al. 2006). Based on these studies, future experiments could be designed by measuring the distance between nucleus and centrosome to assess the nuclear translocation ability, as defects in nuclear translocation have been implicated in migration defect in adult forebrain (Koizumi et al. 2006), and especially given that Slit-Robo-induced Cdc42 inactivation results in leading process shortening (Wong et al. 2001).

Here in this study, we showed that Slit2 expression is regulated downstream PML/PRC2. However, it remains unclear how PML affects the expression or stability of PRC2. As discussed earlier, histone chaperone H3.3 interacts with PRC2 (see Introduction) and it has been implicated in the recruitment of PRC2 to developmental gene promoters (Banaszynski et al. 2013). Work from our lab has shown that PML-interacting protein DAXX is responsible for H3.3 loading in CNS (Michod et al. 2012). Thus, it is plausible to speculate that PML regulates PRC2 via H3.3. Indeed, our unpublished work (Valeria Amodeo) shows that PML loss leads to increased H3.3 expression and loading at Slit2 promoter in aNSCs. Based on these studies and our findings, future experiments could be carried out by knockdown of H3.3 in PML-deficient cells to determine if it phenocopies PML control cells.

In addition to controlling cell migration of aNSC downstream PML, Slit2 could also regulate SVZ neurogenesis via additional mechanisms. In this respect, Slit2 has been implicated in angiogenesis, but, like PML Slit2 exerts a dual role in this process. It either promotes (Kaur et al. 2008; Urbich et al. 2009; Yang et al. 2010b; Rama et al. 2015) or inhibits angiogenesis (Liu et al. 2006b; Jones et al. 2008; Jones et al. 2009). Of note, two independent studies have shown that aNSCs within SVZ are tightly apposed to blood vessels during homeostasis and regeneration, and that SVZ neurogenesis occurs near blood vessels (Shen et al. 2008; Tavazoie et al. 2008). Work from our group and others have

implicated PML in suppression of angiogenesis via multiple mechanisms (Bernardi et al. 2006; Dvorkina et al. 2016). Based on these studies, it would be tempting to speculate that PML loss could affect the vascular structure of adult SVZ via regulation of Slit2 expression. This could in turn affect the spatial organization of the aNSC niche, potentially affecting aNSC behaviour and generation of OB neurons? For instance, we could use whole mount staining of brain sections from $PML^{+/-}$ and $PML^{-/-}$ mice to determine if PML loss affects the SVZ vasculature.

Another avenue for future investigation is whether PML controls neurogenesis and migration in the context of other brain areas. In this respect, our lab has generated a large body of unpublished work implicating PML in regulation of cerebellar postnatal neurogenesis. Specifically, a previous postdoc, in collaboration with Dr Simonetta Pazzaglia (Rome, Italy) has shown that PML loss leads to increased proliferation of cerebellar granule cell progenitors (GCPs) in the external granule layer (EGL) and augmented entry into differentiation. This is however associated with decreased overall number of mature granule neurons in the inner granule layer (IGL). These changes were recapitulated *in vitro* using primary GCPs, where PML loss led to increased proliferation and spontaneous differentiation. This phenotype is reminiscent of the SVZ neurogenesis alterations found in PML KO adult brains. It would be interesting to determine whether a similar PML/Slit axis regulates migration and/or differentiation in the context of cerebellum development. In this respect, as our findings also showed that SHH signalling was reduced in PML KO GCPs, it could be speculated that Slits are involved in regulation of SHH signalling downstream PML. Interestingly, a previous report has shown that Slit2 inhibits SHH expression in the ventral neural tube (Wang et al. 2013). Vice versa, Gata3 positively modulate the expression of Slit2 (Liu et al. 2014). Further work is needed to fully dissect the role of PML during cerebellar development.

A novel role of Twist1 in regulation of adult neurogenesis

This study has demonstrated, for the first time, that Twist1 is expressed at very low levels in aNSCs, but it is markedly induced by PML loss to regulate Slit2 expression, cell migration and cell proliferation. However, in aNSCs Twist1

appears to inhibit cell migration, challenging its canonical role in promoting cell migration/invasion. Interestingly, Twist1 shares commonalities with another member of the bHLH family, Ascl1, which is expressed in aNSCs with respect to cell cycle progression and cell proliferation (see **3.8** for further discussion).

A recent study has suggested that Twist1 is involved in regulation of metabolism. Specifically, Twist1 negatively regulates fatty acid metabolism (FAO) in mice via regulation of PGC1A target genes (Pan et al. 2009). Of note, in HSCs and breast cancer cells, a PML/PPA-δ/FAO metabolism pathway has been shown to promote stem cell maintenance through promotion of asymmetric over symmetric division (Carracedo et al. 2012; Ito et al. 2012). Accordingly, pharmacological inhibition of FAO phenocopies PML loss, resulting in HSC exhaustion (Ito et al. 2012). Given that PML loss leads to upregulation of Twist1, one could speculate that the elevated Twist1 expression inhibits PPA-δ/FAO pathway, thus in turn leading to stem cell exhaustion in the adult SVZ. We are currently assessing i) whether the expression of PGC1A target genes is affected in PML-deficient aNSCs, ii) if these changes are reverted upon Twist1 knockdown and iii) if Twist1-OE in control cells phenocopies PML loss. If indeed some of the PGC1A target genes appear to be regulated by a PML/Twist1 axis, we plan to determine whether PML/Twist1-mediated control fatty acid metabolism could plays a role in aCNS neurogenesis. Finally, it would be important to investigate whether Slit2 could be involved in FA metabolism as well.

PML represses Slit1 (not Slit2) in neoplastic settings

This part is mainly the work of Valeria Amodeo and Joanne Betts, in collaboration with Sebastian Brandner (UCL Institute of Neurology) and Chris Jones' (Institute of Cancer Research, Sutton) lab. I contributed to this part intellectually and provided relevant cells and reagents. As discussed in the Introduction, it is well established that one of the key features of brain cancer cells is their ability to invade the brain parenchyma. Notably, brain cancer share migration routes with normal neuroblasts, suggesting that brain cancer migration has neurobiological roots (Cuddapah et al. 2014). Therefore, it was tempting to speculate whether a PML/Slit axis could regulate cell migration upon neoplastic transformation of aNSCs as well as in GBM cells derived from

established tumours. As mentioned in the Introduction, PML mediates induction of cellular senescence downstream oncogenic RAS. However, given recent studies reporting an oncogenic function of PML (Ito et al. 2008; Carracedo et al. 2012; Ito et al. 2012), it could be postulated that PML mediates RAS oncogenic functions as well. To determine the role of PML in the context of RAS-induced transformation, we utilised a H-RASV12-IRES-GFP (OncRAS) model described before (Bartesaghi et al. 2015). Notably, we found that i) PML expression was increased in response to OncRAS (**Appendix 7. Fig 6B**) and ii) PML loss impaired migration of OncRAS-transformed aNSCs (**Appendix 7. Fig 6C**). Notably, Slit1, not Slit2, was found to be the target for PML-mediated repression upon RAS-driven transformation (**Appendix 7. Fig 6D**). Furthermore, Slit2 was downregulated, suggesting a positive role of PML in regulation of Slit2 expression in neoplastic cells. To assess the involvement of PML in mediating RAS-driven transformation *in vivo*, injection of OncRas-transformed $PML^{+/-}$ and $PML^{-/-}$ aNSCs into NOD-SCID mice was performed. Notably, PML loss delays RAS-driven oncogenesis in orthotopic xenografts (**Appendix 7. Fig 6F**) and impairs invasiveness into adjacent brain tissue (**Appendix 7. Fig 6H**). Given that PML/Slit axis also controls cell migration in neoplastic transformation (OncRAS-transformed aNSCs), we investigated the PML/Slit axis in GBM, as RAS/MAPK activation is believed to contribute to the development of a subset of GBM tumours (see Introduction). We first studied the expression of PML and SLIT/ROBO members in relation to known GBM molecular subtypes using existing datasets. Interestingly, PML was found highly expressed in GBM tumours belonging to the mesenchymal subtype (**Appendix 7. Fig 7A**), which is characterised by loss of the RAS inhibitor NF1 and by an invasion/angiogenesis gene expression signature. Furthermore, PML expression was found inversely correlated with SLIT1 (**Appendix 7. Fig 7B**), whereas it directly correlated with SLIT2 (**Appendix 7. Supplementary Fig 6B**), in accordance with the expression pattern observed in PML-deficient OncRAS-transformed aNSCs. Finally, PML expression directly correlated with tumour stage and was associated with poor prognosis (**Appendix 7. Fig 7E, Supplementary Fig 6D&E**).

We then set out to determine whether PML regulates cell migration in primary GBM cells. PML was expressed at variable levels across a panel of primary

GBM cells (**Appendix 7. Fig 7F**). Notably, PML-KD in PML^{HIGH} G2 cells (**Appendix 7. Fig 7G**) led to reduced migration (**Appendix 7. Fig 7H**), which was associated with SLIT1 upregulation (**Appendix 7. Fig 7I&L**). In contrast, SLIT2 was downregulated upon PML-KD, suggesting that like in OncRAS-transformed aNSCs, SLIT1 (not SLIT2) is the main target of PML in GBM. Conversely, overexpression of the PML-I isoform in PML^{LOW} G1 cells promoted cell migration, whilst it represses SLIT1 expression and enhanced SLIT2 expression (**Appendix 7. Fig 7N&O**). Finally, the PRC2 components EZH2 and SUZ12 were reduced upon PML-KD (**Appendix 7. Fig 7L**), in accordance with the reduced H3K27me3 enrichment at SLIT1 promoter and decreased global H3K27me3 levels (**Appendix 7. Fig 7K&M**). In contrast, an elevated H3K27me3 enrichment was found at the SLIT2 promoter (**Appendix 7. Supplementary Fig 6G**), correlating its reduced expression in response to PML-KD. Our findings reveal a "switch" from SLIT2 to SLIT1 upon PML loss or PML-KD, suggesting that in neoplastic transformation, SLIT1, not SLIT2, is the main target of PML. This correlates with the H3K27me3 enrichment levels at the promoter regions of SLIT1 and SLIT2. Moreover, a similar regulation of PRC2 and H3K27me3 levels downstream PML was observed in GBM cells, whereby PML-KD impairs EZH2 and accordingly the H3K27me3 mark globally. There are several hypotheses that could be postulated to explain the observed 'switch', but I am now discussing one in particular, which I feel to be more plausible. It is possible that RAS signalling could redistribute PRC2 and H3K27me3 from SLIT2 to SLIT1, potentially because SLIT2 might be unable to repress invasion in GBM and/or potentially have pro-tumourigenic functions such as increasing proliferation and/or promoting angiogenesis, as suggested in the literature (Kaur et al. 2008; Urbich et al. 2009; Yang et al. 2010b; Rama et al. 2015; Secq et al. 2015). In this context, PML downregulation via inhibition of PRC2 leads to SLIT1 derepression and inhibition of invasion. How could PML loss negatively affect SLIT2 expression? One could speculate that in GBM cells SLIT1-dependent signalling could lead to inhibition of SLIT2 expression, as part of a negative feedback loop existing between different SLIT family members, which could be in place to control the 'SLIT burden' in the cell. To test this hypothesis, I could first examine whether recombinant SLIT1

(rSLIT1) could repress SLIT2 and whether a decoy ROBO2 receptor (assuming that it would not bind SLIT2) or SLIT1 KD could result in derepression of SLIT2.

More generally, these findings suggest that contrary to paediatric brain tumours (Bender et al. 2013; Chan et al. 2013; Lewis et al. 2013), PRC2 and H3K27me3 may play an oncogenic role in adult GBM, as suggested by other studies. In adult settings, PML would represent a novel regulator of PRC2 function in both normal and cancer settings. In this respect, our findings reveal that PML expression increases with tumour grade and positively correlates with poor prognosis. Moreover, experiments in orthotopic animal model show that PML loss delays the tumourigenesis and impairs cell migration of OncRAS-transformed aNSCs, suggesting an oncogenic role of PML in the adult CNS. This challenges the canonical tumour suppressive role of PML (Gurrieri et al. 2004), as its protein expression is lost or reduced in a number of human tumours from different origins. However, these findings are in line with more recent evidence supporting a pro-oncogenic role of PML in CML and breast cancer (Ito et al. 2008; Carracedo et al. 2012). For instance, PML is found highly expressed in CML patients, and its expression level positively correlates with poor prognosis (Ito et al. 2008). These studies together with our findings reinforce the multifaceted role of PML in tumour and its complexity as a context-dependent factor. It is important to note that unpublished work in our group (Joanne Betts) has shown that PML is highly expressed in medulloblastoma, a tumour of the cerebellum. It would be interesting to determine whether it could play a similar pro-migratory role also in this tumour, which is often associated with invasion and in some instances spinal metastasis (Quenum et al. 2012; Zivkovic et al. 2014).

Taken together, our work uncovers a previously unknown pathway that underpins cell migration in both physiological and neoplastic settings. Since PML can be degraded by As_2O_3 (see discussion in the Introduction), one could speculate that this pathway could be targeted pharmacologically in GBM. However, caution should be taken as more work is needed to better understand the precise molecular mechanisms underlying the function of the PML/SLIT axis in brain cancer.

Appendix

Appendix

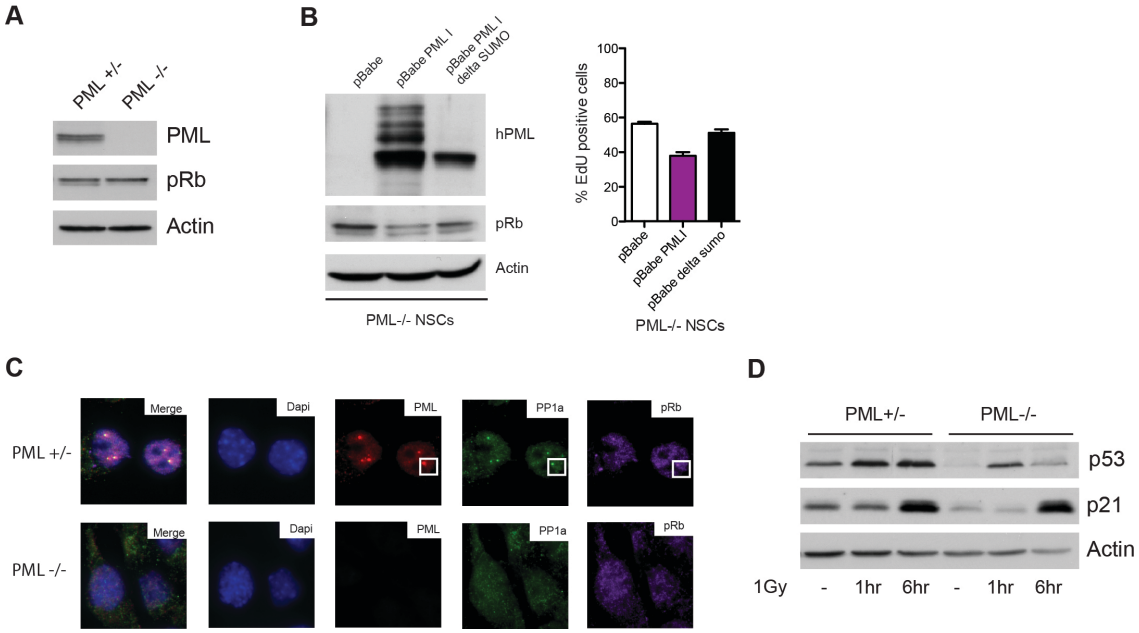

Appendix 1 (Joanne Betts). (A) An increased amount of pRb phosphorylation in PML$^{-/-}$ cells compared to PML control cells. (B) PML-knock-in (KI) in PML-deficient cells impaired pRb phosphorylation, and proliferation. (C) PP1α, and pRb colocalise in PML-NBs in PML control cells, whereas this colocalisation is abolished in PML-deficient cells. (D) WB analysis revealed reduced p53, and p21 protein levels in PML$^{-/-}$ cells. γ-irradiation (1Gy) led to increased p53, and p21 protein levels.

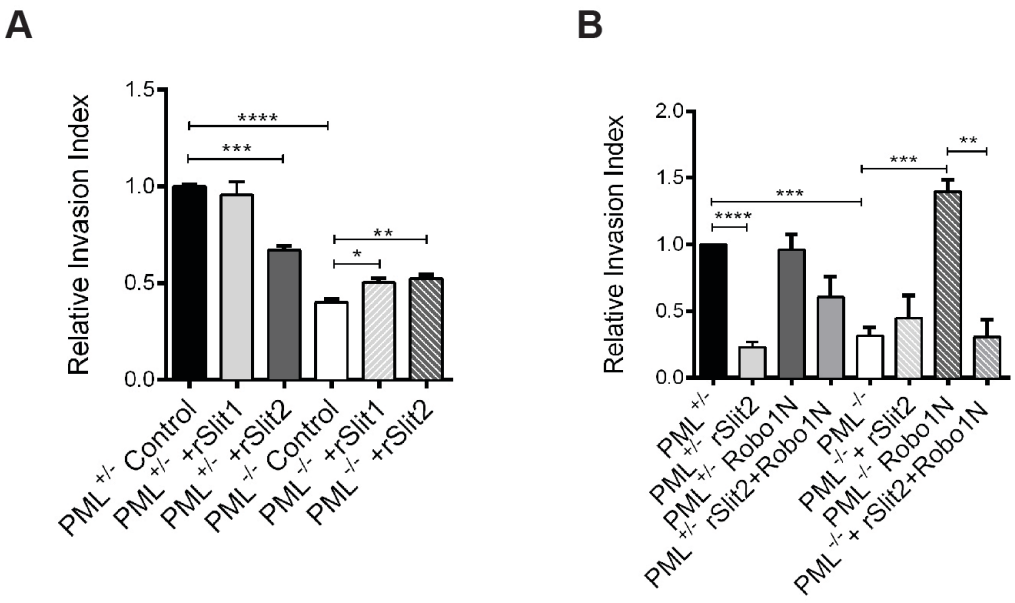

Appendix 2 (Valeria Amodeo). (A) rSlit2 impairs NSCs cell migration. Values represent mean ± SEM (n = 3; *p < 0.05, **p < 0.01, ***P < 0.001; ****P < 0.0001, one-way ANOVA, and unpaired t-test). (B) ECM assay revealed that Robo1N rescues the migration of $PML^{-/-}$ cells. $PML^{+/-}$, and $PML^{-/-}$ cells were treated with rSlit2 (100 ng/mL) and/or with Robo1N (200 ng/mL). Values represent mean ± SEM (n = 3; **p < 0.01; ***p < 0.001; ****p < 0.0001, one-way ANOVA, and unpaired t-test). rSlit1, recombinant Slit1; rSlit2, recombinant Slit2.

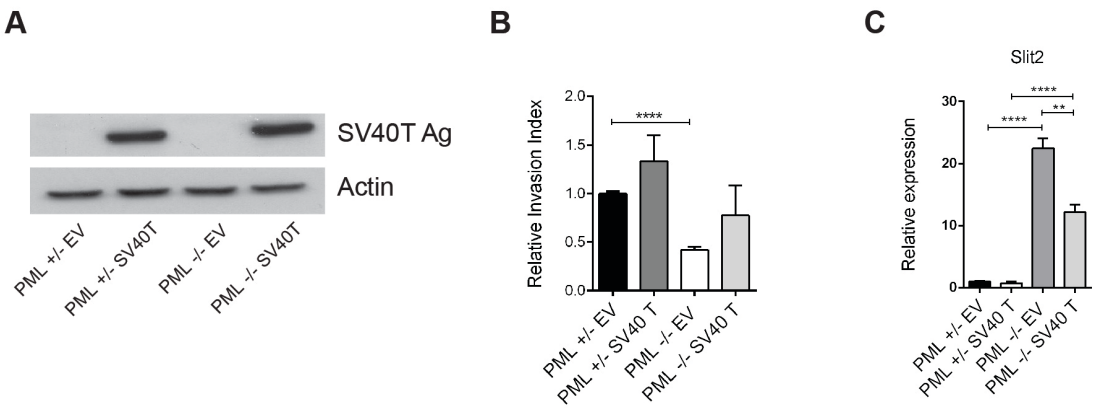

Appendix 3 (Valeria Amodeo). (A) WB revealed successful expression of SV40 LT in PML control, and PML-deficient cells. β-actin was used as loading control. EV, pLXSN-empty vector; SV40T, pLXSN-SV40 LT. (B) ECM assay revealed that SV40 LT did not impede migration in aNSCs. Values represent mean ± SEM (n = 3; ****p < 0.0001, one-way ANOVA). (C) qPCR analysis demonstrated that Slit2 expression was not regulated by SV40 LT in PML control cells. Values represent mean ± SEM (n = 4; **p < 0.01; ****p < 0.0001, one-way ANOVA, and unpaired t-test).

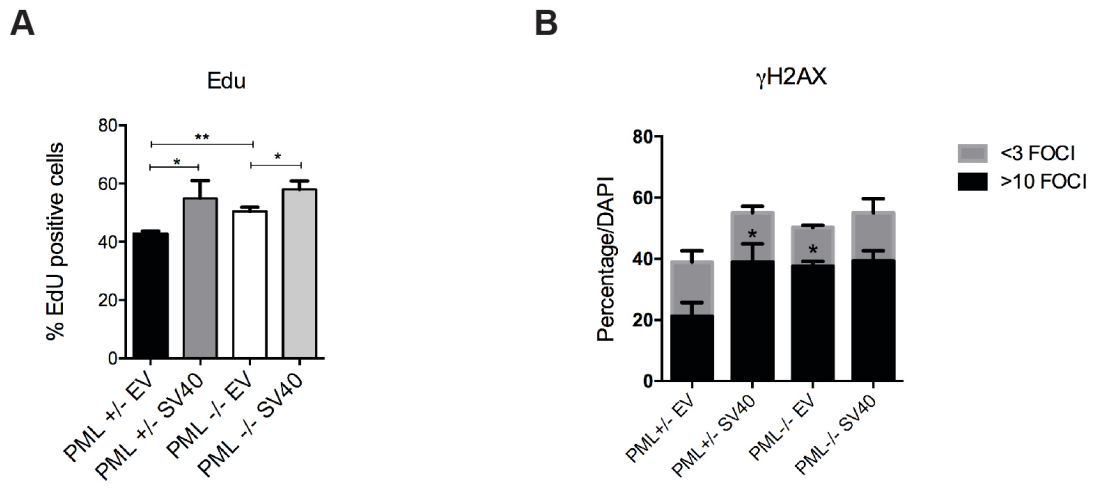

Appendix 4 (Valeria Amodeo). (A) Transduction of SV40 LargeT was sufficient to induce proliferation in $PML^{+/-}$ cells. Values represent mean ± SEM (n = 3; *p < 0.05; **p < 0.01, one-way ANOVA) (B) A positive correlation between increased proliferation upon SV40 LargeT and γH2AX foci formation. Values represent mean ± SEM (n = 3; *p < 0.05, two-way ANOVA).

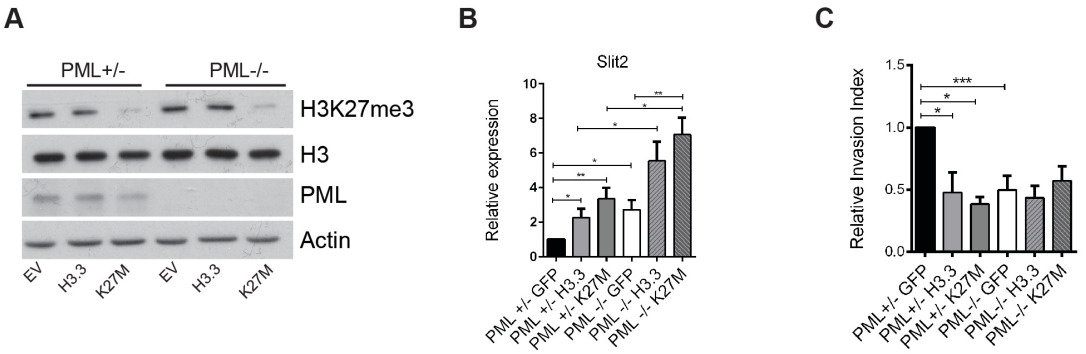

Appendix 5 (in coordination with Valeria Amodeo). (A) WB analysis revealed reduced global levels of H3K27me3 in H3.3K27M-transduced cells (cells derived from 6-month old animals). Note that the global reduction of H3K27me3 in $PML^{-/-}$ cells is not visible in panel A. This may be due to viral transduction and subsequent cell sorting, as control experiment using non-transduced cells (data not shown, Valeria Amodeo) was able to see the reduction as shown in **Fig. 3.11A** (B) Slit2 expression was found increased in H3.3, and H3.3K27M-transduced $PML^{+/-}$, and $PML^{-/-}$ NSCs. Values represent mean ± SEM (n = 5; *p < 0.05; **p < 0.01, one-way ANOVA, and unpaired *t*-test). (C) ECM assay revealed that WT H3.3, and the mutant H3.3K27M significantly decreased the migration ability of $PML^{+/-}$ cells. No further effects were observed in $PML^{-/-}$ cells. Values represent mean ± SEM (n = 3; *p < 0.05, ***p < 0.001, one-way ANOVA).

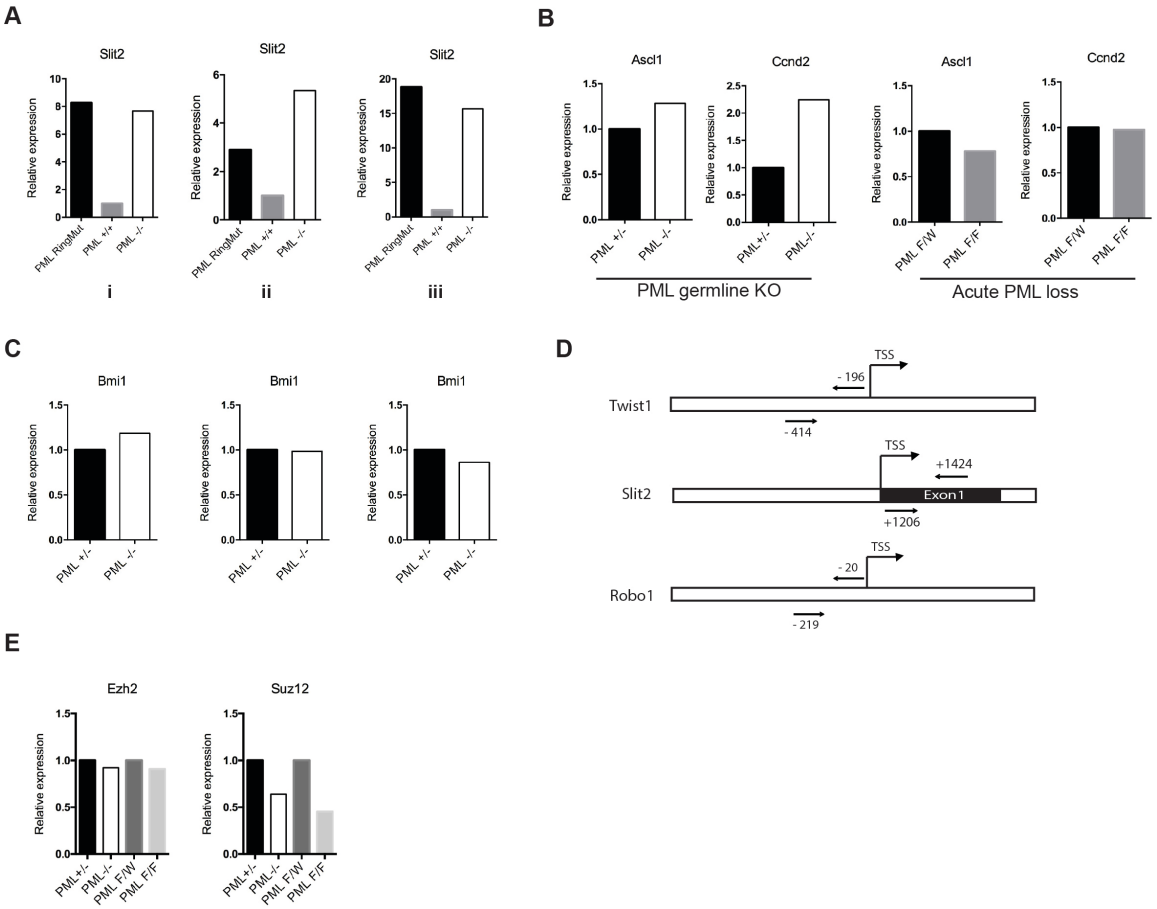

Appendix 6. (A) Three different experiments demonstrating similar patterns of Slit2 expression in PML RingMut cells. (B) Ascl1, and its target Ccnd2 were found upregulated in PML germline KO cells, but not in PML conditional KO cells (n = 1). (C) Bmi1 was not regulated by PML in aNSCs from different preparations. (D) Schematic illustration displays ChIP-qPCR primers amplifying promoter regions of genes of interest. Primers were validated in UCSC Genome Browser based on CpG island overlapping. (E) Ezh2 mRNA was found not to be affected by PML loss. However, Suz12 mRNA was found to be downregulated.

Appendix 7 (PML in neoplastic settings):

Figure 6

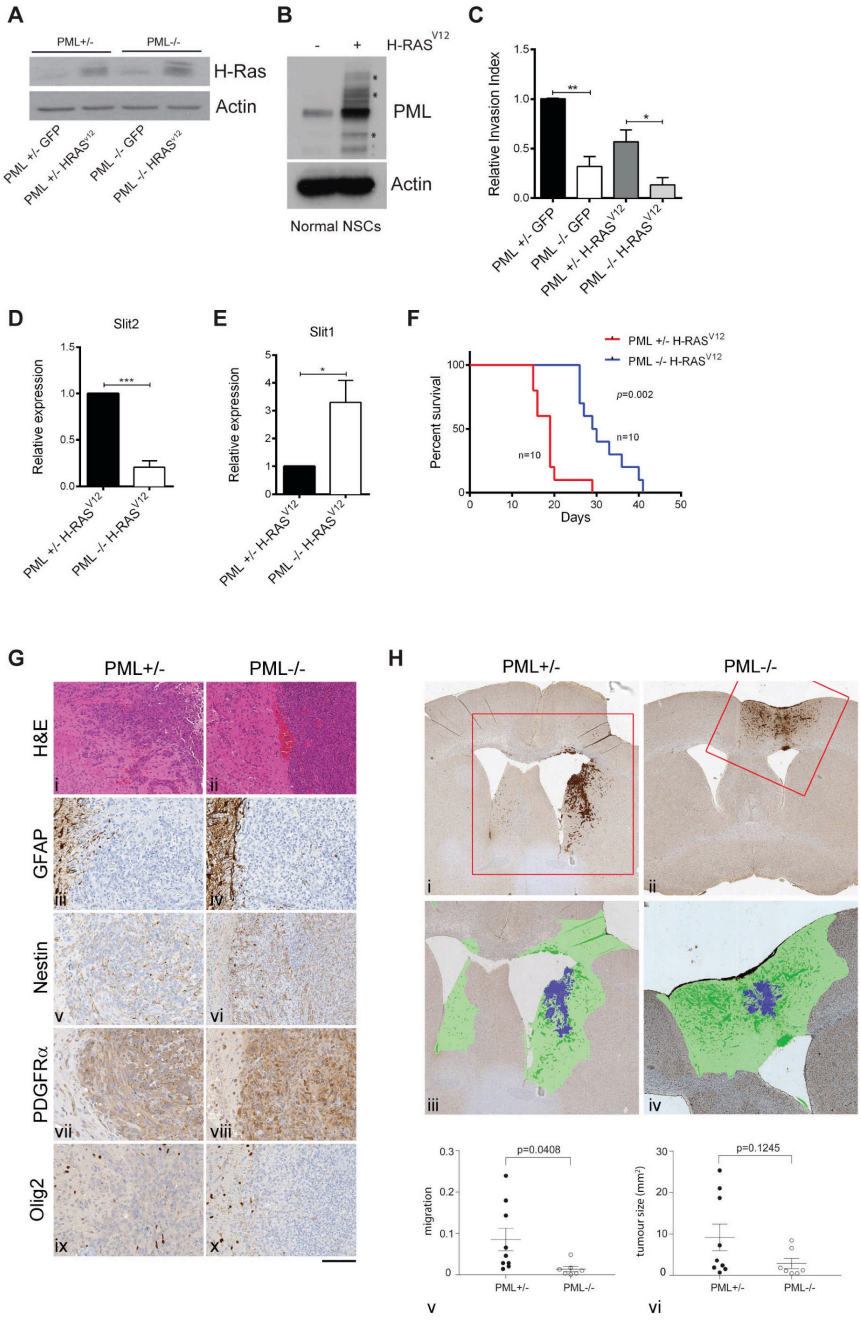

Figure 7

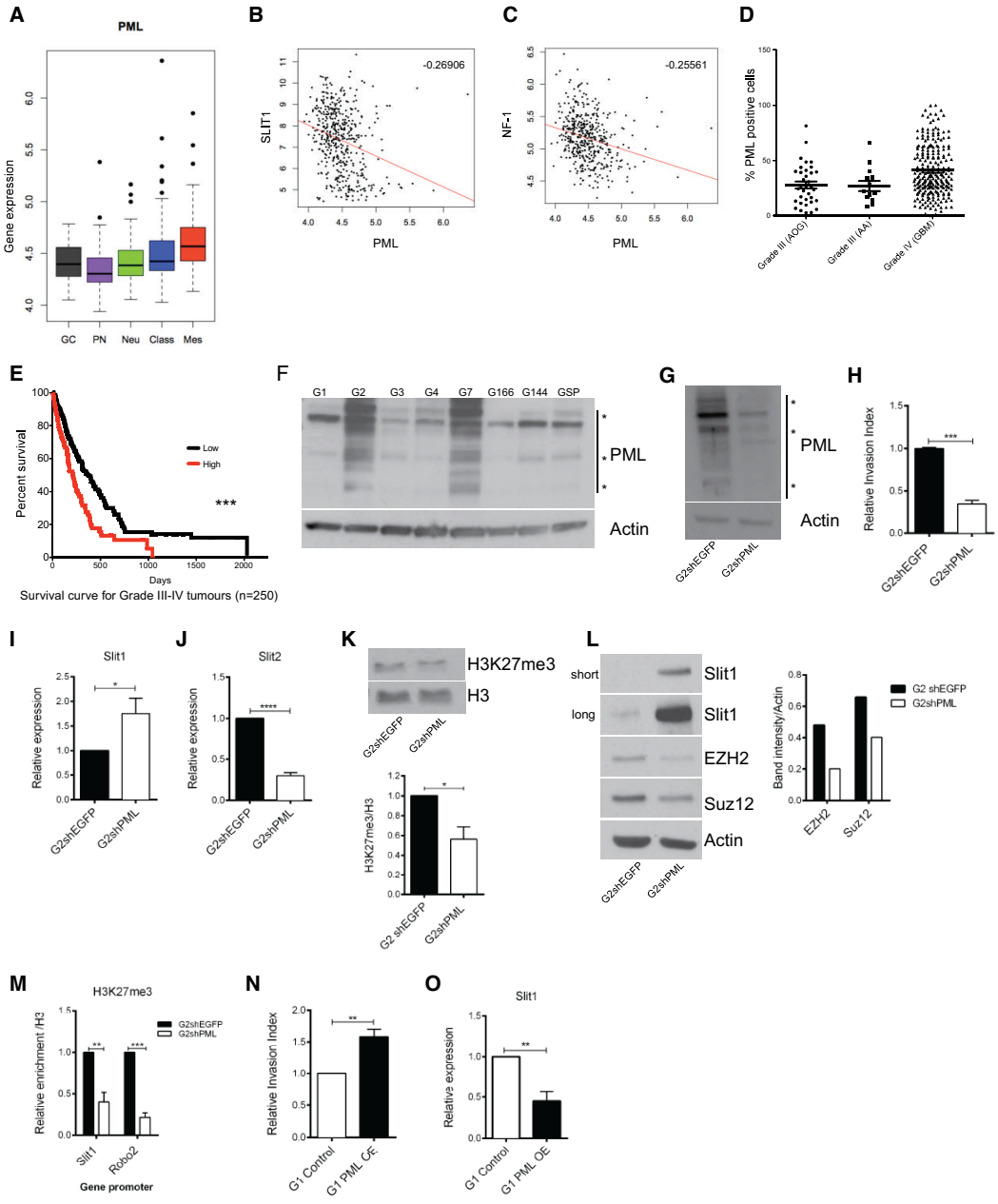
A
PML
Gene expression
GC
PN
Neu
Class
Mes
B
SLIT1
-0.26906
PML
C
NF-1
-0.25561
PML
D
% PML positive cells
Grade III (AOG)
Grade III (AA)
Grade IV (GBM)
E
Percent survival
Low
High
***
Days
Survival curve for Grade III-IV tumours (n=250)
F
G1
G2
G3
G4
G7
G166
G144
GSP
PML
Actin
G
PML
Actin
G2shEGFP
G2shPML
H
Relative Invasion Index
***
G2shEGFP
G2shPML
I
Slit1
Relative expression
*
G2shEGFP
G2shPML
J
Slit2
Relative expression
****
G2shEGFP
G2shPML
K
H3K27me3
H3
G2shEGFP
G2shPML
H3K27me3/H3
*
G2 shEGFP
G2shPML
L
short
long
Slit1
Slit1
EZH2
Suz12
Actin
G2shEGFP
G2shPML
Band intensity/Actin
G2 shEGFP
G2shPML
EZH2
Suz12
M
H3K27me3
Relative enrichment /H3
G2shEGFP
G2shPML
**
***
Slit1
Robo2
Gene promoter
N
Relative Invasion Index
**
G1 Control
G1 PML OE
O
Slit1
Relative expression
**
G1 Control
G1 PML OE

Supplementary Figure 6

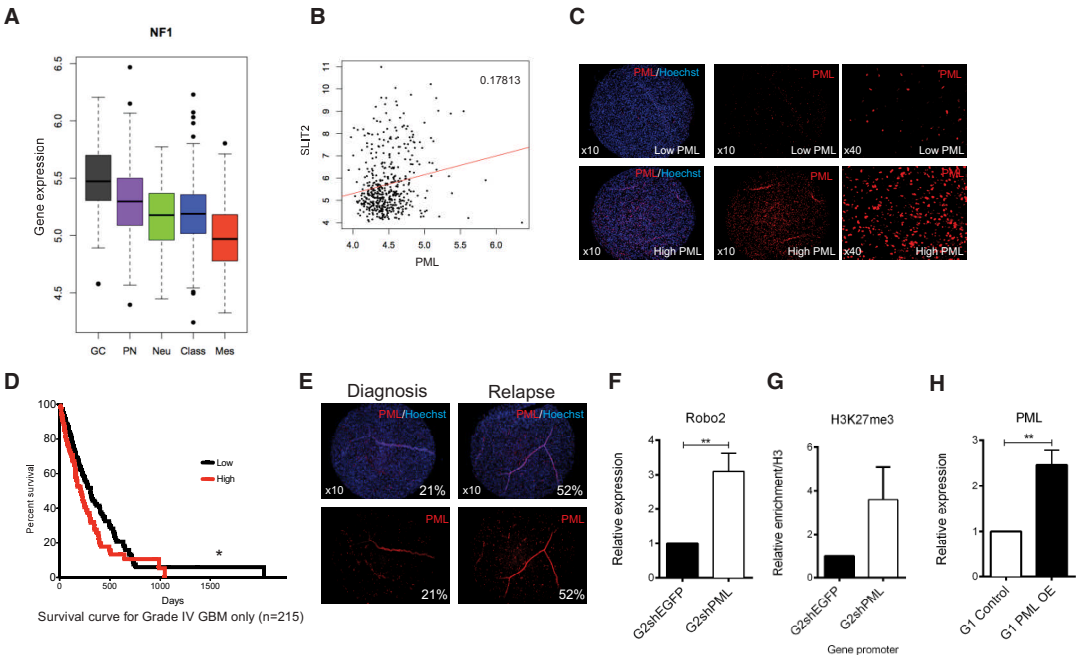

Appendix 8 (*Cell reports*, under revision)

Manuscript

A PML/Slit axis controls physiological cell migration and cancer invasion in the CNS

Deli A[1,2*], Valeria Amodeo[1,2*], Joanne Betts [1,2*], Stefano Bartesaghi[1,2], Ying Zhang[3], Angela Richard-Londt[3], Matthew Ellis[3], Rozita Roshani[1,2], Mikaella Vouri[1,2], Sara Galavotti[1,2], Sarah Oberndorfer[1,2], Ana Leite[1,2], Alan Mackay[4], Ningning Li[3], Eva Wessel Stratford[5], David Dinsdale[6], David Grimwade[7], Chris Jones[4], Pierluigi Nicotera[8], David Michod[1,2,9], Sebastian Brandner[3], and Paolo Salomoni[1,2^]

[1]UCL Cancer Institute, London; [2]Samantha Dickson Brain Cancer Unit; [3]UCL Institute of Neurology, London; [4]Institute of Cancer Research, Sutton, UK; [5]The Norwegian Radium Hospital, Oslo, Norway; [6]MRC Toxicology Unit, Leicester, UK; [7]King's College London, London; [8]DZNE, Bonn, Germany; [9]UCL Institute of Child Health, London.

*Contributed equally to this work

^Corresponding author

Bibliography

References

Acevedo M, Vernier M, Mignacca L, Lessard F, Huot G, Moiseeva O, Bourdeau V, Ferbeyre G. 2016. A CDK4/6-Dependent Epigenetic Mechanism Protects Cancer Cells from PML-induced Senescence. *Cancer Res*.

Acquati S, Greco A, Licastro D, Bhagat H, Ceric D, Rossini Z, Grieve J, Shaked-Rabi M, Henriquez NV, Brandner S et al. 2013. Epigenetic regulation of survivin by Bmi1 is cell type specific during corticogenesis and in gliomas. *Stem Cells* **31**: 190-202.

Aguirre A, Rubio ME, Gallo V. 2010. Notch and EGFR pathway interaction regulates neural stem cell number and self-renewal. *Nature* **467**: 323-327.

Akizu N, García MA, Estarás C, Fueyo R, Badosa C, de la Cruz X, Martínez-Balbás MA. 2016. EZH2 regulates neuroepithelium structure and neuroblast proliferation by repressing p21. *Open Biology* **6**.

Alberts B. 2008. *Molecular Biology of the Cell: Reference edition*. Garland Science.

Albig W, Bramlage B, Gruber K, Klobeck HG, Kunz J, Doenecke D. 1995. The human replacement histone H3.3B gene (H3F3B). *Genomics* **30**: 264-272.

Alcalay M, Tomassoni L, Colombo E, Stoldt S, Grignani F, Fagioli M, Szekely L, Helin K, Pelicci PG. 1998. The promyelocytic leukemia gene product (PML) forms stable complexes with the retinoblastoma protein. *Molecular and Cellular Biology* **18**: 1084-1093.

Alcantara Llaguno S, Chen J, Kwon CH, Jackson EL, Li Y, Burns DK, Alvarez-Buylla A, Parada LF. 2009. Malignant astrocytomas originate from neural stem/progenitor cells in a somatic tumor suppressor mouse model. *Cancer Cell* **15**: 45-56.

Allfrey VG. 1966. Structural modifications of histones and their possible role in the regulation of ribonucleic acid synthesis. *Proc Can Cancer Conf* **6**: 313-335.

Aloia L, Di Stefano B, Di Croce L. 2013. Polycomb complexes in stem cells and embryonic development. *Development* **140**: 2525-2534.

Alvarez-Buylla A, Garcia-Verdugo JM. 2002. Neurogenesis in adult subventricular zone. *J Neurosci* **22**: 629-634.

Alvarez-Buylla A, Kohwi M, Nguyen TM, Merkle FT. 2008. The heterogeneity of adult neural stem cells and the emerging complexity of their niche. *Cold Spring Harb Symp Quant Biol* **73**: 357-365.

Andreu-Agullo C, Maurin T, Thompson CB, Lai EC. 2012. Ars2 maintains neural stem-cell identity through direct transcriptional activation of Sox2. *Nature* **481**: 195-198.

Andrews W, Barber M, Hernadez-Miranda LR, Xian J, Rakic S, Sundaresan V, Rabbitts TH, Pannell R, Rabbitts P, Thompson H et al. 2008. The role of Slit-Robo signaling in the generation, migration and morphological differentiation of cortical interneurons. *Dev Biol* **313**: 648-658.

Andrews W, Liapi A, Plachez C, Camurri L, Zhang J, Mori S, Murakami F, Parnavelas JG, Sundaresan V, Richards LJ. 2006. Robo1 regulates the development of major axon tracts and interneuron migration in the forebrain. *Development* **133**: 2243-2252.

Angot E, Loulier K, Nguyen-Ba-Charvet KT, Gadeau AP, Ruat M, Traiffort E. 2008. Chemoattractive activity of sonic hedgehog in the adult subventricular zone modulates the number of neural precursors reaching the olfactory bulb. *Stem Cells* **26**: 2311-2320.

Ansieau S, Bastid J, Doreau A, Morel AP, Bouchet BP, Thomas C, Fauvet F, Puisieux I, Doglioni C, Piccinin S et al. 2008. Induction of EMT by twist proteins as a

collateral effect of tumor-promoting inactivation of premature senescence. *Cancer Cell* **14**: 79-89.

Arvidsson A, Collin T, Kirik D, Kokaia Z, Lindvall O. 2002. Neuronal replacement from endogenous precursors in the adult brain after stroke. *Nat Med* **8**: 963-970.

Attieh Y, Geng Q-R, DiNardo CD, Zheng H, Jia Y, Fang Z-H, Gañán-Gómez I, Yang H, Wei Y, Kantarjian H et al. 2013. Low frequency of H3.3 mutations and upregulated DAXX expression in MDS. *Blood* **121**: 4009-4011.

Bachmann IM, Halvorsen OJ, Collett K, Stefansson IM, Straume O, Haukaas SA, Salvesen HB, Otte AP, Akslen LA. 2006. EZH2 expression is associated with high proliferation rate and aggressive tumor subgroups in cutaneous melanoma and cancers of the endometrium, prostate, and breast. *J Clin Oncol* **24**: 268-273.

Bagri A, Marin O, Plump AS, Mak J, Pleasure SJ, Rubenstein JL, Tessier-Lavigne M. 2002. Slit proteins prevent midline crossing and determine the dorsoventral position of major axonal pathways in the mammalian forebrain. *Neuron* **33**: 233-248.

Banaszynski LA, Wen D, Dewell S, Whitcomb SJ, Lin M, Diaz N, Elsasser SJ, Chapgier A, Goldberg AD, Canaani E et al. 2013. Hira-dependent histone H3.3 deposition facilitates PRC2 recruitment at developmental loci in ES cells. *Cell* **155**: 107-120.

Barker N, Bartfeld S, Clevers H. 2010. Tissue-resident adult stem cell populations of rapidly self-renewing organs. *Cell Stem Cell* **7**: 656-670.

Barkho BZ, Munoz AE, Li X, Li L, Cunningham LA, Zhao X. 2008. Endogenous matrix metalloproteinase (MMP)-3 and MMP-9 promote the differentiation and migration of adult neural progenitor cells in response to chemokines. *Stem Cells* **26**: 3139-3149.

Bartesaghi S, Graziano V, Galavotti S, Henriquez NV, Betts J, Saxena J, Minieri V, A D, Karlsson A, Martins LM et al. 2015. Inhibition of oxidative metabolism leads to p53 genetic inactivation and transformation in neural stem cells. *Proc Natl Acad Sci U S A* **112**: 1059-1064.

Beauchesne P. 2011. Extra-neural metastases of malignant gliomas: myth or reality? *Cancers (Basel)* **3**: 461-477.

Behesti H, Bhagat H, Dubuc AM, Taylor MD, Marino S. 2013. Bmi1 overexpression in the cerebellar granule cell lineage of mice affects cell proliferation and survival without initiating medulloblastoma formation. *Dis Model Mech* **6**: 49-63.

Behjati S, Tarpey PS, Presneau N, Scheipl S, Pillay N, Van Loo P, Wedge DC, Cooke SL, Gundem G, Davies H et al. 2013. Distinct H3F3A and H3F3B driver mutations define chondroblastoma and giant cell tumor of bone. *Nat Genet* **45**: 1479-1482.

Bender S, Tang Y, Lindroth AM, Hovestadt V, Jones DT, Kool M, Zapatka M, Northcott PA, Sturm D, Wang W et al. 2013. Reduced H3K27me3 and DNA hypomethylation are major drivers of gene expression in K27M mutant pediatric high-grade gliomas. *Cancer Cell* **24**: 660-672.

Benedykcinska A, Ferreira A, Lau J, Broni J, Richard-Loendt A, Henriquez NV, Brandner S. 2016. Generation of brain tumours in mice by Cre-mediated recombination of neural progenitors in situ with the tamoxifen metabolite endoxifen. *Dis Model Mech* **9**: 211-220.

Bergmann O, Liebl J, Bernard S, Alkass K, Yeung Maggie SY, Steier P, Kutschera W, Johnson L, Landén M, Druid H et al. 2012. The Age of Olfactory Bulb Neurons in Humans. *Neuron* **74**: 634-639.

Bernardi R, Guernah I, Jin D, Grisendi S, Alimonti A, Teruya-Feldstein J, Cordon-Cardo C, Simon MC, Rafii S, Pandolfi PP. 2006. PML inhibits HIF-1alpha translation and neoangiogenesis through repression of mTOR. *Nature* **442**: 779-785.

Bernardi R, Pandolfi PP. 2003. Role of PML and the PML-nuclear body in the control of programmed cell death. *Oncogene* **22**: 9048-9057.

-. 2007. Structure, dynamics and functions of promyelocytic leukaemia nuclear bodies. *Nat Rev Mol Cell Biol* **8**: 1006-1016.

Bernstein BE, Mikkelsen TS, Xie X, Kamal M, Huebert DJ, Cuff J, Fry B, Meissner A, Wernig M, Plath K et al. 2006. A bivalent chromatin structure marks key developmental genes in embryonic stem cells. *Cell* **125**: 315-326.

Berube NG, Healy J, Medina CF, Wu S, Hodgson T, Jagla M, Picketts DJ. 2008. Patient mutations alter ATRX targeting to PML nuclear bodies. *Eur J Hum Genet* **16**: 192-201.

Binder E, Rukavina M, Hassani H, Weber M, Nakatani H, Reiff T, Parras C, Taylor V, Rohrer H. 2011. Peripheral nervous system progenitors can be reprogrammed to produce myelinating oligodendrocytes and repair brain lesions. *J Neurosci* **31**: 6379-6391.

Biteau B, Hochmuth CE, Jasper H. 2011. Maintaining tissue homeostasis: dynamic control of somatic stem cell activity. *Cell Stem Cell* **9**: 402-411.

Bjerke L, Mackay A, Nandhabalan M, Burford A, Jury A, Popov S, Bax DA, Carvalho D, Taylor KR, Vinci M et al. 2013. Histone H3.3. mutations drive pediatric glioblastoma through upregulation of MYCN. *Cancer Discov* **3**: 512-519.

Blackledge Neil P, Farcas Anca M, Kondo T, King Hamish W, McGouran Joanna F, Hanssen Lars LP, Ito S, Cooper S, Kondo K, Koseki Y et al. 2014. Variant PRC1 Complex-Dependent H2A Ubiquitylation Drives PRC2 Recruitment and Polycomb Domain Formation. *Cell* **157**: 1445-1459.

Blockus H, Chedotal A. 2014. The multifaceted roles of Slits and Robos in cortical circuits: from proliferation to axon guidance and neurological diseases. *Curr Opin Neurobiol* **27**: 82-88.

Bloomer WA, VanDongen HM, VanDongen AM. 2007. Activity-regulated cytoskeleton-associated protein Arc/Arg3.1 binds to spectrin and associates with nuclear promyelocytic leukemia (PML) bodies. *Brain Res* **1153**: 20-33.

Bonaguidi MA, Wheeler MA, Shapiro JS, Stadel RP, Sun GJ, Ming GL, Song H. 2011. In vivo clonal analysis reveals self-renewing and multipotent adult neural stem cell characteristics. *Cell* **145**: 1142-1155.

Bond AM, Ming G-l, Song H. 2015. Adult Mammalian Neural Stem Cells and Neurogenesis: Five Decades Later. *Cell stem cell* **17**: 385-395.

Bonfanti L. 2006. PSA-NCAM in mammalian structural plasticity and neurogenesis. *Prog Neurobiol* **80**: 129-164.

Bonfanti L, Olive S, Poulain DA, Theodosis DT. 1992. Mapping of the distribution of polysialylated neural cell adhesion molecule throughout the central nervous system of the adult rat: an immunohistochemical study. *Neuroscience* **49**: 419-436.

Bonfanti L, Theodosis DT. 1994. Expression of polysialylated neural cell adhesion molecule by proliferating cells in the subependymal layer of the adult rat, in its rostral extension and in the olfactory bulb. *Neuroscience* **62**: 291-305.

Borden KL. 2002. Pondering the promyelocytic leukemia protein (PML) puzzle: possible functions for PML nuclear bodies. *Mol Cell Biol* **22**: 5259-5269.

Borden KL, Boddy MN, Lally J, O'Reilly NJ, Martin S, Howe K, Solomon E, Freemont PS. 1995. The solution structure of the RING finger domain from the acute promyelocytic leukaemia proto-oncoprotein PML. *EMBO J* **14**: 1532-1541.

Borden KL, Lally JM, Martin SR, O'Reilly NJ, Solomon E, Freemont PS. 1996. In vivo and in vitro characterization of the B1 and B2 zinc-binding domains from the acute promyelocytic leukemia protooncoprotein PML. *Proc Natl Acad Sci U S A* **93**: 1601-1606.

Borrell V, Cardenas A, Ciceri G, Galceran J, Flames N, Pla R, Nobrega-Pereira S, Garcia-Frigola C, Peregrin S, Zhao Z et al. 2012. Slit/Robo signaling modulates the proliferation of central nervous system progenitors. *Neuron* **76**: 338-352.

Bottomley MJ. 2004. Structures of protein domains that create or recognize histone modifications. *EMBO Rep* **5**: 464-469.

Boyer LA, Plath K, Zeitlinger J, Brambrink T, Medeiros LA, Lee TI, Levine SS, Wernig M, Tajonar A, Ray MK et al. 2006. Polycomb complexes repress developmental regulators in murine embryonic stem cells. *Nature* **441**: 349-353.

Bracken AP, Pasini D, Capra M, Prosperini E, Colli E, Helin K. 2003. EZH2 is downstream of the pRB-E2F pathway, essential for proliferation and amplified in cancer. *EMBO J* **22**: 5323-5335.

Brennan CW, Verhaak RG, McKenna A, Campos B, Noushmehr H, Salama SR, Zheng S, Chakravarty D, Sanborn JZ, Berman SH et al. 2013. The somatic genomic landscape of glioblastoma. *Cell* **155**: 462-477.

Breton-Provencher V, Lemasson M, Peralta MR, 3rd, Saghatelyan A. 2009. Interneurons produced in adulthood are required for the normal functioning of the olfactory bulb network and for the execution of selected olfactory behaviors. *J Neurosci* **29**: 15245-15257.

Brose K, Bland KS, Wang KH, Arnott D, Henzel W, Goodman CS, Tessier-Lavigne M, Kidd T. 1999. Slit proteins bind Robo receptors and have an evolutionarily conserved role in repulsive axon guidance. *Cell* **96**: 795-806.

Brunk BP, Martin EC, Adler PN. 1991. Drosophila genes Posterior Sex Combs and Suppressor two of zeste encode proteins with homology to the murine bmi-1 oncogene. *Nature* **353**: 351-353.

Butler K, Martinez LA, Tejada-Simon MV. 2013. Impaired cognitive function and reduced anxiety-related behavior in a promyelocytic leukemia (PML) tumor suppressor protein-deficient mouse. *Genes Brain Behav* **12**: 189-202.

Cakouros D, Isenmann S, Cooper L, Zannettino A, Anderson P, Glackin C, Gronthos S. 2012. Twist-1 induces Ezh2 recruitment regulating histone methylation along the Ink4A/Arf locus in mesenchymal stem cells. *Mol Cell Biol* **32**: 1433-1441.

Calzolari F, Michel J, Baumgart EV, Theis F, Gotz M, Ninkovic J. 2015. Fast clonal expansion and limited neural stem cell self-renewal in the adult subependymal zone. *Nat Neurosci* **18**: 490-492.

Cancer Genome Atlas Research N. 2008. Comprehensive genomic characterization defines human glioblastoma genes and core pathways. *Nature* **455**: 1061-1068.

Cao R, Zhang Y. 2004. SUZ12 is required for both the histone methyltransferase activity and the silencing function of the EED-EZH2 complex. *Mol Cell* **15**: 57-67.

Capilla-Gonzalez V, Guerrero-Cazares H, Bonsu JM, Gonzalez-Perez O, Achanta P, Wong J, Garcia-Verdugo JM, Quinones-Hinojosa A. 2014. The subventricular zone is able to respond to a demyelinating lesion after localized radiation. *Stem Cells* **32**: 59-69.

Capilla-Gonzalez V, Lavell E, Quinones-Hinojosa A, Guerrero-Cazares H. 2015. Regulation of subventricular zone-derived cells migration in the adult brain. *Adv Exp Med Biol* **853**: 1-21.

Caramel J, Papadogeorgakis E, Hill L, Browne Gareth J, Richard G, Wierinckx A, Saldanha G, Osborne J, Hutchinson P, Tse G et al. A Switch in the Expression of Embryonic EMT-Inducers Drives the Development of Malignant Melanoma. *Cancer Cell* **24**: 466-480.

Carbone R, Botrugno OA, Ronzoni S, Insinga A, Di Croce L, Pelicci PG, Minucci S. 2006. Recruitment of the histone methyltransferase SUV39H1 and its role in the oncogenic properties of the leukemia-associated PML-retinoic acid receptor fusion protein. *Mol Cell Biol* **26**: 1288-1296.

Carleton A, Petreanu LT, Lansford R, Alvarez-Buylla A, Lledo PM. 2003. Becoming a new neuron in the adult olfactory bulb. *Nat Neurosci* **6**: 507-518.

Carracedo A, Weiss D, Leliaert AK, Bhasin M, de Boer VC, Laurent G, Adams AC, Sundvall M, Song SJ, Ito K et al. 2012. A metabolic prosurvival role for PML in breast cancer. *J Clin Invest* **122**: 3088-3100.

Casarosa S, Zasso J, Conti L. 2013. Systems for ex-vivo Isolation and culturing of neural stem cells. in *cdnintechopencom*.

Castro DS, Martynoga B, Parras C, Ramesh V, Pacary E, Johnston C, Drechsel D, Lebel-Potter M, Garcia LG, Hunt C et al. 2011. A novel function of the proneural factor Ascl1 in progenitor proliferation identified by genome-wide characterization of its targets. *Genes Dev* **25**: 930-945.

Chan KM, Fang D, Gan H, Hashizume R, Yu C, Schroeder M, Gupta N, Mueller S, James CD, Jenkins R et al. 2013. The histone H3.3K27M mutation in pediatric glioma reprograms H3K27 methylation and gene expression. *Genes Dev* **27**: 985-990.

Chang CJ, Yang JY, Xia W, Chen CT, Xie X, Chao CH, Woodward WA, Hsu JM, Hortobagyi GN, Hung MC. 2011. EZH2 promotes expansion of breast tumor initiating cells through activation of RAF1-beta-catenin signaling. *Cancer Cell* **19**: 86-100.

Chang KS, Fan YH, Andreeff M, Liu J, Mu ZM. 1995. The PML gene encodes a phosphoprotein associated with the nuclear matrix. *Blood* **85**: 3646-3653.

Charruyer A, Barland CO, Yue L, Wessendorf HB, Lu Y, Lawrence HJ, Mancianti ML, Ghadially R. 2009. Transit-amplifying cell frequency and cell cycle kinetics are altered in aged epidermis. *J Invest Dermatol* **129**: 2574-2583.

Chelbi-Alix MK, Pelicano L, Quignon F, Koken MH, Venturini L, Stadler M, Pavlovic J, Degos L, de The H. 1995. Induction of the PML protein by interferons in normal and APL cells. *Leukemia* **9**: 2027-2033.

Chelbi-Alix MK, Quignon F, Pelicano L, Koken MH, de The H. 1998. Resistance to virus infection conferred by the interferon-induced promyelocytic leukemia protein. *J Virol* **72**: 1043-1051.

Chen K, Chen Z, Wu D, Zhang L, Lin X, Su J, Rodriguez B, Xi Y, Xia Z, Chen X et al. 2015. Broad H3K4me3 is associated with increased transcription elongation and enhancer activity at tumor-suppressor genes. *Nat Genet* **47**: 1149-1157.

Chen ZF, Behringer RR. 1995. twist is required in head mesenchyme for cranial neural tube morphogenesis. *Genes Dev* **9**: 686-699.

Cheung NK, Zhang J, Lu C, Parker M, Bahrami A, Tickoo SK, Heguy A, Pappo AS, Federico S, Dalton J et al. 2012. Association of age at diagnosis and genetic mutations in patients with neuroblastoma. *JAMA* **307**: 1062-1071.

Ching RW, Dellaire G, Eskiw CH, Bazett-Jones DP. 2005. PML bodies: a meeting place for genomic loci? *J Cell Sci* **118**: 847-854.

Chow LM, Endersby R, Zhu X, Rankin S, Qu C, Zhang J, Broniscer A, Ellison DW, Baker SJ. 2011. Cooperativity within and among Pten, p53, and Rb pathways induces high-grade astrocytoma in adult brain. *Cancer Cell* **19**: 305-316.

Chuang YS, Huang WH, Park SW, Persaud SD, Hung CH, Ho PC, Wei LN. 2011. Promyelocytic leukemia protein in retinoic acid-induced chromatin remodeling of Oct4 gene promoter. *Stem Cells* **29**: 660-669.

Cohen E, Meininger V. 1987. Ultrastructural analysis of primary cilium in the embryonic nervous tissue of mouse. *Int J Dev Neurosci* **5**: 43-51.

Condemine W, Takahashi Y, Zhu J, Puvion-Dutilleul F, Guegan S, Janin A, de The H. 2006. Characterization of endogenous human promyelocytic leukemia isoforms. *Cancer Res* **66**: 6192-6198.

Conti L, Pollard SM, Gorba T, Reitano E, Toselli M, Biella G, Sun Y, Sanzone S, Ying QL, Cattaneo E et al. 2005. Niche-independent symmetrical self-renewal of a mammalian tissue stem cell. *PLoS Biol* **3**: e283.

Coskun V, Luskin MB. 2002. Intrinsic and extrinsic regulation of the proliferation and differentiation of cells in the rodent rostral migratory stream. *J Neurosci Res* **69**: 795-802.

Courtes S, Vernerey J, Pujadas L, Magalon K, Cremer H, Soriano E, Durbec P, Cayre M. 2011. Reelin controls progenitor cell migration in the healthy and pathological adult mouse brain. *PLoS One* **6**: e20430.

Cremer H, Lange R, Christoph A, Plomann M, Vopper G, Roes J, Brown R, Baldwin S, Kraemer P, Scheff S et al. 1994. Inactivation of the N-CAM gene in mice results in size reduction of the olfactory bulb and deficits in spatial learning. *Nature* **367**: 455-459.

Cuddapah VA, Robel S, Watkins S, Sontheimer H. 2014. A neurocentric perspective on glioma invasion. *Nat Rev Neurosci* **15**: 455-465.

Curtis MA, Kam M, Nannmark U, Anderson MF, Axell MZ, Wikkelso C, Holtas S, van Roon-Mom WM, Bjork-Eriksson T, Nordborg C et al. 2007. Human neuroblasts migrate to the olfactory bulb via a lateral ventricular extension. *Science* **315**: 1243-1249.

De Koning L, Corpet A, Haber JE, Almouzni G. 2007. Histone chaperones: an escort network regulating histone traffic. *Nat Struct Mol Biol* **14**: 997-1007.

de Ruijter AJ, van Gennip AH, Caron HN, Kemp S, van Kuilenburg AB. 2003. Histone deacetylases (HDACs): characterization of the classical HDAC family. *Biochem J* **370**: 737-749.

de The H, Lavau C, Marchio A, Chomienne C, Degos L, Dejean A. 1991. The PML-RAR alpha fusion mRNA generated by the t(15;17) translocation in acute promyelocytic leukemia encodes a functionally altered RAR. *Cell* **66**: 675-684.

de Vries Nienke A, Hulsman D, Akhtar W, de Jong J, Miles Denise C, Blom M, van Tellingen O, Jonkers J, van Lohuizen M. 2015. Prolonged Ezh2 Depletion in Glioblastoma Causes a Robust Switch in Cell Fate Resulting in Tumor Progression. *Cell Reports* **10**: 383-397.

DeCarolis NA, Mechanic M, Petrik D, Carlton A, Ables JL, Malhotra S, Bachoo R, Gotz M, Lagace DC, Eisch AJ. 2013. In vivo contribution of nestin- and GLAST-lineage cells to adult hippocampal neurogenesis. *Hippocampus* **23**: 708-719.

Del Carmen Gomez-Roldan M, Perez-Martin M, Capilla-Gonzalez V, Cifuentes M, Perez J, Garcia-Verdugo JM, Fernandez-Llebrez P. 2008. Neuroblast proliferation on the surface of the adult rat striatal wall after focal ependymal loss by intracerebroventricular injection of neuraminidase. *J Comp Neurol* **507**: 1571-1587.

Delbarre E, Ivanauskiene K, Kuntziger T, Collas P. 2013. DAXX-dependent supply of soluble (H3.3-H4) dimers to PML bodies pending deposition into chromatin. *Genome Res* **23**: 440-451.

Delgado AC, Ferron SR, Vicente D, Porlan E, Perez-Villalba A, Trujillo CM, D'Ocon P, Farinas I. 2014. Endothelial NT-3 delivered by vasculature and CSF promotes quiescence of subependymal neural stem cells through nitric oxide induction. *Neuron* **83**: 572-585.

Dellaire G, Bazett-Jones DP. 2004. PML nuclear bodies: dynamic sensors of DNA damage and cellular stress. *Bioessays* **26**: 963-977.

Dellaire G, Ching RW, Dehghani H, Ren Y, Bazett-Jones DP. 2006. The number of PML nuclear bodies increases in early S phase by a fission mechanism. *J Cell Sci* **119**: 1026-1033.

Deshaies RJ, Joazeiro CA. 2009. RING domain E3 ubiquitin ligases. *Annu Rev Biochem* **78**: 399-434.

Dhavan R, Tsai L-H. 2001. A decade of CDK5. *Nat Rev Mol Cell Biol* **2**: 749-759.

Doetsch F, Alvarez-Buylla A. 1996. Network of tangential pathways for neuronal migration in adult mammalian brain. *Proc Natl Acad Sci U S A* **93**: 14895-14900.

Doetsch F, Caille I, Lim DA, Garcia-Verdugo JM, Alvarez-Buylla A. 1999a. Subventricular zone astrocytes are neural stem cells in the adult mammalian brain. *Cell* **97**: 703-716.

Doetsch F, Garcia-Verdugo JM, Alvarez-Buylla A. 1999b. Regeneration of a germinal layer in the adult mammalian brain. *Proc Natl Acad Sci U S A* **96**: 11619-11624.

Drane P, Ouararhni K, Depaux A, Shuaib M, Hamiche A. 2010. The death-associated protein DAXX is a novel histone chaperone involved in the replication-independent deposition of H3.3. *Genes Dev* **24**: 1253-1265.

Drané P, Ouararhni K, Depaux A, Shuaib M, Hamiche A. 2010. The death-associated protein DAXX is a novel histone chaperone involved in the replication-independent deposition of H3.3. *Genes & Development* **24**: 1253-1265.

Duprez E, Saurin AJ, Desterro JM, Lallemand-Breitenbach V, Howe K, Boddy MN, Solomon E, de The H, Hay RT, Freemont PS. 1999. SUMO-1 modification of

the acute promyelocytic leukaemia protein PML: implications for nuclear localisation. *J Cell Sci* **112 (Pt 3)**: 381-393.

Dvorkina M, Nieddu V, Chakelam S, Pezzolo A, Cantilena S, Leite AP, Chayka O, Regad T, Pistorio A, Sementa AR et al. 2016. A Promyelocytic Leukemia Protein-Thrombospondin-2 Axis and the Risk of Relapse in Neuroblastoma. *Clin Cancer Res* **22**: 3398-3409.

Ehninger D, Kempermann G. 2008. Neurogenesis in the adult hippocampus. *Cell Tissue Res* **331**: 243-250.

Elias MC, Tozer KR, Silber JR, Mikheeva S, Deng M, Morrison RS, Manning TC, Silbergeld DL, Glackin CA, Reh TA et al. 2005. TWIST is expressed in human gliomas and promotes invasion. *Neoplasia* **7**: 824-837.

Elsaesser SJ, Allis CD. 2010. HIRA and Daxx constitute two independent histone H3.3-containing predeposition complexes. *Cold Spring Harb Symp Quant Biol* **75**: 27-34.

Elsasser SJ, Noh K-M, Diaz N, Allis CD, Banaszynski LA. 2015. Histone H3.3 is required for endogenous retroviral element silencing in embryonic stem cells. *Nature* **522**: 240-244.

Emsley JG, Hagg T. 2003. alpha6beta1 integrin directs migration of neuronal precursors in adult mouse forebrain. *Exp Neurol* **183**: 273-285.

Entz-Werle N, Stoetzel C, Berard-Marec P, Kalifa C, Brugiere L, Pacquement H, Schmitt C, Tabone MD, Gentet JC, Quillet R et al. 2005. Frequent genomic abnormalities at TWIST in human pediatric osteosarcomas. *Int J Cancer* **117**: 349-355.

Eom TY, Li J, Anton ES. 2010. Going tubular in the rostral migratory stream: neurons remodel astrocyte tubes to promote directional migration in the adult brain. *Neuron* **67**: 173-175.

Eriksson PS, Perfilieva E, Bjork-Eriksson T, Alborn A-M, Nordborg C, Peterson DA, Gage FH. 1998. Neurogenesis in the adult human hippocampus. *Nat Med* **4**: 1313-1317.

Ernst A, Alkass K, Bernard S, Salehpour M, Perl S, Tisdale J, Possnert G, Druid H, Frisén J. 2014. Neurogenesis in the Striatum of the Adult Human Brain. *Cell* **156**: 1072-1083.

Ernst T, Chase AJ, Score J, Hidalgo-Curtis CE, Bryant C, Jones AV, Waghorn K, Zoi K, Ross FM, Reiter A et al. 2010. Inactivating mutations of the histone methyltransferase gene EZH2 in myeloid disorders. *Nat Genet* **42**: 722-726.

Eskeland R, Leeb M, Grimes GR, Kress C, Boyle S, Sproul D, Gilbert N, Fan Y, Skoultchi AI, Wutz A et al. 2010. Ring1B compacts chromatin structure and represses gene expression independent of histone ubiquitination. *Mol Cell* **38**: 452-464.

Esteller M. 2007. Cancer epigenomics: DNA methylomes and histone-modification maps. *Nat Rev Genet* **8**: 286-298.

Facchino S, Abdouh M, Chatoo W, Bernier G. 2010. BMI1 confers radioresistance to normal and cancerous neural stem cells through recruitment of the DNA damage response machinery. *J Neurosci* **30**: 10096-10111.

Fagioli M, Alcalay M, Tomassoni L, Ferrucci PF, Mencarelli A, Riganelli D, Grignani F, Pozzan T, Nicoletti I, Grignani F et al. 1998. Cooperation between the RING + B1-B2 and coiled-coil domains of PML is necessary for its effects on cell survival. *Oncogene* **16**: 2905-2913.

Faiz M, Sachewsky N, Gascon S, Bang KW, Morshead CM, Nagy A. 2015. Adult Neural Stem Cells from the Subventricular Zone Give Rise to Reactive Astrocytes in the Cortex after Stroke. *Cell Stem Cell* **17**: 624-634.

Farcas AM, Blackledge NP, Sudbery I, Long HK, McGouran JF, Rose NR, Lee S, Sims D, Cerase A, Sheahan TW et al. 2012. KDM2B links the Polycomb Repressive Complex 1 (PRC1) to recognition of CpG islands. *Elife* **1**: e00205.

Fasano CA, Dimos JT, Ivanova NB, Lowry N, Lemischka IR, Temple S. 2007. shRNA knockdown of Bmi-1 reveals a critical role for p21-Rb pathway in NSC self-renewal during development. *Cell Stem Cell* **1**: 87-99.

Fasano CA, Phoenix TN, Kokovay E, Lowry N, Elkabetz Y, Dimos JT, Lemischka IR, Studer L, Temple S. 2009. Bmi-1 cooperates with Foxg1 to maintain neural stem cell self-renewal in the forebrain. *Genes Dev* **23**: 561-574.

Felsenfeld G. 2014. A brief history of epigenetics. *Cold Spring Harb Perspect Biol* **6**.

Felsenfeld G, Groudine M. 2003. Controlling the double helix. *Nature* **421**: 448-453.

Feng X, Juan AH, Wang HA, Ko KD, Zare H, Sartorelli V. 2016. Polycomb Ezh2 controls the fate of GABAergic neurons in the embryonic cerebellum. *Development* **143**: 1971-1980.

Ferbeyre G, de Stanchina E, Querido E, Baptiste N, Prives C, Lowe SW. 2000. PML is induced by oncogenic ras and promotes premature senescence. *Genes Dev* **14**: 2015-2027.

Figeac N, Daczewska M, Marcelle C, Jagla K. 2007. Muscle stem cells and model systems for their investigation. *Dev Dyn* **236**: 3332-3342.

Fiskus W, Pranpat M, Balasis M, Herger B, Rao R, Chinnaiyan A, Atadja P, Bhalla K. 2006. Histone deacetylase inhibitors deplete enhancer of zeste 2 and associated polycomb repressive complex 2 proteins in human acute leukemia cells. *Mol Cancer Ther* **5**: 3096-3104.

Fogal V, Gostissa M, Sandy P, Zacchi P, Sternsdorf T, Jensen K, Pandolfi PP, Will H, Schneider C, Del Sal G. 2000. Regulation of p53 activity in nuclear bodies by a specific PML isoform. *The EMBO journal* **19**: 6185-6195.

Francis F, Koulakoff A, Boucher D, Chafey P, Schaar B, Vinet MC, Friocourt G, McDonnell N, Reiner O, Kahn A et al. 1999. Doublecortin is a developmentally regulated, microtubule-associated protein expressed in migrating and differentiating neurons. *Neuron* **23**: 247-256.

Friedmann-Morvinski D, Bushong EA, Ke E, Soda Y, Marumoto T, Singer O, Ellisman MH, Verma IM. 2012. Dedifferentiation of neurons and astrocytes by oncogenes can induce gliomas in mice. *Science* **338**: 1080-1084.

Fuchtbauer EM. 1995. Expression of M-twist during postimplantation development of the mouse. *Dev Dyn* **204**: 316-322.

Fuentealba LC, Rompani SB, Parraguez JI, Obernier K, Romero R, Cepko CL, Alvarez-Buylla A. 2015. Embryonic Origin of Postnatal Neural Stem Cells. *Cell* **161**: 1644-1655.

Furnari FB, Fenton T, Bachoo RM, Mukasa A, Stommel JM, Stegh A, Hahn WC, Ligon KL, Louis DN, Brennan C et al. 2007. Malignant astrocytic glioma: genetics, biology, and paths to treatment. *Genes Dev* **21**: 2683-2710.

Furutachi S, Matsumoto A, Nakayama KI, Gotoh Y. 2013. p57 controls adult neural stem cell quiescence and modulates the pace of lifelong neurogenesis. *The EMBO Journal* **32**: 970-981.

Furutachi S, Miya H, Watanabe T, Kawai H, Yamasaki N, Harada Y, Imayoshi I, Nelson M, Nakayama KI, Hirabayashi Y et al. 2015. Slowly dividing neural progenitors are an embryonic origin of adult neural stem cells. *Nat Neurosci* **18**: 657-665.

Gage FH. 2000. Mammalian Neural Stem Cells. *Science* **287**: 1433-1438.

Gage FH, Temple S. 2013. Neural stem cells: generating and regenerating the brain. *Neuron* **80**: 588-601.

Gao Z, Zhang J, Bonasio R, Strino F, Sawai A, Parisi F, Kluger Y, Reinberg D. 2012. PCGF homologs, CBX proteins, and RYBP define functionally distinct PRC1 family complexes. *Mol Cell* **45**: 344-356.

Garcia E, Marcos-Gutierrez C, del Mar Lorente M, Moreno JC, Vidal M. 1999. RYBP, a new repressor protein that interacts with components of the mammalian Polycomb complex, and with the transcription factor YY1. *EMBO J* **18**: 3404-3418.

Geoffroy MC, Chelbi-Alix MK. 2011. Role of promyelocytic leukemia protein in host antiviral defense. *J Interferon Cytokine Res* **31**: 145-158.

Gitelman I. 1997. Twist protein in mouse embryogenesis. *Dev Biol* **189**: 205-214.

Gleeson JG, Lin PT, Flanagan LA, Walsh CA. 1999. Doublecortin is a microtubule-associated protein and is expressed widely by migrating neurons. *Neuron* **23**: 257-271.

Goings GE, Sahni V, Szele FG. 2004. Migration patterns of subventricular zone cells in adult mice change after cerebral cortex injury. *Brain Res* **996**: 213-226.

Goldberg AD, Banaszynski LA, Noh KM, Lewis PW, Elsaesser SJ, Stadler S, Dewell S, Law M, Guo X, Li X et al. 2010. Distinct factors control histone variant H3.3 localization at specific genomic regions. *Cell* **140**: 678-691.

Gonzalez-Perez O. 2012. Neural stem cells in the adult human brain. *Biol Biomed Rep* **2**: 59-69.

Gonzalez-Perez O, Romero-Rodriguez R, Soriano-Navarro M, Garcia-Verdugo JM, Alvarez-Buylla A. 2009. Epidermal growth factor induces the progeny of subventricular zone type B cells to migrate and differentiate into oligodendrocytes. *Stem Cells* **27**: 2032-2043.

Gray PA, Fu H, Luo P, Zhao Q, Yu J, Ferrari A, Tenzen T, Yuk DI, Tsung EF, Cai Z et al. 2004. Mouse brain organization revealed through direct genome-scale TF expression analysis. *Science* **306**: 2255-2257.

Gregg C, Weiss S. 2003. Generation of functional radial glial cells by embryonic and adult forebrain neural stem cells. *J Neurosci* **23**: 11587-11601.

Grimwade D, Solomon E. 1997. Characterisation of the PML/RAR alpha rearrangement associated with t(15;17) acute promyelocytic leukaemia. *Curr Top Microbiol Immunol* **220**: 81-112.

Guerrero-Cazares H, Gonzalez-Perez O, Soriano-Navarro M, Zamora-Berridi G, Garcia-Verdugo JM, Quinones-Hinojosa A. 2011. Cytoarchitecture of the lateral ganglionic eminence and rostral extension of the lateral ventricle in the human fetal brain. *J Comp Neurol* **519**: 1165-1180.

Guillemot F. 2005. Cellular and molecular control of neurogenesis in the mammalian telencephalon. *Curr Opin Cell Biol* **17**: 639-647.

Guo A, Salomoni P, Luo J, Shih A, Zhong S, Gu W, Pandolfi PP. 2000. The function of PML in p53-dependent apoptosis. *Nat Cell Biol* **2**: 730-736.

Gurrieri C, Capodieci P, Bernardi R, Scaglioni PP, Nafa K, Rush LJ, Verbel DA, Cordon-Cardo C, Pandolfi PP. 2004. Loss of the tumor suppressor PML in

human cancers of multiple histologic origins. *J Natl Cancer Inst* **96**: 269-279.

Hack I, Bancila M, Loulier K, Carroll P, Cremer H. 2002. Reelin is a detachment signal in tangential chain-migration during postnatal neurogenesis. *Nat Neurosci* **5**: 939-945.

Hamilton JD, Rapp M, Schneiderhan T, Sabel M, Hayman A, Scherer A, Kropil P, Budach W, Gerber P, Kretschmar U et al. 2014. Glioblastoma multiforme metastasis outside the CNS: three case reports and possible mechanisms of escape. *J Clin Oncol* **32**: e80-84.

Hanahan D, Weinberg Robert A. 2011. Hallmarks of Cancer: The Next Generation. *Cell* **144**: 646-674.

Happel N, Doenecke D. 2009. Histone H1 and its isoforms: contribution to chromatin structure and function. *Gene* **431**: 1-12.

Haupt Y, Alexander WS, Barri G, Klinken SP, Adams JM. 1991. Novel zinc finger gene implicated as myc collaborator by retrovirally accelerated lymphomagenesis in E mu-myc transgenic mice. *Cell* **65**: 753-763.

He J, Shen L, Wan M, Taranova O, Wu H, Zhang Y. 2013. Kdm2b maintains murine embryonic stem cell status by recruiting PRC1 complex to CpG islands of developmental genes. *Nat Cell Biol* **15**: 373-384.

He S, Iwashita T, Buchstaller J, Molofsky AV, Thomas D, Morrison SJ. 2009. Bmi-1 over-expression in neural stem/progenitor cells increases proliferation and neurogenesis in culture but has little effect on these functions in vivo. *Dev Biol* **328**: 257-272.

Heaphy CM, de Wilde RF, Jiao Y, Klein AP, Edil BH, Shi C, Bettegowda C, Rodriguez FJ, Eberhart CG, Hebbar S et al. 2011. Altered telomeres in tumors with ATRX and DAXX mutations. *Science* **333**: 425.

Heinemann B, Nielsen JM, Hudlebusch HR, Lees MJ, Larsen DV, Boesen T, Labelle M, Gerlach L-O, Birk P, Helin K. 2014. Inhibition of demethylases by GSK-J1/J4. *Nature* **514**: E1-E2.

Hirabayashi Y, Gotoh Y. 2010. Epigenetic control of neural precursor cell fate during development. *Nat Rev Neurosci* **11**: 377-388.

Hirabayashi Y, Suzki N, Tsuboi M, Endo TA, Toyoda T, Shinga J, Koseki H, Vidal M, Gotoh Y. 2009. Polycomb limits the neurogenic competence of neural precursor cells to promote astrogenic fate transition. *Neuron* **63**: 600-613.

Hirota Y, Ohshima T, Kaneko N, Ikeda M, Iwasato T, Kulkarni AB, Mikoshiba K, Okano H, Sawamoto K. 2007. Cyclin-dependent kinase 5 is required for control of neuroblast migration in the postnatal subventricular zone. *J Neurosci* **27**: 12829-12838.

Hisada K, Sanchez C, Endo TA, Endoh M, Roman-Trufero M, Sharif J, Koseki H, Vidal M. 2012. RYBP represses endogenous retroviruses and preimplantation- and germ line-specific genes in mouse embryonic stem cells. *Mol Cell Biol* **32**: 1139-1149.

Hoek K, Rimm DL, Williams KR, Zhao H, Ariyan S, Lin A, Kluger HM, Berger AJ, Cheng E, Trombetta ES et al. 2004. Expression profiling reveals novel pathways in the transformation of melanocytes to melanomas. *Cancer Res* **64**: 5270-5282.

Holland EC, Celestino J, Dai C, Schaefer L, Sawaya RE, Fuller GN. 2000. Combined activation of Ras and Akt in neural progenitors induces glioblastoma formation in mice. *Nat Genet* **25**: 55-57.

Hollenbach AD, McPherson CJ, Mientjes EJ, Iyengar R, Grosveld G. 2002. Daxx and histone deacetylase II associate with chromatin through an interaction with core histones and the chromatin-associated protein Dek. *J Cell Sci* **115**: 3319-3330.

Hong J, Zhou J, Fu J, He T, Qin J, Wang L, Liao L, Xu J. 2011. Phosphorylation of serine 68 of Twist1 by MAPKs stabilizes Twist1 protein and promotes breast cancer cell invasiveness. *Cancer Res* **71**: 3980-3990.

Hor CH, Tang BL. 2010. Sonic hedgehog as a chemoattractant for adult NPCs. *Cell Adh Migr* **4**: 1-3.

Hu H. 1999. Chemorepulsion of neuronal migration by Slit2 in the developing mammalian forebrain. *Neuron* **23**: 703-711.

Hu H, Rutishauser U. 1996. A Septum-Derived Chemorepulsive Factor for Migrating Olfactory Interneuron Precursors. *Neuron* **16**: 933-940.

Hu H, Tomasiewicz H, Magnuson T, Rutishauser U. 1996. The role of polysialic acid in migration of olfactory bulb interneuron precursors in the subventricular zone. *Neuron* **16**: 735-743.

Hussain M, Rao M, Humphries AE, Hong JA, Liu F, Yang M, Caragacianu D, Schrump DS. 2009. Tobacco smoke induces polycomb-mediated repression of Dickkopf-1 in lung cancer cells. *Cancer Res* **69**: 3570-3578.

Hwang WW, Salinas RD, Siu JJ, Kelley KW, Delgado RN, Paredes MF, Alvarez-Buylla A, Oldham MC, Lim DA. 2014. Distinct and separable roles for EZH2 in neurogenic astroglia. *Elife* **3**: e02439.

Hynes RO. 2002. Integrins: bidirectional, allosteric signaling machines. *Cell* **110**: 673-687.

Ihrie RA, Shah JK, Harwell CC, Levine JH, Guinto CD, Lezameta M, Kriegstein AR, Alvarez-Buylla A. 2011. Persistent sonic hedgehog signaling in adult brain determines neural stem cell positional identity. *Neuron* **71**: 250-262.

Ikeda K, Inoue S. 2012. Trim Proteins as Ring Finger E3 Ubiquitin Ligases. in *TRIM/RBCC Proteins* (ed. G Meroni), pp. 27-37. Springer New York, New York, NY.

Imayoshi I, Kageyama R. 2014. bHLH factors in self-renewal, multipotency, and fate choice of neural progenitor cells. *Neuron* **82**: 9-23.

Imayoshi I, Sakamoto M, Ohtsuka T, Takao K, Miyakawa T, Yamaguchi M, Mori K, Ikeda T, Itohara S, Kageyama R. 2008a. Roles of continuous neurogenesis in the structural and functional integrity of the adult forebrain. *Nat Neurosci* **11**: 1153-1161.

Imayoshi I, Sakamoto M, Ohtsuka T, Takao K, Miyakawa T, Yamaguchi M, Mori K, Ikeda T, Itohara S, Kageyama R. 2008b. Roles of continuous neurogenesis in the structural and functional integrity of the adult forebrain. *Nat Neurosci* **11**: 1153-1161.

Imitola J, Raddassi K, Park KI, Mueller FJ, Nieto M, Teng YD, Frenkel D, Li J, Sidman RL, Walsh CA et al. 2004. Directed migration of neural stem cells to sites of CNS injury by the stromal cell-derived factor 1alpha/CXC chemokine receptor 4 pathway. *Proc Natl Acad Sci U S A* **101**: 18117-18122.

Ingham PW, McMahon AP. 2001. Hedgehog signaling in animal development: paradigms and principles. *Genes Dev* **15**: 3059-3087.

Inta D, Alfonso J, von Engelhardt J, Kreuzberg MM, Meyer AH, van Hooft JA, Monyer H. 2008. Neurogenesis and widespread forebrain migration of distinct GABAergic neurons from the postnatal subventricular zone. *Proc Natl Acad Sci U S A* **105**: 20994-20999.

Ishov AM, Sotnikov AG, Negorev D, Vladimirova OV, Neff N, Kamitani T, Yeh ET, Strauss JF, 3rd, Maul GG. 1999. PML is critical for ND10 formation and recruits the PML-interacting protein daxx to this nuclear structure when modified by SUMO-1. *J Cell Biol* **147**: 221-234.

Ito K, Bernardi R, Morotti A, Matsuoka S, Saglio G, Ikeda Y, Rosenblatt J, Avigan DE, Teruya-Feldstein J, Pandolfi PP. 2008. PML targeting eradicates quiescent leukaemia-initiating cells. *Nature* **453**: 1072-1078.

Ito K, Carracedo A, Weiss D, Arai F, Ala U, Avigan DE, Schafer ZT, Evans RM, Suda T, Lee CH et al. 2012. A PML-PPAR-delta pathway for fatty acid oxidation regulates hematopoietic stem cell maintenance. *Nat Med* **18**: 1350-1358.

Itoh Y, Masuyama N, Nakayama K, Nakayama KI, Gotoh Y. 2007. The cyclin-dependent kinase inhibitors p57 and p27 regulate neuronal migration in the developing mouse neocortex. *J Biol Chem* **282**: 390-396.

Itoh Y, Moriyama Y, Hasegawa T, Endo TA, Toyoda T, Gotoh Y. 2013. Scratch regulates neuronal migration onset via an epithelial-mesenchymal transition-like mechanism. *Nat Neurosci* **16**: 416-425.

Jacobowitz DM, Winsky L. 1991. Immunocytochemical localization of calretinin in the forebrain of the rat. *J Comp Neurol* **304**: 198-218.

Jacques TS, Relvas JB, Nishimura S, Pytela R, Edwards GM, Streuli CH, ffrench-Constant C. 1998. Neural precursor cell chain migration and division are regulated through different beta1 integrins. *Development* **125**: 3167-3177.

Jacques TS, Swales A, Brzozowski MJ, Henriquez NV, Linehan JM, Mirzadeh Z, C OM, Naumann H, Alvarez-Buylla A, Brandner S. 2010. Combinations of genetic mutations in the adult neural stem cell compartment determine brain tumour phenotypes. *EMBO J* **29**: 222-235.

Jadasz JJ, Rivera FJ, Taubert A, Kandasamy M, Sandner B, Weidner N, Aktas O, Hartung HP, Aigner L, Kury P. 2012. p57kip2 regulates glial fate decision in adult neural stem cells. *Development* **139**: 3306-3315.

Jaenisch R, Bird A. 2003. Epigenetic regulation of gene expression: how the genome integrates intrinsic and environmental signals. *Nat Genet* **33 Suppl**: 245-254.

Jaerve A, Muller HW. 2012. Chemokines in CNS injury and repair. *Cell Tissue Res* **349**: 229-248.

Janer A, Martin E, Muriel M-P, Latouche M, Fujigasaki H, Ruberg M, Brice A, Trottier Y, Sittler A. 2006. PML clastosomes prevent nuclear accumulation of mutant ataxin-7 and other polyglutamine proteins. *The Journal of Cell Biology* **174**: 65-76.

Jankovski A, Sotelo C. 1996. Subventricular zone-olfactory bulb migratory pathway in the adult mouse: cellular composition and specificity as determined by heterochronic and heterotopic transplantation. *J Comp Neurol* **371**: 376-396.

Jeanne M, Lallemand-Breitenbach V, Ferhi O, Koken M, Le Bras M, Duffort S, Peres L, Berthier C, Soilihi H, Raught B et al. 2010. PML/RARA oxidation and arsenic binding initiate the antileukemia response of As2O3. *Cancer Cell* **18**: 88-98.

Jensen K, Shiels C, Freemont PS. 2001. PML protein isoforms and the RBCC/TRIM motif. *Oncogene* **20**: 7223-7233.

Jiao Y, Killela PJ, Reitman ZJ, Rasheed AB, Heaphy CM, de Wilde RF, Rodriguez FJ, Rosemberg S, Oba-Shinjo SM, Nagahashi Marie SK et al. 2012. Frequent

ATRX, CIC, FUBP1 and IDH1 mutations refine the classification of malignant gliomas. *Oncotarget* **3**: 709-722.

Jiao Y, Shi C, Edil BH, de Wilde RF, Klimstra DS, Maitra A, Schulick RD, Tang LH, Wolfgang CL, Choti MA et al. 2011. DAXX/ATRX, MEN1, and mTOR pathway genes are frequently altered in pancreatic neuroendocrine tumors. *Science* **331**: 1199-1203.

Joazeiro CA, Weissman AM. 2000. RING finger proteins: mediators of ubiquitin ligase activity. *Cell* **102**: 549-552.

Johansson CB, Momma S, Clarke DL, Risling M, Lendahl U, Frisen J. 1999. Identification of a neural stem cell in the adult mammalian central nervous system. *Cell* **96**: 25-34.

Jones CA, London NR, Chen H, Park KW, Sauvaget D, Stockton RA, Wythe JD, Suh W, Larrieu-Lahargue F, Mukouyama Y-s et al. 2008. Robo4 stabilizes the vascular network by inhibiting pathologic angiogenesis and endothelial hyperpermeability. *Nat Med* **14**: 448-453.

Jones CA, Nishiya N, London NR, Zhu W, Sorensen LK, Chan AC, Lim CJ, Chen H, Zhang Q, Schultz PG et al. 2009. Slit2-Robo4 signalling promotes vascular stability by blocking Arf6 activity. *Nat Cell Biol* **11**: 1325-1331.

Jones DT, Hutter B, Jager N, Korshunov A, Kool M, Warnatz HJ, Zichner T, Lambert SR, Ryzhova M, Quang DA et al. 2013. Recurrent somatic alterations of FGFR1 and NTRK2 in pilocytic astrocytoma. *Nat Genet* **45**: 927-932.

Joseph B, Andersson ER, Vlachos P, Sodersten E, Liu L, Teixeira AI, Hermanson O. 2009. p57Kip2 is a repressor of Mash1 activity and neuronal differentiation in neural stem cells. *Cell Death Differ* **16**: 1256-1265.

Kakizuka A, Miller WH, Jr., Umesono K, Warrell RP, Jr., Frankel SR, Murty VV, Dmitrovsky E, Evans RM. 1991. Chromosomal translocation t(15;17) in human acute promyelocytic leukemia fuses RAR alpha with a novel putative transcription factor, PML. *Cell* **66**: 663-674.

Kalluri R, Weinberg RA. 2009. The basics of epithelial-mesenchymal transition. *The Journal of Clinical Investigation* **119**: 1420-1428.

Kamakaka RT, Biggins S. 2005. Histone variants: deviants? *Genes Dev* **19**: 295-310.

Kaneko N, Marin O, Koike M, Hirota Y, Uchiyama Y, Wu JY, Lu Q, Tessier-Lavigne M, Alvarez-Buylla A, Okano H et al. 2010. New neurons clear the path of astrocytic processes for their rapid migration in the adult brain. *Neuron* **67**: 213-223.

Kaneko N, Sawamoto K. 2007. [Neuronal migration in the adult brain]. *Nihon Shinkei Seishin Yakurigaku Zasshi* **27**: 215-218.

Kang SS, Keasey MP, Arnold SA, Reid R, Geralds J, Hagg T. 2013. Endogenous CNTF mediates stroke-induced adult CNS neurogenesis in mice. *Neurobiol Dis* **49**: 68-78.

Kanno M, Hasegawa M, Ishida A, Isono K, Taniguchi M. 1995. mel-18, a Polycomb group-related mammalian gene, encodes a transcriptional negative regulator with tumor suppressive activity. *EMBO J* **14**: 5672-5678.

Kaplan MS, McNelly NA, Hinds JW. 1985. Population dynamics of adult-formed granule neurons of the rat olfactory bulb. *J Comp Neurol* **239**: 117-125.

Kappeler C, Saillour Y, Baudoin JP, Tuy FP, Alvarez C, Houbron C, Gaspar P, Hamard G, Chelly J, Metin C et al. 2006. Branching and nucleokinesis defects in migrating interneurons derived from doublecortin knockout mice. *Hum Mol Genet* **15**: 1387-1400.

Katsimpardi L, Litterman NK, Schein PA, Miller CM, Loffredo FS, Wojtkiewicz GR, Chen JW, Lee RT, Wagers AJ, Rubin LL. 2014. Vascular and neurogenic rejuvenation of the aging mouse brain by young systemic factors. *Science* **344**: 630-634.

Kaur S, Samant GV, Pramanik K, Loscombe PW, Pendrak ML, Roberts DD, Ramchandran R. 2008. Silencing of directional migration in roundabout4 knockdown endothelial cells. *BMC Cell Biol* **9**: 61.

Kavanagh E, Joseph B. 2011. The hallmarks of CDKN1C (p57, KIP2) in cancer. *Biochim Biophys Acta* **1816**: 50-56.

Kennedy TE, Wang H, Marshall W, Tessier-Lavigne M. 2006. Axon guidance by diffusible chemoattractants: a gradient of netrin protein in the developing spinal cord. *J Neurosci* **26**: 8866-8874.

Khan MM, Nomura T, Kim H, Kaul SC, Wadhwa R, Shinagawa T, Ichikawa-Iwata E, Zhong S, Pandolfi PP, Ishii S. 2001. Role of PML and PML-RARalpha in Mad-mediated transcriptional repression. *Mol Cell* **7**: 1233-1243.

Khochbin S, Verdel A, Lemercier C, Seigneurin-Berny D. 2001. Functional significance of histone deacetylase diversity. *Curr Opin Genet Dev* **11**: 162-166.

Khuong-Quang DA, Buczkowicz P, Rakopoulos P, Liu XY, Fontebasso AM, Bouffet E, Bartels U, Albrecht S, Schwartzentruber J, Letourneau L et al. 2012. K27M mutation in histone H3.3 defines clinically and biologically distinct subgroups of pediatric diffuse intrinsic pontine gliomas. *Acta Neuropathol* **124**: 439-447.

Killock D. 2016. CNS cancer: Breaking boundaries [mdash] IDH mutations in glioma. *Nat Rev Clin Oncol* **13**: 64-65.

Kim JH, Yoon SY, Jeong SH, Kim SY, Moon SK, Joo JH, Lee Y, Choe IS, Kim JW. 2004. Overexpression of Bmi-1 oncoprotein correlates with axillary lymph node metastases in invasive ductal breast cancer. *Breast* **13**: 383-388.

Kim KH, Roberts CWM. 2016. Targeting EZH2 in cancer. *Nat Med* **22**: 128-134.

Kippin TE, Martens DJ, van der Kooy D. 2005. p21 loss compromises the relative quiescence of forebrain stem cell proliferation leading to exhaustion of their proliferation capacity. *Genes Dev* **19**: 756-767.

Kirschenbaum B, Doetsch F, Lois C, Alvarez-Buylla A. 1999. Adult subventricular zone neuronal precursors continue to proliferate and migrate in the absence of the olfactory bulb. *J Neurosci* **19**: 2171-2180.

Kitamura YI, Kitamura T, Kruse JP, Raum JC, Stein R, Gu W, Accili D. 2005. FoxO1 protects against pancreatic beta cell failure through NeuroD and MafA induction. *Cell Metab* **2**: 153-163.

Kleihues P, Louis DN, Scheithauer BW, Rorke LB, Reifenberger G, Burger PC, Cavenee WK. 2002. The WHO classification of tumors of the nervous system. *J Neuropathol Exp Neurol* **61**: 215-225; discussion 226-219.

Klymenko T, Papp B, Fischle W, Kocher T, Schelder M, Fritsch C, Wild B, Wilm M, Muller J. 2006. A Polycomb group protein complex with sequence-specific DNA-binding and selective methyl-lysine-binding activities. *Genes Dev* **20**: 1110-1122.

Knudson AG, Jr. 1971. Mutation and cancer: statistical study of retinoblastoma. *Proc Natl Acad Sci U S A* **68**: 820-823.

Kohwi M, Osumi N, Rubenstein JLR, Alvarez-Buylla A. 2005. Pax6 Is Required for Making Specific Subpopulations of Granule and Periglomerular Neurons in the Olfactory Bulb. *The Journal of Neuroscience* **25**: 6997-7003.

Koizumi H, Higginbotham H, Poon T, Tanaka T, Brinkman BC, Gleeson JG. 2006. Doublecortin maintains bipolar shape and nuclear translocation during migration in the adult forebrain. *Nat Neurosci* **9**: 779-786.

Kojima T, Hirota Y, Ema M, Takahashi S, Miyoshi I, Okano H, Sawamoto K. 2010. Subventricular zone-derived neural progenitor cells migrate along a blood vessel scaffold toward the post-stroke striatum. *Stem Cells* **28**: 545-554.

Koken MH, Linares-Cruz G, Quignon F, Viron A, Chelbi-Alix MK, Sobczak-Thepot J, Juhlin L, Degos L, Calvo F, de The H. 1995. The PML growth-suppressor has an altered expression in human oncogenesis. *Oncogene* **10**: 1315-1324.

Korb E, Wilkinson CL, Delgado RN, Lovero KL, Finkbeiner S. 2013. Arc in the nucleus regulates PML-dependent GluA1 transcription and homeostatic plasticity. *Nat Neurosci* **16**: 874-883.

Kornberg RD. 1974. Chromatin structure: a repeating unit of histones and DNA. *Science* **184**: 868-871.

Kornberg RD, Thomas JO. 1974. Chromatin structure; oligomers of the histones. *Science* **184**: 865-868.

Kosaka K, Aika Y, Toida K, Heizmann CW, Hunziker W, Jacobowitz DM, Nagatsu I, Streit P, Visser TJ, Kosaka T. 1995. Chemically defined neuron groups and their subpopulations in the glomerular layer of the rat main olfactory bulb. *Neurosci Res* **23**: 73-88.

Kosaka K, Toida K, Margolis FL, Kosaka T. 1997. Chemically defined neuron groups and their subpopulations in the glomerular layer of the rat main olfactory bulb--II. Prominent differences in the intraglomerular dendritic arborization and their relationship to olfactory nerve terminals. *Neuroscience* **76**: 775-786.

Kouzarides T. 2007. Chromatin modifications and their function. *Cell* **128**: 693-705.

Kreso A, van Galen P, Pedley NM, Lima-Fernandes E, Frelin C, Davis T, Cao L, Baiazitov R, Du W, Sydorenko N et al. 2014. Self-renewal as a therapeutic target in human colorectal cancer. *Nat Med* **20**: 29-36.

Kruidenier L, Chung CW, Cheng Z, Liddle J, Che K, Joberty G, Bantscheff M, Bountra C, Bridges A, Diallo H et al. 2012. A selective jumonji H3K27 demethylase inhibitor modulates the proinflammatory macrophage response. *Nature* **488**: 404-408.

Kuo HY, Chang CC, Jeng JC, Hu HM, Lin DY, Maul GG, Kwok RP, Shih HM. 2005. SUMO modification negatively modulates the transcriptional activity of CREB-binding protein via the recruitment of Daxx. *Proc Natl Acad Sci U S A* **102**: 16973-16978.

Kwok WK, Ling MT, Lee TW, Lau TC, Zhou C, Zhang X, Chua CW, Chan KW, Chan FL, Glackin C et al. 2005. Up-regulation of TWIST in prostate cancer and its implication as a therapeutic target. *Cancer Res* **65**: 5153-5162.

Lachapelle F, Avellana-Adalid V, Nait-Oumesmar B, Baron-Van Evercooren A. 2002. Fibroblast growth factor-2 (FGF-2) and platelet-derived growth factor AB (PDGF AB) promote adult SVZ-derived oligodendrogenesis in vivo. *Mol Cell Neurosci* **20**: 390-403.

Lallemand-Breitenbach V, de The H. 2010. PML nuclear bodies. *Cold Spring Harb Perspect Biol* **2**: a000661.

Lallemand-Breitenbach V, Zhu J, Chen Z, de Thé H. Curing APL through PML/RARA degradation by As₂O₃. *Trends in Molecular Medicine* **18**: 36-42.

Lamouille S, Xu J, Derynck R. 2014. Molecular mechanisms of epithelial–mesenchymal transition. *Nat Rev Mol Cell Biol* **15**: 178-196.

Lavau C, Marchio A, Fagioli M, Jansen J, Falini B, Lebon P, Grosveld F, Pandolfi PP, Pelicci PG, Dejean A. 1995. The acute promyelocytic leukaemia-associated PML gene is induced by interferon. *Oncogene* **11**: 871-876.

Laywell ED, Rakic P, Kukekov VG, Holland EC, Steindler DA. 2000. Identification of a multipotent astrocytic stem cell in the immature and adult mouse brain. *Proceedings of the National Academy of Sciences of the United States of America* **97**: 13883-13888.

Lazarini F, Mouthon MA, Gheusi G, de Chaumont F, Olivo-Marin JC, Lamarque S, Abrous DN, Boussin FD, Lledo PM. 2009. Cellular and behavioral effects of cranial irradiation of the subventricular zone in adult mice. *PLoS One* **4**: e7017.

Lee TK, Poon RT, Yuen AP, Ling MT, Kwok WK, Wang XH, Wong YC, Guan XY, Man K, Chau KL et al. 2006. Twist overexpression correlates with hepatocellular carcinoma metastasis through induction of epithelial-mesenchymal transition. *Clin Cancer Res* **12**: 5369-5376.

Lee W, Teckie S, Wiesner T, Ran L, Prieto Granada CN, Lin M, Zhu S, Cao Z, Liang Y, Sboner A et al. 2014. PRC2 is recurrently inactivated through EED or SUZ12 loss in malignant peripheral nerve sheath tumors. *Nat Genet* **46**: 1227-1232.

Lessard J, Sauvageau G. 2003. Bmi-1 determines the proliferative capacity of normal and leukaemic stem cells. *Nature* **423**: 255-260.

Leung C, Lingbeek M, Shakhova O, Liu J, Tanger E, Saremaslani P, van Lohuizen M, Marino S. 2004. Bmi1 is essential for cerebellar development and is overexpressed in human medulloblastomas. *Nature* **428**: 337-341.

Levine M, Davidson EH. 2005. Gene regulatory networks for development. *Proceedings of the National Academy of Sciences of the United States of America* **102**: 4936-4942.

Levine SS, Weiss A, Erdjument-Bromage H, Shao Z, Tempst P, Kingston RE. 2002. The core of the polycomb repressive complex is compositionally and functionally conserved in flies and humans. *Mol Cell Biol* **22**: 6070-6078.

Lewis EB. 1978. A gene complex controlling segmentation in Drosophila. *Nature* **276**: 565-570.

Lewis PW, Elsaesser SJ, Noh K-M, Stadler SC, Allis CD. 2010a. Daxx is an H3.3-specific histone chaperone and cooperates with ATRX in replication-independent chromatin assembly at telomeres. *Proceedings of the National Academy of Sciences* **107**: 14075-14080.

Lewis PW, Elsaesser SJ, Noh KM, Stadler SC, Allis CD. 2010b. Daxx is an H3.3-specific histone chaperone and cooperates with ATRX in replication-independent chromatin assembly at telomeres. *Proc Natl Acad Sci U S A* **107**: 14075-14080.

Lewis PW, Muller MM, Koletsky MS, Cordero F, Lin S, Banaszynski LA, Garcia BA, Muir TW, Becher OJ, Allis CD. 2013. Inhibition of PRC2 activity by a gain-of-function H3 mutation found in pediatric glioblastoma. *Science* **340**: 857-861.

Li B, Carey M, Workman JL. 2007. The role of chromatin during transcription. *Cell* **128**: 707-719.

Li G, Margueron R, Ku M, Chambon P, Bernstein BE, Reinberg D. 2010. Jarid2 and PRC2, partners in regulating gene expression. *Genes Dev* **24**: 368-380.

Li H, Leo C, Zhu J, Wu X, O'Neil J, Park EJ, Chen JD. 2000. Sequestration and inhibition of Daxx-mediated transcriptional repression by PML. *Mol Cell Biol* **20**: 1784-1796.

Li HS, Chen JH, Wu W, Fagaly T, Zhou L, Yuan W, Dupuis S, Jiang ZH, Nash W, Gick C et al. 1999. Vertebrate slit, a secreted ligand for the transmembrane protein roundabout, is a repellent for olfactory bulb axons. *Cell* **96**: 807-818.

Li L, Neaves WB. 2006. Normal stem cells and cancer stem cells: the niche matters. *Cancer Res* **66**: 4553-4557.

Li QQ, Xu JD, Wang WJ, Cao XX, Chen Q, Tang F, Chen ZQ, Liu XP, Xu ZD. 2009a. Twist1-mediated adriamycin-induced epithelial-mesenchymal transition relates to multidrug resistance and invasive potential in breast cancer cells. *Clin Cancer Res* **15**: 2657-2665.

Li W, Ferguson BJ, Khaled WT, Tevendale M, Stingl J, Poli V, Rich T, Salomoni P, Watson CJ. 2009b. PML depletion disrupts normal mammary gland development and skews the composition of the mammary luminal cell progenitor pool. *Proceedings of the National Academy of Sciences* **106**: 4725-4730.

Lim DA, Alvarez-Buylla A. 1999. Interaction between astrocytes and adult subventricular zone precursors stimulates neurogenesis. *Proc Natl Acad Sci U S A* **96**: 7526-7531.

-. 2014. Adult neural stem cells stake their ground. *Trends Neurosci* **37**: 563-571.

-. 2016. The Adult Ventricular-Subventricular Zone (V-SVZ) and Olfactory Bulb (OB) Neurogenesis. *Cold Spring Harb Perspect Biol* **8**.

Lim DA, Tramontin AD, Trevejo JM, Herrera DG, Garcia-Verdugo JM, Alvarez-Buylla A. 2000. Noggin antagonizes BMP signaling to create a niche for adult neurogenesis. *Neuron* **28**: 713-726.

Lin HK, Bergmann S, Pandolfi PP. 2004. Cytoplasmic PML function in TGF-beta signalling. *Nature* **431**: 205-211.

Liu BF, Gao EJ, Zeng XZ, Ji M, Cai Q, Lu Q, Yang H, Xu QY. 2006a. Proliferation of neural precursors in the subventricular zone after chemical lesions of the nigrostriatal pathway in rat brain. *Brain Res* **1106**: 30-39.

Liu C, Sage JC, Miller MR, Verhaak RG, Hippenmeyer S, Vogel H, Foreman O, Bronson RT, Nishiyama A, Luo L et al. 2011. Mosaic analysis with double markers reveals tumor cell of origin in glioma. *Cell* **146**: 209-221.

Liu D, Hou J, Hu X, Wang X, Xiao Y, Mou Y, De Leon H. 2006b. Neuronal chemorepellent Slit2 inhibits vascular smooth muscle cell migration by suppressing small GTPase Rac1 activation. *Circ Res* **98**: 480-489.

Liu H-K, Belz T, Bock D, Takacs A, Wu H, Lichter P, Chai M, Schütz G. 2008. The nuclear receptor tailless is required for neurogenesis in the adult subventricular zone. *Genes & Development* **22**: 2473-2478.

Liu J, Wang X, Li J, Wang H, Wei G, Yan J. 2014. Reconstruction of the gene regulatory network involved in the sonic hedgehog pathway with a potential role in early development of the mouse brain. *PLoS Comput Biol* **10**: e1003884.

Liu XY, Gerges N, Korshunov A, Sabha N, Khuong-Quang DA, Fontebasso AM, Fleming A, Hadjadj D, Schwartzentruber J, Majewski J et al. 2012. Frequent ATRX mutations and loss of expression in adult diffuse astrocytic tumors carrying IDH1/IDH2 and TP53 mutations. *Acta Neuropathol* **124**: 615-625.

Livak KJ, Schmittgen TD. 2001. Analysis of relative gene expression data using real-time quantitative PCR and the 2(-Delta Delta C(T)) Method. *Methods* **25**: 402-408.

Lois C, Alvarez-Buylla A. 1994. Long-distance neuronal migration in the adult mammalian brain. *Science* **264**: 1145-1148.

Long H, Sabatier C, Ma L, Plump A, Yuan W, Ornitz DM, Tamada A, Murakami F, Goodman CS, Tessier-Lavigne M. 2004. Conserved roles for Slit and Robo proteins in midline commissural axon guidance. *Neuron* **42**: 213-223.

Lopez-Bendito G, Flames N, Ma L, Fouquet C, Di Meglio T, Chedotal A, Tessier-Lavigne M, Marin O. 2007. Robo1 and Robo2 cooperate to control the guidance of major axonal tracts in the mammalian forebrain. *J Neurosci* **27**: 3395-3407.

Louria-Hayon I, Grossman T, Sionov RV, Alsheich O, Pandolfi PP, Haupt Y. 2003. The promyelocytic leukemia protein protects p53 from Mdm2-mediated inhibition and degradation. *J Biol Chem* **278**: 33134-33141.

Loyola A, Bonaldi T, Roche D, Imhof A, Almouzni G. 2006. PTMs on H3 Variants before Chromatin Assembly Potentiate Their Final Epigenetic State. *Molecular Cell* **24**: 309-316.

Lui Jan H, Hansen David V, Kriegstein Arnold R. 2011. Development and Evolution of the Human Neocortex. *Cell* **146**: 18-36.

Lund AH, van Lohuizen M. 2004. Polycomb complexes and silencing mechansims. pp. 239-246.

Luo GQ, Li JH, Wen JF, Zhou YH, Hu YB, Zhou JH. 2008. Effect and mechanism of the Twist gene on invasion and metastasis of gastric carcinoma cells. *World J Gastroenterol* **14**: 2487-2493.

Lytle C, Forbush B, 3rd. 1996. Regulatory phosphorylation of the secretory Na-K-Cl cotransporter: modulation by cytoplasmic Cl. *Am J Physiol* **270**: C437-448.

Ma DK, Marchetto MC, Guo JU, Ming GL, Gage FH, Song H. 2010. Epigenetic choreographers of neurogenesis in the adult mammalian brain. *Nat Neurosci* **13**: 1338-1344.

Maestro R, Dei Tos AP, Hamamori Y, Krasnokutsky S, Sartorelli V, Kedes L, Doglioni C, Beach DH, Hannon GJ. 1999. Twist is a potential oncogene that inhibits apoptosis. *Genes Dev* **13**: 2207-2217.

Maher EA, Furnari FB, Bachoo RM, Rowitch DH, Louis DN, Cavenee WK, DePinho RA. 2001. Malignant glioma: genetics and biology of a grave matter. *Genes Dev* **15**: 1311-1333.

Mao YS, Zhang B, Spector DL. 2011. Biogenesis and function of nuclear bodies. *Trends Genet* **27**: 295-306.

Margueron R, Reinberg D. 2011. The Polycomb complex PRC2 and its mark in life. *Nature* **469**: 343-349.

Marks P, Rifkind RA, Richon VM, Breslow R, Miller T, Kelly WK. 2001. Histone deacetylases and cancer: causes and therapies. *Nat Rev Cancer* **1**: 194-202.

Marques-Torrejon MA, Porlan E, Banito A, Gomez-Ibarlucea E, Lopez-Contreras AJ, Fernandez-Capetillo O, Vidal A, Gil J, Torres J, Farinas I. 2013. Cyclin-dependent kinase inhibitor p21 controls adult neural stem cell expansion by regulating Sox2 gene expression. *Cell Stem Cell* **12**: 88-100.

Marshall CA, Novitch BG, Goldman JE. 2005. Olig2 directs astrocyte and oligodendrocyte formation in postnatal subventricular zone cells. *J Neurosci* **25**: 7289-7298.

Martens JH, Brinkman AB, Simmer F, Francoijs KJ, Nebbioso A, Ferrara F, Altucci L, Stunnenberg HG. 2010. PML-RARalpha/RXR Alters the Epigenetic Landscape in Acute Promyelocytic Leukemia. *Cancer Cell* **17**: 173-185.

Martin C, Zhang Y. 2005. The diverse functions of histone lysine methylation. *Nat Rev Mol Cell Biol* **6**: 838-849.

Mason HA, Ito S, Corfas G. 2001. Extracellular signals that regulate the tangential migration of olfactory bulb neuronal precursors: inducers, inhibitors, and repellents. *J Neurosci* **21**: 7654-7663.

Maze I, Noh KM, Soshnev AA, Allis CD. 2014. Every amino acid matters: essential contributions of histone variants to mammalian development and disease. *Nat Rev Genet* **15**: 259-271.

Maze I, Wenderski W, Noh K-M, Bagot RC, Tzavaras N, Purushothaman I, Elsässer SJ, Guo Y, Ionete C, Hurd YL et al. 2015. Critical role of histone turnover in neuronal transcription and plasticity. *Neuron* **87**: 77-94.

Mazza M, Pelicci PG. 2013. Is PML a Tumor Suppressor? *Front Oncol* **3**: 174.

McCabe MT, Graves AP, Ganji G, Diaz E, Halsey WS, Jiang Y, Smitheman KN, Ott HM, Pappalardi MB, Allen KE et al. 2012. Mutation of A677 in histone methyltransferase EZH2 in human B-cell lymphoma promotes hypertrimethylation of histone H3 on lysine 27 (H3K27). *Proc Natl Acad Sci U S A* **109**: 2989-2994.

McKinnon PJ. 2009. DNA repair deficiency and neurological disease. *Nat Rev Neurosci* **10**: 100-112.

-. 2013. Maintaining genome stability in the nervous system. *Nat Neurosci* **16**: 1523-1529.

McNally BA, Trgovcich J, Maul GG, Liu Y, Zheng P. 2008. A role for cytoplasmic PML in cellular resistance to viral infection. *PLoS One* **3**: e2277.

Mejia-Gervacio S, Murray K, Lledo PM. 2011. NKCC1 controls GABAergic signaling and neuroblast migration in the postnatal forebrain. *Neural Dev* **6**: 4.

Melnick A, Fruchtman S, Zelent A, Liu M, Huang Q, Boczkowska B, Calasanz M, Fernandez A, Licht JD, Najfeld V. 1999. Identification of novel chromosomal rearrangements in acute myelogenous leukemia involving loci on chromosome 2p23, 15q22 and 17q21. *Leukemia* **13**: 1534-1538.

Menezes JR, Smith CM, Nelson KC, Luskin MB. 1995. The division of neuronal progenitor cells during migration in the neonatal mammalian forebrain. *Mol Cell Neurosci* **6**: 496-508.

Menn B, Garcia-Verdugo JM, Yaschine C, Gonzalez-Perez O, Rowitch D, Alvarez-Buylla A. 2006. Origin of oligodendrocytes in the subventricular zone of the adult brain. *J Neurosci* **26**: 7907-7918.

Merkle FT, Fuentealba LC, Sanders TA, Magno L, Kessaris N, Alvarez-Buylla A. 2014. Adult neural stem cells in distinct microdomains generate previously unknown interneuron types. *Nat Neurosci* **17**: 207-214.

Merkle FT, Mirzadeh Z, Alvarez-Buylla A. 2007. Mosaic Organization of Neural Stem Cells in the Adult Brain. *Science* **317**: 381-384.

Meroni G, Diez-Roux G. 2005. TRIM/RBCC, a novel class of 'single protein RING finger' E3 ubiquitin ligases. *Bioessays* **27**: 1147-1157.

Metzger MB, Hristova VA, Weissman AM. 2012. HECT and RING finger families of E3 ubiquitin ligases at a glance. *J Cell Sci* **125**: 531-537.

Michod D, Bartesaghi S, Khelifi A, Bellodi C, Berliocchi L, Nicotera P, Salomoni P. 2012. Calcium-dependent dephosphorylation of the histone chaperone

DAXX regulates H3.3 loading and transcription upon neuronal activation. *Neuron* **74**: 122-135.

Mikheeva SA, Mikheev AM, Petit A, Beyer R, Oxford RG, Khorasani L, Maxwell JP, Glackin CA, Wakimoto H, Gonzalez-Herrero I et al. 2010. TWIST1 promotes invasion through mesenchymal change in human glioblastoma. *Mol Cancer* **9**: 194.

Miki T, Xu Z, Chen-Goodspeed M, Liu M, Van Oort-Jansen A, Rea MA, Zhao Z, Lee CC, Chang KS. 2012. PML regulates PER2 nuclear localization and circadian function. *EMBO J* **31**: 1427-1439.

Miro X, Zhou X, Boretius S, Michaelis T, Kubisch C, Alvarez-Bolado G, Gruss P. 2009. Haploinsufficiency of the murine polycomb gene Suz12 results in diverse malformations of the brain and neural tube. *Dis Model Mech* **2**: 412-418.

Mobley AK, McCarty JH. 2011. beta8 integrin is essential for neuroblast migration in the rostral migratory stream. *Glia* **59**: 1579-1587.

Molofsky AV, Pardal R, Iwashita T, Park IK, Clarke MF, Morrison SJ. 2003. Bmi-1 dependence distinguishes neural stem cell self-renewal from progenitor proliferation. *Nature* **425**: 962-967.

Moravcsik E, Joannides M, Voisset E, Wessel Stratford E, Zeisig BB, Morris J, Densham R, Palgrave C, Stamp G, Nye E et al. 2013. Disruption Of PML Nuclear Bodies Cooperates In The Pathogenesis Of Acute Promyelocytic Leukemia. *Blood* **122**: 3721-3721.

Moreno MM, Linster C, Escanilla O, Sacquet J, Didier A, Mandairon N. 2009. Olfactory perceptual learning requires adult neurogenesis. *Proc Natl Acad Sci U S A* **106**: 17980-17985.

Mori T, Tanaka K, Buffo A, Wurst W, Kuhn R, Gotz M. 2006. Inducible gene deletion in astroglia and radial glia--a valuable tool for functional and lineage analysis. *Glia* **54**: 21-34.

Morin RD, Johnson NA, Severson TM, Mungall AJ, An J, Goya R, Paul JE, Boyle M, Woolcock BW, Kuchenbauer F et al. 2010. Somatic mutations altering EZH2 (Tyr641) in follicular and diffuse large B-cell lymphomas of germinal-center origin. *Nat Genet* **42**: 181-185.

Morrison SJ, Kimble J. 2006. Asymmetric and symmetric stem-cell divisions in development and cancer. *Nature* **441**: 1068-1074.

Muller J, Hart CM, Francis NJ, Vargas ML, Sengupta A, Wild B, Miller EL, O'Connor MB, Kingston RE, Simon JA. 2002. Histone methyltransferase activity of a Drosophila Polycomb group repressor complex. *Cell* **111**: 197-208.

Nagayama S, Homma R, Imamura F. 2014. Neuronal organization of olfactory bulb circuits. *Frontiers in Neural Circuits* **8**.

Nait-Oumesmar B, Decker L, Lachapelle F, Avellana-Adalid V, Bachelin C, Baron-Van Evercooren A. 1999. Progenitor cells of the adult mouse subventricular zone proliferate, migrate and differentiate into oligodendrocytes after demyelination. *Eur J Neurosci* **11**: 4357-4366.

Nait-Oumesmar B, Picard-Riera N, Kerninon C, Decker L, Seilhean D, Hoglinger GU, Hirsch EC, Reynolds R, Baron-Van Evercooren A. 2007. Activation of the subventricular zone in multiple sclerosis: evidence for early glial progenitors. *Proc Natl Acad Sci U S A* **104**: 4694-4699.

Nam HS, Benezra R. 2009. High levels of Id1 expression define B1 type adult neural stem cells. *Cell Stem Cell* **5**: 515-526.

Nan X, Ng HH, Johnson CA, Laherty CD, Turner BM, Eisenman RN, Bird A. 1998. Transcriptional repression by the methyl-CpG-binding protein MeCP2 involves a histone deacetylase complex. *Nature* **393**: 386-389.

Napolitano LM, Meroni G. 2012. TRIM family: Pleiotropy and diversification through homomultimer and heteromultimer formation. *IUBMB Life* **64**: 64-71.

Nekrasov M, Klymenko T, Fraterman S, Papp B, Oktaba K, Kocher T, Cohen A, Stunnenberg HG, Wilm M, Muller J. 2007. Pcl-PRC2 is needed to generate high levels of H3-K27 trimethylation at Polycomb target genes. *EMBO J* **26**: 4078-4088.

Nguyen LV, Vanner R, Dirks P, Eaves CJ. 2012. Cancer stem cells: an evolving concept. *Nat Rev Cancer* **12**: 133-143.

Nguyen-Ba-Charvet KT, Picard-Riera N, Tessier-Lavigne M, Baron-Van Evercooren A, Sotelo C, Chedotal A. 2004. Multiple roles for slits in the control of cell migration in the rostral migratory stream. *J Neurosci* **24**: 1497-1506.

Nikoloski G, Langemeijer SM, Kuiper RP, Knops R, Massop M, Tonnissen ER, van der Heijden A, Scheele TN, Vandenberghe P, de Witte T et al. 2010. Somatic mutations of the histone methyltransferase gene EZH2 in myelodysplastic syndromes. *Nat Genet* **42**: 665-667.

Ninkovic J, Mori T, Gotz M. 2007. Distinct modes of neuron addition in adult mouse neurogenesis. *J Neurosci* **27**: 10906-10911.

Ntziachristos P, Tsirigos A, Van Vlierberghe P, Nedjic J, Trimarchi T, Flaherty MS, Ferres-Marco D, da Ros V, Tang Z, Siegle J et al. 2012. Genetic inactivation of the polycomb repressive complex 2 in T cell acute lymphoblastic leukemia. *Nat Med* **18**: 298-301.

Nunes MC, Roy NS, Keyoung HM, Goodman RR, McKhann G, 2nd, Jiang L, Kang J, Nedergaard M, Goldman SA. 2003. Identification and isolation of multipotential neural progenitor cells from the subcortical white matter of the adult human brain. *Nat Med* **9**: 439-447.

O'Leary CJ, Bradford D, Chen M, White A, Blackmore DG, Cooper HM. 2015. The Netrin/RGM receptor, Neogenin, controls adult neurogenesis by promoting neuroblast migration and cell cycle exit. *Stem Cells* **33**: 503-514.

O'Rourke MP, Tam PP. 2002. Twist functions in mouse development. *Int J Dev Biol* **46**: 401-413.

Ocbina PJ, Dizon ML, Shin L, Szele FG. 2006. Doublecortin is necessary for the migration of adult subventricular zone cells from neurospheres. *Mol Cell Neurosci* **33**: 126-135.

Ohgaki H, Dessen P, Jourde B, Horstmann S, Nishikawa T, Di Patre PL, Burkhard C, Schuler D, Probst-Hensch NM, Maiorka PC et al. 2004. Genetic pathways to glioblastoma: a population-based study. *Cancer Res* **64**: 6892-6899.

Ohgaki H, Kleihues P. 2013. The definition of primary and secondary glioblastoma. *Clin Cancer Res* **19**: 764-772.

Ono K, Tomasiewicz H, Magnuson T, Rutishauser U. 1994. N-CAM mutation inhibits tangential neuronal migration and is phenocopied by enzymatic removal of polysialic acid. *Neuron* **13**: 595-609.

Orona E, Scott JW, Rainer EC. 1983. Different granule cell populations innervate superficial and deep regions of the external plexiform layer in rat olfactory bulb. *J Comp Neurol* **217**: 227-237.

Ortega F, Gascon S, Masserdotti G, Deshpande A, Simon C, Fischer J, Dimou L, Chichung Lie D, Schroeder T, Berninger B. 2013a. Oligodendrogliogenic and

neurogenic adult subependymal zone neural stem cells constitute distinct lineages and exhibit differential responsiveness to Wnt signalling. *Nat Cell Biol* **15**: 602-613.

Ortega F, Gascón S, Masserdotti G, Deshpande A, Simon C, Fischer J, Dimou L, Chichung Lie D, Schroeder T, Berninger B. 2013b. Oligodendrogliogenic and neurogenic adult subependymal zone neural stem cells constitute distinct lineages and exhibit differential responsiveness to Wnt signalling. *Nat Cell Biol* **15**: 602-613.

Otero L, Zurita M, Bonilla C, Rico MA, Aguayo C, Rodriguez A, Vaquero J. 2012. Endogenous neurogenesis after intracerebral hemorrhage. *Histol Histopathol* **27**: 303-315.

Ottone C, Krusche B, Whitby A, Clements M, Quadrato G, Pitulescu ME, Adams RH, Parrinello S. 2014. Direct cell-cell contact with the vascular niche maintains quiescent neural stem cells. *Nat Cell Biol* **16**: 1045-1056.

P PK, Bischof O, Purbey PK, Notani D, Urlaub H, Dejean A, Galande S. 2007. Functional interaction between PML and SATB1 regulates chromatin-loop architecture and transcription of the MHC class I locus. *Nat Cell Biol* **9**: 45-56.

Palmer TD, Ray J, Gage FH. 1995. FGF-2-responsive neuronal progenitors reside in proliferative and quiescent regions of the adult rodent brain. *Mol Cell Neurosci* **6**: 474-486.

Palmer TD, Takahashi J, Gage FH. 1997. The adult rat hippocampus contains primordial neural stem cells. *Mol Cell Neurosci* **8**: 389-404.

Pan D, Fujimoto M, Lopes A, Wang YX. 2009. Twist-1 is a PPARdelta-inducible, negative-feedback regulator of PGC-1alpha in brown fat metabolism. *Cell* **137**: 73-86.

Parras CM, Galli R, Britz O, Soares S, Galichet C, Battiste J, Johnson JE, Nakafuku M, Vescovi A, Guillemot F. 2004. Mash1 specifies neurons and oligodendrocytes in the postnatal brain. *The EMBO Journal* **23**: 4495-4505.

Parras CM, Schuurmans C, Scardigli R, Kim J, Anderson DJ, Guillemot F. 2002. Divergent functions of the proneural genes Mash1 and Ngn2 in the specification of neuronal subtype identity. *Genes Dev* **16**: 324-338.

Parrish-Aungst S, Shipley MT, Erdelyi F, Szabo G, Puche AC. 2007. Quantitative analysis of neuronal diversity in the mouse olfactory bulb. *J Comp Neurol* **501**: 825-836.

Parseghian MH, Newcomb RL, Hamkalo BA. 2001. Distribution of somatic H1 subtypes is non-random on active vs. inactive chromatin II: distribution in human adult fibroblasts. *J Cell Biochem* **83**: 643-659.

Parsons DW, Jones S, Zhang X, Lin JC, Leary RJ, Angenendt P, Mankoo P, Carter H, Siu IM, Gallia GL et al. 2008. An integrated genomic analysis of human glioblastoma multiforme. *Science* **321**: 1807-1812.

Pasini D, Bracken AP, Jensen MR, Lazzerini Denchi E, Helin K. 2004. Suz12 is essential for mouse development and for EZH2 histone methyltransferase activity. *EMBO J* **23**: 4061-4071.

Patel S, Huang Y-W, Reheman A, Pluthero FG, Chaturvedi S, Mukovozov IM, Tole S, Liu G-Y, Li L, Durocher Y et al. 2012. The Cell Motility Modulator Slit2 Is a Potent Inhibitor of Platelet FunctionClinical Perspective. *Circulation* **126**: 1385-1395.

Pearson M, Carbone R, Sebastiani C, Cioce M, Fagioli M, Saito S, Higashimoto Y, Appella E, Minucci S, Pandolfi PP et al. 2000. PML regulates p53 acetylation

and premature senescence induced by oncogenic Ras. *Nature* **406**: 207-210.

Peinado H, Olmeda D, Cano A. 2007. Snail, Zeb and bHLH factors in tumour progression: an alliance against the epithelial phenotype? *Nat Rev Cancer* **7**: 415-428.

Pencea V, Luskin MB. 2003. Prenatal development of the rodent rostral migratory stream. *J Comp Neurol* **463**: 402-418.

Peng JC, Valouev A, Swigut T, Zhang J, Zhao Y, Sidow A, Wysocka J. 2009. Jarid2/Jumonji coordinates control of PRC2 enzymatic activity and target gene occupancy in pluripotent cells. *Cell* **139**: 1290-1302.

Pereira JD, Sansom SN, Smith J, Dobenecker M-W, Tarakhovsky A, Livesey FJ. 2010. Ezh2, the histone methyltransferase of PRC2, regulates the balance between self-renewal and differentiation in the cerebral cortex. *Proceedings of the National Academy of Sciences* **107**: 15957-15962.

Peretto P, Merighi A, Fasolo A, Bonfanti L. 1997. Glial tubes in the rostral migratory stream of the adult rat. *Brain Res Bull* **42**: 9-21.

Picard-Riera N, Decker L, Delarasse C, Goude K, Nait-Oumesmar B, Liblau R, Pham-Dinh D, Baron-Van Evercooren A. 2002. Experimental autoimmune encephalomyelitis mobilizes neural progenitors from the subventricular zone to undergo oligodendrogenesis in adult mice. *Proc Natl Acad Sci U S A* **99**: 13211-13216.

Piunti A, Shilatifard A. 2016. Epigenetic balance of gene expression by Polycomb and COMPASS families. *Science* **352**: aad9780.

Pollard SM, Conti L, Sun Y, Goffredo D, Smith A. 2006. Adherent neural stem (NS) cells from fetal and adult forebrain. *Cereb Cortex* **16 Suppl 1**: i112-120.

Pollard SM, Wallbank R, Tomlinson S, Grotewold L, Smith A. 2008. Fibroblast growth factor induces a neural stem cell phenotype in foetal forebrain progenitors and during embryonic stem cell differentiation. *Mol Cell Neurosci* **38**: 393-403.

Price JL, Powell TPS. 1970. The Synaptology of the Granule Cells of the Olfactory Bulb. *Journal of Cell Science* **7**: 125-155.

Puisieux A, Valsesia-Wittmann S, Ansieau S. 2006. A twist for survival and cancer progression. *Br J Cancer* **94**: 13-17.

Qin Q, Xu Y, He T, Qin C, Xu J. 2012. Normal and disease-related biological functions of Twist1 and underlying molecular mechanisms. *Cell Res* **22**: 90-106.

Quenum K, Ntalaja J, Onen J, Arkha Y, Derraz S, El Ouahabi A, Sefiani S, ElKhamlichi A. 2012. A Rare Case of Adult Medulloblastoma with Spinal Metastasis. *Case Reports in Neurological Medicine* **2012**: 3.

Quinones-Hinojosa A, Sanai N, Soriano-Navarro M, Gonzalez-Perez O, Mirzadeh Z, Gil-Perotin S, Romero-Rodriguez R, Berger MS, Garcia-Verdugo JM, Alvarez-Buylla A. 2006. Cellular composition and cytoarchitecture of the adult human subventricular zone: a niche of neural stem cells. *J Comp Neurol* **494**: 415-434.

Rama N, Dubrac A, Mathivet T, Ni Charthaigh RA, Genet G, Cristofaro B, Pibouin-Fragner L, Ma L, Eichmann A, Chedotal A. 2015. Slit2 signaling through Robo1 and Robo2 is required for retinal neovascularization. *Nat Med* **21**: 483-491.

Regad T, Bellodi C, Nicotera P, Salomoni P. 2009. The tumor suppressor Pml regulates cell fate in the developing neocortex. *Nat Neurosci* **12**: 132-140.

Renault VM, Rafalski VA, Morgan AA, Salih DA, Brett JO, Webb AE, Villeda SA, Thekkat PU, Guillerey C, Denko NC et al. 2009. FoxO3 regulates neural stem cell homeostasis. *Cell Stem Cell* **5**: 527-539.

Reya T, Morrison SJ, Clarke MF, Weissman IL. 2001. Stem cells, cancer, and cancer stem cells. *Nature* **414**: 105-111.

Reymond A, Meroni G, Fantozzi A, Merla G, Cairo S, Luzi L, Riganelli D, Zanaria E, Messali S, Cainarca S et al. 2001. The tripartite motif family identifies cell compartments. *EMBO J* **20**: 2140-2151.

Reynolds BA, Weiss S. 1992. Generation of neurons and astrocytes from isolated cells of the adult mammalian central nervous system. *Science* **255**: 1707-1710.

Rogakou EP, Boon C, Redon C, Bonner WM. 1999. Megabase chromatin domains involved in DNA double-strand breaks in vivo. *J Cell Biol* **146**: 905-916.

Rosivatz E, Becker I, Specht K, Fricke E, Luber B, Busch R, Höfler H, Becker K-F. 2002. Differential Expression of the Epithelial-Mesenchymal Transition Regulators Snail, SIP1, and Twist in Gastric Cancer. *The American Journal of Pathology* **161**: 1881-1891.

Roth SY, Denu JM, Allis CD. 2001. Histone acetyltransferases. *Annu Rev Biochem* **70**: 81-120.

Rowe FA, Edwards DA. 1972. Olfactory bulb removal: Influences on the mating behavior of male mice. *Physiology & Behavior* **8**: 37-41.

Sahay A, Hen R. 2007. Adult hippocampal neurogenesis in depression. *Nat Neurosci* **10**: 1110-1115.

Salomoni P. 2013. The PML-Interacting Protein DAXX: Histone Loading Gets into the Picture. *Front Oncol* **3**: 152.

Salomoni P, Bellodi C. 2007. New insights into the cytoplasmic function of PML. *Histol Histopathol* **22**: 937-946.

Salomoni P, Calegari F. 2010. Cell cycle control of mammalian neural stem cells: putting a speed limit on G1. *Trends Cell Biol* **20**: 233-243.

Salomoni P, Dvorkina M, Michod D. 2012. Role of the promyelocytic leukaemia protein in cell death regulation. *Cell Death Dis* **3**: e247.

Salomoni P, Ferguson BJ, Wyllie AH, Rich T. 2008. New insights into the role of PML in tumour suppression. *Cell Res* **18**: 622-640.

Salomoni P, Pandolfi PP. 2002. The role of PML in tumor suppression. *Cell* **108**: 165-170.

Sanai N, Alvarez-Buylla A, Berger MS. 2005. Neural stem cells and the origin of gliomas. *N Engl J Med* **353**: 811-822.

Sanai N, Nguyen T, Ihrie RA, Mirzadeh Z, Tsai HH, Wong M, Gupta N, Berger MS, Huang E, Garcia-Verdugo JM et al. 2011. Corridors of migrating neurons in the human brain and their decline during infancy. *Nature* **478**: 382-386.

Sanai N, Tramontin AD, Quinones-Hinojosa A, Barbaro NM, Gupta N, Kunwar S, Lawton MT, McDermott MW, Parsa AT, Manuel-Garcia Verdugo J et al. 2004. Unique astrocyte ribbon in adult human brain contains neural stem cells but lacks chain migration. *Nature* **427**: 740-744.

Sashida G, Harada H, Matsui H, Oshima M, Yui M, Harada Y, Tanaka S, Mochizuki-Kashio M, Wang C, Saraya A et al. 2014. Ezh2 loss promotes development of myelodysplastic syndrome but attenuates its predisposition to leukaemic transformation. *Nat Commun* **5**: 4177.

Sawa M, Yamamoto K, Yokozawa T, Kiyoi H, Hishida A, Kajiguchi T, Seto M, Kohno A, Kitamura K, Itoh Y et al. 2005. BMI-1 is highly expressed in M0-subtype acute myeloid leukemia. *Int J Hematol* **82**: 42-47.

Sawamoto K, Wichterle H, Gonzalez-Perez O, Cholfin JA, Yamada M, Spassky N, Murcia NS, Garcia-Verdugo JM, Marin O, Rubenstein JL et al. 2006. New neurons follow the flow of cerebrospinal fluid in the adult brain. *Science* **311**: 629-632.

Schaar BT, McConnell SK. 2005. Cytoskeletal coordination during neuronal migration. *Proc Natl Acad Sci U S A* **102**: 13652-13657.

Scheffler B, Walton NM, Lin DD, Goetz AK, Enikolopov G, Roper SN, Steindler DA. 2005. Phenotypic and functional characterization of adult brain neuropoiesis. *Proc Natl Acad Sci U S A* **102**: 9353-9358.

Scheuermann JC, de Ayala Alonso AG, Oktaba K, Ly-Hartig N, McGinty RK, Fraterman S, Wilm M, Muir TW, Muller J. 2010. Histone H2A deubiquitinase activity of the Polycomb repressive complex PR-DUB. *Nature* **465**: 243-247.

Schuettengruber B, Chourrout D, Vervoort M, Leblanc B, Cavalli G. 2007. Genome regulation by polycomb and trithorax proteins. *Cell* **128**: 735-745.

Schuurmans C, Guillemot F. 2002. Molecular mechanisms underlying cell fate specification in the developing telencephalon. *Curr Opin Neurobiol* **12**: 26-34.

Schwartzentruber J, Korshunov A, Liu XY, Jones DT, Pfaff E, Jacob K, Sturm D, Fontebasso AM, Quang DA, Tonjes M et al. 2012. Driver mutations in histone H3.3 and chromatin remodelling genes in paediatric glioblastoma. *Nature* **482**: 226-231.

Secq V, Leca J, Bressy C, Guillaumond F, Skrobuk P, Nigri J, Lac S, Lavaut MN, Bui TT, Thakur AK et al. 2015. Stromal SLIT2 impacts on pancreatic cancer-associated neural remodeling. *Cell Death Dis* **6**: e1592.

Shen Q, Wang Y, Kokovay E, Lin G, Chuang S-M, Goderie SK, Roysam B, Temple S. 2008. Adult SVZ stem cells lie in a vascular niche: A quantitative analysis of niche cell-cell interactions. *Cell stem cell* **3**: 289-300.

Shen TH, Lin HK, Scaglioni PP, Yung TM, Pandolfi PP. 2006. The mechanisms of PML-nuclear body formation. *Mol Cell* **24**: 331-339.

Shi Y, Lan F, Matson C, Mulligan P, Whetstine JR, Cole PA, Casero RA, Shi Y. 2004. Histone demethylation mediated by the nuclear amine oxidase homolog LSD1. *Cell* **119**: 941-953.

Simon C, Chagraoui J, Krosl J, Gendron P, Wilhelm B, Lemieux S, Boucher G, Chagnon P, Drouin S, Lambert R et al. 2012. A key role for EZH2 and associated genes in mouse and human adult T-cell acute leukemia. *Genes Dev* **26**: 651-656.

Singh SK, Hawkins C, Clarke ID, Squire JA, Bayani J, Hide T, Henkelman RM, Cusimano MD, Dirks PB. 2004. Identification of human brain tumour initiating cells. *Nature* **432**: 396-401.

Sit S-T, Manser E. 2011. Rho GTPases and their role in organizing the actin cytoskeleton. *Journal of Cell Science* **124**: 679.

Skene PJ, Henikoff S. 2013. Histone variants in pluripotency and disease. *Development* **140**: 2513-2524.

Sneeringer CJ, Scott MP, Kuntz KW, Knutson SK, Pollock RM, Richon VM, Copeland RA. 2010. Coordinated activities of wild-type plus mutant EZH2 drive tumor-associated hypertrimethylation of lysine 27 on histone H3 (H3K27) in human B-cell lymphomas. *Proc Natl Acad Sci U S A* **107**: 20980-20985.

Solecki DJ, Model L, Gaetz J, Kapoor TM, Hatten ME. 2004. Par6alpha signaling controls glial-guided neuronal migration. *Nat Neurosci* **7**: 1195-1203.

Song MS, Salmena L, Carracedo A, Egia A, Lo-Coco F, Teruya-Feldstein J, Pandolfi PP. 2008. The deubiquitinylation and localization of PTEN are regulated by a HAUSP–PML network. *Nature* **455**: 813-817.

Song X, Gao T, Wang N, Feng Q, You X, Ye T, Lei Q, Zhu Y, Xiong M, Xia Y et al. 2016. Selective inhibition of EZH2 by ZLD1039 blocks H3K27 methylation and leads to potent anti-tumor activity in breast cancer. *Sci Rep* **6**: 20864.

Spalding Kirsty L, Bergmann O, Alkass K, Bernard S, Salehpour M, Huttner Hagen B, Boström E, Westerlund I, Vial C, Buchholz Bruce A et al. 2013. Dynamics of Hippocampal Neurogenesis in Adult Humans. *Cell* **153**: 1219-1227.

Sparmann A, van Lohuizen M. 2006. Polycomb silencers control cell fate, development and cancer. *Nat Rev Cancer* **6**: 846-856.

Sparmann A, Xie Y, Verhoeven E, Vermeulen M, Lancini C, Gargiulo G, Hulsman D, Mann M, Knoblich JA, van Lohuizen M. 2013. The chromodomain helicase Chd4 is required for Polycomb‐mediated inhibition of astroglial differentiation. *The EMBO Journal* **32**: 1598-1612.

Srivastava J, Rho O, Youssef RM, DiGiovanni J. 2016. Twist1 regulates keratinocyte proliferation and skin tumor promotion. *Mol Carcinog* **55**: 941-952.

Stenman J, Toresson H, Campbell K. 2003. Identification of two distinct progenitor populations in the lateral ganglionic eminence: implications for striatal and olfactory bulb neurogenesis. *J Neurosci* **23**: 167-174.

Strange K. 2004. Cellular volume homeostasis. *Adv Physiol Educ* **28**: 155-159.

Sturm D, Witt H, Hovestadt V, Khuong-Quang DA, Jones DT, Konermann C, Pfaff E, Tonjes M, Sill M, Bender S et al. 2012. Hotspot mutations in H3F3A and IDH1 define distinct epigenetic and biological subgroups of glioblastoma. *Cancer Cell* **22**: 425-437.

Sudo T, Utsunomiya T, Mimori K, Nagahara H, Ogawa K, Inoue H, Wakiyama S, Fujita H, Shirouzu K, Mori M. 2005. Clinicopathological significance of EZH2 mRNA expression in patients with hepatocellular carcinoma. *Br J Cancer* **92**: 1754-1758.

Sultan S, Mandairon N, Kermen F, Garcia S, Sacquet J, Didier A. 2010. Learning-dependent neurogenesis in the olfactory bulb determines long-term olfactory memory. *FASEB J* **24**: 2355-2363.

Sun W, Kim H, Moon Y. 2010. Control of neuronal migration through rostral migration stream in mice. *Anat Cell Biol* **43**: 269-279.

Sundholm-Peters NL, Yang HK, Goings GE, Walker AS, Szele FG. 2005. Subventricular zone neuroblasts emigrate toward cortical lesions. *J Neuropathol Exp Neurol* **64**: 1089-1100.

Szenker E, Ray-Gallet D, Almouzni G. 2011. The double face of the histone variant H3.3. *Cell Res* **21**: 421-434.

Tagami H, Ray-Gallet D, Almouzni G, Nakatani Y. 2004. Histone H3.1 and H3.3 complexes mediate nucleosome assembly pathways dependent or independent of DNA synthesis. *Cell* **116**: 51-61.

Tan J, Yang X, Zhuang L, Jiang X, Chen W, Lee PL, Karuturi RK, Tan PB, Liu ET, Yu Q. 2007. Pharmacologic disruption of Polycomb-repressive complex 2-mediated gene repression selectively induces apoptosis in cancer cells. *Genes Dev* **21**: 1050-1063.

Tanaka T, Serneo FF, Higgins C, Gambello MJ, Wynshaw-Boris A, Gleeson JG. 2004. Lis1 and doublecortin function with dynein to mediate coupling of the nucleus to the centrosome in neuronal migration. *J Cell Biol* **165**: 709-721.

Tavares L, Dimitrova E, Oxley D, Webster J, Poot R, Demmers J, Bezstarosti K, Taylor S, Ura H, Koide H et al. 2012. RYBP-PRC1 complexes mediate H2A ubiquitylation at polycomb target sites independently of PRC2 and H3K27me3. *Cell* **148**: 664-678.

Tavazoie M, Van der Veken L, Silva-Vargas V, Louissaint M, Colonna L, Zaidi B, Garcia-Verdugo JM, Doetsch F. 2008. A specialized vascular niche for adult neural stem cells. *Cell Stem Cell* **3**: 279-288.

Temple S, Alvarez-Buylla A. 1999. Stem cells in the adult mammalian central nervous system. *Curr Opin Neurobiol* **9**: 135-141.

Terme JM, Sese B, Millan-Arino L, Mayor R, Izpisua Belmonte JC, Barrero MJ, Jordan A. 2011. Histone H1 variants are differentially expressed and incorporated into chromatin during differentiation and reprogramming to pluripotency. *J Biol Chem* **286**: 35347-35357.

Thiery JP. 2002. Epithelial-mesenchymal transitions in tumour progression. *Nat Rev Cancer* **2**: 442-454.

Thiery JP, Acloque H, Huang RY, Nieto MA. 2009. Epithelial-mesenchymal transitions in development and disease. *Cell* **139**: 871-890.

Tomasiewicz H, Ono K, Yee D, Thompson C, Goridis C, Rutishauser U, Magnuson T. 1993. Genetic deletion of a neural cell adhesion molecule variant (N-CAM-180) produces distinct defects in the central nervous system. *Neuron* **11**: 1163-1174.

Tran DD, Corsa CA, Biswas H, Aft RL, Longmore GD. 2011. Temporal and spatial cooperation of Snail1 and Twist1 during epithelial-mesenchymal transition predicts for human breast cancer recurrence. *Mol Cancer Res* **9**: 1644-1657.

Trotman LC, Alimonti A, Scaglioni PP, Koutcher JA, Cordon-Cardo C, Pandolfi PP. 2006. Identification of a tumour suppressor network opposing nuclear Akt function. *Nature* **441**: 523-527.

Trounson A, McDonald C. 2015. Stem Cell Therapies in Clinical Trials: Progress and Challenges. *Cell Stem Cell* **17**: 11-22.

Tsai LH, Gleeson JG. 2005. Nucleokinesis in neuronal migration. *Neuron* **46**: 383-388.

Tse C, Sera T, Wolffe AP, Hansen JC. 1998. Disruption of higher-order folding by core histone acetylation dramatically enhances transcription of nucleosomal arrays by RNA polymerase III. *Mol Cell Biol* **18**: 4629-4638.

Urban N, Guillemot F. 2014. Neurogenesis in the embryonic and adult brain: same regulators, different roles. *Front Cell Neurosci* **8**: 396.

Urban N, van den Berg DL, Forget A, Andersen J, Demmers JA, Hunt C, Ayrault O, Guillemot F. 2016. Return to quiescence of mouse neural stem cells by degradation of a proactivation protein. *Science* **353**: 292-295.

Urbich C, Rössig L, Kaluza D, Potente M, Boeckel J-N, Knau A, Diehl F, Geng J-G, Hofmann W-K, Zeiher AM et al. 2009. HDAC5 is a repressor of angiogenesis and determines the angiogenic gene expression pattern of endothelial cells. *Blood* **113**: 5669.

Valley MT, Mullen TR, Schultz LC, Sagdullaev BT, Firestein S. 2009. Ablation of mouse adult neurogenesis alters olfactory bulb structure and olfactory fear conditioning. *Front Neurosci* **3**: 51.

van Lohuizen M, Verbeek S, Scheijen B, Wientjens E, van der Gulden H, Berns A. 1991. Identification of cooperating oncogenes in E mu-myc transgenic mice by provirus tagging. *Cell* **65**: 737-752.

van Praag H, Schinder AF, Christie BR, Toni N, Palmer TD, Gage FH. 2002. Functional neurogenesis in the adult hippocampus. *Nature* **415**: 1030-1034.

Varambally S, Dhanasekaran SM, Zhou M, Barrette TR, Kumar-Sinha C, Sanda MG, Ghosh D, Pienta KJ, Sewalt RG, Otte AP et al. 2002. The polycomb group protein EZH2 is involved in progression of prostate cancer. *Nature* **419**: 624-629.

Varjosalo M, Taipale J. 2008. Hedgehog: functions and mechanisms. *Genes Dev* **22**: 2454-2472.

Venneti S, Garimella MT, Sullivan LM, Martinez D, Huse JT, Heguy A, Santi M, Thompson CB, Judkins AR. 2013. Evaluation of histone 3 lysine 27 trimethylation (H3K27me3) and enhancer of Zest 2 (EZH2) in pediatric glial and glioneuronal tumors shows decreased H3K27me3 in H3F3A K27M mutant glioblastomas. *Brain Pathol* **23**: 558-564.

Verhaak RG, Hoadley KA, Purdom E, Wang V, Qi Y, Wilkerson MD, Miller CR, Ding L, Golub T, Mesirov JP et al. 2010. Integrated genomic analysis identifies clinically relevant subtypes of glioblastoma characterized by abnormalities in PDGFRA, IDH1, EGFR, and NF1. *Cancer Cell* **17**: 98-110.

Verma SK, Tian X, LaFrance LV, Duquenne C, Suarez DP, Newlander KA, Romeril SP, Burgess JL, Grant SW, Brackley JA et al. 2012. Identification of Potent, Selective, Cell-Active Inhibitors of the Histone Lysine Methyltransferase EZH2. *ACS Medicinal Chemistry Letters* **3**: 1091-1096.

Vernier M, Bourdeau V, Gaumont-Leclerc MF, Moiseeva O, Begin V, Saad F, Mes-Masson AM, Ferbeyre G. 2011. Regulation of E2Fs and senescence by PML nuclear bodies. *Genes Dev* **25**: 41-50.

Vescovi AL, Galli R, Reynolds BA. 2006. Brain tumour stem cells. *Nat Rev Cancer* **6**: 425-436.

Vesuna F, van Diest P, Chen JH, Raman V. 2008. Twist is a transcriptional repressor of E-cadherin gene expression in breast cancer. *Biochemical and biophysical research communications* **367**: 235-241.

Villa R, Pasini D, Gutierrez A, Morey L, Occhionorelli M, Vire E, Nomdedeu JF, Jenuwein T, Pelicci PG, Minucci S et al. 2007. Role of the polycomb repressive complex 2 in acute promyelocytic leukemia. *Cancer Cell* **11**: 513-525.

Villa R, Pasini D, Gutierrez A, Morey L, Occhionorelli M, Viré E, Nomdedeu JF, Jenuwein T, Pelicci PG, Minucci S et al. Role of the Polycomb Repressive Complex 2 in Acute Promyelocytic Leukemia. *Cancer Cell* **11**: 513-525.

Villagra NT, Navascues J, Casafont I, Val-Bernal JF, Lafarga M, Berciano MT. 2006. The PML-nuclear inclusion of human supraoptic neurons: a new compartment with SUMO-1- and ubiquitin-proteasome-associated domains. *Neurobiol Dis* **21**: 181-193.

Visvader JE. 2011. Cells of origin in cancer. *Nature* **469**: 314-322.

Voigt P, Tee WW, Reinberg D. 2013. A double take on bivalent promoters. *Genes Dev* **27**: 1318-1338.

von Campe G, Spencer DD, de Lanerolle NC. 1997. Morphology of dentate granule cells in the human epileptogenic hippocampus. *Hippocampus* **7**: 472-488.

Vonlanthen S, Heighway J, Altermatt HJ, Gugger M, Kappeler A, Borner MM, van Lohuizen M, Betticher DC. 2001. The bmi-1 oncoprotein is differentially expressed in non-small cell lung cancer and correlates with INK4A-ARF locus expression. *Br J Cancer* **84**: 1372-1376.

Vu TH, Werb Z. 2000. Matrix metalloproteinases: effectors of development and normal physiology. *Genes Dev* **14**: 2123-2133.

Wagers AJ, Weissman IL. 2004. Plasticity of Adult Stem Cells. *Cell* **116**: 639-648.

Wang C, Liu F, Liu YY, Zhao CH, You Y, Wang L, Zhang J, Wei B, Ma T, Zhang Q et al. 2011. Identification and characterization of neuroblasts in the subventricular zone and rostral migratory stream of the adult human brain. *Cell Res* **21**: 1534-1550.

Wang G, Li Y, Wang XY, Han Z, Chuai M, Wang LJ, Ho Lee KK, Geng JG, Yang X. 2013. Slit/Robo1 signaling regulates neural tube development by balancing neuroepithelial cell proliferation and differentiation. *Exp Cell Res* **319**: 1083-1093.

Wang H, Wang L, Erdjument-Bromage H, Vidal M, Tempst P, Jones RS, Zhang Y. 2004a. Role of histone H2A ubiquitination in Polycomb silencing. *Nature* **431**: 873-878.

Wang J, Shiels C, Sasieni P, Wu PJ, Islam SA, Freemont PS, Sheer D. 2004b. Promyelocytic leukemia nuclear bodies associate with transcriptionally active genomic regions. *J Cell Biol* **164**: 515-526.

Wang L, Brown JL, Cao R, Zhang Y, Kassis JA, Jones RS. 2004c. Hierarchical recruitment of polycomb group silencing complexes. *Mol Cell* **14**: 637-646.

Wang Y, Jin K, Mao XO, Xie L, Banwait S, Marti HH, Greenberg DA. 2007. VEGF-overexpressing transgenic mice show enhanced post-ischemic neurogenesis and neuromigration. *J Neurosci Res* **85**: 740-747.

Watanabe O, Imamura H, Shimizu T, Kinoshita J, Okabe T, Hirano A, Yoshimatsu K, Konno S, Aiba M, Ogawa K. 2004. Expression of twist and wnt in human breast cancer. *Anticancer Res* **24**: 3851-3856.

Weber M, Apostolova G, Widera D, Mittelbronn M, Dechant G, Kaltschmidt B, Rohrer H. 2015. Alternative generation of CNS neural stem cells and PNS derivatives from neural crest-derived peripheral stem cells. *Stem Cells* **33**: 574-588.

Wei PC, Chang AN, Kao J, Du Z, Meyers RM, Alt FW, Schwer B. 2016. Long Neural Genes Harbor Recurrent DNA Break Clusters in Neural Stem/Progenitor Cells. *Cell* **164**: 644-655.

Weickert CS, Webster MJ, Colvin SM, Herman MM, Hyde TM, Weinberger DR, Kleinman JE. 2000. Localization of epidermal growth factor receptors and putative neuroblasts in human subependymal zone. *J Comp Neurol* **423**: 359-372.

Weissman IL. 2000. Stem cells: units of development, units of regeneration, and units in evolution. *cell* **100**: 157-168.

Weissman IL. 2015. Stem cells are units of natural selection for tissue formation, for germline development, and in cancer development. *Proceedings of the National Academy of Sciences* **112**: 8922-8928.

Wells D, Hoffman D, Kedes L. 1987. Unusual structure, evolutionary conservation of non-coding sequences and numerous pseudogenes characterize the human H3.3 histone multigene family. *Nucleic Acids Res* **15**: 2871-2889.

Wen PY, Kesari S. 2008. Malignant gliomas in adults. *N Engl J Med* **359**: 492-507.

Wheelock MJ, Shintani Y, Maeda M, Fukumoto Y, Johnson KR. 2008. Cadherin switching. *J Cell Sci* **121**: 727-735.

Whitcomb SJ, Basu A, Allis CD, Bernstein E. 2007. Polycomb Group proteins: an evolutionary perspective. *Trends Genet* **23**: 494-502.

Wichterle H, Garcia-Verdugo JM, Alvarez-Buylla A. 1997. Direct evidence for homotypic, glia-independent neuronal migration. *Neuron* **18**: 779-791.

Wilson BG, Wang X, Shen X, McKenna ES, Lemieux ME, Cho Y-J, Koellhoffer EC, Pomeroy SL, Orkin SH, Roberts CWM. 2010. Epigenetic Antagonism between Polycomb and SWI/SNF Complexes during Oncogenic Transformation. *Cancer Cell* **18**: 316-328.

Winner B, Cooper-Kuhn CM, Aigner R, Winkler J, Kuhn HG. 2002. Long-term survival and cell death of newly generated neurons in the adult rat olfactory bulb. *Eur J Neurosci* **16**: 1681-1689.

Witt O, Albig W, Doenecke D. 1997. Transcriptional regulation of the human replacement histone gene H3.3B. *FEBS Lett* **408**: 255-260.

Wong K, Ren XR, Huang YZ, Xie Y, Liu G, Saito H, Tang H, Wen L, Brady-Kalnay SM, Mei L et al. 2001. Signal transduction in neuronal migration: roles of GTPase activating proteins and the small GTPase Cdc42 in the Slit-Robo pathway. *Cell* **107**: 209-221.

Woulfe J, Gray D, Prichett-Pejic W, Munoz DG, Chretien M. 2004. Intranuclear rodlets in the substantia nigra: interactions with marinesco bodies, ubiquitin, and promyelocytic leukemia protein. *J Neuropathol Exp Neurol* **63**: 1200-1207.

Woulfe JM, Prichett-Pejic W, Rippstein P, Munoz DG. 2007. Promyelocytic leukaemia-immunoreactive neuronal intranuclear rodlets in the human brain. *Neuropathol Appl Neurobiol* **33**: 56-66.

Wu G, Broniscer A, McEachron TA, Lu C, Paugh BS, Becksfort J, Qu C, Ding L, Huether R, Parker M et al. 2012. Somatic histone H3 alterations in pediatric diffuse intrinsic pontine gliomas and non-brainstem glioblastomas. *Nat Genet* **44**: 251-253.

Wu W, Wong K, Chen J, Jiang Z, Dupuis S, Wu JY, Rao Y. 1999. Directional guidance of neuronal migration in the olfactory system by the protein Slit. *Nature* **400**: 331-336.

Wu X, Johansen JV, Helin K. 2013. Fbxl10/Kdm2b recruits polycomb repressive complex 1 to CpG islands and regulates H2A ubiquitylation. *Mol Cell* **49**: 1134-1146.

Xing YL, Röth PT, Stratton JAS, Chuang BHA, Danne J, Ellis SL, Ng SW, Kilpatrick TJ, Merson TD. 2014. Adult Neural Precursor Cells from the Subventricular Zone Contribute Significantly to Oligodendrocyte Regeneration and Remyelination. *The Journal of Neuroscience* **34**: 14128-14146.

Xu J, Lamouille S, Derynck R. 2009. TGF-beta-induced epithelial to mesenchymal transition. *Cell Res* **19**: 156-172.

Xue Y, Gibbons R, Yan Z, Yang D, McDowell TL, Sechi S, Qin J, Zhou S, Higgs D, Wang W. 2003. The ATRX syndrome protein forms a chromatin-remodeling complex with Daxx and localizes in promyelocytic leukemia nuclear bodies. *Proc Natl Acad Sci U S A* **100**: 10635-10640.

Yadirgi G, Leinster V, Acquati S, Bhagat H, Shakhova O, Marino S. 2011. Conditional activation of Bmi1 expression regulates self-renewal, apoptosis, and differentiation of neural stem/progenitor cells in vitro and in vivo. *Stem Cells* **29**: 700-712.

Yamashita T, Ninomiya M, Hernandez Acosta P, Garcia-Verdugo JM, Sunabori T, Sakaguchi M, Adachi K, Kojima T, Hirota Y, Kawase T et al. 2006. Subventricular zone-derived neuroblasts migrate and differentiate into mature neurons in the post-stroke adult striatum. *J Neurosci* **26**: 6627-6636.

Yan H, Parsons DW, Jin G, McLendon R, Rasheed BA, Yuan W, Kos I, Batinic-Haberle I, Jones S, Riggins GJ et al. 2009. IDH1 and IDH2 mutations in gliomas. *N Engl J Med* **360**: 765-773.

Yan YP, Sailor KA, Vemuganti R, Dempsey RJ. 2006. Insulin-like growth factor-1 is an endogenous mediator of focal ischemia-induced neural progenitor proliferation. *Eur J Neurosci* **24**: 45-54.

Yang J, Mani SA, Donaher JL, Ramaswamy S, Itzykson RA, Come C, Savagner P, Gitelman I, Richardson A, Weinberg RA. 2004. Twist, a master regulator of morphogenesis, plays an essential role in tumor metastasis. *Cell* **117**: 927-939.

Yang MH, Hsu DS, Wang HW, Wang HJ, Lan HY, Yang WH, Huang CH, Kao SY, Tzeng CH, Tai SK et al. 2010a. Bmi1 is essential in Twist1-induced epithelial-mesenchymal transition. *Nat Cell Biol* **12**: 982-992.

Yang P, Yin X, Rutishauser U. 1992. Intercellular space is affected by the polysialic acid content of NCAM. *J Cell Biol* **116**: 1487-1496.

Yang S, Kuo C, Bisi JE, Kim MK. 2002. PML-dependent apoptosis after DNA damage is regulated by the checkpoint kinase hCds1/Chk2. *Nat Cell Biol* **4**: 865-870.

Yang X-M, Han H-X, Sui F, Dai Y-M, Chen M, Geng J-G. 2010b. Slit–Robo signaling mediates lymphangiogenesis and promotes tumor lymphatic metastasis. *Biochemical and Biophysical Research Communications* **396**: 571-577.

Yao B, Christian KM, He C, Jin P, Ming GL, Song H. 2016. Epigenetic mechanisms in neurogenesis. *Nat Rev Neurosci*.

Yao B, Jin P. 2014. Unlocking epigenetic codes in neurogenesis. *Genes Dev* **28**: 1253-1271.

Yeh ML, Gonda Y, Mommersteeg MT, Barber M, Ypsilanti AR, Hanashima C, Parnavelas JG, Andrews WD. 2014. Robo1 modulates proliferation and neurogenesis in the developing neocortex. *J Neurosci* **34**: 5717-5731.

Yiin J-J, Hu B, Jarzynka MJ, Feng H, Liu K-W, Wu JY, Ma H-I, Cheng S-Y. 2009. Slit2 inhibits glioma cell invasion in the brain by suppression of Cdc42 activity. *Neuro-Oncology* **11**: 779-789.

Yu J, Cao Q, Yu J, Wu L, Dallol A, Li J, Chen G, Grasso C, Cao X, Lonigro RJ et al. 2010. The neuronal repellent SLIT2 is a target for repression by EZH2 in prostate cancer. *Oncogene* **29**: 5370-5380.

Yuen Benjamin TK, Knoepfler Paul S. 2013. Histone H3.3 Mutations: A Variant Path to Cancer. *Cancer Cell* **24**: 567-574.

Zee BM, Levin RS, Xu B, LeRoy G, Wingreen NS, Garcia BA. 2010. In vivo residue-specific histone methylation dynamics. *J Biol Chem* **285**: 3341-3350.

Zhang J, Ji F, Liu Y, Lei X, Li H, Ji G, Yuan Z, Jiao J. 2014. Ezh2 regulates adult hippocampal neurogenesis and memory. *J Neurosci* **34**: 5184-5199.

Zhang J, Wu G, Miller CP, Tatevossian RG, Dalton JD, Tang B, Orisme W, Punchihewa C, Parker M, Qaddoumi I et al. 2013. Whole-genome sequencing identifies genetic alterations in pediatric low-grade gliomas. *Nat Genet* **45**: 602-612.

Zhang RL, LeTourneau Y, Gregg SR, Wang Y, Toh Y, Robin AM, Zhang ZG, Chopp M. 2007. Neuroblast division during migration toward the ischemic striatum:

a study of dynamic migratory and proliferative characteristics of neuroblasts from the subventricular zone. *J Neurosci* **27**: 3157-3162.

Zhang X-W, Yan X-J, Zhou Z-R, Yang F-F, Wu Z-Y, Sun H-B, Liang W-X, Song A-X, Lallemand-Breitenbach V, Jeanne M et al. 2010. Arsenic Trioxide Controls the Fate of the PML-RARα Oncoprotein by Directly Binding PML. *Science* **328**: 240-243.

Zhang Y, Reinberg D. 2001. Transcription regulation by histone methylation: interplay between different covalent modifications of the core histone tails. *Genes Dev* **15**: 2343-2360.

Zhao C, Deng W, Gage FH. 2008. Mechanisms and Functional Implications of Adult Neurogenesis. *Cell* **132**: 645-660.

Zhao L, Li J, Ma Y, Wang J, Pan W, Gao K, Zhang Z, Lu T, Ruan Y, Yue W et al. 2015. Ezh2 is involved in radial neuronal migration through regulating Reelin expression in cerebral cortex. *Sci Rep* **5**: 15484.

Zhao P, Hoffman EP. 2004. Embryonic myogenesis pathways in muscle regeneration. *Dev Dyn* **229**: 380-392.

Zheng C, Hayes JJ. 2003. Intra- and inter-nucleosomal protein-DNA interactions of the core histone tail domains in a model system. *J Biol Chem* **278**: 24217-24224.

Zhong S, Muller S, Ronchetti S, Freemont PS, Dejean A, Pandolfi PP. 2000. Role of SUMO-1-modified PML in nuclear body formation. *Blood* **95**: 2748-2752.

Zhou J, Pérès L, Honoré N, Nasr R, Zhu J, de Thé H. 2006. Dimerization-induced corepressor binding and relaxed DNA-binding specificity are critical for PML/RARA-induced immortalization. *Proceedings of the National Academy of Sciences* **103**: 9238-9243.

Zhu J, Zhou J, Peres L, Riaucoux F, Honore N, Kogan S, de The H. 2005a. A sumoylation site in PML/RARA is essential for leukemic transformation. *Cancer Cell* **7**: 143-153.

Zhu Y, Guignard F, Zhao D, Liu L, Burns DK, Mason RP, Messing A, Parada LF. 2005b. Early inactivation of p53 tumor suppressor gene cooperating with NF1 loss induces malignant astrocytoma. *Cancer Cell* **8**: 119-130.

Zink LM, Hake SB. 2016. Histone variants: nuclear function and disease. *Curr Opin Genet Dev* **37**: 82-89.

Zivkovic N, Berisavac I, Markovic M, Milenkovic S. 2014. Spinal metastasis of medulloblastoma in adults: a case report. *Srp Arh Celok Lek* **142**: 713-716.

Zong H, Parada LF, Baker SJ. 2015. Cell of origin for malignant gliomas and its implication in therapeutic development. *Cold Spring Harb Perspect Biol* **7**.